

**EXTRACTION AND SEPARATION STUDIES OF URANIUM
AND THORIUM FROM VARIOUS AQUEOUS MEDIA USING
ORGANOPHOSPHOROUS EXTRACTANTS**

By

SUJOY BISWAS

CHEM012008040020, dt. 01/09/2008

URANIUM EXTRACTION DIVISION

BHABHA ATOMIC RESEARCH CENTRE, INDIA

A thesis submitted to the

Boards of Studies in Chemical Science Discipline

In partial fulfillment of requirements

For the Degree of

DOCTOR OF PHILOSOPHY

of

HOMI BHABHA NATIONAL INSTITUTE



May, 2014

Homi Bhabha National Institute

Recommendations of the Viva Voce Board

As members of Viva Voce Board we certify that we have read the dissertation prepared by Sujoy Biswas entitled “**Extraction and Separation Studies of Uranium and Thorium from Various Aqueous Media Using Organophosphorous Extractants**” and recommended that it may be accepted as fulfilling the dissertation requirement for the Degree of Doctor of Philosophy.

Chairperson- Prof. A. Goswami _____ date_____

Convener- Prof. P.N.Pathak_____ date_____

External Examiner: Prof. Sukalyan Basu_____ date_____

Member 1- Dr. B.S. Tomar_____ date_____

Member 2- Dr. P.K. Mohapatra_____ date_____

Member 3- Dr. Manmohan Kumar_____ date_____

Final approval and acceptance of this dissertation is contingent upon the candidate's submission of final copies of the dissertation to HBNI.

We here by certify that we have read this dissertation prepared under our direction and recommended that it may be accepted as fulfilling the dissertation requirement.

Guide- Prof. P.N. Pathak _____ date

STATEMENT BY AUTHOR

This dissertation has been submitted in partial fulfillment of requirements for an advanced degree at Homi Bhabha National Institute (HBNI) and is deposited in the Library to be made available to borrowers under rules of the HBNI.

Brief quotations from this dissertation are allowable without special permission, provided that accurate acknowledgement of the source is made. Request for permission for quotation from or reproduction of this manuscript in whole or in part may be granted by the Competent Authority of HBNI when in his or her judgment the proposed use of the material is in the interest of scholarship. In all other instance however, permission must be obtained from the author.

Sujoy Biswas

DECLARATION

I hereby declare that the work presented in this thesis entitled “**Extraction and Separation Studies of Uranium and Thorium from Various Aqueous Media Using Organophosphorous Extractants**” is original and has not been submitted to this or any other University/ Institution for the award of any other degree or diploma.

Sujoy Biswas

Research Student

DEDICATED TO MY MOTHER

SMT. MAHAMAYA BISWAS

ACKNOWLEDGEMENTS

I am highly indebted to my research guide Dr. P. N. Pathak, SO/G, Radiochemistry Division, Bhabha Atomic Research Centre for accepting me as his student and providing me his invaluable guidance.

It is my great privilege to acknowledge Dr. (Smt) S. B. Roy, Head, UED and Shri K. N. Hareendran, Incharge, QCS, UED, for permitting me to undertake this programme. I am especially thankful to Dr. D. K. Singh, REDS, for his constant help and encouragement. Chairman (Prof. A. Goswami) and members (Dr. B.S. Tomar, Dr. P.K. Mohapatra and Dr. Manmohan Kumar) of the doctoral committee are gratefully acknowledged for their critical review and suggestion during progress review and pre-synopsis viva-voce. I also want to express my warmest appreciation to all my colleagues at UED, who have contributed, directly or indirectly, to the success of this programme.

May 2014

Sujoy Biswas

UED, BARC

CONTENTS

	Page No.
SYNOPSIS	xiv
LIST OF FIGURES	xxiii
LIST OF TABLES	xxxi
CHAPTER 1: INTRODUCTION	1
1.1. India's Nuclear Power Programme	2
1.2. Nuclear Fuel Cycle and its Various Steps	3
1.3. Uranium	4
1.3.1. Natural occurrence of uranium	5
1.3.2. Metallurgical extraction of uranium	6
1.3.3. Uranium metal preparation and its properties	9
1.5. Thorium	10
1.5.1. Natural occurrence of thorium	11
1.5.2. Recovery of thorium from monazite	12
1.5.3. Uses of thorium	15
1.6. Chemist's Role in Nuclear Fuel Cycle	15
1.7. The Actinide Elements	16
1.7.1. Electronic configuration	16
1.7.2. Oxidation states	18
1.7.3. Complexes and stereochemistry	20

1.7.4. Disproportionation	21
1.7.5. Hydrolysis and polymerization	21
1.7.6. Atomic spectra	22
1.8. Separation Methods	23
1.8.1 Solvent extraction	23
1.8.1.1. Solvent extraction equilibria and distribution ratio (<i>D</i>)	24
1.8.1.3. Separation factor (β)	25
1.8.1.4. Extraction isotherm	25
1.8.1.5. Multiple extractions	26
1.8.1.6. Co-current extraction	26
1.8.1.7. Counter-current extraction	27
1.8.1.8. Factors influencing the distribution of solutes	30
1.8.1.9. Classification of extractants	31
1.8.1.10. Criteria for the selection of extractants	32
1.8.2 Membrane Based Separation	33
1.8.2.1. Supported liquid membranes (SLMs)	35
1.8.2.2. Transport in SLM	35
1.9. Aim and Scope of the Thesis	37
CHAPTER II: EXPERIMENTAL	41
2.1. Introduction	42
2.2. Extractants	42
2.3. Synthesis of Di-nonyl Phenyl Phosphoric Acid (DNPPA)	43
2.4. Purification of DNPPA	43

2.4.1. Purification by Nd-salt Method	43
2.4.2. Purification by Mono Ethylene Glycol Treatment	44
2.4.3. Characterization of DNPPA: Potentiometric titration	45
2.5. Other Materials	46
2.6. Instruments	47
2.7. Solution Preparations	48
2.7.1. Standard solution of uranium & thorium	48
2.7.2. Solution for Spectrophotometric Measurement of Uranium	48
2.7.2.1. Preparation of complexing solution	48
2.7.2.2. Buffer solution	48
2.7.2.3. Br-PADAP solution (0.05%)	49
2.7.2.4. Mixture of PC88A and TOPO solution (0.1M + 0.05 M)	49
2.7.3. Composition of Uranyl Nitrate Raffinate (UNR)	49
2.7.4. Uranium ore leach solution	50
2.8. Experimental Procedure for Solvent Extraction	51
2.9. Experimental Procedure Membrane Transport Studies	52
2.9.1. Transport equation	52
2.10. Dynamic Light Scattering (DLS) Measurements	54
2.12. Quantitative Determination of Thorium	55
2.12.1. Spectrophotometry	55
2.12.2. Complexometric titration	55
2.13. Estimation of Uranium	56
2.13.1. Spectrophotometry	56

2.13.2. Davies Gray titration	57
CHAPTER III: SYNERGISTIC EXTRACTION OF URANIUM WITH MIXTURES OF ORGANOPHOSPHOROUS ACIDIC AND NEUTRAL EXTRACTANTS	58
3.1. Introduction	59
3.2. The present work	60
3.3. Results and Discussion	61
3.3.1. Extraction of U(VI) from nitric acid medium with PC88A and neutral donors	61
3.3.1.1. Effect of nitric acid concentration	61
3.3.1.2. Effect of temperature	64
3.3.1.3. Effect of diluents	65
3.3.1.4. Synergistic extraction	66
3.3.1.5. Recovery of uranium from raffinate waste	69
3.3.1.5.1. Evaluation of different extractants	69
3.3.1.5.2. Uranium recovery from actual waste samples	71
3.3.2. Extraction of U(VI) from nitric acid medium with DNPPA and neutral donors	71
3.3.2.1. Effect of nitric acid and extractant concentration	72
3.3.2.2 Comparison with other acidic organophosphorous extractants	75
3.3.2.3. Synergistic extraction	76
3.4. Conclusions	78
CHAPTER IV: EMPIRICAL MODELING OF SOLVENT EXTRACTION DATA OF U(VI) FROM SULPHATE MEDIUM USING PC88A AND NEUTRAL OXODONORS	80
4.1. Introduction	81
4.2 The present work	82

4.3. Results and Discussion	83
4.3.1. Extraction of U(VI) studies from sulphate medium	83
4.3.2. Extraction equilibrium	84
4. 3.3. Stoichiometry of the extracted species	85
4. 3.4. Non-linear least square regression	88
4. 3.5. Development of mathematical model	90
4. 3.6. Mathematical model for synergistic extraction	92
4. 4. Conclusions	96
CHAPTER V: SEPARATION OF U(VI) AND Th(IV) FROM MONAZITE USING TRIS(2-ETHYLHEXYL) PHOSPHATE (TEHP)/ <i>n</i>-PARAFFIN	98
5.1. Introduction	99
5.2. The present work	101
5.3. Results and Discussion	101
5.3.1. Extraction of U(VI) from nitric acid medium	101
5.3.2. Extraction behavior of Th(IV)	103
5.3.3. Effect of extractant concentration	104
5.3.4. Separation of U(VI) from Th(IV)	106
5.3.5. Separation of U(VI) from a mixture of U(VI) and Y(III)	109
5.3.6. Separation of U(VI) from a mixture of U(VI), Th(IV), and Y(III)	110
5.3.7. Separation of U(VI) from multi-component system	110
5.3.8. McCabe-Thiele diagram for extraction and stripping of U(VI)	111
5.3.9. Conceptual process flow-sheet	113

5.4. Conclusions	115
CHAPTER VI: URANIUM PERMEATION STUDIES FROM NITRIC ACID MEDIUM ACROSS SUPPORTED LIQUID MEMBRANE USING ORGANOPHOSPHOROUS EXTRACTANTS	116
6.1. Introduction	117
6.2. The present work	118
6.3. Results and Discussion	119
6.3.1. Uranium permeation studies from HNO ₃ medium using neutral organophosphorous extractants	119
6.3.1.2. Effect of feed acidity	121
6.3.1.3. Effect of extractant concentration	123
6.3.1.4. Effect of uranium concentration	124
6.3.1.5. Effect of pore	126
6.3.1.6. Effect of membrane thickness	127
6.3.2. Uranium permeation studies using acidic organophosphorous extractants and their synergistic mixtures	128
6.3.2.1. Evaluation of acidic extractants	128
6.3.2.2 Evaluation of different strippants as receiver phase	129
6.3.2.3 Effect of neutral donors	131
6.3.2.4 Effect of H ₂ SO ₄ concentration on uranium transport in the receiver phase	132
6.3.2.5. Effect of feed acidity	134
6.3.2.6. Effect of U(VI) concentration	135
6.3.2.7. Effect of membrane thickness	137
6.3.2.8. Effect of membrane pore size	139

6.3.3. Transport studies using DNPPA and its mixture with neutral donors	140
6.3.3.1. Kinetic Modeling	140
6.3.3.2. Effect of membrane thickness	144
6.3.3.3. Synergistic transport of uranium	146
5.2.3.4. Effect of variation of mole ratio of extractants	148
5.2.3.5. Comparison of U(VI) permeation with other synergistic solvent mixture	150
6.2.4. Recovery of U(VI) from UNR solution	151
6.3. Conclusions	152
CHAPTER VII: STUDY ON AGGREGATION BEHAVIOR OF DINONYL PHENYL PHOSPHORIC ACID (DNPPA)	153
7.1. Introduction	154
7.2. The present work	154
7.3. Results and Discussion	155
7.3.1. Effect of feed acidity and diluents on aggregation of DNPPA	155
7.3.2. Effect of DNPPA concentration on aggregation	158
7.3.3 Effect of metal ions on aggregation	159
7.3.4. Influence of neutral donors on aggregation behavior	160
7.4. Conclusions	163
CHAPTERVIII: DEVELOPMENT OF EXTRACTIVE SPECTROPHOTOMETRIC METHOD FOR THE ANALYSIS OF URANIUM	165
8.1. Introduction	166
8.2. The present work	167
8.3. Experimental procedure	169
8.4. Results and Discussion	170

8.4.1. Effect of time on color stability	170
8.4.2. Optimization of ethanol concentration	172
8.4.3. Accuracy of the analytical method	173
8.4.4. Effect of other ions	174
8.4.5. Precision of the developed method	175
8.4.6. t and F test	176
8.4.7. Evaluation of detection limit	178
8.4.8. Application of the developed method to real samples	179
8.5. Conclusions	180
RECOMMENDATION FOR FURTHER RESEARCH	182
References	183
Statement under section 0.771	200



Homi Bhabha National Institute

Ph. D. PROGRAMME

- 1. Name of the Student: Sujoy Biswas**
- 2. Name of the Constituent Institution: Bhabha Atomic Research Centre, Mumbai, India**
- 3. Enrolment No. : CHEM 012008040020, dt. 01/09/2008**
- 4. Title of the Thesis: “Extraction and Separation Studies of Uranium and Thorium from Various Aqueous Media Using Organophosphorous Extractants”**
- 5. Board of Studies: Chemical Sciences**

SYNOPSIS

Separation and purification of actinide elements such as uranium and thorium from their ore bodies, irradiated fuel dissolver solution, and waste solutions etc. is of vital importance in the nuclear fuel cycle [1-2]. Different methods such as ion exchange, precipitation, solvent extraction, and membrane based separations are used for this purpose [1-6]. Whereas solvent extraction is useful for large scale recovery and separation of metal ions from high concentration feed solutions, membrane based separations appear promising for lean aqueous media. The present study deals with the separation/recovery of uranium and thorium from various aqueous

solutions by solvent extraction as well as supported liquid membrane (SLM) techniques using various organophosphorous extractants.

High purity is essential for the production and processing of uranium and thorium for their use as fuel materials in nuclear reactors with the concentration of some specific elements in ppm-ppb level (e.g. Boron :120 ppb). The deployment of a new solvent extraction process requires the generation of basic data for evaluating the efficiency of different extractants. This includes the evaluation of distribution ratio (D), decontamination factor (DF), separation factor (SF), stoichiometry, stability/extraction constants of extracted species, influence of pH/acidity, temperature, nature of diluents, and stripping agents etc. Similarly, the recovery of trace concentrations of metal ions from different waste solutions using SLM needs generation of basic data with respect to the choice of the solid support, membrane pore size, nature and concentration of carrier solvent, time required for quantitative transport, permeability coefficient (P) calculation, effect of various strippants, feed acidity, diluents, selectivity, stability of membrane, and finally the scale up of the process etc.

Commercially available organophosphorous extractants have been used for the recovery and separation of uranium and thorium from various feed solutions [7-13]. In the present work, the extraction and transport behavior of uranium and thorium has been studied using acidic extractants (HA) such as (i) 2-ethylhexyl phosphonic acid 2-ethylhexyl monoester (PC88A), (ii) dinonylphenyl phosphoric acid (DNPPA), (iii) bis(2,4,4-trimethylpentyl) phosphonic acid (Cyanex 272), and (iv) di(2-ethylhexyl) phosphoric acid (D2EHPA); and neutral extractants (S) such as (i) tributyl phosphate (TBP), (ii) tris(2-ethylhexyl) phosphate (TEHP), (iii) trioctyl phosphine oxide (TOPO), (iv) Cyanex 923 (a mixture of four trialkyl phosphine oxides viz.

R_3PO , $R_2R'PO$, RR'_2PO and R'_3PO where R: *n*-octyl and R': *n*-hexyl chain), (v) dioctyl sulphoxide (DOSO), and (vi) methyl isobutyl ketone (MIBK).

The thesis is divided in to eight chapters. A brief description of each chapter is given below:

Chapter 1: This chapter deals with solution chemistry of actinides, different types of extractants, basic principles of solvent extraction and transport of metal ions across supported liquid membranes.

Chapter 2: This chapter deals with the experimental details of solvent extraction and supported liquid membrane based metal transport studies. The preparation of different supported liquid membranes and their experimental set up are described. Details of equipments used for the determination of metal ions and acidity in different phases are mentioned. This chapter also includes the methods of preparation of stock solutions of metal ions, extractants and their properties.

Chapter 3: This chapter presents the results obtained for the extraction of uranium from nitric acid medium using acidic extractants such as PC88A, DNPPA, D2EHPA either alone or their synergistic mixtures with neutral donors such as TBP, TEHP, TOPO, Cyanex 923 under different experimental conditions. Extraction data of U(VI) from nitric acid medium using PC88A shows that extraction occurs via cation exchange at low HNO_3 concentration and then by solvation mechanism at high HNO_3 concentration. The stoichiometry of the extracted species has been found to be $UO_2(NO_3).HA_2(H_2A_2)$ type of complex at $< 3 M HNO_3$ concentration and at high acidities $UO_2(NO_3)_2.(2H_2A_2)$ is formed where H_2A_2 refers to the dimeric form of PC88A. The

use of mixtures of PC88A with neutral donors such as TBP, TOPO, DOSO, MIBK shows synergism during U(VI) extraction from nitric acid medium. The synergistic extraction of U(VI) by PC88A along with neutral donors varies in the order : MIBK < TBP < DOSO < TOPO which is in agreement with their basicity/ acid uptake constant (K_H). On the other hand, U(VI) extraction using DNPPA from HNO_3 medium showed the formation of $UO_2(HA_2)_2$ type of complex in the organic phase. The presence of neutral oxodonor like TBP, TEHP, Cyanex 923 along with DNPPA showed synergistic enhancement in the extraction of U(VI) in the order: Cyanex 923 > TBP > TEHP. Stoichiometry of the extracted species was determined as $UO_2(HA_2)_2 \cdot 2S$ in the organic phase. The optimized conditions have been tested for uranium recovery from uranyl nitrate raffinate (UNR) solutions emanating from uranium purification plant.

Chapter 4: This chapter deals with the extraction of U(VI) from sulphate medium with PC88A in *n*-dodecane under a wide range of conditions such as variation of feed acidity, metal ion and extractant concentration etc. The experimental data on the distribution ratio of U(VI) (D_U) against initial acidity (H_i) at varying initial uranium concentration (C_i) has been determined and utilized to develop an empirical correlation between D_U , H_i and C_i . This can be used to predict the concentration of uranium in organic as well as in aqueous phase at any C_i and H_i under the present experimental conditions.

Chapter 5: In this chapter, the separation of trace amount of U(VI) from monazite leach solution is investigated using TEHP as extractant. The effects of experimental variables such as diluents, HNO_3 , extractant and metal ion concentration etc. are investigated with respect to U(VI) and

Th(IV) extraction. The separation of U(VI) from a binary mixture of metal ion containing Th(IV) and Y(III) at different HNO₃ concentrations are studied using varying concentration of TEHP/*n*-paraffin and results are compared under identical conditions using TBP. It is observed that the separation factors of uranium in case of TEHP are better TBP at all HNO₃ concentrations. McCabe-Thiele diagram for the extraction and stripping of U(VI) from nitric acid medium shows that for a feed solution containing 1 g/L U(VI) at 2 M HNO₃, 0.2 M TEHP/*n*-paraffin as solvent and water as strippant, 3 stages are sufficient for quantitative extraction (> 99.9%) of U(VI) from the solution. The optimized conditions have been successfully applied for the separation of U(VI) from simulated monazite leach solution in HNO₃ medium.

Chapter 6: During the purification of yellow cake (diuranate) by TBP/Kerosene route, the UNR solution contains significant amounts of uranium (0.3-1 g/L) along with other impurities, is currently treated with MgO to precipitate uranium as magnesium diuranate and disposed as a solid waste. It is desirable to recover uranium from UNR solutions before its disposal as solid waste. This chapter presents SLM based studies of the recovery of U(VI) from UNR solution. Different types of extractants used for preparation of SLM were DNPPA, Cyanex 272, PC88A, D2EHPA, TBP, TEHP, TEBP, TOPO, Cyanex 923 and their different combination dissolved in *n*-paraffin. These experiments have been carried out using PTFE membranes, in two compartment glass cell. The solutions have been stirred using magnetic spin bars at a constant speed of 200 r.p.m. Different parameters such as nature and concentration of strippants, concentration of metal ions and acid in feed solution, diluents and pore size variation are optimized to achieve effective uranium transport with minimum time.

A simple kinetic model has been proposed to evaluate the diffusion coefficient of U-DNPPA and U-DNPPA-Cyanex 923 complexes across SLM. The transport experiments are also carried out using genuine UNR solution and % transport of uranium along with the impurities. A comparative study has been made on the recovery of uranium from UNR solution using SLM technique employing different combinations of carrier solutions and receiver phases. Based on the experimental results the 0.1 M Cyanex 272 + 0.05 M Cyanex 923/ *n*-paraffin as carrier and 2 M H₂SO₄ as receiver phase has been found to be best combination for selective recovery of uranium from UNR solution.

Chapter 7: This chapter deals with the aggregation behavior of DNPPA under varying experimental conditions such as aqueous phase acidity, nature of diluents, and ligand concentration using dynamic light scattering (DLS), and spectrophotometry. The aggregation tendency of 0.05 M DNPPA/*n*-dodecane decreased with increased aqueous phase acidity from 3.23 nm (0.5 M HNO₃) to 2.31 nm (8 M HNO₃), which followed the extraction pattern of uranium and rare earths. This observation was further supported by changes in absorption spectra of DNPPA pre-equilibrated with increasing concentrations of nitric acid. DNPPA/*n*-dodecane had a single characteristics absorption peak at 288 nm, and a new peak appeared at 353 nm on equilibration with increasing concentrations of nitric acid suggesting the interaction of DNPPA-HNO₃ molecules. However, the presence of neutral oxodonors such as tri-*n*-butyl phosphate (TBP) and Cyanex 923 suppressed the interaction of DNPPA and HNO₃ molecules. This behavior was attributed to preferential formation of TBP/Cyanex 923-HNO₃ adducts, which was supported by changes in the absorption spectra.

Chapter 8: An extractive spectrophotometric analytical method for the determination of uranium in ore leach solution is described in this chapter. The method is based on the selective extraction of uranium from multielement system using a synergistic mixture of PC88A + TOPO in cyclohexane and color development from organic phase using 2-(5-bromo-2-pyridylazo)-5-diethylaminophenol (Br-PADAP) as chromogenic reagent. The absorption maximum of the U(VI)-Br-PADAP complex has been observed at 576 nm and molar extension coefficient (ϵ) was calculated to be $36747.20 \pm 241 \text{ Lmol}^{-1}\text{cm}^{-1}$ in the presence of 64 % ethanol at pH ~ 7.8 . The effects of various parameters such as stability of complex, ethanol, ore matrix etc. on the determination of uranium are evaluated. Analysis of synthetic standard as well as ore leach solution shows that for 10 determinations relative standard deviation (RSD) is $< 2 \%$. The accuracy has been checked by determining uranium using standard addition methods in the range of $10 \mu\text{m/mL}$ to $200 \mu\text{g/mL}$ and it is found to be accurate with a 98- 105 % recovery rate.

In summary, the important highlights of this thesis are as follows:

1. Organophosphorous acidic extractants such as PC88A, DNPPA have been tested for extraction of U(VI) from nitric acid medium and extraction parameters are optimized for the recovery of U(VI) from UNR solution generated during the purification of yellow cake.
2. The extraction of uranium with PC88A in *n*-dodecane from sulphate medium has indicated the formation of a monomeric neutral complex, $\text{UO}_2(\text{HA}_2)_2$. An empirical correlation, $(D = (12.98 \pm 0.90) / C_i^{(-0.75 \pm 0.05)} \times [\text{H}_i]^2)$ has been developed which can be used to predict the extraction behavior of U(VI) with PC88A under the wide experimental conditions.

3. A solvent extraction process for the recovery of U(VI) from a mixture of U(VI), Th(IV) and R.E has been developed using TEHP as extractant and its performance has been compared vis-à-vis TBP under identical conditions. The process has been used successfully for the recovery of U(VI) from monazite leach solution (HNO₃ medium).
4. Permeation of U(VI) across SLM has been investigated using various organo-phosphorous extractants either alone or their mixtures with neutral oxodonors. The process was successfully applied for the recovery of U(VI) from genuine UNR solution generated during purification of yellow cake in Uranium Metal Plant, BARC.
5. The aggregation behavior of DNPPA in different diluents has been studied to explain the extraction of metal ions from aqueous medium. A direct correlation between DNPPA aggregate size and the extraction profile of metal ions has been observed in U(VI)-HNO₃-DNPPA system.
6. An extractive spectrophotometric method has been developed for the estimation of uranium in ore leach solution. This technique is based on the selective extraction of uranium from multi-element system using a synergistic mixture of PC88A + TOPO in cyclohexane and simultaneous color development in organic phase using Br-PADAP as chromogenic reagent. The technique developed can be used to determine 2.5- 250 µg/mL uranium in ore leach solution with high accuracy and precision.

The studies carried out during the present work and the methodologies developed have led to publications in peer reviewed International Journals (11 Nos) and national symposia (12 Nos).

References

1. Mukherjee T.K., and Singh H., INSAC, Kalpokkam, 2003, IT-1.
2. Gupta C.K., Singh H., Uranium Resource Processing: secondary Resources, Springer, Germany, 2003.
3. Thompson R., September Special Publication No. 40, (1980) p.p. 403–443.
4. Singh S.K., Misra S.K., Tripathi S.C., Singh D.K., Desalination 250 (2010) 19-20.
5. Singh S.K., Dhami P.S., Dakshinamoorthy A., Sundersanan M., Sep. Sci. Technol., 44 (2009) 491-505.
6. Kedari C.S., Pandit S.S., Misra S.K., Ramanujam A., Hydrometallurgy. 62 (2001) 47-56.
7. Singh R.K., Dhadke P.M., J. Radioanal. Nucl. Chem., 254 (2002) 607-612.
8. Behera P., Mishra M.S., Mohanty M.I., Chakravortty V., J. Radioanal. Nucl. Chem., 178 (1994) 179-192.
9. Singh D.K., Singh H., Mathur J.N., Radiochim. Acta, 89 (2001) 573–578.
10. Rout K.C., Mishra P.K., Chakravortty V., and Dash K.C., Radiochim. Acta, 62 (1993) 203–206.
11. Mansingh P.S., Chakravortty V., and Dash K.C., Radiochim. Acta, 73 (1996) 139–143.
12. Godbole A.G., Mapara P.M., Swarup R., J. Radioanal. Nucl. Chem., 200 (1995) 1-8.
13. Chetty K.V., Gamare J.S., Godbole A.G., Vaidya V.N., J. Radioanal. Nucl. Chem., 269 (2006) 15-20.

LIST OF FIGURES

	Page No.
Figure 1.1 : Various steps of a typical nuclear fuel cycle	3
Figure 1.2 : Alkali digestion process flow-sheet of Monazite/Xenotime	12
Figure 1.3 : Acid digestion process flow-sheet of Monazite/Xenotime	13
Figure 1.4 : Redox potential of actinide ions in 1M HClO ₄ (Volts)	19
Figure 1.5 : Co-current extraction in three stages	27
Figure 1.6 : Counter-current extraction scheme	28
Figure 1.7 : Pictorial view of supported liquid membrane	35
Figure 1.8 : Co- transport steps in SLM	36
Figure 1.9 : Counter-transport steps in SLM	37
Figure 2.1 : Potentiometric titration of DNPPA with standard 0.1 M NaOH using Phenolphthalein as indicator; EP: End Point	46
Figure 2.2 : A typical membrane transport cell used in the present study	52
Figure 3.1 : Variation of D_U with aqueous phase acidity; [U(VI)]: 0.1 M; Diluent: <i>n</i> -dodecane; T: 298 K	62
Figure 3.2 : Variation of D_U with hydrogen ion concentration; [PC88A]: 5×10^{-3} M; [U(VI)]: 1×10^{-3} M; [NO ₃ ⁻]: 3 M; Diluent: <i>n</i> -dodecane T: 298 K	62
Figure 3.3 : Variation of D_U with PC88A concentration; Diluent: <i>n</i> -dodecane; [U(VI)]: 0.1 M; T: 298 K	63

Figure 3.4	: Variation of D_U with nitrate ion concentration; [U(VI)]: 0.1 M; [PC88A]: 0.025 M; Diluent: <i>n</i> -dodecane; [H ⁺]: 0.3 M; T: 298 K	64
Figure 3.5	: Variation of D_U with temperature; [U(VI)]: 0.1 M; [HNO ₃]: 4 M; [PC88A]: 0.5 F; Diluent: <i>n</i> -dodecane	65
Figure 3.6	: Variation of D_U with aqueous phase acidity; [DNPPA]: 0.01 M; Diluent: <i>n</i> -paraffin; T: 298 K	72
Figure 3.7	: Variation of D_U with hydrogen ion concentration; [U(VI)]: 1×10^{-3} M; Diluents: <i>n</i> -paraffin; [NO ₃ ⁻]: 3 M; T: 298 K	73
Figure 3.8	: Variation of D_U with DNPPA concentration; [HNO ₃]: 3 M; Diluent: <i>n</i> -paraffin; T: 298 K	74
Figure 3.9	: Comparison of variation of D_U with nitric acid concentration using various organophosphorous acidic extractants; [U(VI)]: 0.1 M; Diluent: <i>n</i> -paraffin; T: 298 K	75
Figure 4.1	: Variation of D_U with H ₂ SO ₄ concentration; Diluent: <i>n</i> -dodecane; T: 298 K	83
Figure 4.2	: Effect of [H ⁺] on distribution ratio of uranium; [PC88A]: 0.05 M; Diluent: <i>n</i> -dodecane; T: 298 K	86
Figure 4.3	: Dependence of distribution ratio on extractant concentrations for the extraction of U(VI); [U(VI)]: 0.02 M; [H ⁺]: 3 M; Diluent: <i>n</i> -dodecane; T: 298 K	87
Figure 4.4	: Non linear least square regression plot for the extraction of various concentrations of U(VI) with 0.5 M PC88A; Diluent: <i>n</i> -dodecane; T: 298 K.	89

Figure 4.5	: Dependence of distribution ratio on acidity at various concentrations of U(VI); [PC88A] : 0.5 M; Diluent: <i>n</i> -dodecane, T: 298 K	90
Figure 4.6	: Plot of D_{exp} vs D_{cal} using mathematical model; Refer Equation 4.11	92
Figure 4.7	: Variation of % extraction (% E) of U(VI) with PC88A concentration at constant neutral donor (TOPO) concentration; [U(VI)]: 0.015 M; [TOPO] : 0.015 M; [H ⁺]: 3 M	93
Figure 4.8	: Variation of % extraction (% E) of U(VI) with TOPO concentration at constant PC88A concentration; [U(VI)]: 0.015 M; [PC88A] : 0.1 M; [H ⁺]: 3 M	94
Figure 4.9	: Plot of % E_{exp} vs % E_{cal} using mathematical model	96
Figure 5.1	: Variation of D_U with HNO ₃ concentration for 1.1M TEHP and TBP, Diluents: <i>n</i> -paraffin; T: 298 K	102
Figure 5.2	: Variation of D_{Th} with HNO ₃ concentration for 1.1M TEHP and TBP; Diluents: <i>n</i> -paraffin; T: 298 K.	104
Figure 5.3	: Variation of log D vs log [TEHP]; [HNO ₃] : 4 M; [U(VI)] : 2×10^{-3} M; [Th(IV)] : 2×10^{-3} M; Diluents: <i>n</i> -paraffin; T: 298 K	105
Figure 5.4	: McCabe-Thiele diagram of extraction of U(VI) from 2 M HNO ₃ medium using 0.2 M TEHP, Diluent: <i>n</i> -paraffin; T: 298 K	112
Figure 5.5	: McCabe-Thiele diagram of stripping of U(VI) from 0.2 M TEHP; Strippant: water; Diluent: <i>n</i> -paraffin; T: 298 K	112

Figure 5.6	: Process flow-sheet for separation of U(VI), Th(IV), REEs during processing of Monazite mineral, TEHP: 0.2 M, Diluent: <i>n</i> -paraffin; T: 298 K.	114
Figure 6.1	: Uranium transport behavior of various organophosphorous carrier in the membrane phase; $[U(VI)]_{\text{feed}}: 2 \times 10^{-3} \text{ M}$ at 1.12 M HNO_3 ; Carrier concentration: 1.1 M in <i>n</i> -paraffin	120
Figure 6.2	: Comparison of uranium transport across PTFE supported membrane impregnated with different carriers and with different feed solutions; Carrier(s): 1.1 M TBP/TBEP/TEHP in <i>n</i> -paraffin; Feed solution(s): $2 \times 10^{-3} \text{ M U(VI)}$ at 1.1 - 3.3 M HNO_3 ; Strippant: Distilled Water	121
Figure 6.3	: Effect of acidity on uranium transport using 1.1M TBEP in <i>n</i> -paraffin as a carrier; $[U(VI)]_{\text{feed}}: 2 \times 10^{-3} \text{ M}$; Strippant: Distilled Water	122
Figure 6.4	: Transport steps of uranium in SLM in presence of neutral extractant	123
Figure 6.5	: Variation of flux (J) with U(VI) concentration in the feed solution; Carrier: 1.1 M TEHP/ <i>n</i> -paraffin; Feed acidity: 2 M; Receiver phase: Distilled Water	125
Figure 6.6	: Effect of U(VI) concentration in the feed solution on its permeation; Feed acidity: 2 M HNO_3 ; Carrier: 1.1 M TEHP in <i>n</i> -paraffin; Receiver phase: Distilled Water	125

Figure 6.7	: Effect of membrane pore size on U(VI) transport across SLM employing 1.1 M TEHP/ <i>n</i> -paraffin; Feed: 2×10^{-3} M U(VI) at 2 M HNO ₃ ; Receiver phase: Distilled Water	126
Figure 6.8	: Effect of membrane thickness on U(VI) transport across SLM employing 1.1M TEHP/ <i>n</i> -paraffin; Feed: 2×10^{-3} M U(VI) at 2 M HNO ₃ ; Receiver phase: Distilled Water	127
Figure 6.9	: Uranium transport across SLM impregnated with various acidic extractants as carrier; [U(VI)] _{feed} : 2×10^{-3} M at 2 M HNO ₃ ; Carrier: 0.1 M in <i>n</i> -paraffin; Receiver phase: 2 M H ₂ SO ₄	129
Figure 6.10	: Effect of receiver phase on U(VI) transport; [U(VI)] _{feed} : 2×10^{-3} M at 2 M HNO ₃ ; Carrier: 0.1 M Cyanex 272 in <i>n</i> -paraffin	130
Figure 6.11	: Effect of various neutral donors in the carrier solution in presence of 0.1 M Cyanex 272 on uranium transport; Feed: 2×10^{-3} M U(VI) at 2 M HNO ₃ ; Diluent: <i>n</i> -paraffin; Receiver phase: 2 M H ₂ SO ₄	131
Figure 6.12	: Uranium transport as a function of H ₂ SO ₄ concentration in the receiver phase; [U(VI)] _{feed} : 2×10^{-3} M at 2 M HNO ₃ ; Carrier: 0.1 M Cyanex 272 + 0.05 M Cyanex 923 in <i>n</i> -paraffin	133
Figure 6.13	: Uranium transport as a function of feed acidity; Carrier: 0.1 M Cyanex 272 + 0.05M Cyanex 923 in <i>n</i> -paraffin; [U(VI)] _{feed} : 2×10^{-3} M; Receiver phase: 2 M H ₂ SO ₄	134
Figure 6.14	: Counter-current U(VI) transport steps in SLM using acidic extractants (H ₂ A ₂)	135

Figure 6.15	: Effect of U(VI) concentration in the feed solution on its permeation; Carrier: 0.1 M Cyanex 272 + 0.05 M Cyanex 923 in <i>n</i> -paraffin; Feed acidity: 2 M HNO ₃ ; Receiver phase: 2 M H ₂ SO ₄	136
Figure 6.16	: Variation of flux (J) with U concentration in the feed solution; Carrier: 0.1 M Cyanex 272 + 0.05 M Cyanex 923/ <i>n</i> -paraffin; Receiver phase: 2 M H ₂ SO ₄	137
Figure 6.17	: Variation of U(VI) transport with membrane thickness; Feed: 2x10 ⁻³ M U(VI) at 2 M HNO ₃ ; Carrier: 0.1 M Cyanex 272 + 0.05 M Cyanex 923 in <i>n</i> -paraffin; Receiver phase: 2 M H ₂ SO ₄	138
Figure 6.18	: Variation of U(VI) permeability with membrane thickness; [U(VI)] _{feed} : 2x10 ⁻³ M; Receiver phase: 2 M H ₂ SO ₄ ; Carrier: 0.1 M Cyanex 272 + 0.05 M Cyanex 923 in <i>n</i> -paraffin	138
Figure 6.19	: Effect of pore size on U(VI) permeation; Feed: 2x10 ⁻³ M U(VI) at 2 M HNO ₃ ; Carrier: 0.1 M Cyanex 272 + 0.05 M Cyanex 923 in <i>n</i> -paraffin; Receiver phase: 2 M H ₂ SO ₄	139
Figure 6.20	: Plot of 1/P vs 1/K at different DNPPA concentration; Feed acid: 2 M HNO ₃ ; U(VI): 2x 10 ⁻³ M Receiver phase: 6 H ₂ SO ₄ , [U(VI)] _{feed} : 2x10 ⁻³ M	143
Figure 6.21	: Variation of U(VI) transport with membrane thickness; Feed: 2x10 ⁻³ M U(VI) at 2 M HNO ₃ ; Carrier: 0.1 M DNPPA in <i>n</i> -paraffin; Receiver phase: 6 M H ₂ SO ₄	145
Figure 6.22	: Variation of U(VI) permeability with membrane thickness; [U(VI)] _{feed} : 2x10 ⁻³ M; Receiver phase: 6 M H ₂ SO ₄ ; Carrier: 0.1 M DNPPA in <i>n</i> -paraffin	145

Figure 6.23	: Effect of different neutral donors on U(VI) transport across SLM containing 0.1M DNPPA/ <i>n</i> -paraffin in the membrane phase; Feed: 2×10^{-3} M U(VI) in 2 M HNO ₃ ; Receiver phase: 2 M H ₂ SO ₄	147
Figure 6.24	: Effect of varying concentrations of Cyanex 923 on U(VI) transport across SLM; [DNPPA]: 0.1 M DNPPA; Diluent: <i>n</i> -paraffin; Feed: 2×10^{-3} M U(VI) in 2 M HNO ₃ ; Receiver phase: 2 M H ₂ SO ₄	149
Figure 7.1	: Effect of diluents on the aggregation behavior of 0.05 M DNPPA pre-equilibrated with different nitric acid solutions; [DNPPA] : 0.05M; Temperature: 25 °C	155
Figure 7.2	: Absorbance spectra of DNPPA solutions dissolved in <i>n</i> -dodecane and pre-equilibrated with different nitric acid solutions [#] 5×10^{-3} M DNPPA; ^{##} 5×10^{-4} M DNPPA	156
Figure 7.3	: Variation of D _U with aqueous phase acidity; [U(VI)]: 1×10^{-3} M; Extractant: 1×10^{-2} M DNPPA; Diluent: <i>n</i> -dodecane; temperature: 25 °C	157
Figure 7.4	: Effect of DNPPA concentration on its aggregation behavior pre-equilibrated with 1 & 3 M HNO ₃ ; Diluent: <i>n</i> -dodecane; Temperature: 25 °C	159
Figure 7.5	: Absorbance spectra of DNPPA solutions dissolved in <i>n</i> -dodecane and pre-equilibrated with 3 M HNO ₃	159
Figure 7.6	: Effect of Eu(III)/U(VI) on the aggregation behavior of 0.05 M DNPPA pre-equilibrated with different nitric acid solutions; Diluent: <i>n</i> -dodecane; temperature: 25 °C	160

Figure 7.7	: Effect of neutral donors on the aggregation behavior of 0.05 M DNPPA in <i>n</i> -dodecane pre-equilibrated with different nitric acid solutions; temperature: 25 °C	161
Figure 7.8	: Absorbance spectra of 5×10^{-4} M DNPPA + 5×10^{-4} M Cyanex 923 solutions in <i>n</i> -dodecane pre-equilibrated with different nitric acid solutions	162
Figure 7.9 (a)	: Absorbance spectra of 5×10^{-4} M DNPPA + 5×10^{-4} M TBP solutions in <i>n</i> -dodecane pre-equilibrated with 0.1 -0.5 M HNO ₃	162
Figure 7.9(b)	: Absorbance spectra of 5×10^{-4} M DNPPA + 5×10^{-4} M TBP solutions in <i>n</i> -dodecane pre-equilibrated with 2- 8 M HNO ₃	163
Figure 8.1	: Absorption spectra of U-Br-PADAP complexes in PC88A+TOPO/Cyclohexane medium	169
Figure 8.2	: Calibration plot of determination of U(VI) in sulphate medium using Br-PADAP in 0.1M PC88A + 0.05M TOPO/Cyclohexane organic medium	172
Figure 8.3	: Effect of ethanol content in absorbance of U(VI)-Br-PADAP complexes in 0.1M PC88A+ 0.05M TOPO/cyclohexane medium	173

LIST OF TABLES

	Page No
Table 1.1 : Electronic configurations of actinide elements	17
Table 1.2 : Oxidation states of the actinides	19
Table 1.3 : Extractants employed in nuclear hydrometallurgy	32
Table 2.1 : Purity and yield obtained after purification of different batches of DNPPA	45
Table 2.2 : Major components of a typical raffinate solution (of uranium purification cycle)	49
Table 2.3 : ICP-AES analysis of a typical raffinate solution	50
Table 2.4 : Typical analysis of an ore leach solution containing large amount of impurities	50
Table 3.1 : Effect of various diluents on extraction of uranium; Extractant: 0.5 F PC88A; Aqueous phase: 0.1 M U(VI) at 4 M HNO ₃ ; Organic-to-aqueous phase ratio (O/A): 1; T: 298 K	66
Table 3.2 : Variation of D_U with nitric acid concentration; [U(VI)]: 2×10^{-3} M; Extractant(s): 3×10^{-2} M TBP, 3×10^{-2} F PC88A and their mixture in <i>n</i> -dodecane; T: 298 K	67
Table 3.3 : Variation of D_U with nitric acid concentration; [U(VI)]: 2×10^{-3} M; Extractant(s): 3×10^{-2} M TOPO, 3×10^{-2} F PC88A and their mixture in <i>n</i> -dodecane; T: 298 K	67

Table 3.4	:	Variation of D_U with nitric acid concentration; [U(VI)]: 2×10^{-3} M; Extractant(s): 3×10^{-2} M DOSO, 3×10^{-2} F PC88A and their mixture in <i>n</i> -dodecane; T: 298 K	68
Table 3.5	:	Variation of D_U with nitric acid concentration; [U(VI)]: 2×10^{-3} M; Extractant(s): 3×10^{-2} M MIBK, 3×10^{-2} F PC88A and their mixture in <i>n</i> -dodecane; T: 298 K	68
Table 3.6	:	Extraction of U(VI) from 0.4g/L uranyl nitrate raffinate at 1.12 M HNO ₃ by various extractants; Diluent: <i>n</i> -dodecane; T: 298 K	69
Table 3.7	:	Stripping of uranium from loaded organic phases using various strippants; Diluent: <i>n</i> -dodecane; T: 298 K	70
Table 3.8	:	Uranium recovery from different batches of uranyl nitrate raffinate (UNR) waste; Extractant: 1.1 M TBP/ <i>n</i> -dodecane; O/A: 1; T: 298 K	71
Table 3.9	:	Variation of D_U with nitric acid concentration; [U]: 2×10^{-3} M; Extractant(s): 2×10^{-2} M TBP, 2×10^{-2} M DNPPA and their mixture in <i>n</i> -paraffin; T: 298 K	77
Table 3.10	:	Variation of D_U with nitric acid concentration; [U]: 2×10^{-3} M; Extractant(s): 2×10^{-2} M TEHP, 2×10^{-2} M DNPPA and their mixture in <i>n</i> -paraffin; T: 298 K	77
Table 3.11	:	Variation of D_U with nitric acid concentration; [U]: 2×10^{-3} M; Extractant(s): 2×10^{-2} M Cyanex 923, 2×10^{-2} M DNPPA and their mixture in <i>n</i> -paraffin; T: 298 K	78

Table 4.1	:	Relation between $\log D_U$ and $\log [H^+]$ for the extraction of various concentrations of U(VI) with PC88A in <i>n</i> -dodecane	86
Table 4.2	:	$\log K_{ex}$ values at various uranium and H^+ concentrations, [Extractant]: 0.5 M PC88A/ <i>n</i> -dodecane; O/A: 1	87
Table 4.3	:	$\log K_{ex}$ values at various PC88A concentrations; [U(VI)]: 2×10^{-2} M; $[H^+]_i$: 3.0 M; O/A: 1	88
Table 4.4	:	Values of n , K and chi-square (χ^2) obtained by non-linear least square regression analysis of the extraction of different concentrations of uranium (C_i) from sulphate medium using 0.5 M PC88A in <i>n</i> -dodecane as the extractant, O/A: 1	89
Table 4.5	:	Values of n , K and chi-square (χ^2) obtained by non-linear least square regression analysis of the extraction of different concentrations of uranium (C_i) from sulphate medium using 0.5 M PC88A in <i>n</i> -dodecane as the extractant, O/A: 1	91
Table 4.6	:	Values of n and chi-square (χ^2) and $\log A$ obtained by non-linear regression analysis for extraction of U(VI)	95
Table 5.1	:	Separation factor (β) of U(VI), Th(IV) extracted from various concentration of nitric acid medium using 1.1M TEHP and TBP in <i>n</i> -paraffin; $[U]_{aq,in}$ or $[Th]_{aq,in}$: 2×10^{-3} M; T: 298 K	107
Table 5.2	:	Result of evaluation of separation factor (β) for U(VI), Th(IV) mixture under different aqueous phase acidity and at various TEHP concentrations; $[U]_{aq,in}$ or $[Th]_{aq,in}$: 2×10^{-3} M; Diluent: <i>n</i> -paraffin, T: 298 K	107

Table 5.3	: Maximum loading capacity of uranium at various concentrations of TEHP in <i>n</i> -paraffin; [HNO ₃]: 2 M; T: 298 K	108
Table 5.4	: Separation factors of U(VI), Th(IV) under various feed concentrations; Extractant: 0.2 M TEHP in <i>n</i> -paraffin; [HNO ₃]: 2M; T: 298 K	108
Table 5.5	: Separation factors of U(VI), Y(III) from nitric acid medium using and TBP in <i>n</i> -paraffin; [U] _{aq,in} or [Y] _{aq,in} : 2x10 ⁻³ M; T: 298 K	109
Table 5.6	: Separation of U(VI) from a mixture of U(VI), Th(IV) and Y(III) from nitric acid medium using TBP and TEHP; Diluent: <i>n</i> -paraffin; [U] _{aq,in} : 1g/L; [Th] _{aq,in} : 20g/L; [Y] _{aq,in} : 20g/L; [HNO ₃]: 2M; T: 298 K	110
Table 5.7	: Separation of U(VI) from multi component metal ion system using 1.1 M TEHP/ TBP in <i>n</i> -paraffin; U(VI) : 1x10 ⁻² M; [HNO ₃] : 4 M; T: 298 K.	111
Table 6.1	: Effect of carrier concentration on U(VI) transport from HNO ₃ medium using TEHP/ <i>n</i> -paraffin, U(VI): 2x10 ⁻³ M, Volume of feed & strip solutions: 25mL; Feed acidity: 4 M HNO ₃ ; Strippant: Distilled water; Stirring speed: 200 rpm	124
Table 6.2	: Variation of carrier (DNPPA) / <i>n</i> -paraffin concentration; U(VI): 2x10 ⁻³ M; Feed acidity 2 M HNO ₃ ; Receiver phase: 6 M H ₂ SO ₄ ; Duration: 4h	142
Table 6.3	: Comparison of diffusion coefficient $D_{(o)}$ of different metal ion extractant systems	144

Table 6.4	:	Synergistic transport of uranium using DNPPA and various neutral donors in presence of 2 M H ₂ SO ₄ as a receiver phase; [U(VI)]: 2x10 ⁻³ M; Feed acidity 2 M HNO ₃ ; Duration: 4 hour	148
Table 6.5	:	Viscosity and density measurements of different concentration of synergistic mixture containing 0.1M DNPPA and varying concentration of Cyanex 923 dissolved in <i>n</i> -paraffin	149
Table 6.6	:	Comparison of uranium transport with different synergistic solvent system	150
Table 6.7	:	Transport behavior of different metal ions present in a typical UNR solution at 1.1 M HNO ₃ employing various combinations of carrier and receiver phases; Diluent: <i>n</i> -paraffin; Duration: 4 hours; Stirring speed: 200 r.p.m.	151
Table 8.1	:	Metal tested for the ability to bind Br-PADAP	168
Table 8.2	:	Color Stability of U(VI)-Br-PADAP complex, λ _{max} : 576 nm	171
Table 8.3	:	Recovery study of the analytical technique on the basis of added/found concentration of uranium standards	174
Table 8.4	:	Effect of various ions on the determination of U(VI) concentration in ore leach solution; [U(VI)]: 200 µg mL ⁻¹	175
Table 8.5	:	Evaluation of relative standard deviation of the methods	176
Table 8.6	:	t and F- Test comparison of means from two (ICPAES and Br-PADAP) methods using a single ore leach solution	178
Table 8.7	:	Evaluation of detection limit of the method for measurement of uranium in ore-leach solution	179

Table 8.8	: Comparison of extraction spectrometric and ICPAES analysis of some typical ore leach solutions	180
Table 8.9	: Comparison of Br-PADAP method with the other existing methods	181

CHAPTER I

INTRODUCTION

1.1. India's Nuclear Power Programme

Dr. Homi Jehangir Bhabha, the founder of Indian Nuclear Programme, initiated the generation of nuclear power in three steps to meet India's energy demand [1]. (a) first stage: construction and operation of sufficient number of Pressurized Heavy Water Reactors (PHWRs) with natural uranium as fuel and associated fuel cycle facilities, (b) second stage: Fast Breeder Reactors (FBRs) using plutonium as fuel with thorium as blanket and backed by suitable reprocessing plants, and (c) third stage: two options are available, firstly construction of Advanced Heavy Water Reactors (AHWRs) with plutonium-thorium-uranium based fuel and secondly, construction of light water reactor with the help of ^{233}U generated for thorium blanket in the second stage.

India's primary energy consumption more than doubled between 1990 and 2012. India's dependence on imported energy resources and the inconsistent reform of the energy sector are challenges to satisfying rising demand. Electricity demand in India is increasing rapidly, and the 960 billion kilowatt hours gross produced in 2010 was more than triple the 1990 output, though still represented only some 750 kWh per capita for the year. The per capita electricity consumption figure is expected to double by 2020, with 6.3% annual growth, and reach 5000-6000 kWh by 2050, requiring about 8000 TWh/year then. There is an acute demand for more and more reliable power supplies. Nuclear power supplied 20 billion kWh (3.7%) of India's electricity in 2011 from 4.4 GWe (of 180 GWe total) capacities and after a dip in 2008-09 this is increasing as imported uranium becomes available and new plants become operative. Some 350 reactor-years of operation had been achieved by the end of 2011. India's fuel situation, with shortage of fossil fuels, is driving the nuclear investment for electricity, and 25% nuclear contribution is the ambition for 2050, when 1094 GWe of base-load capacity is expected to be required [3].

1.2. Nuclear Fuel Cycle and its Various Steps

It refers to the steps by which fissionable (for example ^{233}U , ^{235}U , ^{239}Pu) and fertile (for example, ^{238}U , ^{232}Th) materials are prepared for use in, and recycled or discarded after discharge from, the nuclear reactor. These steps include mining and milling of uranium or thorium bearing ores to form concentrates. **Figure 1.1** shows the different steps of a typical nuclear fuel cycle.

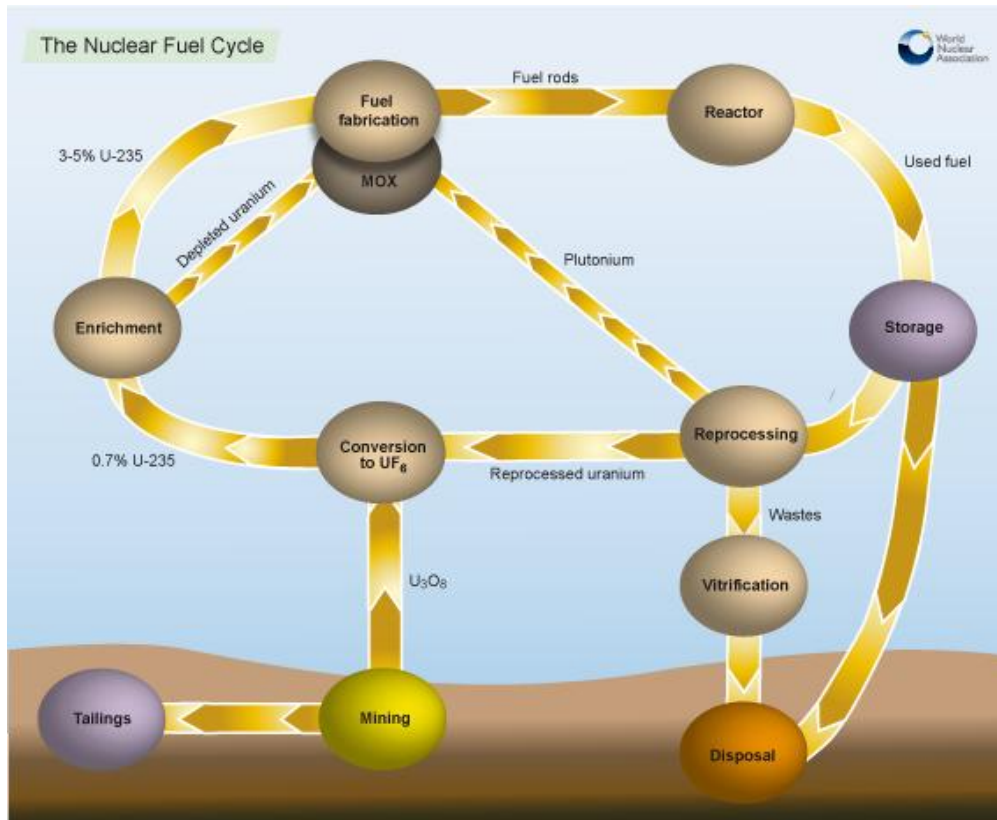


Figure 1.1. Various steps of a typical nuclear fuel cycle

The uranium concentrate is converted to the volatile uranium hexafluoride (UF_6) that is used in the separation of isotopes to produce uranium enriched in the fissile ^{235}U . Next step of the fuel cycle is the fabrication of the enriched uranium into fuel assemblies. After the fuel has liberated the desired amount of heat in the reactor, the spent fuel assemblies are reprocessed to separate the remaining fissionable and fertile material (uranium and plutonium) from the nuclear wastes. Finally, waste management includes the treatment, storage, and disposal of radioactive wastes

from the many other parts of the fuel cycle. The fuel cycle for a thorium based reactor requires, in addition to the uranium fuel cycle steps outlined above, the mining, milling, and purification of thorium and the reprocessing of thorium containing fuel into its components, which include unused thorium, uranium in the form of fissionable ^{233}U , and nuclear waste.

1.3. Uranium

A chemical element, symbol U, atomic number 92, atomic weight 238.03; one of the elements of actinide series, in which the 5f shell is being filled. The name is derived from the planet Uranus. The valence electron configuration is $[\text{Rn}] 5f^3 6d^1 s^2$. Uranium was isolated in 1789 by Martin Heinrich Klaproth in a sample of pitchblende from Saxony [4]. In 1896, Antoine-Henri Becquerel discovered that uranium undergoes radioactive decay. Discovery of the nuclear fission phenomenon by Otto Hahn and Fritz Strassmann in 1939 vaulted uranium from a position of relative obscurity to a role of major importance. Uranium in nature is a mixture of three isotopes: ^{234}U (0.00054%), ^{235}U ($0.72 \pm 0.030\%$), and ^{238}U (99.275%). These values may vary somewhat, depending on the origin or on the degree of depletion of the sample [5]. Half-lives of the three isotopes are $(2.446 \pm 0.007) \times 10^5$ years (^{234}U), $(7.038 \pm 0.005) \times 10^7$ years (^{235}U), and $(4.4683 \pm 0.0024) \times 10^9$ years (^{238}U). ^{235}U , which was discovered by A. J. Dempster in 1936, undergoes fission with slow neutrons to release large amounts of energy. ^{238}U absorbs slow neutrons to form ^{239}U , which in turn decays to fissile ^{239}Pu by the emission of two beta particles. Other isotopes of uranium ranging in mass from ^{226}U to ^{240}U have been prepared by radioactive processes. Among these, fissile ^{233}U is obtained by the irradiation of natural thorium with neutrons. ^{232}Th , the major component in natural thorium, absorbs slow neutrons to form ^{233}Th , which decays to fissile ^{233}U by the emission of two beta particles [6].

1.3.1. Natural occurrence of uranium

Uranium is believed to be concentrated largely in the Earth's crust, where the average concentration is 4 parts per million (ppm). For comparison, the crust contains 0.1 ppm silver and 0.5 ppm mercury. Basic rocks (basalts) contain less than 1 ppm uranium, whereas acidic rocks (granites) may have 8 ppm or more. Estimates for sedimentary rocks are 2 ppm, and for ocean water 0.0033 ppm. The total uranium content of the Earth's crust to a depth of 25 km is calculated to be 4.5×10^{17} kg; the oceans may contain 4.5×10^{13} kg of uranium [7]. Several uranium-containing minerals have been identified, but only a few are of commercial interest. Uraninite, as found in pegmatites, usually occurs in rather small amounts which are of little economic significance. The euxenite-polycrase series, brannerite, and davidite are complex pegmatitic minerals. Pitchblende, a variety of uraninite found in hydrothermal veins, is the most important mineral of uranium. It is usually poorly crystalline, contains very little thorium or rare earths, and is frequently found associated with sulfide minerals. Coffinite, first identified in 1951, is recognized as an important mineral on the Colorado Plateau. Prior to 1942, uranium was obtained principally as a by-product of radium mining operations. With the discovery of nuclear fission and the potential of atomic power, the possession of uranium reserves became vitally important. Uranium reserves containing more than 1 g U_3O_8 /kg of ore, for that part of the world for which statistics are available, are estimated at about 2.2×10^9 kg U_3O_8 , and those of the United States are about 10^9 kg U_3O_8 . Deposits containing as little as 0.1% uranium are being mined [8-11]. Some of the largest occurrences are the sandstone-impregnated Colorado Plateau deposits, the Blind River conglomerates (Ontario, Canada), and the reefs of the Witwatersrand (South Africa), from which uranium is produced as a by-product of the gold industry. The vein deposits at Great Bear Lake (Northwest Territories, Canada) and Lake Athabasca (west-central

Canada) are also important sources of uranium, but the Shinkolobwe, Zaire, deposits are virtually exhausted. An interesting deposit is the one at Oklo, Gabon, where in primordial times a spontaneous fission chain reaction occurred which caused a shift in the isotopic composition of the uranium in the deposit. In addition to the occurrence mentioned, extensive reserves of low-grade ore (0.005 to 0.02% uranium) exist in phosphate deposits (Florida, Brazil, Soviet Union, and North Africa), in bituminous shales (Soviet Union, Sweden, and Tennessee), and in lignites (the Dakotas) [12].

In India, the major uranium deposit sites are: a) Jaduguda, b) Bhatin, c) Narwapahar, d) Turamdih, e) Mohuldih and f) Bagjata, located in eastern region. In addition to that 14 middle Proterozoic basins have been identified since 1990 which are expected to possess geological settings conducive to host this type of deposit. These are: 1. Kadapah (Tummalapalle), 2. Bhima, 3. Kaladgi, 4. Pakhal, 5. Ampani, 6. Indravathi, 7. Kharihar, 8. Amhujmar, 9. Chhattisgarh, 10. Khairagarh, 11. Vindhyan, 12. Delhi, 13. Kunjar and 14. Shillong. Out of these 4-5 Proterozoic basins have been identified to have high grade in nature. These are: 1. Kadapah basin (Andhra Pradesh), 2. Shillong basin (Meghalaya), 3. Kunjar basin (Orissa), 4. Vindhyan basin (Madhya Pradesh) and 5. Delhi-Aravalli basin (Rajasthan). Further, the deposit of Tummalapalle is lower grade (~0.042 % U_3O_8) but reasonably large reserve and it is confined in the host rock of alkali (dolomite and calcite).

1.3.2. Metallurgical extraction of uranium

These are well defined areas of uranium hydrometallurgy where solvent extraction as well as membrane separations play an important role in: (i) the recovery of uranium from low grade ores and production of a concentrate called a yellow cake, (ii) the refining of uranium from the yellow cake to nuclear purity grade, and (iii) the recovery of uranium as by product from the industrial

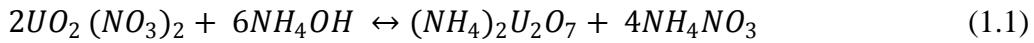
wet phosphoric acids. Uranium production is generally carried out from its ores such as pitchblend ($x\text{UO}_2.y\text{UO}_3$, carnotite ($\text{K}_2\text{O}.2\text{UO}_3.V_2\text{O}_5.x\text{H}_2\text{O}$), autunite ($\text{CaO}.2\text{UO}_3.\text{P}_2\text{O}_5.x\text{H}_2\text{O}$, etc [13]. Secondary resources of uranium include rock phosphate, monazite, xenotime, coal ash, copper tailing and sea water. Phosphate rocks contain roughly 0.1 to 0.2 kg U_3O_8 /tonne. This concentration seems to be unsuitable for exploration as an ore. Fortunately all the phosphate rock has to be processed by fertilizer industries, and uranium will be available as a by-product. The world production of phosphate rock is almost 140 million tonnes per year, which contains nearly 12000 tonnes of U_3O_8 per year. In USA, almost 25 % demand of U_3O_8 was met by processing of this particular resource [14]. Uranium recovery from ores is achieved invariably by hydrometallurgy. Most of the ores of low grade contain 1-5 kg U_3O_8 per tonne. The mined ore is concentrated in uranium mills by a chemical process, which depends on the nature of the ore. Ores with large amounts of calcium carbonate are leached with sodium carbonate to dissolve uranium or they are leached with sulphuric acid. Acid leaching is the most commonly used technique for recovery of uranium from the ground ores. The leach liquor after filtration is used for the production of uranium concentrate. Of the various methods for treating acid and alkaline solutions of uranium in order to obtain the concentrates, two well established techniques, are ion-exchange and solvent extraction. For purification of uranium from leach solutions, use of DAPEX process or AMEX processes are only of historical importance [15]. The recovery of uranium from wet phosphoric acid (WPA) is important not only for production of uranium as a by-product for nuclear industry, but also for preventing its spread with fertilizer in to the food chain. Several reports are available for recovery of uranium from wet phosphoric acid (WPA) using solvent extraction as well as supported liquid membrane (SLM) [16-19]. A synergistic mixture of 0.5 M di (2-ethyl hexyl) phosphoric acid (D2EHPA) and 0.125 M tri-*n*-octyl

phosphine oxide (TOPO) dissolved in kerosene has been used to separate uranium from phosphoric acid [16]. Recently Singh et al. have reported the recovery of uranium from phosphoric acid using novel synergistic solvent di nonylphenyl phosphoric acid (DNPPA) and neutral donors such as TOPO, tri-*n*-butyl phosphate (TBP), TRPO (a mixture of four trialkyl phosphine oxides viz. R_3PO , $R_2R'PO$, RR'_2PO and R'_3PO where R: *n*-octyl and R': *n*-hexyl chain)[17-19]. The uranium from organic phase was stripped back using ammonium carbonate solution [20]. Separation of uranium from phosphoric acid has also been carried out using supported liquid membrane where various extractants such as D2EHPA, 2-ethyl hexyl phosphonic acid 2-ethyl hexyl monoester (PC88A), bis (2,4,4-trimethylpentyl) phosphonic acid (Cyanex 272) either along or mixed with various neutral donors were used in membrane phase and polytetrafluoroethylene (PTFE) membrane were used as solid support [21-25]. Uranium was precipitated with ammonium carbonate as ammonium uranyl carbonate (AUC), which is calcined to produce 98 % U_3O_8 . Most commonly route of uranium recovery from ore leach solution is the ion exchange followed by precipitation with magnesium oxide (formation of magnesium di uranate called yellow cake). The yellow cake, so produced is further refined using TBP process to give nuclear grade uranium. From the pure uranyl nitrate, uranium oxide, uranium fluoride or uranium metal can be obtained. The oxide is used as fuel in power reactors and metal for research reactors while fluoride for enrichment respectively. The use of TBP, TOPO, D2EHPA, dibutyl butyl phosphonate (DBBP), dioctyl phenyl phosphoric acid (DOPPA) etc have been well established for purifying uranium from various sources [26]. Extraction of uranium with D2EHPA and Cyanex 272 has also been studied both from the view points of understanding of the mechanism of extraction and application to practical problems [27,28]. Synergistic extraction of U(VI) and

Th(IV) has been investigated using the mixture of PC88A and micelles of di nonyl naphthalene sulphonic acid (HDNNS) [29].

1.3.3. Uranium metal preparation and its properties

Uranium is a very dense, strongly electropositive, reactive metal; it is ductile and malleable, but a poor conductor of electricity. It is most conveniently prepared by the reduction of a halide (UF_4) with calcium or magnesium in a sealed bomb at 1200-1400°C (2190-2550°F) [7,30]. The steps involved in preparation of the metal from uranyl nitrate are summarized by reactions (1.1)-(1.5).



Uranium metal exists in three crystalline modifications: (a) uranium (25-668°C or 68-1234°F) is orthorhombic, with four atoms per unit cell, and density of 19.04 g/cm³. Its structure is interpreted as a distorted hexagonal lattice containing corrugated sheets of uranium atoms; (b) The beta phase (668-775°C or 1234-1427°F) is a complex tetragonal structure, with 30 atoms per cell, and a density of 18.13 at 720°C (1328°F); and (c) Uranium (775-1132°C or 1427-2070°F) is body-centered cubic, with two atoms per cell, and density of 18.06 g/cm³ at 805°C (1481°F) [7]. The beta phase can be stabilized at room temperature by addition of small amounts of chromium, the gamma form with molybdenum. The unique nature of the room-temperature gamma structure curtails solid solution of uranium with many metals. Aluminum, beryllium, bismuth, cadmium, cobalt, gallium, germanium, gold, indium, iron, lead, manganese, mercury, nickel, tin, titanium,

zinc, and zirconium can form one or more inter-metallic compounds with uranium [12]. Chromium, magnesium, silver, tantalum, thorium, tungsten, and vanadium, as well as calcium, sodium, and some of the rare-earth metals, form neither compounds nor extensive solid solutions. Many uranium alloys are of great interest in nuclear technology because the pure metal is chemically active and anisotropic and has poor mechanical properties. However, cylindrical rods of pure uranium coated with silicon and canned in aluminum tubes (slags) are used in production reactors. Uranium alloys can also be useful in diluting enriched uranium for reactors and in providing liquid fuels. Uranium depleted of the fissile isotope ^{235}U has been used in shielded containers for storage and transport of radioactive materials. Uranium reacts with nearly all nonmetallic elements and their binary compounds. Uranium dissolves in hydrochloric acid to leave a black residue of uranium hydroxy hydride. Addition of fluorosilicate prevents formation of this residue. Nitric acid dissolves the metal, but non-oxidizing acids, such as sulfuric, phosphoric, or hydrofluoric acid, react very slowly. Usually a trace of mercuric nitrate tends to catalyze the dissolution. Uranium metal is inert to alkali metals, but addition of peroxide causes formation of water-soluble peruranates.

1.5. Thorium

It was discovered by J. J. Berzelius in 1828. However, little use was found for thorium before the development of the incandescent gas mantle by C. A. von Welsbach in 1885. Thorium has an atomic weight of 232. The metal has a density of 11.7 g/cm^3 . Good-quality thorium metal is relatively soft and ductile. It can be shaped readily by any of the ordinary metal-forming operations. It must be protected, however, to prevent oxidation in treatments involving high temperatures. The massive metal is silvery in color, but it tarnishes on long exposure to the atmosphere; finely divided thorium has a tendency to be pyrophoric in air. The atoms of thorium

in the metal are arranged in a face-centered cubic system at all temperatures below 1400°C (2600°F). On heating, the atoms rearrange at this temperature into a body-centered cubic pattern which is stable up to the melting temperature. However, the temperature at which pure thorium melts is not known with certainty; it is thought to be not far from 1750°C (3200°F). Thorium is a member of the actinide series of elements, which includes protactinium, uranium, and the synthetic trans-uranic elements. It is radioactive with a half-life of about 1.4×10^{10} years. It is the first member of the radioactive decay series which in a chain of 10 successive disintegrations finally terminates as ^{208}Pb . All of the nonmetallic elements, except the rare gases, form binary compounds with thorium. Binary inter-metallic compounds have been reported for thorium with beryllium, magnesium, boron, aluminum, and silicon, and with all of the metallic elements in the three long periods of the periodic chart in groups positioned to the right of the manganese group [31,32]. However, a number of the inter-metallic compounds of thorium, especially those with copper, silver, and gold, are quite pyrophoric. A study of the binary alloy systems formed by thorium metal and metals of the scandium, titanium, vanadium, and chromium groups, including the rare earths, shows no evidence of inter-metallic compound formation.

1.5.1. Natural occurrence of thorium

Monazite, the most common and commercially important thorium-bearing mineral, is widely distributed in nature. Important deposits occur along the shores of India, Brazil, and Srilanka. Other extensive deposits of monazite are found in South Africa, Russia, Scandinavia, and Australia. Sources in the United States include deposits in Florida, Idaho, and the Carolinas. Monazite is chiefly obtained as sand, which is separated from other sands by physical or mechanical means, following dredging operations [33]. The monazite sand concentrate is essentially an orthophosphate of rare-earth elements, and generally contains 3-10 % ThO_2 [2].

Other thorium-bearing minerals of lesser importance include thorite, thorianite, and uranothorite [34-36].

1.5.2. Recovery of thorium from monazite

Processes for thorium recovery generally start by digestion of the monazite sand with either hot concentrated sulfuric acid or hot concentrated caustic soda (**Figure 1.2 and 1.3**). Subsequent chemical treatments, varying greatly even with the same initial treatment, yield a concentrate of impure thorium. This impure concentrate may be further treated by a liquid-liquid extraction process to yield high-purity thorium [37, 38].

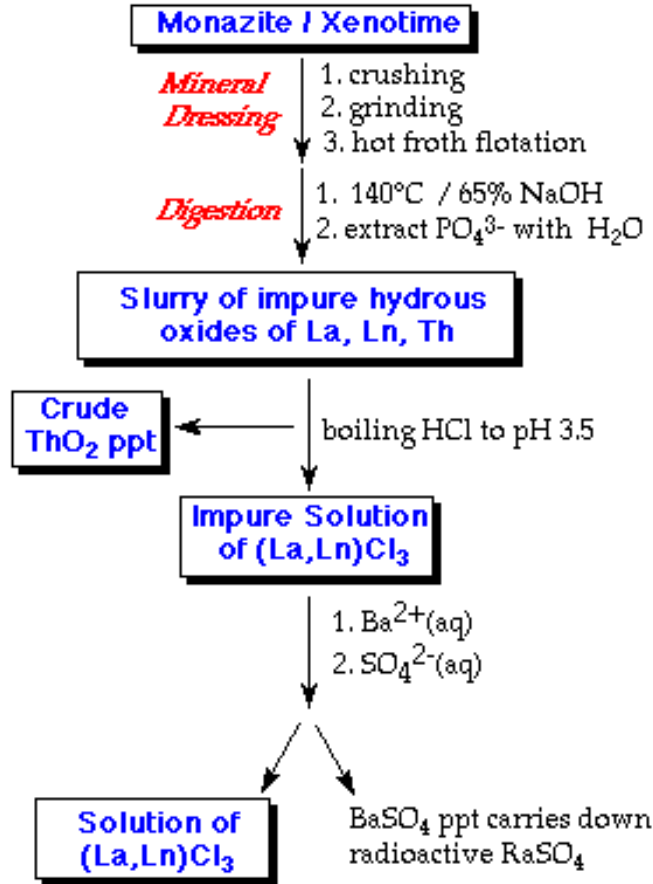


Figure 1.2. Alkali digestion process flow-sheet of Monazite/Xenotime [39]

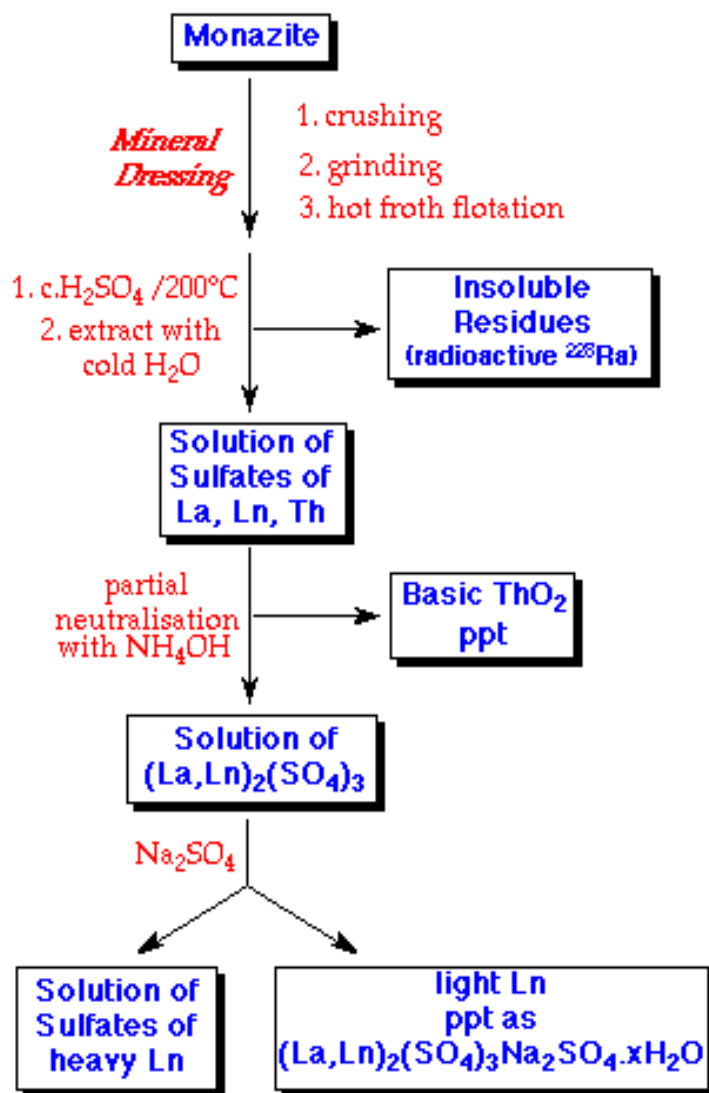


Figure 1.3. Acid digestion process flow-sheet of Monazite/Xenotime [39]

For a system consisting of water, TBP, nitric acid, thorium, and the associated impurities, an extractor can be set up to remove thorium with the water-immiscible TBP phase, while the impurities are carried away in the aqueous phase. Generally, the purified thorium is back-extracted to an aqueous solution and either crystallized from solution as the nitrate or precipitated as the oxalate. From these pure salts, the oxide or other compounds of thorium can be prepared. Because thorium is quite reactive, some difficulty is experienced in preparing thorium metal. Only by electrolysis or by treatment with elements high in the electromotive force

series (the alkali and alkaline-earth metals) has good-quality thorium metal been satisfactorily prepared directly from its compounds. The calcium reduction of ThO_2 has been widely used for many years to prepare thorium metal [32]. In this process, granular calcium metal is mixed with thorium oxide and charged into a lined iron crucible which is then filled with an inert gas and heated to almost 1000°C (1830°F) to form thorium metal powder and calcium oxide. After cooling to room temperature, the thorium powder is recovered by leaching and then drying. Powder metallurgy techniques are employed to obtain massive metal. The electro-deposition of thorium from a bath, consisting of thorium chlorides or fluorides dissolved in fused alkali halides, yields granular thorium which may be pressed and sintered to give massive pieces of ductile metal. Large-scale production of thorium metal has been carried out by a bomb process [40-42]. The charge, consisting of a mixture of thorium tetra-fluoride, granular calcium metal, and zinc chloride, is placed in a refractory-lined vessel that is closed by a lid. The charged bomb is placed in a furnace held at about 650°C (1200°F) where, after several minutes, the charge ignites spontaneously and the resulting reaction yields a slag of calcium fluoride and calcium chloride and an alloy of thorium and zinc. The temperature reached by the reaction in the charge is sufficient to melt the products, and the thorium-rich alloy collects as a molten pool under the liquid slag. The bomb is allowed to cool, and then the solid piece of thorium alloy is removed and cleaned of adhering slag. Next, the zinc is removed by heating the alloy in a vacuum at a temperature of 1100°C (2000°F), leaving the thorium metal as a sponge. Solid ingots of thorium metal are prepared by vacuum-induction-melting the sponge in a crucible or by shaping the sponge in the form of bars and melting these by consumable electrode arc melting. Good-quality thorium metal can be readily worked to shape by standard methods of fabrication.

1.5.3. Uses of thorium

For many years, thorium oxide has been incorporated in tungsten metal, which is used for electric light filaments; also small amounts of the oxide have been found to be useful in other metals and alloys [42]. The oxide is employed in catalysts for the promotion of certain organic chemical reactions. Thorium oxide has special uses as a high-temperature ceramic material. The metal or its oxide is employed in some electronic tubes, photocells, and special welding electrodes. The metal can serve as a getter in vacuum systems and in gas purification and it is also used as a scavenger in some metals. Because of its high density, chemical reactivity, mediocre mechanical properties, and relatively high cost, thorium metal has no market value as a structural material. However, many alloys containing thorium metal have been studied in some detail and thorium does have important applications as an alloying agent in some structural metals. Perhaps, the principal use for thorium metal beyond its use in the nuclear field, is in magnesium technology. Approximately 3 % thorium, added as an alloying ingredient, imparts to magnesium metal high-strength properties and creep resistance at elevated temperatures. The magnesium alloys containing thorium, because of their light weight and desirable strength properties are being used in aircraft engines and in airframe construction. Thorium can be converted in a nuclear reactor to ^{233}U , an atomic fuel. The system of thorium and ^{233}U gives promise of complete utilization of all thorium in the production of atomic power. The energy available from the world's supply of thorium has been estimated as greater than the energy available from all of the world's uranium, coal, and oil combined [43].

1.6. Chemist's Role in Nuclear Fuel Cycle

The fuel cycle is made up of a series of processes that manufacture reactor fuel, burn the fuel in a reactor to generate electricity, and manage the spent reactor fuel (**Figure 1.1**). These processes

are grouped into three steps; (i) the front end, which includes all activities prior to placement of the fuel in the reactor, (ii) the service period, when the fuel is converted into energy in the reactor, and (iii) the back end, which covers all activities dealing with spent fuel from the reactor. If the spent fuel is sent to storage, the cycle is referred to as open. If it is reprocessed to recover useful components, it is known as closed. The recovery of nuclear fuel materials such as uranium and thorium from the ore to the fuel repressing, the role of a chemist is tremendously important. Every step of nuclear fuel cycle has associated with lot of chemistry involvements form dissolution, separation, purification to waste management.

1.7. The Actinide Elements

The 14 elements which follows the properties of actinium ($Z = 89$) are called as actinide elements. It forms a separate series in the periodic table called actinide series. In this series, with increasing atomic number the added electron go into the internal 5f orbital. Hence they are alternatively termed as inner transition elements or **5f** elements [44]. Most of the members of this group are synthesized and all of their isotopes are radioactive [45]. They form unique class because of their unique physical and chemical properties and have great similarity with analogous **4f** series, the lanthanides. The actinide elements (such as U, Pu, and Th) play an important role in the nuclear industry and modern inorganic chemistry because of their interesting nuclear and chemical properties.

1.7.1. Electronic configuration

The electronic structure of the elements in the series is presented in **Table 1.1**. Evidences suggest that the **5f** electron shell is undergoing filling similar to **4f** series in the lanthanide group. Hence

Table 1.1. Electronic configurations of actinide elements

Atomic Number	Symbol	Elements Name	Electronic structure [Rn core ⁺]
89	Ac	Actinium	6d ¹ 7s ²
90	Th	Thorium	6d ² 7s ²
91	Pa	Protactinium	5f ² 6d ¹ 7s ²
92	U	Uranium	5f ³ 6d ¹ 7s ²
93	Np	Neptunium	5f ⁵ 7s ²
94	Pu	Plutonium	5f ⁶ 7s ²
95	Am	Americium	5f ⁷ 7s ²
96	Cm	Curium	5f ⁷ 6d ¹ 7s ²
97	Bk	Berkelium	5f ⁸ 6d ¹ 7s ² /5f ⁹ 7s ²
98	Cf	Californium	5f ¹⁰ 7s ²
99	Es	Einsteinium	5f ¹¹ 7s ²
100	Fm	Fermium	5f ¹² 7s ²
101	Md	Mendelevium	5f ¹³ 7s ²
102	No	Nobelium	5f ¹⁴ 7s ²
103	Lr	Lawrencium	5f ¹⁴ 6d ¹ 7s ²

the elements of two series have similarities in their chemical behavior. Still the relatively low binding energy and less effective shielding of the **5f** electrons by the outer orbitals of the actinides as compared to the **4f** electrons of the lanthanides, make important differences between the two series. For the early members of the actinide series, the electron prefer **6d** orbitals as the

5f and **6d** orbital have comparable energies. With increasing atomic number, the **5f** level becomes progressively lower in energy and the electron starts entering the **5f** orbital [46]. The series begins after the element actinium, and the first of the fourteen **5f** electrons are added formally through not necessary – from thorium ($Z = 90$). For uranium and succeeding members, the **5f** electrons are present and shell is completed with the element lawrencium ($Z= 103$). Similar to the lanthanide series of elements, actinides also show a significant and steady decrease in the size of their atoms and ions with increasing atomic number. This actinide contraction is due to the increase in effective nuclear charge on the **5f** electrons as the series proceeds, causing a reduction in the size of the atomic and ionic radii.

1.7.2. Oxidation states

Redox chemistry of the actinide elements is extremely complicated [47]. The most common and dominant oxidation state of the elements, Am and beyond in the series is +3. The elements, specially the earlier members, show multiple oxidation states ranging from +2 to +7 in solution. On going down the series, the increase in nuclear charge caused a successive contraction. The shell will be better shielded from the field of neighboring atoms and the energy difference between the **5f** and the outer orbital will grow. As a consequence the participation of the **5f** electrons in bonding becomes more difficult, resulting in a very marked stabilization of the trivalent oxidation state for the heavier actinides [48]. The oxidation numbers of the elements are given in **Table 1.2**. The redox potential diagrams of early actinides such as U, Np and Pu at 25°C in 1M HClO₄ are shown in **Figure 1.4**. It has been found that the M^{3+}/M^{4+} and MO_2^+/MO_2^{2+} couples are reversible and fast as they involve the transfer of only single electron. On the other hand, the other couples are irreversible and achieve equilibrium slowly as they involve the formation or rupture of metal oxygen bonds. The solution chemistries and oxidation–reduction

potentials are further complicated by the formation in presence of ions other than perchlorate, of cationic, neutral or anionic complexes.

Table 1.2: Oxidation states of the actinides

89	90	91	92	93	94	95	96	97	98	99	100	101	102	103
Ac	Th	Pa	U	Np	Pu	Am	Cm	Bk	Cf	Es	Fm	Md	No	Lr
						(2)		(2)				(2)	(2)	
3	3	3	3	3	3	3	3	3	3	3	3	3	3	3
	4	4	4	4	4	4	4	4						
		5	5	5	5	5								
			6	6	6	6								
				7	7									

Red numbers refer to the most stable oxidation states; Blue numbers in parantheses refer to the oxidation states which are not known in solution

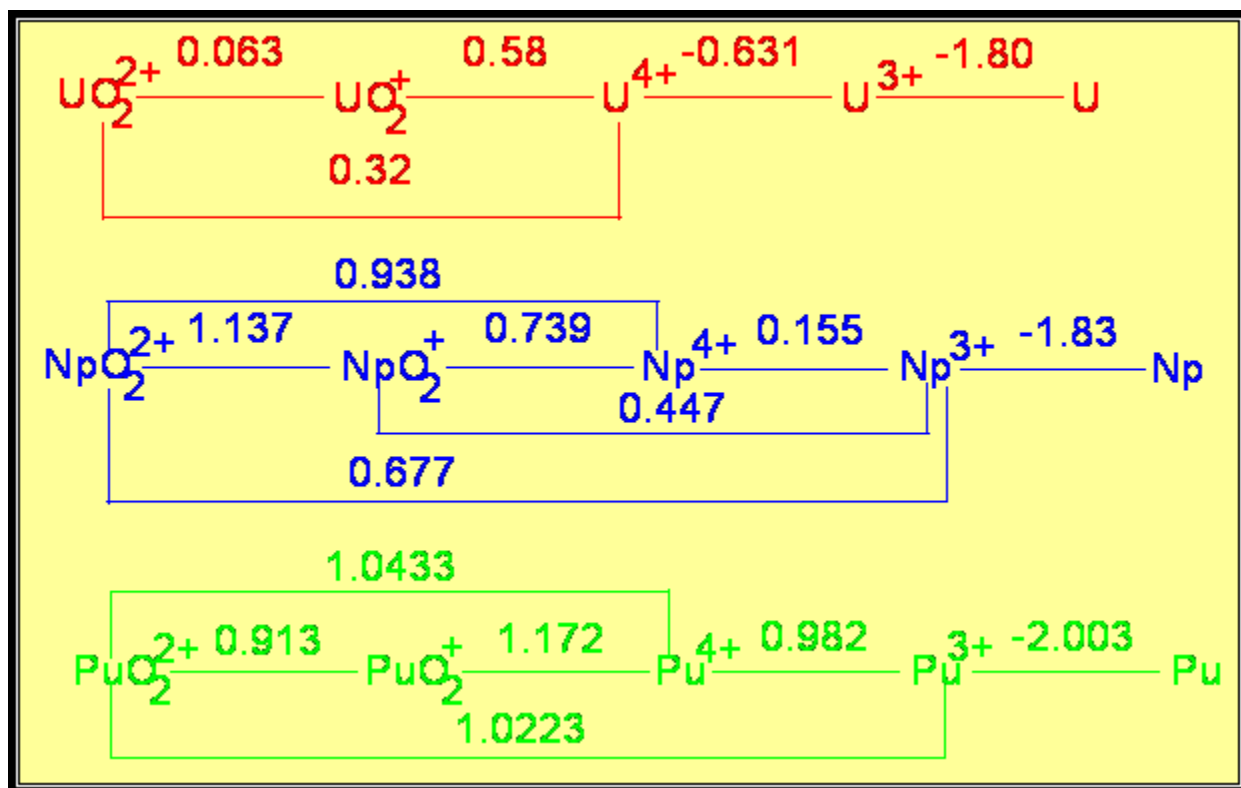


Figure 1.4. Redox potential of actinide ions in 1M HClO₄ (Volts)

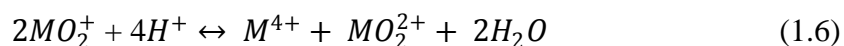
1.7.3. Complexes and stereochemistry

The actinides have a far greater tendency to form complexes than their analog lanthanides. There are extensive series of complexes with oxo anions of all types (RCOO^- , NO_3^- , SO_4^{2-} , CO_3^- , $\text{H}_n\text{PO}_{4-3}^{+n}$, $\text{C}_2\text{O}_4^{2-}$, where R is the alkyl group), halide ions, BH_4^- , and other ligands, especially chelating ones. A vast amount of data exist on complex formation in solution, since this has been of primary importance in connection with solvent extraction, ion exchange behavior, and precipitation reaction involved in the technology of actinide separation and purification. The general tendency to complex ion formation decreases in the direction controlled by factors such as ionic size and charge, so that order is generally $\text{M}^{4+} > \text{MO}_2^{2+} > \text{M}^{3+} > \text{MO}_2^+$. For anions the order of complexing ability is generally: uni-negative ions, $\text{F}^- > \text{NO}_3^- > \text{Cl}^- > \text{ClO}_4^-$; bi-negative ions, $\text{CO}_3^{2-} > \text{Ox}^{2-} > \text{SO}_4^{2-}$, where Ox^{2-} indicate oxalate ion. There are many actinide nitrate complexes which are important in separation procedure whereby the elements are extracted from aqueous nitric acid in to non polar solvents. Of these, the UO_2^{2+} complexes are best characterized; they are typically 8-coordinated with two bi dentate NO_3^- ions and two neutral ligands (H_2O , tetra hydro furan (THF), di methyl sulphoxide (DMSO), and tri alkyl phosphine oxide (R_3PO)) forming a distorted equatorial hexagon [47, 48]. Because of enormous variety of ligands that form actinides complexes and the number of oxidation states, the stereochemistry found in complexes and compounds of actinides is extraordinary. The relatively large size of actinide ions coupled with the high electrostatic attraction due to formal charges of + 3 to + 6, all lead to the higher coordination numbers, specially 8 and 9, are very common. For the + 3 oxidation state, where there is much resemblance to the lanthanides, octahedral coordination is often found along with coordination number 9. Eight coordination number is very common for the +4 oxidation state. In the +5 oxidation state the AnF_8^{3-} ion afford rare examples of discrete

cubic coordination. In oxidation +6, the hexafluoride are strictly octahedral. The stereochemistry of the MO_2^{2+} complexes varies considerably. Thus for uranium the O=U=O unit can have 4-6 ligand atoms in, or close to, the equatorial plane, giving tetragonal, pentagonal, or hexagonal bipyramidal coordination. The 6 coordinated species are least common and 8-coordinated species most numerous. The latter commonly have an essentially flat equatorial six-member ring as in $UO_2(NO_3)_2(OPPh_2)_2$, but puckered ring are also formed.

1.7.4. Disproportionation

In aqueous solutions the cationic species of the actinide elements, particularly uranium, plutonium, neptunium and americium can co-exist in appreciable concentration, at different oxidation states. Due to the closeness of the redox potentials of different oxidation states, they can undergo self oxidation- reduction. This is called disproportionation reaction. For example, all the four oxidation states of plutonium, ranging from + 3 to + 6 co-exist in acidic solutions under the same experimental conditions [45]. The disproportionation equilibrium for the MO_2^{2+} ion (M = U, Pu, Np or Am) in acidic medium can be represented as,



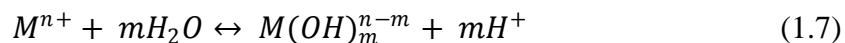
For U the equilibrium constant (K) of the above reaction is 1.7×10^7 .

1.7.5. Hydrolysis and polymerization

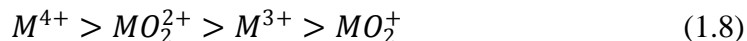
Hydrolysis is a complex formation reaction where the hydroxide ion serves as the ligands. However, this is generally considered as a separate process because it can lead to precipitation or formation of polymeric species or both. The oxidation number and the radius of metal ion are the important factors for determining the hydrolysis of a hydrated metal ion. High oxidation number favors an extensive hydrolysis while the large radii of the ions make them less prone to

hydrolysis. The extent of hydrolysis of the ions also depends on the parameters such as pH, concentration of actinide ions, temperature, presence of complexing ligands etc.

The equilibrium can be represented by the equation,



The degree of hydrolysis for a given actinide follows the order:



Polymerization can be suppressed by the presence of complexing ions.

1.7.6. Atomic spectra

The ionic solution of the actinide elements possesses characteristic absorption bands in the near ultra violet, visible and near infrared regions. The bright colors exhibited by their solutions are because of the selective absorption of visible light by the species. There are three different types of electronic transitions causing the absorption for the actinides [49]. In the first type, the transition takes place between two **f** levels within inner electron orbital. As the electron occupying higher orbitals largely screen the inner orbitals, the absorption bands are narrow and relatively unaffected by the influence from the environment. This type of transition is Laporte forbidden and the absorption bands are not very intense with low molar absorptivity. Electronic transition can also occur between the **5f** and **6d** orbitals of the ions. Since the outer shell is also involved, the environment influences the transitions of this type and the bands are broad. The absorption is intense with molar absorptivity over 1000 L.mol⁻¹ cm⁻¹. The third type of absorption is the charge transfer where the electronic transition is occurring between the **5f** shell of the metal ion and the orbitals of the coordinated ligands. The characteristic color of many actinide complexes in solution are generally due to the charge transfer absorption bands. The transitions depend on the electronic configuration of the ligands also and its spectra are affected

by the environmental influences leading to broad bands. For analytical purpose, the species which exhibit charge transfer absorption are very important due to high molar absorptivity ($\epsilon_{\max} > 10000 \text{ L mol}^{-1} \text{ cm}^{-1}$) [50]. The spectra provide highly sensitive means for detecting and determining the absorbing species.

1.8. Separation Methods

1.8.1 Solvent extraction

Separation of a metal ion or a compound from a mixture of components is very old problem in science. Different separation techniques applied for selective recovery of a component depends upon their various properties. Recovery of metal ion from an aqueous phase can be carried out by precipitation, crystallization, evaporation and solvent extraction. Solvent extraction name itself implies the phenomena of transfer of solute (metal ions) from one phase (generally aqueous phase) to another immiscible phase (organic phase). Due to the process simplicity, easy operation, large scale operation and high efficiency solvent extraction gets wide applicability in separation industry. In 1872 Berthlot [51] first enunciated a law governing the distribution of a metal species between two immiscible phases. Since then the theory and the technique of solvent extraction has progressed step by step along with the advantages in the knowledge of solution chemistry and complexing behavior of metal ions. The application of solvent extraction in hydrometallurgy as a viable technique commenced mainly due to the demand for effective beneficiation of low grade ores of copper and uranium. The major thrust for this technique and its use in large scale separations has come from the nuclear industry [52]. This technique now finds wide spread for commercial applications in the recovery of several metal such as copper, nickel, cobalt, uranium, vanadium, molybdenum, tungsten, zinc, rare earths, platinum group metals, tantalum/niobium, zirconium/hafnium etc. [53-57]. Approximately, 25,000 tonnes of

uranium and 200,000 tonnes of copper are being processed per year by solvent extraction. The successful application of solvent extraction in hydrometallurgy for this purpose has stimulated studies of new types of extractants and equipment to suit specific needs.

1.8.1.1. Solvent extraction equilibria and distribution ratio (D)

The solvent extraction principle is based on the Nerst Distribution law according to the law if $[A]_{org}$ and $[A]_{aq}$ the concentrations of a solute distributed between two immiscible solvents (organic and aqueous) at constant temperature and pressure the ratio of activities of the solute in two phases is constant. For simplicity, if we consider one phase is aqueous and another is organic, the equilibrium of solute A in two phases could be represented as



The distribution coefficient is defined as the ratio of activity of the solute A in organic phase to activity of solute A in aqueous phase. But determination of the activity of a solute is often difficult, and hence the activity terms are replaced by more general term concentration and distribution coefficient become distribution ratio (D).

$$D = \frac{[A]_{org}}{[A]_{aq}} \quad (1.10)$$

The distribution ratio unlike distribution coefficient depends on various parameters like temperature, pressure, phase ratio, metal ion concentration in aqueous phase etc.

1.8.1.2. Percentage extraction, % E

For practical purpose as in industrial application, it is often more popular to use the percentage extraction, % E, which is given as

$$\%E = \frac{100D}{(D + V_{org}/V_{aq})} \quad (1.11)$$

Where D = distribution ratio of the solute/ desired components, V_{org} and V_{aq} are the volume of organic phase and aqueous phase used in the extraction process. A requirement for practical use of solvent extraction is that a reasonable fraction of the desired component is extracted in a single operation.

1.8.1.3. Separation factor (β)

In solvent extraction process, selective separation of a metal ion is very important. The selectivity of a separation process is defined by the separation factor (β), which is defined as

$$\beta = D_A/D_B \quad (1.12)$$

Where D_A is distribution ratio of component A and D_B is distribution ratio of component B. For selective separation $D_A \gg D_B$, hence β must be greater than one. The separation factor can be maximized by judicious choice of the extractant and extraction condition.

1.8.1.4. Extraction isotherm

Determination of extraction isotherm is an important initial step in establishing any solvent extraction process. Aliquots of aqueous solutions containing varying amounts of metal salts are contacted with varying volumes of the solvent and thoroughly mixed for a predetermined time. The two phases are separated and their metal contents are determined. Different quantities of metal ions get extracted in the solvent depending upon the distribution coefficient, solvent volume and initial metal concentration. The extraction isotherm is obtained by plotting the metal concentration in the aqueous phase along the x-axis and that in the organic phase along the y-axis. A knowledge of the distribution ratio (D) values for the metal ions at low concentration helps to compare the different solvent systems.

1.8.1.5. Multiple extractions

In order to achieve quantitative extraction of metal, the aqueous phase (containing the metal) is repeatedly brought in contact with the organic phase. The multiple extraction of metal is carried out in either of the following two ways:

1.8.1.6. Co-current extraction

In these processes, a solvent is added to the mixture to be separated, whereupon - after equilibrium has been established and the phases have been separated, the raffinate phase is again treated with solvent (Fig. 1.4). The process is repeated as many times as required. Each of the treatments with the solvent is termed as an “*ideal or theoretical extraction stage*”.

Distribution ratio (D) can be expressed as follows:

$$D = [(W - W_1)/V_o] / (W_1/V_a) \quad (1.13)$$

where V_o = volume of the organic phase; V_a = volume of the aqueous phase.

It can be shown that after first extraction:

$$W_1 = [1 / (1 + D \cdot V_o/V_a)] \times W \quad (1.14)$$

and after the n th contact of the raffinate with V_o volume of fresh solvent, W_n = weight of the metal left in the aqueous solution

$$W_n = [1 / (1 + D \cdot V_o/V_a)]^n \times W \quad (1.15)$$

where W = Initial weight of the metal in the aqueous solution.

To extract metal ion quantitatively, W_n should be as low as possible. This can be achieved by the high values for ‘ V_o/V_a ’ and ‘ n ’. If only one contact is attempted, V_o/V_a has to be maintained at a very high value. A more practical approach is to keep V_o small and resort to an increase of the number of contacts.

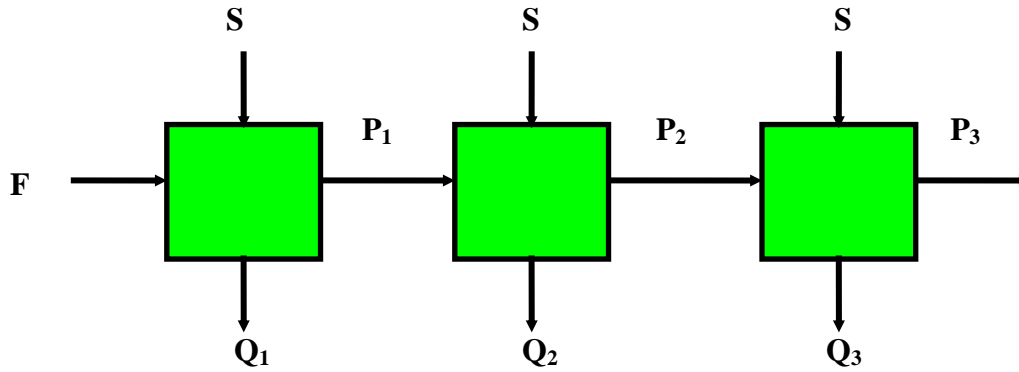


Figure 1.5. Co-current extraction in three stages

where S = solvent, F = feed, P = raffinate and Q = loaded organic phase.

Co-current extraction scheme is associated with the following limitations:

- (a) large solvent inventory,
- (b) dilute organic extract and
- (c) inefficient use of the solvent.

1.8.1.7. Counter-current extraction

In view of the above mentioned limitations of co-current extraction, it is therefore desirable to adopt the counter current method of extraction. In such a procedure, the fresh solvent is brought in contact with aqueous solution containing the least amount of the metal (1st stage) and the aqueous solution having the highest concentration (n^{th} stage) is contacted with the solvent which is reaching its maximum loading capacity (**Figure 1.6**): where n = no. of stages i.e. 1, 2, 3,....., X = metal content in the aqueous phase, Y = metal content in the organic phase, V_o = volume of the organic phase and V_a = volume of the aqueous phase. By mass balance of the metal species distributed between the solvent and the aqueous phases, one gets the following expression:

[Metal content in the fresh solvent + metal content in the fresh aqueous solution] =

[Metal content in the loaded solvent + metal content in the aqueous raffinate]

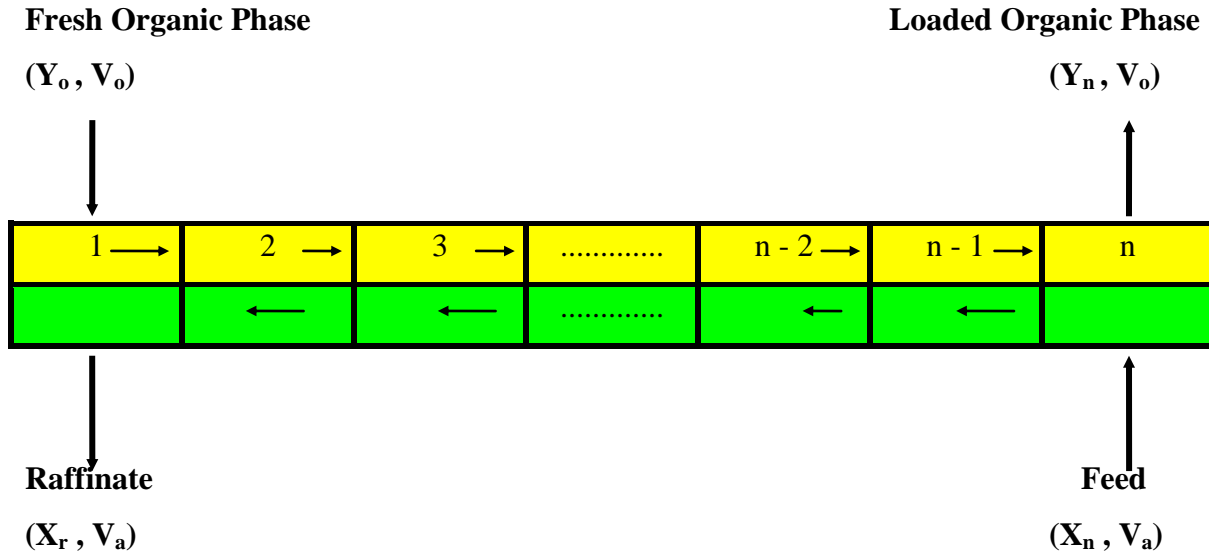


Figure 1.6. Counter-current extraction scheme

Therefore,

$$Y_n V_o + X_r V_a = Y_o V_o + X_n V_a \quad (1.16)$$

$$\text{or, } Y_n = (V_a / V_o) X_n + (Y_o - X_r V_a / V_o) \quad (1.17)$$

X_n and Y_o refer to the metal concentration in the feed and fresh organic phase respectively.

Assuming the metal concentration in the raffinate to be negligible, i.e. $X_r \sim 0$ and $Y_o \sim 0$ (for fresh solvent), We can write

$$Y_n = (V_a / V_o) X_n \quad (1.18)$$

i.e. concentration of metal in (exit) loaded solvent = (V_a / V_o) x concentration of metal in feed solution.

This is an equation of straight line if concentrations of metal in the solvent and aqueous phases are plotted along y- and x-axis respectively. The slope of this line is numerically equal to V_a / V_o and as a first approximation starts at the origin of the graph. This plot is known as “**operating line**” and expresses the material balance of the extraction system. It conveys mathematically the fact that during extraction at any stage, the increase in the metal concentration in the organic

phase is equal to decrease of that in the aqueous phase multiplied by the relative volume of the two phases.

The number of stages required to carry out any counter current extraction operation is determined by drawing the “*McCabe-Thiele*” diagram. It consists of an extraction isotherm and the operating line drawn on the same graph. “*Kremser equation*” (given below) is used to determine the number of stages for extraction or scrubbing stages during counter current continuous operations [58]. The graphical methods for determining the number of theoretical stages required to extract a particular solute quantitatively from one phase into another are widely employed in solvent extraction.

(a) Extraction

$$\begin{aligned}
 [X_r - (Y_o / D)] / [X_n - (Y_o / D)] &= [\varepsilon - 1] / [\varepsilon^{n+1} - 1] \text{ for } \varepsilon \neq 1.0 \\
 &= [1 / (n + 1)] \text{ for } \varepsilon = 1.0
 \end{aligned}
 \tag{1.19}$$

where X_r = Metal concentration in raffinate

X_n = Metal concentration in feed

Y_o = Metal concentration in the barren organic phase ≈ 0

D = Metal distribution ratio

ε = Metal extraction factor = $D (V_o / V_a)$ and

n = Number of stages

On simplification

$$[X_r] / [X_n] = [\varepsilon - 1] / [\varepsilon^{n+1} - 1]
 \tag{1.20}$$

where $[X_r] / [X_n]$ refers to the unextracted fraction of the metal ion and ε is assumed to be constant during the process.

(b) Scrubbing

$$[Y_r - X_s \cdot D] / [Y_o - X_s \cdot D] = [(1/\varepsilon) - 1] / [(1/\varepsilon)^{n+1} - 1] \quad (1.21)$$

where Y_o = Metal concentration in the organic phase before scrubbing

Y_r = Metal concentration in the organic phase after scrubbing

X_s = Metal concentration in the aqueous phase before scrubbing ≈ 0

On simplification

$$[Y_r / Y_o] = [(1/\varepsilon) - 1] / [(1/\varepsilon)^{n+1} - 1] \quad (1.22)$$

In these calculations, the general assumptions made are:

1. the organic and aqueous phases are completely immiscible,
2. the volume of the aqueous and organic phases remain unchanged during the course of extraction and
3. there is no back mixing.

1.8.1.8. Factors influencing the distribution of solutes

The main factors which influence the distribution process are [59,60]:

- (1) Nature and concentration of solute viz. metal ions,
- (2) Nature and concentration of the extractant / diluent,
- (3) Nature and concentration of the complexing agent present in the aqueous phase,
- (4) Presence of salting agent in the aqueous phase,
- (5) Acidity of the aqueous phase and
- (6) Temperature

It is extremely important to control the distribution ratio values (D) to achieve the desired separation.

1.8.1.9. Classification of extractants

The extractants have been classified based on the mechanism of extraction in the following groups:

- (i) **Chelation:** Extraction of metal ions proceeds via the formation of chelate, e.g. the extraction of Pu(IV) by HTTA in benzene.
- (ii) **Solvation:** Extraction of metal ion complexes proceeds via the replacement of water molecules by the neutral extractant with basic donor atoms like O or N. The well known example for this type is TBP extraction of U(VI) from nitric acid medium.
- (iii) **Ion Pair Formation:** Extraction proceeds via the formation of ion pair species. Metal ions can be either in cationic or in complexed anionic form and accordingly ion pair formation involves two types of extractants viz.
 - (a) **Acidic Extractants:** These provide anions which complex with metal cations by liberating protons, sulphonic acids, carboxylic acids and organophosphoric acids.
 - (b) **Basic Extractants:** These provide cations for aqueous anionic species, e.g. amines and quaternary ammonium salts.
- (iv) **Synergism:** This refers to a phenomenon wherein the extraction of metal ion in the presence of two or more extractants is more than that expected from the addition of the distribution ratios of either of the extractants, e.g. the extraction of Pu(IV) from nitric acid medium with a mixture of HTTA and tri-*n*-octyl phosphine oxide (TOPO) in benzene [58].

Table 1.3 lists the extractants which are often being used or hold promise for nuclear hydrometallurgy.

Table 1.3: Extractants employed in nuclear hydrometallurgy

Class	Extractant	Application
Acidic	HDEHP, (Di-2-ethylhexyl phosphoric acid)	Uranium extraction from ores, Actinides and rare earths separation
	PC88A, (dialkyl phosphinic acid)	Rare earths separation
	Versatic acid	Rare earths separation
Basic	Alamine 336	Uranium extraction from ores, Zr/Hf separation
	Aliquat 336	Rare earths separation
	Trilauryl amine	Pu purification
Neutral	TBP	U and Th purification Zr/Hf separation Nb/Ta separation Fuel reprocessing
	TOPO	U recovery from phosphoric acid
	Mono amides*	Fuel reprocessing
	CMP, CMPO and diamides*	Recovery of minor actinides from high level waste

* *Promising but yet to be applied for process applications;*

CMP: Carbamoyl methyl phosphonate;

CMPO: Carbamoyl methyl phosphine oxide.

1.8.1.10. Criteria for the selection of extractants

A number of factors are taken into consideration while selecting a particular extractant for commercial operations [60]. These are as follows:

1. High solubility in the diluent and low solubility in the aqueous phase,
2. Better complexation ability and high solubility of the metal complex in the organic phase,
3. Easy stripping of the metal ion from the organic phase,
4. Ease of regeneration of the extractant for recycling,

5. Reasonably high selectivity for the metal ion of interest over other metal ions present in the aqueous solution,
6. Low viscosity for ease of flow and high Inter Facial Tension (IFT) to enable a faster rate of phase disengagement,
7. Nonvolatility, nontoxicity and noninflammability,
8. High resistance to radiolytic and chemical degradation during operation and
9. Easy availability at a reasonable cost.

1.8.2 Membrane Based Separation

The membrane based separation processes have gained attention in the past few decades for the treatment of industrial effluents, water purification and gas separation etc. [61-63]. Carrier mediated transport of metal ions across liquid membranes is one of the promising options for the recovery of valuable metals from various waste streams [64-67]. This is of great relevance in the nuclear industry in view of the stringent nuclear waste management regulations [68-70]. Liquid membranes are considered to be an improved version of solvent extraction which is widely used in hydrometallurgical separations, because of its high efficiencies, selectivity, less power consumption, as well as use of lower extractant inventory. The transport of metal ions across a liquid membrane (LM) is generally considered as a combination of extraction and stripping processes simultaneously. The transport mechanism is basically same as in liquid-liquid extraction, but the transport process is governed by various diffusion parameters across the membrane interface. Several studies on the recovery of actinides like uranium, plutonium, americium etc. from solutions of different nature/origin using various extractants by supported liquid membranes have been described earlier [71-75]. Separation of uranium from fission products using TBP as carrier for the SLM has been reported [76,78]. Alamine-336 (tri-

octyl/decyl amine), LIX-63 (5,8-diethyl-7-hydroxy-6-dodecanone oxime) and crown ethers have also been employed as carrier in SLM by several authors to separate uranium from various acidic solutions. Shukla *et al.* demonstrated that SLM technique can be used for the recovery of metal ions from radioactive waste solutions [78]. Membrane based separation system combines extraction and stripping processes into one step and offers a possibility of high pre-concentration factor. The chemistry involved in the formation of metal – extractant complex in case of the carrier – facilitated membrane is identical to that of solvent extraction process, but overall separation process in such a membrane based system is governed by the kinetics of the chemical reactions at the aqueous–membrane interfaces and diffusion across the organic phase immobilized in the pores of membrane support. When reaction is too fast, the metal ions transport across the membrane is governed by the viscosity of immobilized organic phase, effective thickness and surface area (porosity) of the membrane. The membrane processes are now finding use in the treatment of large volumes of low level radioactive liquid effluents generated in the various stages of nuclear fuel cycle of the nuclear industry. These processes are primarily used for significant volume reduction of liquid wastes for further processing by conventional methods. This will help reduce the equipment size of the conventional plants, the energy used and the required chemicals. The two configurations of the membranes that are generally used for facilitated transport of the metal ions are emulsion liquid membrane (ELM) and supported liquid membrane (SLM).

There are several reasons for use of SLM over ELM which are stated below:

1. In ELM, anything affecting the emulsion stability must be controlled i.e. ionic strengths, pH, etc.
2. If, for any reason, the membrane does not remain intact during operation, the separation achieved to that point is destroyed.

3. In order to recover the receiving phase, and in order to replenish the carrier phase, the emulsion has to be broken down. This is a difficult task, since in order to make the emulsion stable; one has to work against the ease of its breaking it back down.

1.8.2.1. Supported liquid membranes (SLMs)

The most simplistic in design, the thin sheet supported liquid membrane can be utilized at laboratory scale, but cannot be scaled up for industrial use. Essentially, this is just a porous polymer membrane whose pores are filled with the organic liquid extractant dissolved in suitable solvent, set in between source phase (feed solution) and receiving phase (strip solution), which are being gently stirred as shown in **Figure 1.7**.

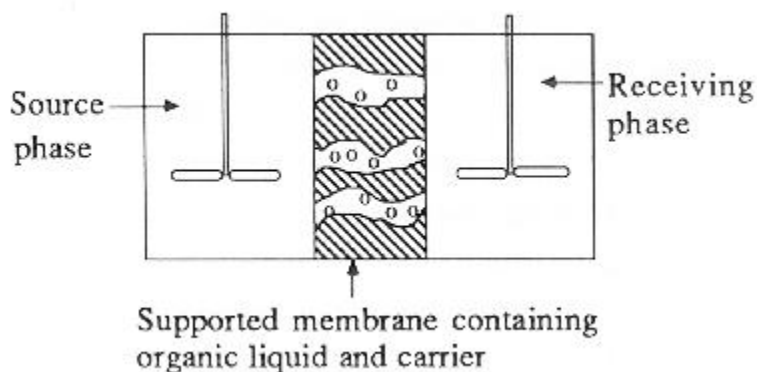


Figure 1.7. Pictorial view of supported liquid membrane

The impregnated membrane acts as a common interface between the feed and strip solutions which are kept in compartments on each side of the membrane. In this system, we can probably guess that the way to instability is to somehow get rid of the carrier or organic liquid in the pores of the supporting membrane. There are two possible ways for this to occur. One is through carrier or solvent evaporation, and the other is by creating a large pressure differential across the membrane, effectively pushing the fluid out [79].

1.8.2.2. Transport in SLM

In the extraction of metal ion, the extractant molecules in the membrane pick up metal ions/species from the feed side forming a complex, which diffuses to the other side of the membrane, where the complex is broken up by a strip solution freeing the extractant molecules

to extract and shuttle more of metal ions. This coupled transport through the SLM can be performed in two ways:

(a).Co-transport: In this process, the metal ions are transported across the SLM, along with the counter ions from the feed solution. If the extractant is neutral or basic, the driving force is the difference in distribution coefficient, K_d , between the feed and the strip solutions. This is generally achieved by maintaining concentration gradient of the counter ions between the feed and the strip phases. The negative counter ions accompanying the metal cations form a complex with the extractant E in the membrane. This complex then diffuses to the other side of the membrane and the metal and the counter ions are dislodged to the strip solution. Pictorial representation is shown in **Figure 1.8** [79].

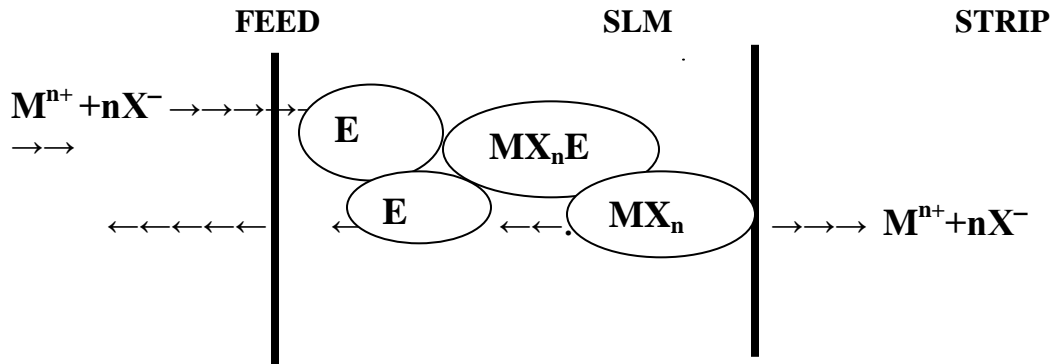


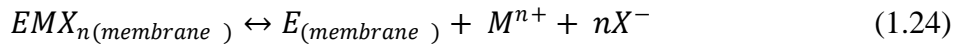
Figure 1.8. Co- transport steps in SLM

The chemical reaction for this coupled transport is given as follows:

For extraction:



For stripping:



The liberated extractant molecules diffuse back to feed-SLM interface, pick up more ions with counter ion and the process continues, till the final equilibrium is attained.

(b).Counter-transport: In the counter-transport phenomenon, an acidic extractant HX forms a complex with metal cation, at the feed-SLM interface. The complex diffuses to the SLM-strip interface and then liberates the metal cation to the strip solution and

simultaneously picks up H^+ ions from the strip solution. The HX species formed diffuse back to feed SLM interface, pick up more metal ions and the process continues. The extractant molecules shuttles between feed and strip interfaces as shown in **Figure 1.9** [79].

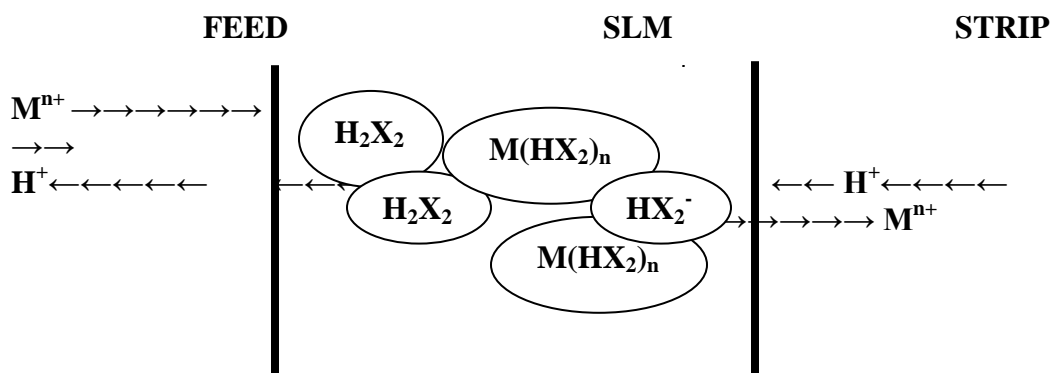


Figure 1.9. Counter-transport steps in SLM

For extraction:



For stripping:



1.9. Aim and Scope of the Thesis

PC88A and DNPPA are the close analog of D2EHPA. Extraction of metal ions using these extractants occurs mostly via cation exchange mechanism. Extraction studies of U(VI), Zr(IV) and Th(IV) from $HClO_4$, HCl , H_2SO_4 medium using PC88A have been reported in literature [80-86]. Our literature survey shows that no detailed study has been done on extraction behavior of U(VI) from nitric acid medium using PC88A as well as DNPPA as extractants. Therefore, the aim of the present thesis is to investigate the extraction behavior of U(VI) from HNO_3 medium using these extractants to establish the extraction mechanism and the evaluation of the effects of various parameters such as diluents, extractant and metal ion concentration,

temperature and stripping agents. The presence of neutral donors such as TBP, TOPO, MIBK (methyl isobutyl ketone), DOSO (di octyl sulphoxide), Cyanex 923 showed synergism. Synergistic coefficients (S.C) at different nitric acid concentrations were calculated and correlated with their acid uptake constants. An attempt has been made to develop empirical model for the U(VI) extraction from H₂SO₄ medium using PC88A and its mixture with neutral donors like TOPO in *n*-dodecane.

Indian monazite is a rare earths (REs) phosphate which also contains thorium and uranium as associates. The leaching of monazite leads to the generation of RE concentrate containing U, Th and phosphate. The monazite sand is processed by either of the two methods: (i) the alkali leaching process with sodium hydroxide where U and Th are separated as hydroxide cakes, and (ii) the acid leaching process with concentrated sulphuric acid where liquor containing RE elements, U and Th is generated [2]. The recovery of uranium from monazite leach solution called “thorium concentrate” is accomplished liquid-liquid extraction technique using Alamine 336 (mixture of tetraalkyl amine, C₈-C₁₀) as an extractant [13,14]. However, this process is associated with limitations such as: (a) corrosion of structural material due to presence of Cl⁻, (b) Alamine 336 forms third-phase and crude oil, (c) loss of solvent in the aqueous phase and (d) lower loading capacity [14]. In view of these problems, several studies have been carried out to identify alternative solvent for separation of U(VI) from U(VI) / Th(IV) mixture from nitric acid medium [87,88]. TEHP (tris-2-ethyl hexyl phosphate) is one of the promising extractants for the separation of U(VI) from a mixture of U(VI) / Th(IV). Present study deals with the separation of U(VI) from a mixture of U(VI) / Th(IV) from nitric medium and the conditions have been optimized for the separation of U(VI) from simulated monazite leach solution in HNO₃ medium.

Liquid-liquid extraction is widely used in the processing of uranium from different resources [80-86]. However, a great majority of effluents are dilute streams and are unsuitable to be treated by conventional liquid-liquid extraction process. Thus, there is always a need for the development of alternative economic separation technologies which may be effectively utilized for the separation of metal values such as uranium from such lean sources. In this context, liquid-membrane based separation holds promise for the recovery of metal ions from lean sources and therefore, has received considerable attention in separation science and technology [62-68]. Uranyl nitrate raffinate (UNR) waste generated from uranium purification plant is an important secondary source of uranium which contains <1 g/L uranium and a large number of other metal ions as impurities. In this thesis an attempt has been made for SLM treatment to recover high purity uranium from this raffinate. Different organophosphorous extractants such as (a) acidic (HA): PC88A, Cyanex 272, DNPPA, D2EHPA; (b) neutral (S): TBP, TEHP, TOPO, TEBP, Cyanex 923 and their different synergistic combination dissolved in *n*-paraffin were used as carriers impregnated in polytetrafluoroethylene (PTFE) membrane.

Investigation have also been carried out on the aggregation behavior of DNPPA under varying experimental conditions such as aqueous phase acidity, nature of diluents, and ligand concentration using Dynamic Light Scattering (DLS), spectrophotometry. The aggregation behavior has been correlated with the extraction properties of metal ions such as U(VI) from HNO₃ medium.

Determination of U(VI) in ore leach solution is a challenging task as it contains a number of other metal ions and anions which often interfere in the analysis [89-92]. Several methods are used for the determination of U(VI) in ore leach solution such as inductively coupled plasma emission spectroscopy (ICP-AES), inductively coupled plasma mass spectroscopy (ICP-MS),

neutron activation analysis (NAA) etc [93-98]. However, these techniques require either huge capital investment or nuclear reactors. In this context simple spectrophotometric technique is described in this thesis for the determination of uranium in ore leach solutions. The technique is based on the selective extraction of uranium from multi-elemental system using a synergistic mixture of PC88A + TOPO in cyclohexane and simultaneous color development in organic phase using 2-(5-bromo-2-pyridylozo)-5-diethyl aminophenol (Br-PADAP) as chromogenic reagent [99-101].

CHAPTER II

EXPERIMENTAL

2.1. Introduction

In the present work, the extraction behavior of U(VI) and Th(IV) has been investigated under different experimental conditions employing various organophosphorous compounds as extractants. The transport behavior of U(VI) from nitric acid medium has also been carried out using supported liquid membrane based technique (SLM). The physiochemical properties of extractants and metal ion complexes have been evaluated using viscosity and dynamic light scattering (DLS). Based on solvent extraction technique, a novel spectrophotometric analytical method has been developed for determination of U(VI) in ore leach solution with high precision and accuracy. This chapter, therefore, deals with the synthesis and characterization of organophosphorous extractant (di nonyl phenyl phosphoric acid i.e. DNPPA) and techniques used for the separation studies of metal ions using solvent extraction and supported liquid membrane (SLM). The details of various apparatus, materials, experimental procedures as well as analytical techniques used in the present work are discussed in this chapter

2.2. Extractants

2-ethylhexyl phosphonic acid mono 2-ethylhexyl ester (PC88A) (95 % pure) was obtained from Diahachi Chemical Industry Co Ltd. Japan and bis(2,4,4-trimethyl pentyl phosphonic acid commercially known as Cyanex 272 (Purity 90 %) was obtained from American Cyanamide Co. USA. Tributyl phosphate (TBP, purity: 97 %, B.D.H), di n octyl sulphoxide (DOSO, purity: 95 %, Thomas Baker), trioctyl phosphine oxide (TOPO, purity: 98 %, American Cyanamide Co. USA), and Cyanex 923 (a mixture of four trialkyl phosphine oxides viz. R_3PO , $R_2R'PO$, RR'_2PO and R'_3PO where R: *n*-octyl and R': *n*-hexyl chain, purity: 97 %, American Cyanamide Co. USA) were used without further purification. Di-nonyl phenyl phosphoric acid (DNPPA) was synthesized and purified before its use in the experiments.

2.3. Synthesis of Di-nonyl Phenyl Phosphoric Acid (DNPPA)

The synthesis route consists of esterification, hydrolysis and purification [102]. Esterification involves reaction of $POCl_3$ with two moles of *p*-nonyl phenol in the presence of pyridine at controlled temperature. The mole ratio of *p*-nonyl phenol, pyridine and $POCl_3$ was 2:1:2, respectively. The esterification reaction can be represented as follows:



Hydrolysis of the alkyl phospho-chloro ester was carried out with 6 M HCl at 80 °C to yield the product. The product obtained was having un-reacted nonyl phenol and byproduct mono nonyl phenyl phosphoric acid as major impurities. The hydrolysis reaction can be represented as:



R = nonyl phenyl group

2.4. Purification of DNPPA

DNPPA synthesized indigenously contained 87-90 % diester, 4-5 % mono ester and 7-8 % neutral (nonyl phenol). It has been observed that the presence of impurities such as unreacted nonyl phenol (neutral) and mono nonyl phosphoric acid (MNPPA) adversely affects the extraction of U(VI) from aqueous medium. The presence of mono ester in DNPPA leads to (a) reduced uranium extraction efficiency, (b) difficult phase separation, (c) poor stripping of uranium, and (d) reduced stability of extractant [103]. It, is therefore, essential to purify DNPPA from these impurities prior to its use in solvent extraction. Two methods have been described for purification of DNPPA as given below:

2.4.1. Purification by Nd-salt Method

Weighed quantity of impure DNPPA product was dissolved in benzene and treated with 70 % methanol 3-4 times maintaining organic-to-aqueous phase ratio (O/A) as 1. Due to

hydrophilic nature, the mono ester fraction present in DNPPA got dissolved in methanol phase and was separated out. The resulting DNPPA/benzene phase obtained after methanol wash was then loaded with Nd(III) by equilibrating it with 30-40 g/L NdCl_3 at pH 2 and maintaining O/A as 1. The Nd(III) loaded DNPPA in benzene was poured in to excess of acetone to precipitate out Nd(III)-DNPPA salt. This precipitate was given two-three washes of acetone and finally redissolved in benzene. This treatment further removed mono-ester as only diester forms complex with Nd(III). The loaded organic phase was contacted with 10 % oxalic acid / 6 M HCl 2-3 times at O/A = 1 to strip Nd(III) and to get free and pure DNPPA dissolved in benzene. Finally, the organic phase after washing with water and drying over sodium sulphate 10 % solution was subjected to evaporation of benzene. The purity of DNPPA (diester) was found to be ~95 %, however, the recovery yield was poor (50-60 %).

2.4.2. Purification by Mono Ethylene Glycol Treatment

The indigenously synthesized DNPPA product was given successive washings with NaOH solution and mono ethylene glycol to remove impurities like nonyl phenol and mono-nonyl phenyl phosphoric acid. Nonyl phenol was separated from the product by NaOH wash in the form of insoluble third phase. This process was continued till the formation of third phase was negligible. After removal of nonyl phenol by alkali wash, the resulting DNPPA product was subjected for mono ethylene glycol washing to remove mono nonyl phenyl phosphoric acid. The washed and dried product was finally distilled using centrifugal molecular distillation unit at 100 °C and 0.01 mm Hg pressure to yield high purity DNPPA containing > 95 % diester and less than 0.5 % monoester. **Table 2.1** lists the yield and purity obtained from different batches of DNPPA after employing the two purification methods. Purification of DNPPA by mono ethylene

glycol wash yielded better recovery and purity of the product. The purified product was further analyzed by potentiometry titration technique to establish its purity.

Table 2.1. Purity and yield obtained after purification of different batches of DNPPA

Method	Batch No.	Diester, %	Monoester, %	Neutrals, %	Yield, %
<i>Untreated</i>	<i>1</i>	88.0	2.5	9.5	-
Nd – salt	1	94	1.5	4.3	55
method	2	95	1.6	3.8	52
Mono ethylene	1	96	0.5	4.5	94
glycol method	2	96	0.4	4.0	92

2.4.3. Characterization of DNPPA: Potentiometric titration

Weighed quantity of DNPPA (~0.5 g) was dissolved in a beaker containing ~50 mL acetone and ~10 mL water. This solution was titrated potentiometrically as well as employing phenolphthalein as indicator simultaneously against standard alkali (0.1 M NaOH) [104]. This helped in clearly identifying the end points both by visual observation and by the changes in pH values. DNPPA and MNPPA being monobasic and dibasic acids showed two inflection points in the potentiometric titration curve. The differential titration curve was plotted using ORIGIN software where the two end points were clearly located. From the two end points the concentration of di-ester, monoester and neutral fractions of DNPPA were calculated. **Figure 2.1** shows a typical titration graph for DNPPA assay.

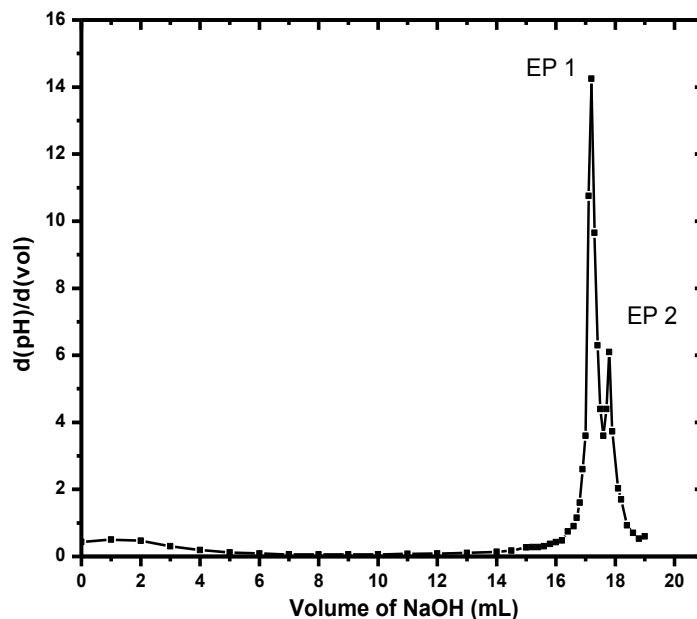


Figure 2.1. Potentiometric titration of DNPPA with standard 0.1 M NaOH using Phenolphthalein as indicator; EP: End Point

2.5. Other Materials

During the experiments, various A.R. grade chemicals like HCl, HNO₃, H₂SO₄, oxalic acid, sodium carbonate, ammonium carbonate, citric acid, phenolphthalein, bromocresol purple, xylenol orange etc. procured from Prabhat Chemical, Mumbai, India were used. Cyclohexanediaminetetra acidic acid (CyDTA), di sodium salt of ethylenediaminetetraacidic acid (Na₂EDTA) sodium fluoride, sulphosalicylic acid (SSA), triethanolamine (TEA) were procured from Sigma, USA. The chromogenic reagent 2-(5-bromo-2-pyridylazo-5-diethylaminophenol) (Br-PADAP) was purchased from Fluka, Germany. Diluents like *n*-dodecane, xylene, chlorobenzene, dichlorobenzene, isodecanol were of A.R. grade while *n*-paraffin was of commercial grade used for preparation of solutions. Nuclear grade uranium metal was collected from Uranium Extraction Divisions (UED), BARC and thorium nitrate was

procured from IRE Ltd. Rare Earth oxides and yttrium oxide, > 99% purity were procured from IRE Ltd. $ZrOCl_2$, $(NH_4)_4MoO_6$, $Al(NO_3)_3$, $CdCl_2$, Cr_2O_3 , $NiSO_4 \cdot 6H_2O$ used in solvent extraction as well as in transport studies were of A.R. grade. For SLM studies commercially available poly tetrafluoroethylene (PTFE) membranes (pore size: $0.45\mu m$; diameter: 47 mm) procured from Sartorius, Germany, were used as a solid support. Porosity of the membrane was determined as 72% by measuring the volume of *n*-dodecane that membrane could hold in the pores and by SEM technique [75].

2.6. Instruments

Solvent extraction experiments were carried out using glass stoppered separating funnels with manual agitation. Double beam Unicam UV 500 (UV-visible) spectrophotometer controlled by microprocessor was used for the measurement of optical density of the desired metal ions. An Inductively Coupled Plasma Emission Spectrophotometer (ICPAES) Jobinyvon Emission, Model No. JY 328 was used to determine trace elements in solutions. The detection limit (3σ) of the instrument for non-transition elements: < 0.2 ppb, transition elements: < 1 ppb and rear earths elements: < 3 ppb. An Energy Dispersive X-ray Fluorescence (EDXRF) Spectrophotometer, Jordon Valley (Model No Ex-3600M) was used for determination of elements in solid samples as well as in solution. The spectrometer contains six filter (Cu, Fe, Mo, Rh, Sn and Ti) and a Si(Li) detector with Be window. The instrument contains 10 sample positions along with 5 internal standards. The instrument can handle solid, powder and liquid samples. nExt software is used for spectrum acquisition and analysis.

The aggregate size measurements in the organic phase were performed using Zetasizer-3000 DLS spectrometer (Malvern Instrument Company, UK) with a 10mW He-Ne laser beam at a wavelength of 488 nm. All the measurements were performed at a scattering angle of 90° in a

cell of 4 mm path length at room temperature (25 ± 1 °C). The instrument was calibrated using standard colloidal suspension (polystyrene, latex) before the size measurement of the actual samples. Each measurement was repeated at least three times to check the reproducibility of the data. The reported value is a mean of these values and deviations are within $\pm 5\%$.

2.7. Solution Preparations

2.7.1. Standard solution of uranium & thorium

Nuclear grade uranium metal turnings were cleaned with alcohol and acetone to remove grease etc and then it was treated with concentrated HNO₃ solution. The whole solution was heated till complete dissolution of uranium. The solution was evaporated to dryness and after evaporation the solution was made up to 250 mL with distilled water with the addition of few drops of nitric acid to prevent hydrolysis. The uranium solution was standardized by Davie and Gray method [105]. Dilute solutions of uranium in different concentrations of nitric acid were prepared by adding requisite amount of nitric acid and distilled water. Thorium nitrate solution was prepared by dissolving requisite amount of nitrate salt in nitric acid solution and the solution was standardized EDTA complexometric titration.

2.7.2. Solution for Spectrophotometric Measurement of Uranium

2.7.2.1. Preparation of complexing solution

To 40 mL of redistilled water, 1.25 g of CyDTA, 0.25 g sodium fluoride and 3.25 g of sulphosalicylic acid were dissolved. The pH of the solution was adjusted to 7.8 using 40% NaOH and the final volume was made up to 100 mL.

2.7.2.2. Buffer solution

To 80 mL of redistilled water 14.2 mL of TEA was dissolved and pH of this solution was adjusted to 7.8 by adding concentrated perchloric acid. The solution was left to stand overnight

and pH of the solution again readjusted to 7.8. The solution was further diluted to 100 mL using double distilled water.

2.7.2.3. *Br-PADAP solution (0.05%)*

0.05 g of Br-PADAP indicator was dissolved in 100 mL absolute ethanol.

2.7.2.4. *Mixture of PC88A and TOPO solution (0.1M + 0.05 M)*

6.31 g PC88A and 1.93 g of TOPO was dissolved in 100mL cyclohexane.

2.7.3. *Composition of Uranyl Nitrate Raffinate (UNR)*

UNR solution generated in the purification of yellow cake by TBP-kerosene rout was collected from Uranium Metal Plant (UMP) of Uranium Extraction Division. The typical specification of the UNR is as follows:

Table 2.2. Major components of a typical raffinate solution (of uranium purification cycle)

Component	Concentration
U	~0.5- 1g/L
Free acidity	~1.1 M
Soluble Solid [#]	~6.4 % (w/v)
Suspended Solids [#]	~0.2 % (w/v)

[#]determined by gravimetry

Table 2.3. ICP-AES analysis of a typical raffinate solution

Element	Concentration, $\mu\text{g/mL}$	Element	Concentration, $\mu\text{g/mL}$
Al	257	Fe	238
B	0.4	Mg	37.5
Cd	0.5	Mn	3.8
Ce	0.6	Ni	6.7
Co	0.4	Sm	<0.1
Cr	9.3	Y	0.3
Dy	<0.1	Yb	<0.1
Eu	<0.1		

Detection limit (3σ) of non-transition elements: <0.2 ppb, transition elements: <1 ppb and rare earths elements: <3 ppb. Standard deviation of the measurements are within 2-5%.

2.7.4. Uranium ore leach solution

A typical analysis of ore leach solution (sulphuric acid leaching) used in the experiments as given in **Table 2.4**.

Table 2.4. Typical analysis of an ore leach solution containing large amount of impurities

Element	Concentration, $\mu\text{g/mL}$	Element	Concentration, $\mu\text{g/mL}$
U	193.9	Eu	0.6
Al	1214.5	Fe	3330.4
B	2.2	Gd	5.2
Ce	43.7	Mg	1017.06
Cr	19.7	Mn	3440.9
Co	1.6	Ni	6
Dy	4.6	Sm	6.7
Er	2.1	Y	14.7

2.8. Experimental Procedure for Solvent Extraction

The solvent extraction experiments were carried out at least in duplicate by equilibrating equal volumes (15mL each) of aqueous and pre-equilibrated organic phases for 5-10 minutes in a separating funnel (60 mL capacity) at room temperature (298 K). This time was found sufficient for achieving equilibrium condition. The organic and aqueous phases were allowed to settle and then separated. The concentrations of metal ions in the aqueous phases were determined by various analytical methods described in next sections. The concentrations of metal ions in organic phases were calculated by the difference of the metal ions concentration in the aqueous phase before and after extraction. The distribution ratio (D_M) of metal ion was calculated as:

$$D = \frac{[M]_{org,eq}}{[M]_{aq,eq}} \quad (2.3)$$

where, $[M]_{org}$ and $[M]_{aq}$ refer to metal ion concentrations in organic and aqueous phases, respectively, under equilibrium condition.

Percentage extraction (%E) and stripping (%S) of metal ions were defined as:

$$\%E = \frac{([M]_{aq,in} - [M]_{aq,eq}) * 100}{[M]_{aq,in}} \quad (2.4)$$

$$\%S = \frac{([M]_{org,in} - [M]_{org,eq}) * 100}{[M]_{org,eq}} \quad (2.5)$$

For Synergistic extraction studies:

$$\text{Synergistic coefficient, } S.C. = \log \frac{D_{mix}}{(D_1 + D_2)} \quad (2.6)$$

where, $[M]_{aq,in}$ = Initial metal ion concentration in the aqueous phase

$[M]_{aq,eq}$ = metal ion concentration in the aqueous phase at equilibrium

$D_{mix} = D_M$ for the synergistic mixture of acidic extractant and neutral donors

$D_1 \& D_2 = D_M$ for pure solvents

Reproducibility of the experimental data and the material balance were within error limits (± 5 -10 %).

2.9. Experimental Procedure Membrane Transport Studies

The transport studies were performed using a Pyrex glass cell consisting of two equal compartments each having 25 mL capacity. The measured effective membrane area was 4.94 cm². Various strippants such as distilled water, H₂SO₄, Na₂CO₃, citric acid, oxalic acid etc. were used as strip solutions. The feed and strip solutions were stirred using Teflon coated magnetic spin bar at constant speed, 200 rpm and at room temperature. The SLM was positioned between the two compartments of the glass cell, joined by glass flanges. The concentrations of metal ions in feed as well as in strip solutions were monitored by taking 0.1 mL samples at fixed time intervals (generally 30 min).

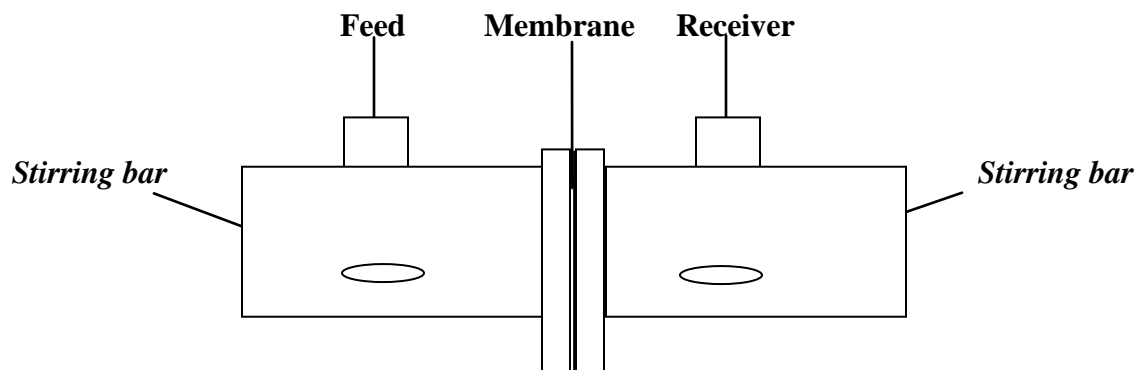


Figure 2.2: A typical membrane transport cell used in the present study

2.9.1. Transport equation

Transport process in the supported liquid membranes can be divided into three basic steps, viz. extraction at the feed membrane interface, diffusion inside the membrane and stripping at the membrane –receiver interface. The driving force behind the transport of metal ion across SLM is the concentration gradient of metal ion in feed as well as in receiver phases. Assuming the

transport of the metal ion across the SLM is diffusion control and the distribution ratio is much greater at the feed-membrane interface as compared to the membrane receiver-interface, the flux (J) of the system is given as [79, 106,107].

$$J = P \cdot C_f \quad (2.7)$$

where P is the permeability coefficient at the feed- membrane interface and C_f is the concentration of the metal ion at the feed side. Alternatively, the flux (J) can be calculated by the following equation:

$$J = - \frac{d(V_f C_f)}{Q \cdot dt} \quad (2.8)$$

where V_f is the feed volume and Q is the effective surface area of the membrane used in the experiment. Combining equations 1 and 2, and by integrating one gets:

$$- \ln \left\{ \frac{V_{f,o} C_{f,o}}{V_{f,t} C_{f,t}} \right\} = P \cdot Q \cdot t / V_f \quad (2.9)$$

where $V_{f,o}$, $C_{f,o}$, $V_{f,t}$ and $C_{f,t}$ represent the volume and concentration of feed at time 0 and after time t , respectively. If volume of the feed does not change significantly during the experiment, then we get the following equation:

$$\ln(C_{f,t}/C_{f,0}) = -QPt/V_f \quad (2.10)$$

where Q represents the effective surface area and is the product of geometrical surface area (A) and the porosity (ϵ). The permeability coefficient (P) values were calculated by the equation (2.10). The percentage transport of metal ions ($\% T$) across SLM was calculated as:

$$\%T = (C_{t,r}/C_{0,f}).100 \quad (2.11)$$

where $C_{0,f}$ and $C_{t,r}$ are the concentrations of metal ions in feed and receiver compartments at time 0 and t (s), respectively.

2.10. Dynamic Light Scattering (DLS) Measurements

The reverse micelles suspended in a liquid (organic diluents in present case) are under constant Brownian motion due to random collision between the micelles and liquid molecules. When a monochromatic and coherent light beam falls on such a suspension, the scattered light photons carry the information about the size of the particle. DLS technique measures the fluctuations, in the intensity of the scattered photons, which occur over short time intervals due to scattering of the particles undergoing Brownian motion in the solution. The behaviour of these fluctuations is described quantitatively by the intensity of the autocorrelation function, $C(\tau)$ of scattered intensity as follows [108,109]:

$$C(\tau) = A(1 + \beta \int_0^{\infty} P(\Gamma) \exp(-\Gamma\tau) d\Gamma) \quad (2.12)$$

where A is the baseline value, β is an instrumental constant and Γ is the characteristic line width of the distribution function $P(\Gamma)$ and is related to the diffusion coefficient (D) of the species by the following expression:

$$\Gamma = Dq^2 \quad (2.13)$$

where q is the scattering vector which is constant for a given observation angle and wavelength of the incident light. Assuming the scattering species as hard sphere, the apparent hydrodynamic radius (r_h) of the species can be calculated by Stokes–Einstein equation:

$$D = k_B T / (6\pi\eta r) \quad (2.14)$$

where k_B is Boltzmann constant, T is the absolute temperature and η is the viscosity of the dispersion medium. However, it is important to mention that the DLS data obtained in the present work provides a gross size of the extractant species in the organic phase.

2.12. Quantitative Determination of Thorium

Some analytical techniques used for determination of thorium are described as follows:

2.12.1. Spectrophotometry

Thorium in microgram quantities in aqueous samples could be determined by spectrophotometric method [110]. Thorium forms a purple colored complex with Arsenazo-III at 5-6 M acidity (HCl) which shows absorption maxima at 665 nm with a molar extinction coefficient of $\sim 100,000$. For sample preparation a suitable aliquot of Th was taken in a standard flask (10 mL) followed by addition of 1mL of 1M sulphamic acid, 4mL of concentrated nitric acid and 1mL of 0.1% Arsenazo-III. The final volume was made up with distilled water and absorbance was recorded at 665nm after 15min of the colour development. The role of sulphamic acid is to remove any trace of nitrous acid which interferes in the method. The calibration plot was constructed by measuring the absorbance of standard solutions of thorium between the concentration range of $1 \times 10^{-5} \text{M}$ to $1 \times 10^{-6} \text{M}$. The concentration of unknown analyte samples was determined from the calibration curve.

2.12.2. Complexometric titration

When the concentration of thorium was in milligram quantities, the conventional complexometric titration was followed. A suitable aliquot of Th solution was titrated against standard EDTA (ethylenediamine tetraacetic acid) solution at pH 3 using xylenol orange as an indicator [111]. The end point of the reaction was the change of colour from deep purple to lemon yellow. The precision of these analyses was $\pm 2\%$ ($\sim 5 \text{mg Th}$). Similarly, the organic phase was also titrated with a precision of $\pm 5\%$. In the case of organic samples, the aliquot size was restricted to 0.5 mL.

2.13. Estimation of Uranium

Numerous procedures are available for the quantitative determination of uranium. Macro quantities of uranium may be analyzed by gravimetric or volumetric methods. Gravimetric procedures usually utilize U_3O_8 ignited in air or 8-hydroxy-quinolate [110, 111]. Volumetric methods are based on reduction of uranium to U(IV) with lead or zinc, followed by titration with an oxidizing agent such as potassium dichromate, ceric sulfate, potassium bromate, or potassium permanganate. Small amounts of uranium may be determined by coulometric, polarographic, colorimetric, fluorescence, or spectroscopic methods. The isotopic composition may be determined by mass spectroscopy or, in the case of U^{235} , by fission counting. Some analytical techniques used for determination of uranium are described here.

2.13.1. Spectrophotometry

Uranium in the aqueous phase as well as in the organic phase could be determined by spectrophotometry using Br-PADAP as a chromogenic reagent [99]. Uranyl ion forms stable intense violet coloured complex with Br-PADAP at pH 7-8 in the alcoholic medium buffered with TEA which shows absorption maxima at 575 nm with molar extinction coefficient of $\sim 70,000$. To a known volume of uranium solution in standard flask (10mL), 1mL of complexing solution, 1mL buffer solution and 0.8mL Br-PADAP solution were added, respectively. For organic samples the final volume (10mL) was made up with ethanol. On the other hand, for aqueous samples the final volume (10mL) was adjusted with distilled water after addition of 4mL of ethanol. The final absorption measurements were performed after 30 min of colour development at 576 nm. This method was found to be very sensitive and no interference of Pu, Th, Al and Fe was observed. The calibration curve was plotted in the concentration range of

1×10^{-5} M to 1×10^{-6} M with standard uranium solution. The concentrations of unknown samples were determined from the calibration plot.

2.13.2. Davies Gray titration

Uranium in the concentration range 50-200 $\mu\text{g/mL}$ was estimated volumetrically by Davis-Gray method employing potentiometric end point detection [105]. The sample size was varied between 1-3mL. This method involves the reduction of U(VI) to U(IV) by Fe(II) in the presence of concentrated phosphoric acid solution containing sulphamic acid. Then the excess Fe(II) is selectively oxidized by nitric acid in the presence of Mo(VI) which acts as a catalyst. The role of sulphamic acid is to destroy any trace of nitrous acid present in the solution which may oxidize Fe(II) and U(IV). The resulting U(IV) phosphate solution is then titrated with standard potassium dichromate solution to potentiometric end point. A small amount of vanadium (IV) sulphate is added in the solution which sharpens the end point. The concentration of uranium in the analyte solution is calculated from the volume of standard potassium dichromate solution consumed.

CHAPTER III

SYNERGISTIC EXTRACTION OF URANIUM WITH MIXTURES OF ORGANOPHOSPHOROUS ACIDIC AND NEUTRAL EXTRACTANTS

3.1. Introduction

Solvent extraction has played a key role in the separation of actinides both for industrial scale as well as for analytical applications. New challenges in nuclear industry relate to the recovery of uranium from its lean resources including effluent wastes of uranium plants. During the purification of diuranate by tri *n*-butyl phosphate (TBP) route, uranyl nitrate raffinate (UNR) is generated as waste containing 0.3-1 g/L U [112]. In view of the presence of the large concentrations of uranium in uranyl nitrate raffinate waste, it is imperative to optimize the conditions of its recovery. Extraction, separation and purification of U(VI) from nitric acid medium are generally carried out by organophosphorous extractants. The most commonly used organophosphorous extractants are TBP [113,114], tri *n*-Octyl phosphine oxide (TOPO) [3], di (2 ethyl hexyl) phosphoric acid (D2EHPA) [4]. 2-ethyl hexyl phosphonic acid 2-ethyl hexyl monoester (PC88A) is an acidic organophosphorous extractant (HA), which is widely used in extractive metallurgy of rare earths and base metals [115-117]. Several synergistic extractions studies of metal ions are reported with neutral oxodons from different acid media [118,119]. Major advantages of the synergistic extraction include low ligand inventory and possibility of extraction from high concentration of acids or complexing agents. Singh *et al.* studied the synergistic extraction of U(VI) from hydrochloric acid medium using PC88A and its mixture with neutral oxodons TBP, TOPO, and Cyanex 923 [120]. Mishra and Chakravorty reported the synergistic extraction of U(VI) from phosphoric acid medium using a binary mixture of Aliquat 336 (tricaprylmethyl ammonium chloride) and PC88A in xylene [121]. Godbole *et al.* observed synergism in U(VI) extraction by a mixture of PC88A and TOPO from sulphuric acid medium [122]. Several studies have been reported on the evaluation of phenyl phosphoric acids either alone or in combination with various synergistic agents for the extraction of uranium from

phosphate media [123-127]. Di nonylphenyl phosphoric acid (DNPPA) finds special place as a powerful extractant for uranium recovery from phosphoric acid solutions [128]. These studies suggested that synergistic mixture DNPPA+ TBP can be used for recovery of uranium from wet phosphoric acid (WPA). Some feasibility studies were also carried out on uranium extraction from merchant grade phosphoric acid (55-60 % P_2O_5 , 0.2-0.3 g/L U_3O_8) [129]. However, no sufficient data are available on extraction of uranium from nitrate media using PC88A and DNPPA as an extractant. This is relevant for the recovery of uranium from different waste solutions generated during its extraction and purification.

3.2. The present work

In the present study, uranium extraction from nitrate medium was investigated using PC88A/DNPPA (acidic extractants, HA) either alone or its mixture with neutral donors such as TBP, TOPO, Cyanex 923 (a mixture of four trialkyl phosphine oxides viz. R_3PO , $R_2R'PO$, RR'_2PO and R'_3PO where R: *n*-octyl and R': *n*-hexyl chain), di-*n*-Octyl sulphoxide (DOSO), and methyl isobutyl ketone (MIBK) in *n*-dodecane/*n*-paraffin as extractants. The effects of different experimental parameters such as aqueous phase acidity, temperature, diluents and nature of strippants on the extraction/stripping behavior of U(VI) were investigated. Synergistic coefficient were calculated and correlated with the basicity of neutral oxodonor ligands. Further, the conditions for the recovery of uranium from the uranyl nitrate waste solutions were through liquid-liquid extraction route optimized using extractants PC88A and its mixtures with TBP, TOPO and DOSO. Extraction efficiencies of different organophosphoric acids such as D2EHPA, PC88A, and dioctyl phenyl phosphoric acid (DOPPA) for uranium from nitric acid medium have been evaluated vis-à-vis DNPPA.

3.3. Results and Discussion

3.3.1. Extraction of U(VI) from nitric acid medium with PC88A and neutral donors

3.3.1.1. Effect of nitric acid concentration

The extraction of U(VI) (0.1 M) from nitric acid medium (0.1 to 10 M HNO₃) was carried out with 0.25 and 0.5 F (F = formality) PC88A in *n*-dodecane. **Figure 3.1** shows decrease in D_U values with increased nitric acid concentration. This was attributed to the acidic nature of PC88A, which extracts uranium by cation exchange process up to 3 M HNO₃ concentration liberating H⁺ ion in the aqueous solution. **Figure 3.2** shows the plot of $\log D_U$ vs $\log [H^+]$ with a slope of 1.02(±0.05), which means for each mole of complex formation there is a liberation of one mole of H⁺ ion. However, the extraction mechanism (**Equation 3.5**) of uranium apparently change at HNO₃ concentration >3M where the solvation process rather than cation exchange. There was a drastic decrease in D_U value beyond 8M which was attributed to the competition of nitric acid extraction with U(VI) extraction by the solvent. Similar observations have been reported during the extraction of uranium using other acidic extractants such as D2EHPA and bis (2,4,4-trimethylpentyl) phosphonic acid (Cyanex 272) different aqueous media [**118,129**]. Ligand variation experiments were done to determine the stoichiometry of the extracted species. **Figures 3.3 & 3.4** represent the variation of $\log D_U$ with $\log [H_2A_2]$ (H_2A_2 = dimeric form of PC88A) and $\log [NO_3^-]$ and their corresponding slopes are ~ 2.0 and 1.04 ± 0.01, respectively. This suggests that each mole of uranium in the organic phase is associated with two moles of PC88A dimer and one mole of nitrate ion. So, the extracted species in the organic phase has the composition of $UO_2(NO_3)(HA_2) \cdot H_2A_2$. This observation is in sharp contrast to that of uranium extraction using PC88A from HCl medium. The reported extracted species in the case of latter is $UO_2(HA_2)_2$ showing no involvement of chloride anion [**121**]. Chetty *et al.* on the other hand, demonstrated

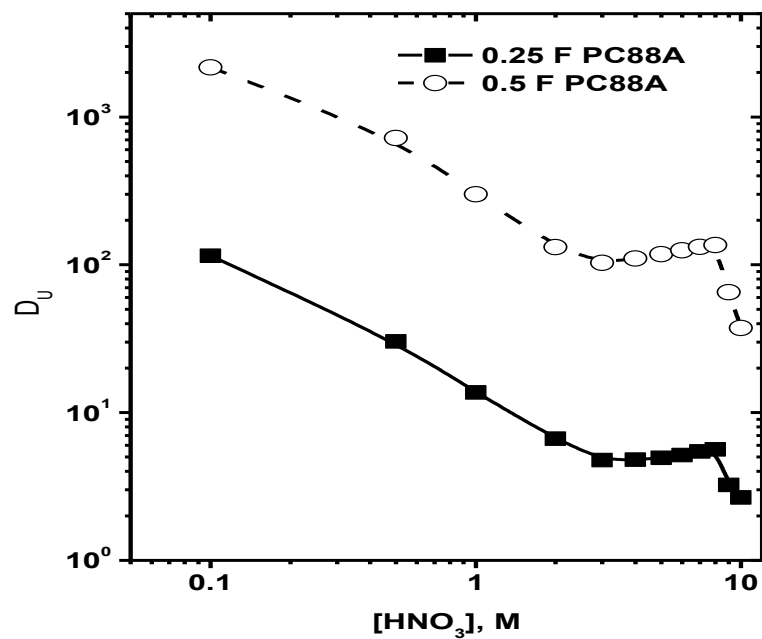


Figure 3.1. Variation of D_U with aqueous phase acidity; [U(VI)]: 0.1 M; Diluent: *n*-dodecane; T: 298 K

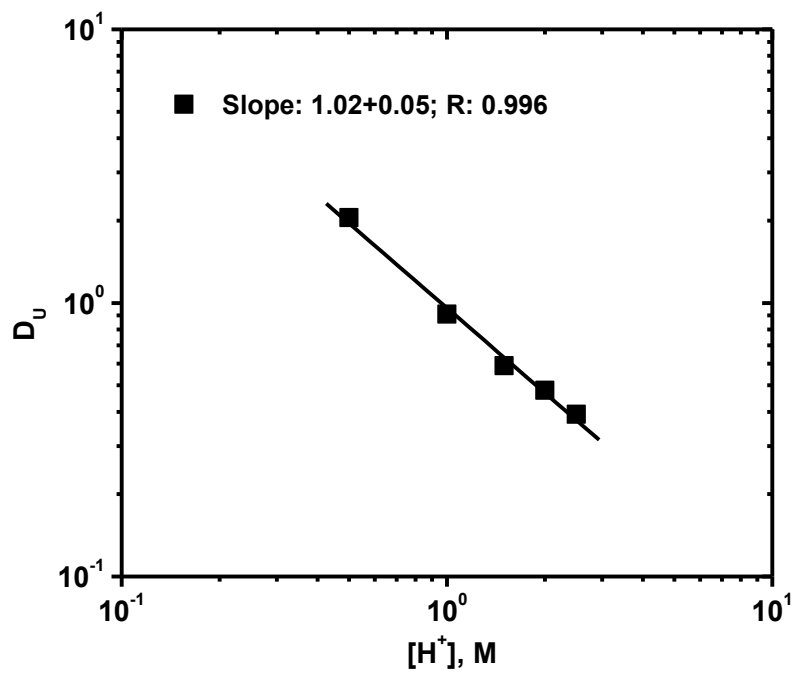
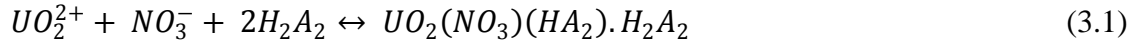


Figure 3.2. Variation of D_U with hydrogen ion concentration; [PC88A]: 5×10^{-3} M; [U(VI)]: 1×10^{-3} M; [NO₃⁻]: 3 M; Diluent: *n*-dodecane T: 298 K

the involvement of nitrate ion in the extracted species of Pu(IV) using PC88A as the extractant [86]. The extraction mechanism of uranium from HNO₃ medium using PC88A/*n*-paraffin can be summarized as follows:

At low nitric acid concentration ($0.1 \text{ M} < [\text{HNO}_3] \leq 3 \text{ M}$):



$$K_{ex} = \frac{([\text{UO}_2(\text{NO}_3)(\text{HA}_2)\text{H}_2\text{A}_2]_{org} [\text{H}^+]_{aq})}{([\text{UO}_2^{2+}]_{aq} [\text{NO}_3^-]_{aq} [\text{H}_2\text{A}_2]_{org}^2)} \quad (3.2)$$

$$K_{ex} = \frac{(D_U [\text{H}^+]_{aq})}{([\text{NO}_3^-]_{aq} [\text{H}_2\text{A}_2]_{org}^2)} \quad (3.3)$$

$$\log D_U = \log K_{ex} + \log [\text{NO}_3^-] + 2 \log [\text{H}_2\text{A}_2] - \log [\text{H}^+] \quad (3.4)$$

At high nitric acid concentration ($[\text{HNO}_3] \geq 3 \text{ M}$):

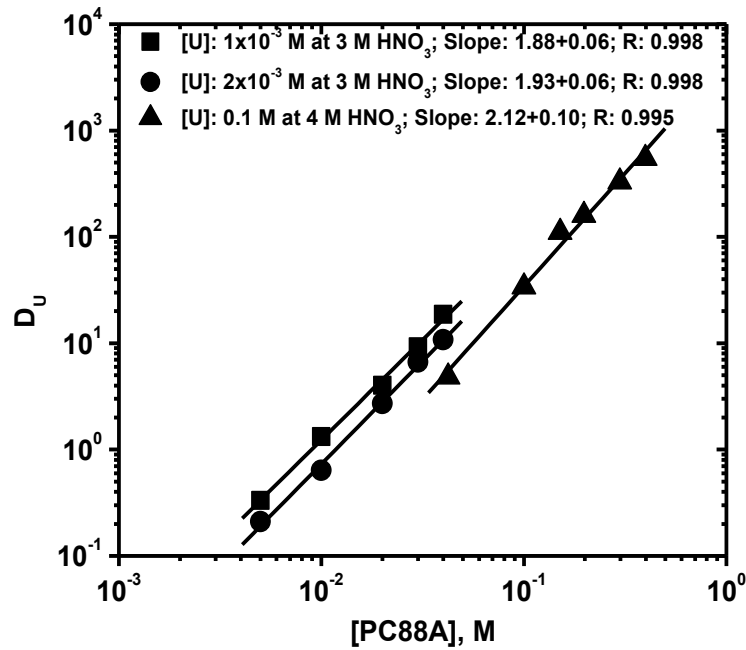
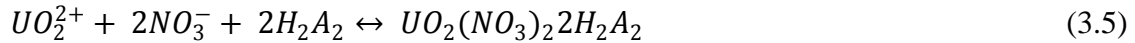


Figure 3.3. Variation of D_U with PC88A concentration; Diluent: *n*-dodecane; [U(VI)]: 0.1 M; T: 298 K

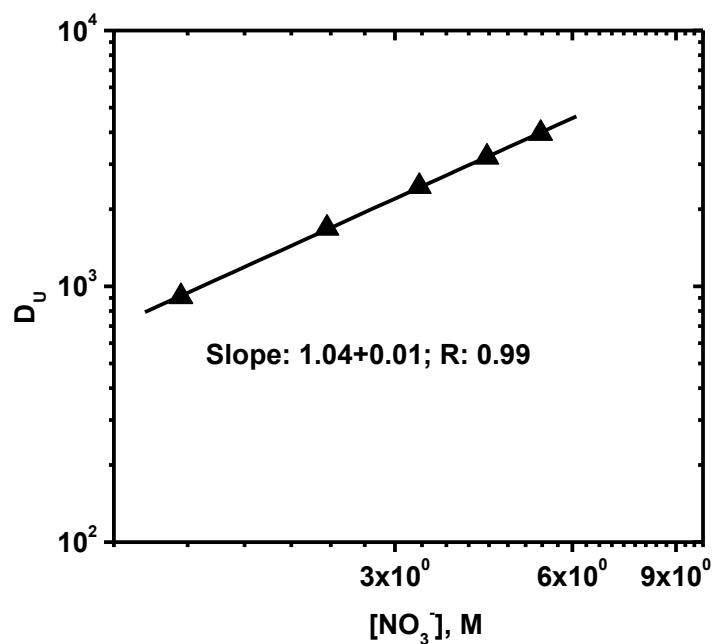


Figure 3.4. Variation of D_U with nitrate ion concentration; [U(VI)]: 0.1 M; [PC88A]: 0.0.25 M; Diluent: *n*-dodecane; [H⁺]: 0.3 M; T: 298 K

Similarly, nitrate coordination has been reported for the extraction of U(VI) from HNO₃ medium using Cyanex 272 as extractant [129].

3.3.1.2. Effect of temperature

Extraction of uranium by 0.5 F PC88A in dodecane was carried out at different temperature and the data were plotted in **Figure 3.5**. It is observed that $\log D_U$ vs $1/T$ (K⁻¹) is a straight line with the slope and intercept values as 399.74(±40.14), and 0.71(±0.13), respectively. The enthalpy change (ΔH) for the above extraction process was calculated from the slope as -7.65(±0.77) kJ mol⁻¹ suggesting the exothermic nature of the extraction process [18]. This result indicates that high temperature may favor the stripping of uranium from organic medium.

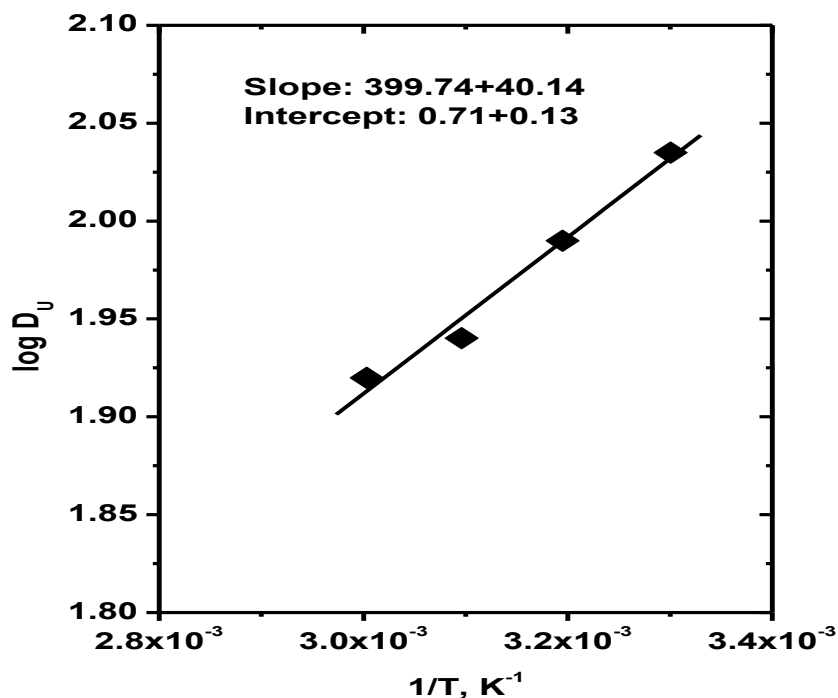


Figure 3.5. Variation of D_U with temperature; [U(VI)]: 0.1 M; [HNO₃]: 4 M; [PC88A]: 0.5 F; Diluent: *n*-dodecane

3.3.1.3. Effect of diluents

Nature of the diluents influences the extraction and solubilization of the extracted species containing metal ions in the organic phase. It was therefore, desirable to investigate the influence of different diluents on the extraction of uranium from nitric acid medium using 0.5 F PC88A as extractant at 298 K. Extraction efficiency increased in the order: xylene < carbon tetrachloride (CCl₄) < *n*-dodecane < MIBK (**Table 3.1**). There is marginal variation of D_U values for Xylene, CCl₄ and dodecane as diluents, but D_U value for MIBK is distinctly larger suggesting higher solubility of extracted species.

Table 3.1. Effect of various diluents on extraction of uranium; Extractant: 0.5 F PC88A;Aqueous phase: 0.1 M U(VI) at 4 M HNO₃; Organic-to-aqueous phase ratio (O/A): 1; T: 298 K

Diluent	D_U	%E
Xylene	72.2	98.6
CCl ₄	72.5	98.6
<i>n</i> -dodecane	113.0	99.1
MIBK	255.0	99.9

3.3.1.4. Synergistic extraction

Tables 3.2-3.5 list the distribution data of uranium at different acidities (0.05 – 6 M HNO₃) using 0.03 F PC88A either alone as a mixture of 0.03 F PC88A and 0.03 M of oxodonors such as TBP/TOPO/DOSO/MIBK in *n*-dodecane as extractants. It is evident that D_U increases with aqueous phase acidity for TBP and reaches a maximum at 5 M HNO₃ whereas for PC88A, the D_U values decrease up to 3 M HNO₃ and then increase slowly. For PC88A–TBP mixture, there is an overall enhancement in D_U values, which decrease with increase in aqueous phase acidity. This enhancement in extraction with binary mixture may be explained as due to the formation of synergistic adduct species. The synergistic extraction is due to the more organophilic nature of the extracted species formed by the enhanced dehydration of uranium by neutral extractants. At low acidity, the synergistic coefficient (S.C.) for uranium extraction varies with the basicity of neutral oxodonors, i.e. TOPO > TBP > DOSO > MIBK [130]. The S.C. values increase with aqueous phase acidity up to ~ 2-3 M HNO₃ for all the neutral donors (except TOPO), and thereafter decrease marginally. The different behavior appears to be due to larger interaction of TOPO with HNO₃ resulting reduced free TOPO concentration available for adduct formation.

Table 3.2. Variation of D_U with nitric acid concentration; [U(VI)]: 2×10^{-3} M; Extractant(s): 3×10^{-2} M TBP, 3×10^{-2} F PC88A and their mixture in *n*-dodecane; T: 298 K

[HNO ₃], M	D_1	D_2	D_{mix}	ΔD	<i>S.C.</i>
0.05	0.02	15.2	34.4	19.2	0.36
1	0.04	5.64	24.9	19.2	0.64
2	0.14	2.13	20.5	18.3	0.96
3	0.21	1.76	16.8	14.8	0.93
4	0.32	1.85	13.7	11.5	0.80
5	0.58	1.89	12.7	10.2	0.71
6	0.45	2.32	11.8	9.0	0.63

$D_1: 3 \times 10^{-2}$ M TBP, $D_2: 3 \times 10^{-2}$ F PC88A, $D_{mix}: 3 \times 10^{-2}$ M TBP + 3×10^{-2} F PC88A

Table 3.3. Variation of D_U with nitric acid concentration; [U(VI)]: 2×10^{-3} M; Extractant(s): 3×10^{-2} M TOPO, 3×10^{-2} F PC88A and their mixture in *n*-dodecane; T: 298 K

[HNO ₃], M	D_1	D_2	D_{mix}	ΔD	<i>S.C.</i>
0.05	73.8	15.2	907.8	818.8	1.00
1	72.3	5.64	524.3	446.4	0.83
2	71.9	2.13	480.6	406.6	0.81
3	45.2	1.76	299.4	252.4	0.80
4	31.6	1.85	194.5	161.0	0.76
5	25.9	1.89	168.3	140.5	0.78
6	22.7	2.32	145.0	119.9	0.76

$D_1: 3 \times 10^{-2}$ M TOPO, $D_2: 3 \times 10^{-2}$ F PC88A, $D_{mix}: 3 \times 10^{-2}$ M TOPO + 3×10^{-2} F PC88A;

Table 3.4. Variation of D_U with nitric acid concentration; [U(VI)]: 2×10^{-3} M; Extractant(s): 3×10^{-2} M DOSO, 3×10^{-2} F PC88A and their mixture in *n*-dodecane; T: 298 K.

[HNO ₃], M	D_1	D_2	D_{mix}	ΔD	S.C.
0.05	0.06	15.2	30.3	15.0	0.30
1	0.07	5.64	28.1	22.4	0.69
2	0.10	2.13	25.5	23.3	1.06
3	0.12	1.76	17.9	16.0	0.98
4	0.14	1.85	14.2	12.2	0.58
5	0.22	1.89	13.1	11.0	0.79
6	0.17	2.32	11.9	9.41	0.68

$D_1: 3 \times 10^{-2}$ M DOSO, $D_2: 3 \times 10^{-2}$ F PC88A, $D_{mix}: 3 \times 10^{-2}$ M DOSO + 3×10^{-2} F PC88A

Table 3.5. Variation of D_U with nitric acid concentration; [U(VI)]: 2×10^{-3} M; Extractant(s): 3×10^{-2} M MIBK, 3×10^{-2} F PC88A and their mixture in *n*-dodecane; T: 298 K

[HNO ₃], M	D_1	D_2	D_{mix}	ΔD	S.C.
0.05	0.01	15.2	16.3	1.11	0.03
1	0.03	5.64	6.53	0.86	0.06
2	0.05	2.13	3.26	1.08	0.17
3	0.08	1.76	2.83	1.00	0.19
4	0.15	1.85	2.78	0.78	0.14
5	0.20	1.89	2.70	0.61	0.11
6	0.25	2.32	2.62	0.05	0.01

$D_1: 3 \times 10^{-2}$ M MIBK, $D_2: 3 \times 10^{-2}$ F PC88A, $D_{mix}: 3 \times 10^{-2}$ M MIBK 3×10^{-2} F PC88A

3.3.1.5. Recovery of uranium from raffinate waste

3.3.1.5.1. Evaluation of different extractants

An attempt was made to optimize the conditions for the recovery of uranium from the raffinate solution (generated during uranium purification by TBP solvent extraction) through solvent extraction route using different extractants such as PC88A and oxodonors (TBP, TOPO, PC88A, DOSO) either alone or as their mixtures. **Table 3.6** shows the value of %E of uranium from a typical uranium raffinate waste containing 0.4 g/L U in 1.12 M HNO₃ medium using different extractants.

Table 3.6. Extraction of U(VI) from 0.4g/L uranyl nitrate raffinate at 1.12 M HNO₃ by various extractants; Diluent: *n*-dodecane; T: 298 K

Sr.No.	Extractant	% E
1	0.03 M TBP	10.5
2	1.1 M TBP	~ 90.0
3	3×10 ⁻² M DOSO	10.2
4	3×10 ⁻² F PC88A	87.4
5	3×10 ⁻² M TOPO	99.3
6	3×10 ⁻² F PC88A + 3×10 ⁻² M TBP	95.9
7	3×10 ⁻² F PC88A + 3×10 ⁻² M DOSO	96.9
8	3×10 ⁻² F PC88A + 3×10 ⁻² M TOPO	99.7

It is evident that any combination of PC88A with neutral donors gives high extraction of uranium (>95 %) due to synergistic effect and the order of synergism TOPO > DOSO > TBP, follows their basicities. Whereas quantitative extraction (>99 %) of uranium was achieved using 0.03 M TOPO/*n*-dodecane solution; only ~10 % uranium recovery was observed using 0.03 M TBP/*n*-dodecane solution as extractant. The highest extraction in case of TOPO is obviously due

to of its very high basicity ($K_H = 8.6$). However, the use of 1.1 M TBP or 3×10^{-2} F PC88A solutions in *n*-dodecane as extractants showed ~ 90 % uranium recovery from the waste solutions. These extractants were further evaluated by performing stripping studies. **Table 3.7** lists the stripping (%) data of uranium from various loaded organic phases employing 5 % $(\text{NH}_4)_2\text{CO}_3$, 8 M HCl and 8 M HNO_3 , as the strippants. 8 M HCl and 8 M HNO_3 are not effective strippants of uranium. Though 3×10^{-2} M TOPO either alone or its synergistic mixture with 3×10^{-2} F PC88A in *n*-dodecane showed quantitative recovery of uranium, its stripping from the organic phase was very poor. By contrast, other extract combinations of PC88A with TBP and DOSO displayed relatively easy stripping of uranium. In view of efficient extraction and stripping considerations, it is suggested that 30% TBP/*n*-dodecane or 3×10^{-2} F PC88A + 3×10^{-2} M TBP mixture in *n*-dodecane may be used for the recovery of uranium from raffinate solution. It is evident that only $(\text{NH}_4)_2\text{CO}_3$ can effectively strip uranium from the loaded organic phase.

Table 3.7. Stripping of uranium from loaded organic phases using various strippants; Diluent: *n*-dodecane; T: 298 K

Organic Phase	Stripping (%)		
	5% $(\text{NH}_4)_2\text{CO}_3$	8 M HCl	8 M HNO_3
1.1 M TBP [#]	> 95	--	--
3×10^{-2} F PC88A	90.8	9.2	98.0
0.03 M TOPO	29.3	1.1	11.1
3×10^{-2} F PC88A + 3×10^{-2} M TBP	98.0	7.3	17.3
3×10^{-2} F PC88A + 3×10^{-2} M DOSO	97.5	8.5	19.9
3×10^{-2} F PC88A + 3×10^{-2} M TOPO	< 1	< 1	< 1

[#]Water: ~ 45 % stripping in one stage

3.3.1.5.2. Uranium recovery from actual waste samples

Based on these studies, the recovery of uranium was attempted from different batches of uranyl nitrate raffinate waste samples of varying concentrations of uranium and nitric acid using 1.1 M TBP/*n*-dodecane as extractant and (NH₄)₂CO₃ as the strippant. It is evident from **Table 3.8** that three extraction stages are sufficient for quantitative recovery (~99.9 %) of uranium from uranyl nitrate raffinate waste. The extracted uranium could easily be stripped by 5 % (NH₄)₂CO₃ solution.

Table 3.8. Uranium recovery from different batches of uranyl nitrate raffinate (UNR) waste; Extractant: 1.1 M TBP/*n*-dodecane; O/A: 1; T: 298 K

Batch No.	[HNO ₃]	[U(VI)]; g/L	<i>D_U</i>	%E [#]
1	2.0	1.35	11.5	92.0
2	1.7	0.35	8.7	89.7
3	1.97	0.34	9.3	90.3
4	1.72	0.39	8.3	89.2
5	1.76	0.35	7.8	88.6
6	1.73	0.46	8.8	89.8

[#]: one stage

3.3.2. Extraction of U(VI) from nitric acid medium with DNPPA and neutral donors

Synergistic extraction of metal ions has been noted in several extraction systems [115,119,121, 129,130]. The present study deals with the synergistic extraction of U(VI) by organophosphorous compounds such as DNPPA in combination with TBP, TEHP, Cyanex 923 in *n*-paraffin medium.

3.3.2.1. Effect of nitric acid and extractant concentration

Figure 3.6 shows the variation of distribution ratio values of U(VI) with aqueous phase acidity (1-8 M HNO₃) and uranium concentration (1×10⁻³ -1×10⁻² M) employing using 1×10⁻² M DNPPA solution in *n*-paraffin as extractant. The D_U values decreased gradually with increased nitric acid

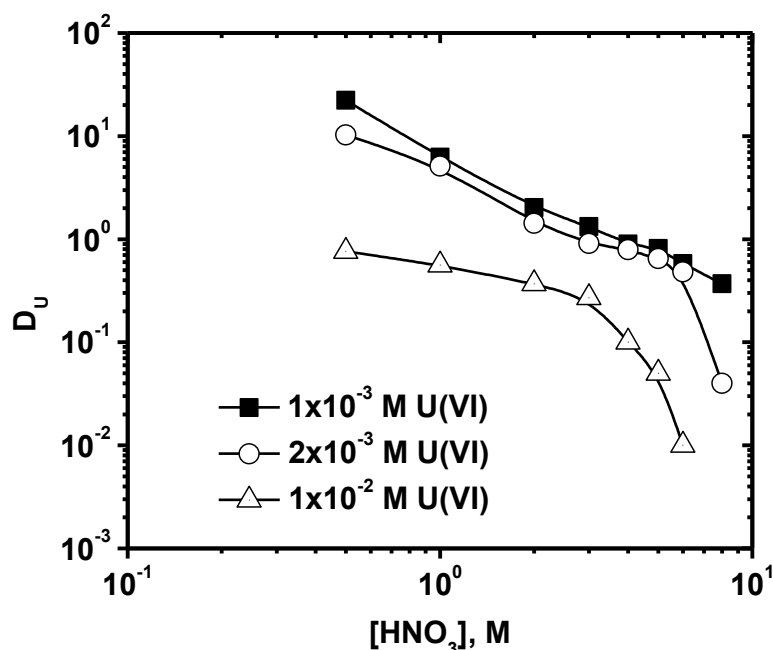


Figure 3.6. Variation of D_U with aqueous phase acidity; [DNPPA]: 0.01 M; Diluent: *n*-paraffin; T: 298 K

and uranium concentrations in the aqueous phase. This observation was attributed to acidic nature of DNPPA and that of uranium loading in the organic phase. The decrease in uranium extraction with aqueous phase acidity is typical of acidic extractants suggesting the involvement of cation exchange mechanism. Similar observations have been reported during the extraction of uranium using other acidic extractants such as D2EHPA, DOPPA, PC88A, and Cyanex 272 (bis(2,4,4-trimethylpentyl)phosphinic acid) in different aqueous media [116, 82, 83, 84,129]. The

extraction mechanism and stoichiometry of the extracted species in organic phase were determined using slop techniques. **Figure 3.7** shows the variation of $\log D_U$ with $\log [H^+]$ at a fixed nitrate ion concentration (3 M) with a slope of ~ 2 . This indicates that for each mole of complex formation, there is liberation of at least two moles of H^+ ions in the aqueous phase.

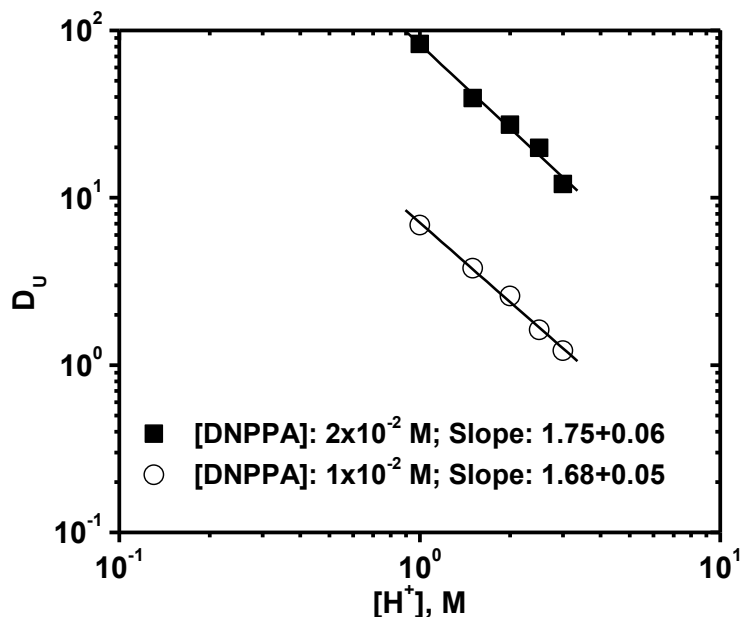


Figure 3.7. Variation of D_U with hydrogen ion concentration; $[U(VI)]: 1 \times 10^{-3}$ M; Diluents: *n*-paraffin; $[NO_3^-]: 3$ M; T: 298 K

Figure 3.8 represents the variation of $\log D_U$ with $\log [H_2A_2]$ at fixed nitric acid concentration (3 M) with a slope ~ 2 . This suggests that two moles of DNPPA dimer are associated with each mole of uranium extracted in the organic phase. However, nitrate ions are not a part of the moiety extracted in the organic phase. Based on these observations, the stoichiometry of the extracted species in the organic phase was proposed as $UO_2(HA_2)_2$ where HA and H_2A_2 are the monomeric and dimeric forms of DNPPA, respectively.

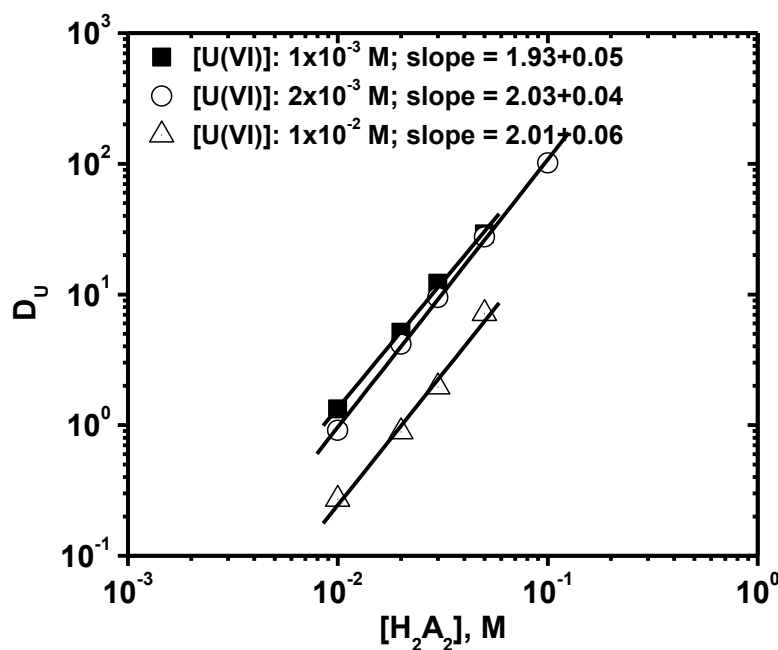
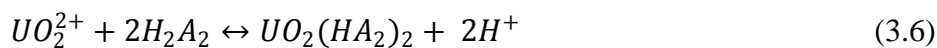


Figure 3.8. Variation of D_U with DNPPA concentration; $[\text{HNO}_3]$: 3 M; Diluent: *n*-paraffin; T: 298 K

The extraction mechanism of uranium in HNO_3 medium using DNPPA can be shown as follows:



$$K_{ex} = \frac{([\text{UO}_2(\text{HA}_2)_2]_{org} [\text{H}^+]_{aq}^2)}{([\text{UO}_2^{2+}]_{aq} [\text{H}_2\text{A}_2]_{org}^2)} \quad (3.7)$$

$$K_{ex} = \frac{(D_U [\text{H}^+]_{aq}^2)}{[\text{H}_2\text{A}_2]_{org}^2} \quad (3.8)$$

$$\log D_U = \log K_{ex} + 2 \log [\text{H}_2\text{A}_2] - 2 \log [\text{H}^+] \quad (3.9)$$

where ‘aq’ and ‘org’ represent the aqueous and organic phases, respectively and K_{ex} is the conditional extraction constant. It is interesting to note that nitrate ion is not involved in the extracted species of U(VI) with DNPPA. However, with increased nitric acid concentration in the aqueous phase, nitrate ion gets involved in the extracted species as $\text{UO}_2(\text{NO}_3)(\text{HA}_2) \cdot \text{H}_2\text{A}_2$ [131].

3.3.2.2 Comparison with other acidic organophosphorous extractants

Figure 3.9 shows the extraction of U(VI) from nitric acid medium using various acidic organophosphorous extractants like DNPPA, D2EHPA, PC88A and Cyanex 272 (0.02 M) in *n*-paraffin under identical conditions. It was observed that for DNPPA, D_U decreased with increased in HNO_3 concentration (up to 8 M) conforming cation exchange mechanism of U(VI) extraction.

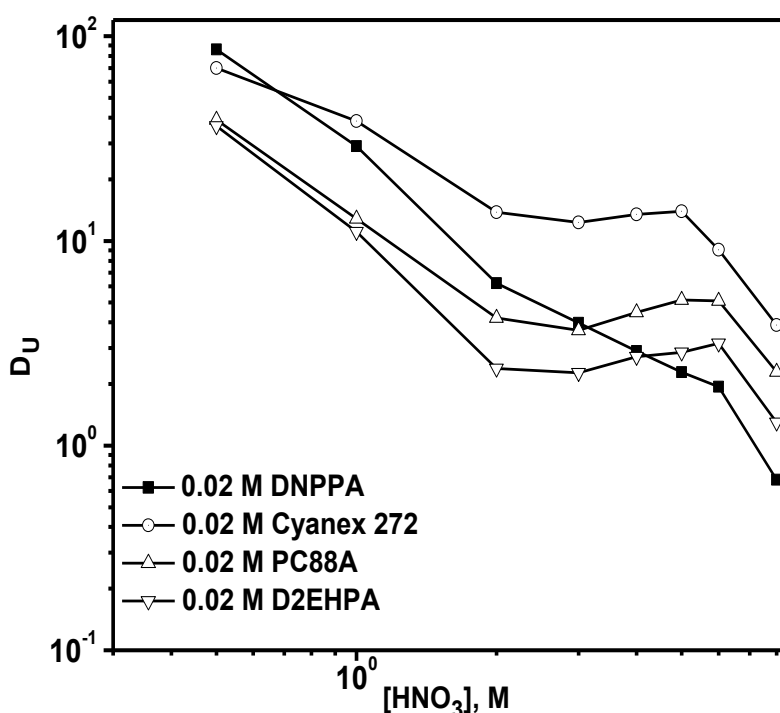


Figure 3.9. Comparison of variation of D_U with nitric acid concentration using various organophosphorous acidic extractants; [U(VI)]: 0.1 M; Diluent: *n*-paraffin; T: 298 K

Similarly, for D2EHPA, PC88A and Cyanex 272, D_U decreased with increased in HNO_3 concentration up to 3M and then increased up to 5 M (6 M for D2EHPA) beyond 5 M D_U decreased. Extraction of U(VI) using D2EHPA, PC88A and Cyanex 272 at low HNO_3 concentration occurred via cation exchange mechanism (up to 3M) and above 3 M via salivation mechanism [116,82,83,84,129]. The order of U(VI) extraction using various organophosphorous extractants up to 3M is: Cyanex 272 > DNPPA > PC88A > D2EHPA and above 4M: Cyanex

272 > PC88A > D2EHPA > DNPPA. The U(VI) extraction profile from HNO₃ can be explained on the basis of pK_a values of the extractants. The anomalous behavior of DNPPA at low HNO₃ concentration may be due to presence of phenyl substituents in the extractant.

3.3.2.3. Synergistic extraction

Addition of neutral donors to DNPPA like TBP, TEHP, Cyanex 923 increase the distribution ratio of U(VI) significantly as compared to pure extractants. This phenomenon is called synergism in hydrometallurgy. **Tables 3.9, 3.10** and **3.11** represent the distribution ratio, D_U and synergistic coefficient (S.C.) values for 2×10^{-2} M DNPPA in combination with 2×10^{-2} M neutral donors (dissolved in *n*-paraffin) at 0.5-8 M HNO₃. As expected, the D_U values for TBP/TEHP increased with acid concentration and maximum was attained at 4-5 M HNO₃ and those with DNPPA decreased sharply with increased nitric acid concentration in the aqueous phase. However, the D_U values were higher in the case of Cyanex 923 at lower acidities. Interestingly, there was a synergistic enhancement in D_U values for binary mixtures of DNPPA – TBP/TEHP/Cyanex 923 mixtures at lower acidities, which decreased at higher nitric acid concentrations. This enhancement in extraction with extractant mixtures was attributed to the formation of hydrophobic adducts. The synergistic coefficient (S.C.) calculation showed that the synergistic effect by the neutral donors followed the order: Cyanex 923 >> TBP ≥ TEHP. The higher synergism in case of Cyanex 923 was due its higher basicity ($K_H = 8.5$) [82] and lower enhancement in the case of TEHP was attributed to the steric hindrance exerted by branched 2-ethylhexyl group. DNPPA being acidic in nature extracts U(VI) from nitric acid medium by cation exchange mechanism and D_U value decrease with increase in aqueous phase acidity. Similar observations were made during the extraction of uranium using acidic extractants like DEHPA, PC88A, and Cyanex 272 and their mixtures with neutral oxodonors [116, 82,129].

Table 3.9. Variation of D_U with nitric acid concentration; [U]: 2×10^{-3} M; Extractant(s): 2×10^{-2} M TBP, 2×10^{-2} M DNPPA and their mixture in *n*-paraffin; T: 298 K

[HNO ₃], M	D_1	D_2	D_{mix}	ΔD	S.C.
0.5	0.02	86.03	222.32	136.27	0.41
1	0.06	29.05	131.27	102.16	0.65
2	0.9	6.22	29.48	22.36	0.62
3	0.12	3.98	19.86	15.76	0.68
4	0.14	2.89	13.43	10.40	0.65
5	0.15	2.28	10.08	7.65	0.62
6	0.11	1.94	7.51	5.46	0.56
8	0.07	0.68	2.93	2.18	0.59

D_1 : 2×10^{-2} M TBP, D_2 : 2×10^{-2} M DNPPA, D_{mix} : 2×10^{-2} M TBP + 2×10^{-2} M DNPPA

Table 3.10. Variation of D_U with nitric acid concentration; [U]: 2×10^{-3} M; Extractant(s): 2×10^{-2} M TEHP, 2×10^{-2} M DNPPA and their mixture in *n*-paraffin; T: 298 K

[HNO ₃], M	D_1	D_2	D_{mix}	ΔD	S.C.
0.5	0.06	86.03	214.19	128.1	0.39
1	0.11	29.05	99.89	70.73	0.54
2	0.13	6.22	21.77	15.42	0.54
3	0.17	3.98	14.77	10.62	0.55
4	0.21	2.89	10.46	7.36	0.53
5	0.33	2.28	8.08	5.47	0.49
6	0.18	1.94	6.75	4.63	0.50
8	0.09	0.68	2.63	1.86	0.53

D_1 = 2×10^{-2} M TEHP, D_2 = 2×10^{-2} M DNPPA, D_{mix} = 2×10^{-2} M TEHP + 2×10^{-2} M DNPPA

Table 3.11. Variation of D_U with nitric acid concentration; [U]: 2×10^{-3} M; Extractant(s): 2×10^{-2} M Cyanex 923, 2×10^{-2} M DNPPA and their mixture in *n*-paraffin; T: 298 K

[HNO ₃], M	D_1	D_2	D_{mix}	ΔD	S.C.
0.5	156.13	86.03	3927.26	3685.1	1.21
1	83.63	29.05	3233.33	3120.65	1.46
2	37.25	6.22	1193.88	1150.41	1.44
3	24.10	3.98	736.52	708.44	1.42
4	16.64	2.89	559.89	540.36	1.46
5	14.36	2.28	421.59	404.95	1.40
6	11.32	1.94	309.73	296.47	1.37
8	3.71	0.68	91.66	87.27	1.32

D_1 : 2×10^{-2} M Cyanex 923, D_2 : 2×10^{-2} M DNPPA, D_{mix} : 2×10^{-2} M Cyanex 923 + 2×10^{-2} M DNPPA

3.4. Conclusions

PC88A in combination with neutral extractants such as TBP, TOPO, and DOSO shows synergistic enhancement in uranium extraction from nitric acid medium (0.5-6 M HNO₃). The extracted species of uranium using PC88A as extractant were identified as UO₂(NO₃)(HA₂)·H₂A₂ (low acidity: < 3 M HNO₃) and UO₂(NO₃)₂·2(H₂A₂) (high acidity: > 3 M HNO₃). Use of MIBK as diluent also showed significant enhancement in uranium due to synergistic extraction. Temperature variation studies using PC88A as extractant showed exothermic nature of extraction process and stripping was more favored at elevated temperatures. Batch extraction studies were carried out to optimize the conditions for the recovery of uranium from raffinate generated during the purification of uranium using different extractants. 1.1M

TBP was the more efficient extractant and 5% $(\text{NH}_4)_2\text{CO}_3$ was the most effective uranium stripping agent.

Similarly, extraction of U(VI) from nitric acid medium using DNPPA showed that with increase in acid concentration there was a decrease in D_U , indicating cation exchange mechanism of the U(VI) extraction. Slope ratio analysis indicate the formation of $\text{UO}_2(\text{HA}_2)_2$ type of complex in the organic phase. Presence of neutral donors like TBP, TEHP and Cyanex 923 along with DNPPA in the organic phase increase D_U due to synergism and calculation of synergistic coefficient showed the order of synergism: Cyanex 923 \gg TBP \geq TEHP.

CHAPTER IV

**EMPERICAL MODELING OF SOLVENT EXTRACTION DATA
OF U(VI) FROM SULPHATE MEDIUM USING PC88A AND
NEUTRAL OXODONORS**

4.1. Introduction

Organophosphorous class of extractants finds an important place due to their wide ranging hydrometallurgical applications in the front- and the back-end of nuclear fuel cycle. Several extractants such as tri *n*-butyl phosphate (TBP), tri *n*-Octyl phosphine oxide (TOPO), di (2 ethyl hexyl) phosphoric acid (D2EHPA), 2-ethyl hexyl phosphonic acid 2-ethyl hexyl monoester (PC88A), and di(octylphenyl) phosphoric acid (DOPPA) have been extensively evaluated and used for the recovery of various metal values e.g., uranium from various sources mainly acidic solutions [116,82,83,84,129]. Based on the experimental data, there is a need to develop suitable models for predicting the extraction behavior of metal ions under specified experimental conditions. It should be noted that stoichiometric equilibrium constants for the extraction of nitric acid and of metal ions like UO_2^{2+} with extractants like TBP cannot be universal. Therefore, it can not characterize the extraction isotherm in the whole range of nitric acid, uranyl nitrate, and TBP concentrations. Thermodynamic equilibrium constants, on the other hand, involving activities of the interacting/extracting species can help in such predictions. However, a complete thermodynamic description of the distribution equilibrium has been difficult to realize due to the limited knowledge of organic-phase activities of the extracting species. In this context, the developments of empirical correlations/ mathematical models based on different chemical equilibria appear to be a good compromise approach. Kolarik reported the development of empirical calculation methods, yielding apparent concentration equilibrium constants or distribution ratios as a function of different concentration variables for TBP dissolved in an alkane as extractant and uranyl nitrate/nitric acid in the aqueous phase [132]. Jozef *et al.* developed relatively simple relationships for the simultaneous distribution of nitric acid and

uranyl nitrate for a wide range of TBP concentrations. These equations were used to predict distribution data for the extraction system in uranium processing technology and in reprocessing of spent nuclear fuel [133]. This model found applications in the computation of the steady-state concentrations of metal ion/nitric acid, distribution coefficients, and the number of theoretical stages, which permits the determination of the efficiency of extraction processes and optimization for nitric acid and uranyl nitrate distribution in a countercurrent apparatus.

PC88A is an acidic extractant ($pK_a = 7.1$) and is a close analog of D2EHPA. Several studies are reported in literature on the extraction behavior of metal ions like U(VI), Th(IV) and Zr(IV) from various aqueous media [80-87]. These studies were aimed at understanding the extraction mechanism under varying experimental conditions such as nature of acid/diluent etc. Some interesting observations were made during the synergistic extraction of U(VI) from HCl medium using the mixtures of PC88A and neutral oxodonor like TBP, TOPO, Cyanex 923 (a mixture of four trialkyl phosphine oxides viz. R_3PO , $R_2R'PO$, RR'_2PO and R'_3PO where R: *n*-octyl and R': *n*-hexyl chain) [82]. Synergistic enhancement in the extraction of U(VI) varied in the order: Cyanex 923 > TOPO > TBP. Whereas synergism in the extraction of U(VI) from HNO_3 and H_2SO_4 medium was observed for PC88A and Aliquat 336 (methyl octyl ammonium chloride) mixture; the presence of dialkyl amide or TBP showed antagonism in U(VI) extraction from H_2SO_4 medium [85]. The extraction behavior of Th(IV) from HNO_3 , H_2SO_4 and HCl media resulted in different extraction profiles [80,134]. These studies suggest that nature of aqueous phase, diluent and the neutral donors affect significantly the extraction behavior of metal ions.

4.2 The present work

The extraction of uranium from H_2SO_4 medium has been investigated using PC88A and a synergistic mixture of PC88A with neutral donors TOPO. Treatment of distribution data by slope

analysis technique showed the formation of a monomeric species $\text{UO}_2(\text{HA}_2)_2$. Formation of this species was also confirmed by non-linear least square regression of the distribution data to the mathematical expression correlating percentage extraction and acidity. The experimental data on the distribution ratio (D_U) of U(VI) against initial acidity (H_i) at varying initial uranium concentration (C_i) has been determined and utilized to develop a mathematical model correlating D_U with H_i and C_i .

4.3. Results and Discussion

4.3.1. Extraction of U(VI) studies from sulphate medium

Figure 4.1 shows the variation of D_U values with aqueous phase acid concentration (H_2SO_4) employing 0.3 M PC88A, 0.03 M TOPO, and 0.3 M PC88A + 0.03 M TOPO dissolved in *n*-dodecane as solvent. The D_U values decreased with increased acid concentration in the case of PC88A/ H_2SO_4 system.

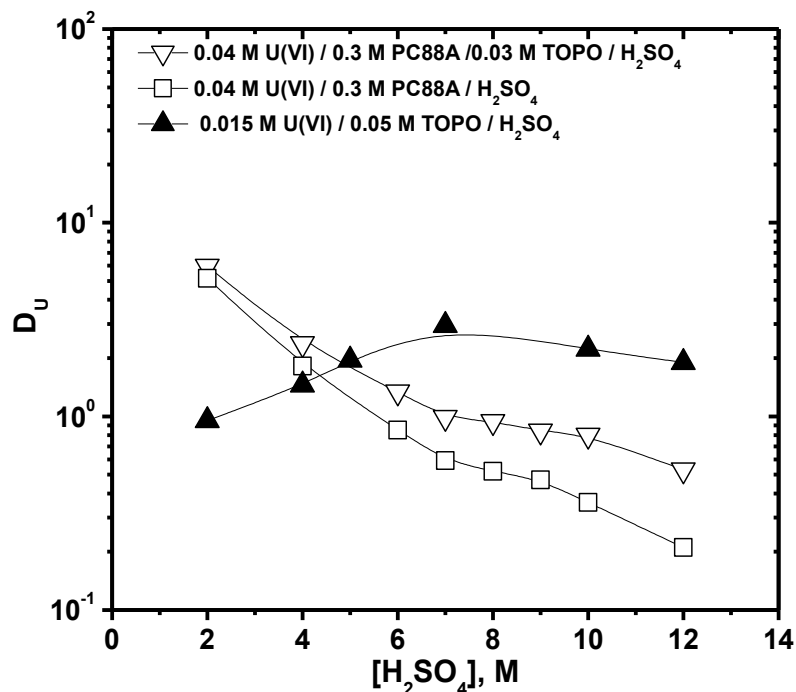
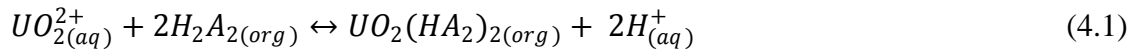


Figure 4.1. Variation of D_U with H_2SO_4 concentration; Diluent: *n*-dodecane; T: 298 K

This suggested that uranium extraction in sulphuric acid medium was predominantly by cation exchange mechanism. Sato reported a similar observation while extracting U(VI) from sulphuric acid medium using D2EHPA as extractant [135]. Similar trends were observed during the extraction of uranium for the mixtures of PC88A and TOPO as extractant from HCl and H_2SO_4 media, respectively [80,134]. A synergistic enhancement in the extraction of uranium was observed for PC88A and TOPO mixture irrespective of aqueous medium, however, HCl medium offered more extraction of uranium than that in H_2SO_4 medium [83,134]. Chetty *et al.* observed synergistic extraction of U(VI) from sulphate medium using the combination of D2EHPA and TBP or TOPO [86]. Even though, TOPO extraction led to higher D_U values in HCl than that in H_2SO_4 medium, the trend for the extraction of uranium for both these aqueous systems appeared to be similar. This behavior can be attributed to the higher stability constant values for uranium complexation with SO_4^{2-} ($\beta_1 = 1.81$ at $I = 1.0$) as compared to that of Cl^- ($\beta_1 = 0.1$ at $I = 1.0$).

4.3.2. Extraction equilibrium

Generally, alkyl phosphoric acid (HA) such as PC88A, D2EHPA etc. exist as dimers (H_2A_2) and the extraction of U(VI) with H_2A_2 dimer of PC88A can be expressed by the following equation: [134,135],



$$K_{ex} = \frac{([UO_2(HA_2)_2]_{(org)}[H^+]_{(aq)}^2)}{([UO_2^{2+}]_{(aq)}[H_2A_2]_{(org)}^2)} \quad (4.2)$$

$$D_U = \frac{[UO_2(HA_2)_2]_{(org)} \cdot [H^+]_{(aq)}^2}{[UO_2^{2+}]_{(aq)}} \quad (4.3)$$

$$K_{ex} = \frac{(D_U [H^+]_{(aq)}^2)}{[H_2A_2]_{(org)}^2} \quad (4.4)$$

Where K_{ex} is the conditional extraction constant and subscripts (aq) and (org) represent the aqueous and organic phases, respectively. Assuming that the activity coefficients of the species were constant under experimental conditions and that $[UO_2(A_2H)_2]_{(org)}$ and $[UO_2^{2+}]_{(aq)}$ were the only species in the organic and aqueous phase, no correction was applied to evaluate the D_U or K_{ex} values.

Taking logarithm and after rearranging, Equation 4.4 can be simplified as:

$$\log D_U = \log K_{ex} + 2 \log [H_2A_2]_{(org)} - 2 \log [H^+]_{(aq)} \quad (4.5)$$

The free $[H_2A_2]_{(o)}$ concentration was calculated as follows:

$$[H_2A_2]_{(free)} = [H_2A_2]_{(initial)} - n \cdot M_{(org)} \quad (4.6)$$

Where $[M]_{(org)}$ refers to the metal ion concentration in the organic phase.

4. 3.3. Stoichiometry of the extracted species

Slope analysis technique was employed for the determination of stoichiometry of the extracted species of U(VI) with PC88A in *n*-dodecane. **Figures 4.2 and 4.3** show the linear variation of $\log D_U$ vs $\log [H^+]$ at 0.5 M PC88A concentration and $\log D_U$ vs $\log [PC88A]$ concentration at fixed $[H^+] = 3$ M with a slope values of -2 and +2, respectively. These results conform to the formation of monomeric neutral complex species of the type $[UO_2(A_2H)_2]$ into the organic phase. Similar results have been reported elsewhere on the extraction of U(VI) by PC88A and its analog 2-ethylhexyl phenyl phosphonic acid from different acid solutions [**116, 82, 83, 84,129**]. **Table 4.1** lists the relation between D_U and $[H^+]$ along with corresponding correlation coefficients obtained by least square regression method. The intercept term corresponds to the terms $\log K_{ex} + x \log [H_2A_2]$ for different concentrations of uranium(VI) in the aqueous phase. These

values decrease with increased uranium concentration in the aqueous phase, which is attributed to the decrease in free $[H_2A_2]$ concentration with increased metal ion loading in the organic phase. **Equation (4.5)** indicates that the $\log D_U$ varies linearly with $\log[H_2A_2]$ at a fixed aqueous phase acidity. Based on least square method (**Figures 4.3**), the relation between $\log D_U$ and $\log[H_2A_2]$ for the extraction of U(VI) with PC88A was obtained as:

$$\log D_U = (1.98) + 1.92 \log[H_2A_2]; R: 0.998 \quad (4.7)$$

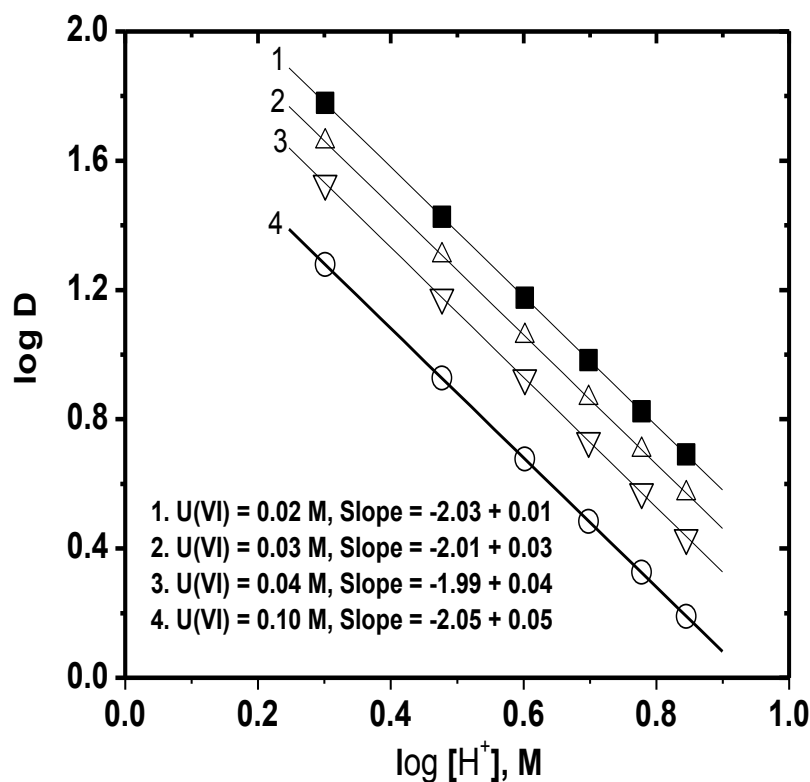


Figure 4.2. Effect of $[H^+]$ on distribution ratio of uranium; [PC88A]: 0.05 M; Diluent: *n*-dodecane; T: 298 K

Table 4.1. Relation between $\log D_U$ and $\log [H^+]$ for the extraction of various concentrations of U(VI) with PC88A in *n*-dodecane

[U(VI)], M	Expression	Correlation Coefficient, R
0.02	$\log D_U = 2.38 - 2.03 \log [H^+]$	0.999
0.03	$\log D_U = 2.26 - 2.01 \log [H^+]$	0.999

0.04	$\log D_U = 2.14 - 1.99 \log [H^+]$	0.999
0.10	$\log D_U = 1.88 - 2.05 \log [H^+]$	0.999

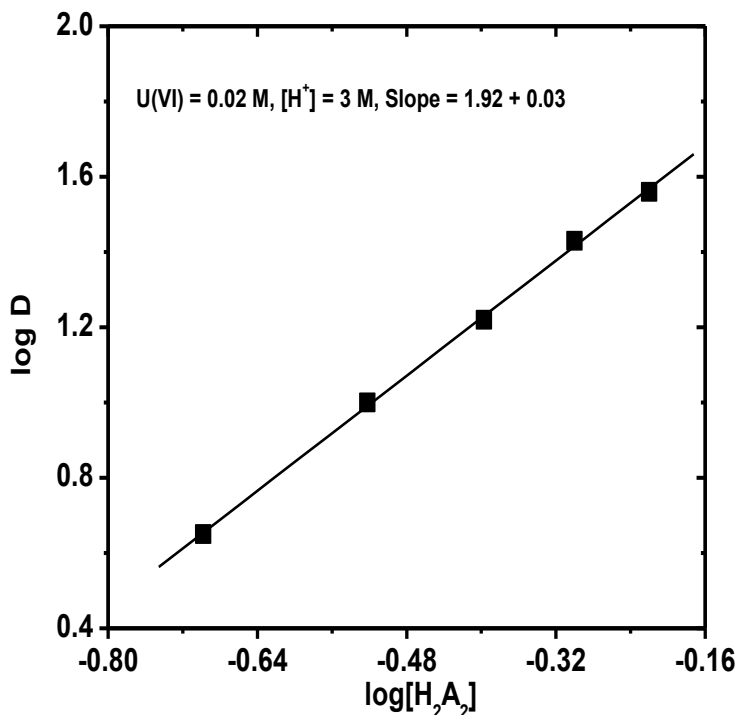


Figure 4.3. Dependence of distribution ratio on extractant concentrations for the extraction of U(VI); [U(VI)]: 0.02 M; [H⁺]: 3 M; Diluent: *n*-dodecane; T: 298 K

Tables 4.2 and **4.3** list the $\log K_{ex}$ values for various uranium and PC88A concentrations in *n*-dodecane. There is fairly good agreement in $\log K_{ex}$ values, which confirms the formation of proposed species described by **Equation 4.1**.

Table 4.2. $\log K_{ex}$ values at various uranium and H⁺ concentrations, [Extractant]: 0.5 M PC88A/*n*-dodecane; O/A: 1

[H _i], M	log K _{ex} at varying [U(VI)], M			
	0.02	0.03	0.04	0.10
2	3.73	3.71	3.68	3.65
3	3.72	3.71	3.67	3.63
4	3.72	3.70	3.68	3.64
5	3.71	3.69	3.64	3.63
6	3.70	3.68	3.62	3.65

7 3.70 3.69 3.63 3.62

Average $\log K_{ex} = 3.68 \pm 0.04$

Table 4.3. $\log K_{ex}$ values at various PC88A concentrations; [U(VI)]: 2×10^{-2} M; $[H^+]_i$: 3.0 M; O/A: 1

[PC88A], M	$\log K_{ex}$
0.2	3.80
0.3	3.75
0.4	3.73
0.5	3.72
0.6	3.68

Average $\log K_{ex} = 3.73 \pm 0.05$

4. 3.4. Non-linear least square regression

The results of slope analysis were verified by calculating the percent extraction (%E) at various uranium concentrations and acidities employing 0.5 M PC88A dissolved in *n*-dodecane using the following relation:

$$\%E = \frac{100K}{\{K + [H^+]^n\}} \quad (4.8)$$

where $K = K_{ex} \cdot [H_2A_2]^2$

The non-linear plots obtained using the mathematical software (ORIGIN 6.1) are shown in **Figure 4.4** and the corresponding values of *n* and K with chi square (χ^2) are given in **Table 4.4**. The lower values of χ^2 indicate good fit of the data to the predicted line. The values of *n*, i.e., the number of hydrogen ion liberated for each metal ion extracted for all the systems studied correspond to ~ 2 , which confirm the results of slope analysis technique. In addition, the

calculated $\log K_{ex}$ values (Table 4.4), are in reasonable agreement with those listed in Table 4.1 (obtained by linear fit equation). These results confirm that under the conditions of these studies, $UO_2(HA_2)_2$ was the predominant extractable species.

Table 4.4. Values of n , K and chi-square (χ^2) obtained by non-linear least square regression analysis of the extraction of different concentrations of uranium (C_i) from sulphate medium using 0.5 M PC88A in n -dodecane as the extractant, O/A: 1

$[C_i], M$	n	$\log K_{ex}$	χ^2
0.02	2.06	2.38	3.0×10^{-4}
0.03	1.99	2.24	1.6×10^{-2}
0.04	2.03	2.15	1.1×10^{-2}
0.10	2.09	1.87	1.5×10^{-2}

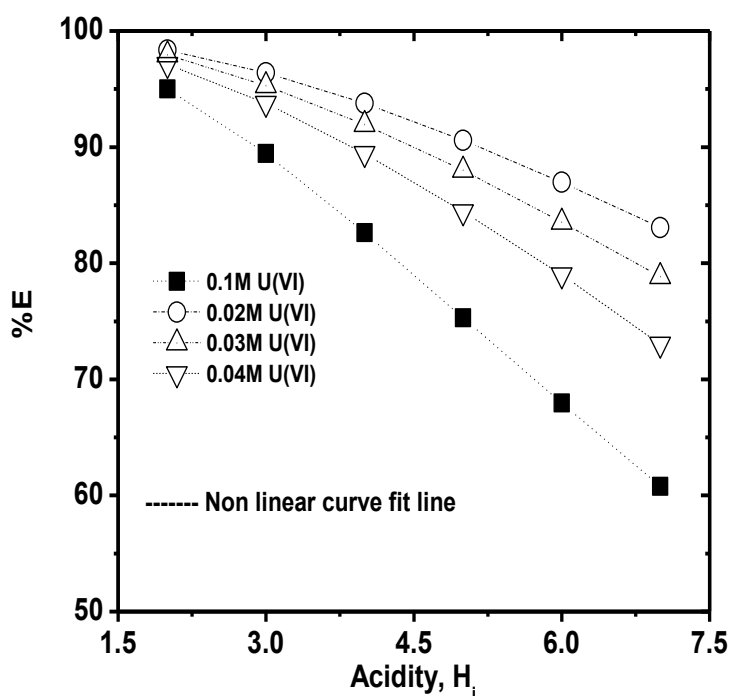


Figure 4.4. Non linear least square regression plot for the extraction of various concentrations of U(VI) with 0.5 M PC88A; Diluent: n -dodecane; T: 298 K.

4. 3.5. Development of mathematical model

A mathematical model correlating D_U with initial uranium concentration (C_i) and acidity (H_i) was developed using ORIGIN 6.1 software. The data of D_U and H_i at various concentrations of uranium were fitted to the equation:

$$D_U = \frac{K_i}{[H_i]^2} \quad (4.9)$$

where K_i is a constant = $K_{ex} \cdot [H_2A_2]^x$ and the term x represents the number of extractant molecules attached to the metal ion in the extracted species. The generated values of D_U decreased with increased C_i and H_i values. **Figure 4.5** shows the variation of D_U with $[H_i]$ at various concentrations of uranium.

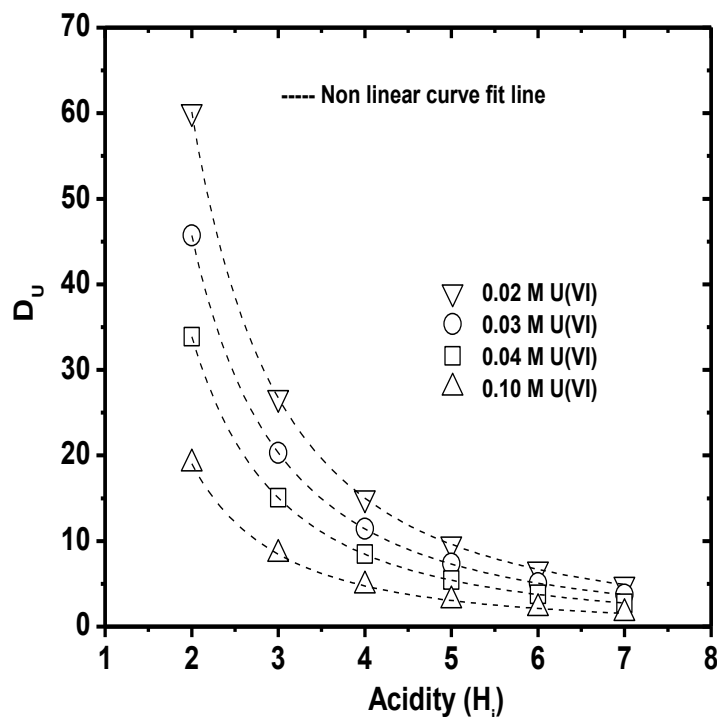


Figure 4.5. Dependence of distribution ratio on acidity at various concentrations of U(VI); [PC88A] : 0.5 M; Diluent: *n*-dodecane, T: 298 K

The values of K_i for each C_i (**Table 4.5**) vary inversely and therefore can be represented as:

$$K_i = K^* \cdot (C_i)^{-n} \quad (4.10)$$

where K^* is a curve fitting parameter and is a constant, and n is another constant. Further, using a mathematical software the values of K_i and C_i were fitted using **equation (4.10)** to obtain the values of K^* and n . The best fit data values of K^* and of n were found to be $12.98(\pm 0.90)$, and $-0.75(\pm 0.05)$, respectively. Using these values, one can express K_i in terms of C_i (Equation 3.26) and finally D_U (**Equation 4.9**) can be calculated using the following relation:

$$D_U = \frac{12.98 (\pm 0.90)}{\{C_i^{-0.75 (\pm 0.05)} [H_i]^2\}} \quad (4.11)$$

Table 4.5. Values of n , K and chi-square (χ^2) obtained by non-linear least square regression analysis of the extraction of different concentrations of uranium (C_i) from sulphate medium using 0.5 M PC88A in *n*-dodecane as the extractant, O/A: 1

$[C_i], M$	n	$\log K_{ex}$	χ^2
0.02	2.06	2.38	3.0×10^{-4}
0.03	1.99	2.24	1.6×10^{-2}
0.04	2.03	2.15	1.1×10^{-2}
0.10	2.09	1.87	1.5×10^{-2}

Equation (3.27) is a general mathematical expression for the extraction of uranium from sulphate medium using PC88A under the experimental conditions of this study. This model may find application in predicting the concentration of uranium ion in the organic and the aqueous phases at any initial concentration of uranium and at any acidity. **Figure 4.6** is the parity plot showing fairly good agreement in the calculated and experimental D_U values obtained in this study.

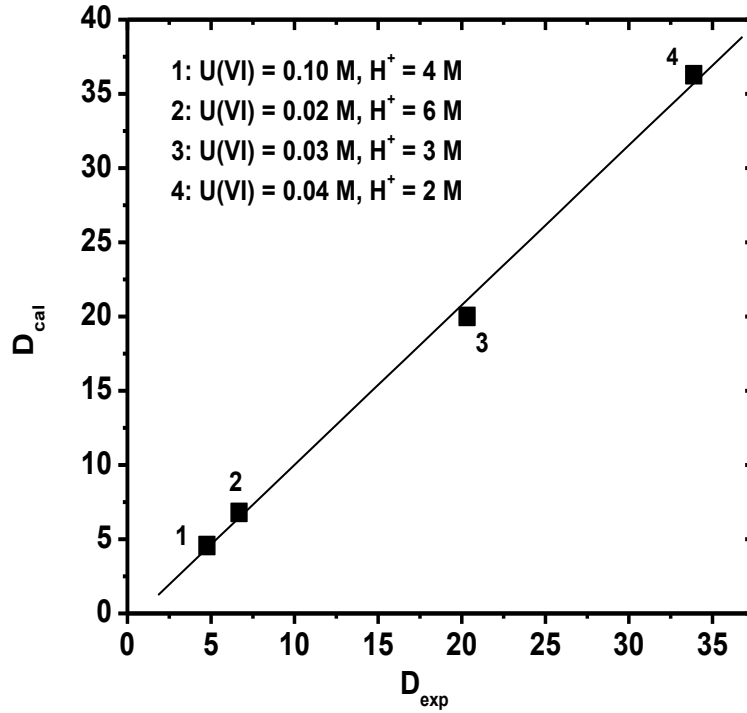
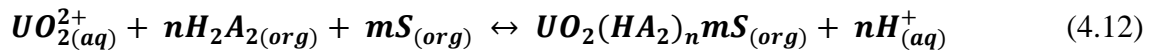


Figure 4.6. Plot of D_{exp} vs D_{cal} using mathematical model; Refer **Equation 4.11**

4. 3.6. Mathematical model for synergistic extraction

The two phase extraction mechanism of U(VI) by synergistic mixture of PC88A and TOPO (S) (**Figure 4.1**) can be expressed as:



$$K_{ex,syn} = \frac{\{[UO_2(HA_2)_n mS]_{(org)}[H^+]_{(aq)}^n\}}{\{[UO_2^{2+}]_{(aq)}[H_2A_2]_{(org)}^n[S]_{(org)}^m\}} \quad (4.13)$$

Where $K_{ex,syn}$ is the conditional extraction constant using synergistic mixture. Assuming that the activity coefficients of the species involved in the extraction process were constant under experimental conditions, the values of n and m were determined by conducting uranium extraction experiments at 3 M $[H^+]$ (i) at varying PC88A concentrations in the presence of 0.015 M TOPO, and (ii) at varying concentration of TOPO in the presence of fixed concentration of

PC88A. The relationship between $\log D_U$ and $\log [H_2A_2]$ at constant TOPO concentration obtained by non-linear regression (**Figure 4.7**) for the extraction of U(VI) can be written as:

$$\log D_U = (2.46) + 1.88 \log [H_2A_2]; R: 0.999 \quad (4.14)$$

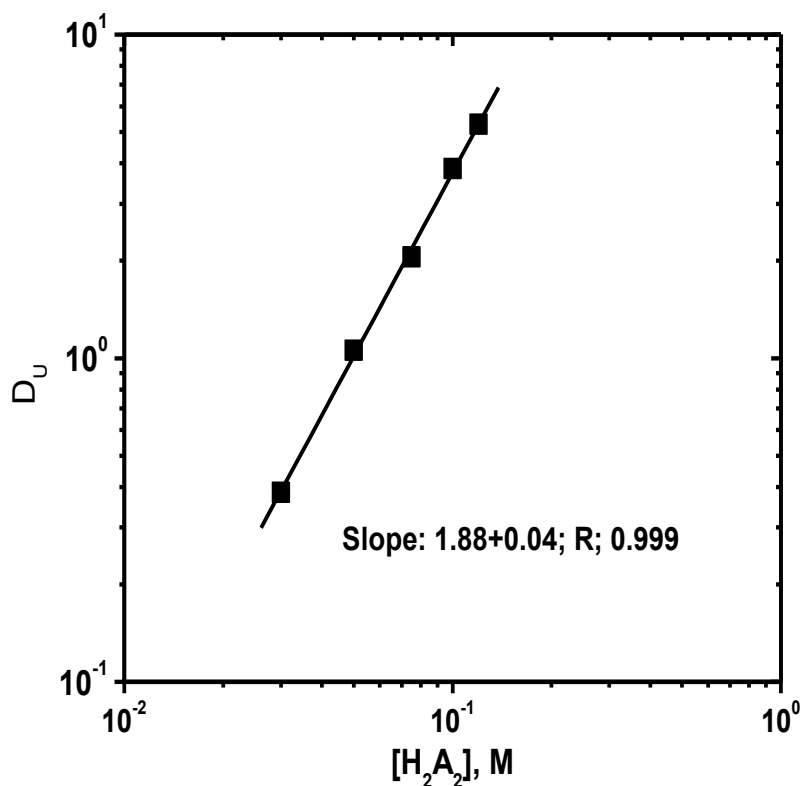


Figure 4.7. Variation of % extraction (% E) of U(VI) with PC88A concentration at constant neutral donor (TOPO) concentration; [U(VI)]: 0.015 M; [TOPO] : 0.015 M; [H⁺]: 3 M

Similarly, the relationship between $\log D_U$ and $\log [TOPO]$ at constant PC88A concentration obtained by non-linear regression for the extraction of U(VI) (**Figure 4.8**) can be written as:

$$\log D_U = (2.30) + 0.93 \log [TOPO]; R: 0.994 \quad (4.15)$$

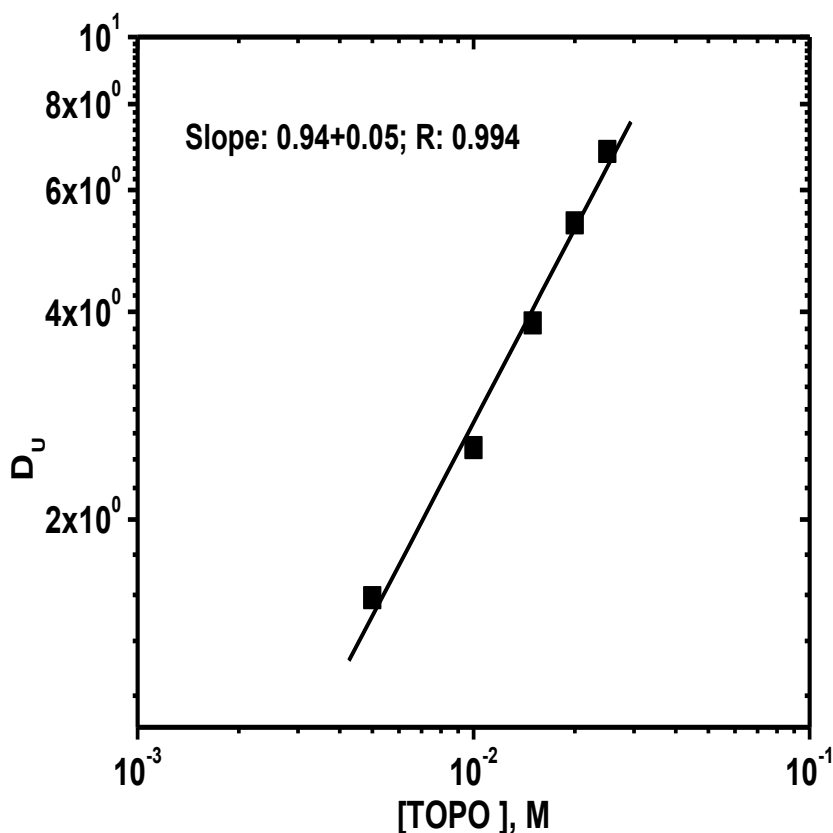


Figure 4.8. Variation of % extraction (% E) of U(VI) with TOPO concentration at constant PC88A concentration; [U(VI)]: 0.015 M; [PC88A] : 0.1 M; [H⁺]: 3 M

The values of n and m obtained from the slopes (**Equations 4.14 and 4.15**) suggested the formation of neutral complex species of the type $[UO_2(A_2H)_2 \cdot TOPO]$ into the organic phase. The non-linear least square regression method was applied to authenticate the findings of slope analysis technique, for the present system. For organic-to-aqueous phase ratio (O/A) as 1, the %E can be calculated from D_U values using the following relation:

$$E = \frac{100D_U}{(1 + D_U)} \quad (4.16)$$

Using equation (4) and (6), the relation between E with the extractants' (S and PC88A) concentration can be shown as:

$$E = 100 \cdot A \cdot S^m / (A \cdot S^m + 1) \quad (4.17)$$

This equation is valid for a fixed concentration of PC88A, and

$$A = K_{ex} \cdot [H_2A_2]_{(org)}^n / [H^+]_{(aq)}^n \quad (4.18)$$

When concentration of neutral donor, S, is kept constant, it can be written as:

$$E = (100 \cdot A \cdot [H_2A_2]^n) / (A \cdot [H_2A_2]^n + 1) \quad (4.19)$$

where $A = K_{ex, syn} \cdot S^m_{(o)} / [H^+]^n_{(a)}$

Equations (18) and (19) represent the empirical relationship between percentage extraction of uranium with variation of TOPO and PC88A concentrations. The value of A , n and m can be obtained by plotting the % extraction (E) with concentration of H_2A_2 (PC88A) and S (TOPO) and the results are summarized in **Table 4.6**. Origin 6.1 mathematical software was used to calculate the values of $\%E_{cal}$ employing **Equations 4.18** and **4.19** under varying experimental conditions. These empirical relationships were found to be useful in predicting the extraction behavior of U(VI) (a) with varying PC88A concentration and at fixed TOPO concentration, and (b) with varying TOPO concentration and at fixed PC88A concentration as shown in parity plot (**Figure 4.9**).

Table 4.6. Values of n and chi-square (χ^2) and log A obtained by non-linear regression analysis for extraction of U(VI)

Experimental condition(s)	n or m	log A	χ^2
Varying [PC88A] at fixed [S]	1.94	2.54	0.93
Varying [TOPO] at fixed [H_2A_2]	0.92	2.46	0.72

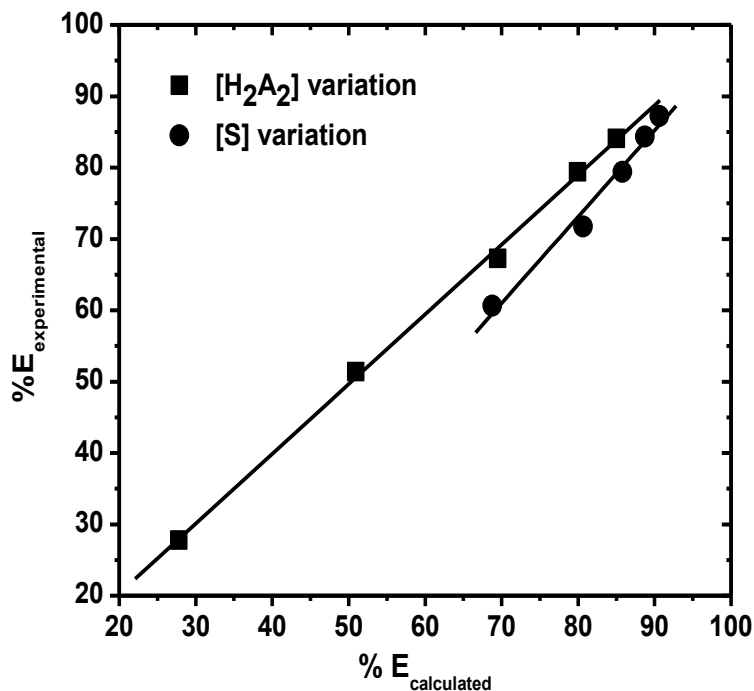


Figure 4.9. Plot of % E_{exp} vs % E_{cal} using mathematical model

4. 4. Conclusions

The extraction of uranium from sulphate medium using with PC88A in *n*-dodecane has indicated the formation of a monomeric neutral complex $[UO_2(HA_2)_2]$ under the conditions of present study. A mathematical model was developed correlating the distribution ratio of uranium with those of uranium concentration and the aqueous phase acidity which can be useful to predict the extraction behaviour of U(VI) with PC88A from sulphuric acid media. Uranium extraction profile using PC88A as extractant showed decrease in D_U values with increase in sulphuric acid concentration due to cation exchange mechanism. Using TOPO alone as the extractant, uranium extraction increased up to 7 M in H_2SO_4 system and then decreased with increased acidity. By contrast, the mixture of PC88A and TOPO showed a synergistic enhancement in uranium extraction for sulphate media. A mathematical equation was developed correlating the %E of uranium with varying concentration of PC88A and TOPO at constant uranium concentration and

constant aqueous phase acidity. The model $D_U = 12.98(\pm 0.90) / \{C_i^{-0.75(\pm 0.05)} \times [H_i]^2\}$ can be used to predict the concentration of uranium in organic as well as in aqueous phase at any C_i and H_i . The extraction constant (K_{ex}) has been calculated. These mathematical correlations may find application in the computation of the steady-state concentrations of metal ion/acid, distribution coefficients, and the number of theoretical stages. This exercise permits the determination of the efficiency of extraction processes.

CHAPTER V

**SEPARATION OF U(VI) AND Th(IV) FROM MONAZITE
USING TRIS(2-ETHYLHEXYL) PHOSPHATE (TEHP)/ *n*-
PARAFFIN**

5.1. Introduction

Monazite is a phosphate ore of thorium and of rare earth elements (REEs) and it invariably contains relatively lower quantities of uranium. Therefore it is considered an important secondary source of uranium. India is blessed with vast resources of thorium as monazite sand which typically contains 0.35 % U_3O_8 , besides 60 % rare earths oxides (REOs), 8 % ThO_2 , 27 % $P_2O_5 \geq 3$ % insoluble materials and other minor oxides [136]. The presence of thorium along with uranium creates problems during recovery of uranium as yellow cake and hence needs to be separated [13]. The leaching of monazite leads to the dissolution of REEs along with U, Th and phosphate. It is performed by either of the following two routes: (i) the alkali leaching process using NaOH where U and Th are separated as hydroxides, and (ii) the acid leaching process employing concentrated sulphuric acid where liquor containing REEs elements, U and Th is generated [137-141]. The recovery of uranium from monazite leach solution called “*thorium concentrate*” is accomplished by a various methods [142-144]. Alamine 336 (trialkyl amine, C_8-C_{10}) is generally used as an extractant for uranium recovery from HCl leach solution of thorium concentrate obtained after processing of monazite minerals by caustic soda digestion. However, this extraction process has certain limitations such as: (a) corrosive nature of HCl medium, (b) low loading capacity of Alamine 336, (c) third-phase leading to crud formation, and (d) amine entrainment to the aqueous phase [15]. The alternate route is based on the use of tri-*n*-butyl phosphate (TBP)-Kerosene as the solvent for the separation of uranium from thorium concentrate dissolved in nitric acid. TBP plays an important role in the front-end and as well as in the back-end of nuclear fuel cycle [145-149]. Even though TBP is the work horse for nuclear industry, it is associated with certain limitations such as high tendency to form third-phase during the extraction of tetravalent metal ions such as Th(IV), Pu(IV), and Zr(IV), and high aqueous

solubility. The aqueous solubility of TBP can lead to the red-oil formation when aqueous solutions generated from solvent extraction process are subjected to volume reduction operations. The degradations products of TBP such as dibutyl phosphate (DBP) and monobutyl phosphate (MBP) create stripping problems of metal ion from organic phase. Crud formation tendency has also been studied which shows a decrease in the dispersion band heights [15]. In view of these problems, several studies have been performed for identifying alternative extractants for uranium recovery from different feed solutions. Suresh *et al.* reported the separation of U(VI) and Th(IV) by tri-*sec*-butyl phosphate (TsBP) and tri-*iso*-butyl phosphate (TiAP) as alternative for TBP [150,151]. Koladkar studied the separation of U(VI) and Th(IV) from nitric acid medium using bis(2-ethylhexyl) phosphinic acid (PIA) and di(2-ethylhexyl) phosphate (HDEHP) as extractants [152]. Higher homologs of TBP e.g. trihexyl phosphate (THP), tris(2-ethylhexyl) phosphate (TEHP) have been reported to have higher loading capacity for U(VI) as well as less tendency towards third-phase formation [153-155]. In addition, TEHP displays better separation for U(VI) over Th(IV) than TBP from nitric acid medium [153]. Pathak *et al.*, studied the separation of ^{233}U from a mixture of thorium uranium in nitric acid medium using di(2-ethylhexyl) isobutyramide (D2EHIBA) as extractant [156]. Mowafy and Aly. reported a higher separation factor of U(VI) and Th(IV) from nitric acid medium employing amides compared to TBP under comparable experimental conditions [157]. Separation of U(VI) from a mixture of U(VI) and Th(IV) has also been investigated using tetra(2-ethylhexyl) diglycolamide (TEHDGA) as an extractant [158]. It was of interest to compare the performance of TEHP and TBP as extractants (from same class) for selective recovery of U(VI) from a mixture of U(VI), Th(IV) and rare earths from nitric acid medium which may be relevant for the processing of monazite leach solutions.

5.2. The present work

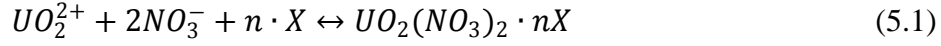
Separation of U(VI) from thorium in nitric acid medium, containing Th(IV) and a number of other metal ions has been investigated using TEHP in *n*-paraffin. Effect of experimental variables such as diluents, nitric acid concentration, extractant concentration, metal ion concentration etc. were investigated on the extraction of U(VI) and Th(IV). The effect of diverse cations such as Th(IV), Zr(IV), Y(III) on extraction of U(VI) has been investigated and results have been compared with same concentration of TBP under comparable conditions. It was observed that the separation factors of all the metal ions in case of TEHP are higher than for the same concentration of TBP at all nitric acid concentrations. The McCabe-Thiele diagrams for extraction and stripping of U(VI) using TEHP from has been constructed. A separation process flow-sheet was developed to recover U(VI) from thorium concentrate after dissolving it in nitric acid medium.

5.3. Results and Discussion

5.3.1. Extraction of U(VI) from nitric acid medium

Figure 5.1 represent the effect of nitric acid concentration on extraction of U(VI) by 1.1M TEHP/*n*-paraffin at different U(VI) concentration and results were compared with same concentration of TBP under comparable conditions. It was observed that with increase in nitric acid concentration the D_U value increase up to 5 M HNO₃ beyond which it is decrease for both the extractants, but at any nitric acid concentration the D_U value for 1.1M TEHP is always higher than for same concentration of TBP. The higher value of D_U for TEHP is due to the branching of alkyl group in second position of the carbon chain in tri alkyl phosphate. Suresh *et al.*, also observed similar trend for extraction of U(VI) from nitric acid medium using tri alkyl phosphate

[139]. The extraction mechanism of U(VI) from nitric acid medium using TEHP/TBP neutral organophosphorous extractant (X) can be summarized as:



At low acidity region, with increase in HNO₃ concentration D_U increase due to availability of more NO₃⁻ ions which acts as salting out agent for uranium extraction up to 5 M, beyond this the complexation of HNO₃ with extractant become predominate and there is a decrease in free extractant which decrease the extraction of uranium. The main difference of extraction behavior between Th(IV) and U(VI) is the rate of increase of distribution ratio with nitric acid concentration.

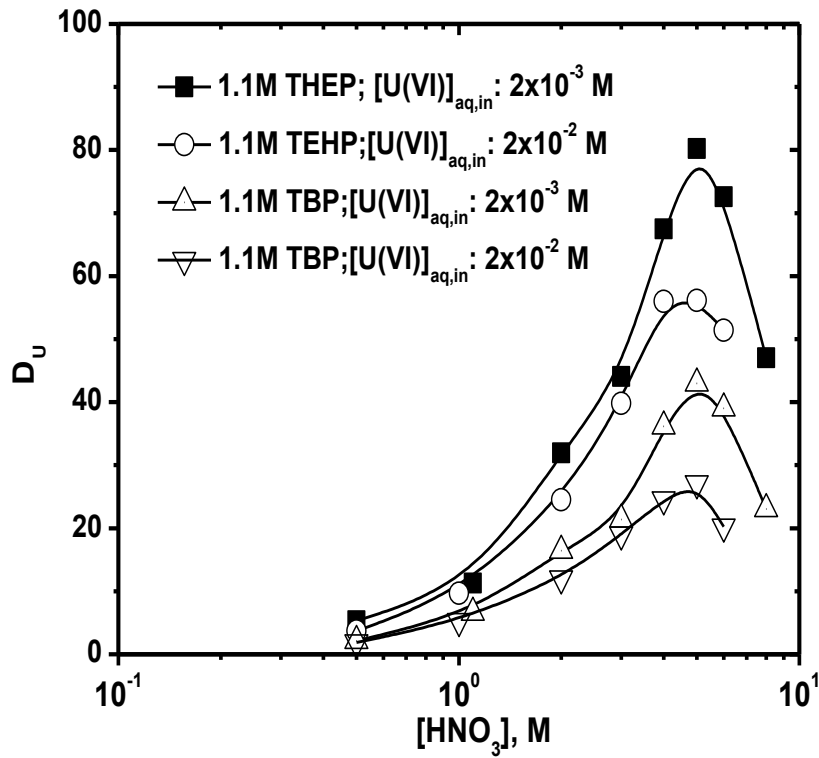
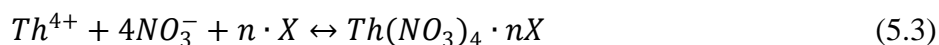


Figure 5.1. Variation of D_U with HNO₃ concentration for 1.1M TEHP and TBP, Diluents: *n*-paraffin; T: 298 K

For Th(IV), the distribution ratio does not change much up to 3M HNO₃, after 3 M it is increased rapidly, where as for U(VI), the distribution ratio increase smoothly from low HNO₃ concentration.

5.3.2. Extraction behavior of Th(IV)

Extraction of Th(IV) from nitric acid medium were investigated using 1.1M TEHP in *n*-paraffin and result was compared with same concentration of TBP under identical conditions. **Figure 5.2** shows the plot of variation of distribution ratio of Th(IV) at different nitric acid concentration using 1.1M TEHP/TBP dissolved in *n*-paraffin. The concentration of Th(IV) was varied from 2x10⁻³ M and 6x10⁻³ M. In both cases it was observed that the extraction of Th(IV) is not significantly affected by changing the alkyl group rather it was decreased in case of TEHP due to introduction of branching in the second carbon atom of the trialkyl phosphate. With increase in nitric acid concentration the distribution ratio of Th(IV) for both the extractant TBP/TEHP increase and reach a maximum at 5M HNO₃, beyond this D_{Th} value decrease due to more up take of nitric acid by the extractant. The data indicates that the extraction mechanism of Th(IV) by TEHP is similar to TBP. Similar behavior in extraction of Th(IV) by tri alkyl phosphate from nitric acid medium has been reported in literature [156,157]. The extraction mechanism of Th(IV) from nitric acid medium using neutral organophosphorous extractant (X) can be presented as:



With increase in nitric acid concentration more nitrate are available for coordinate to Th(IV) which shift equilibrium to the right *ie.*, D_{Th} increase with increase in nitric acid concentration in aqueous phase. Beyond 5 M HNO_3 , the complexation of TBP/TEHP with nitric acid increased and concentration of free TBP/TEHP for extraction of metal ions decreased, which leads to the reduction in distribution coefficient.

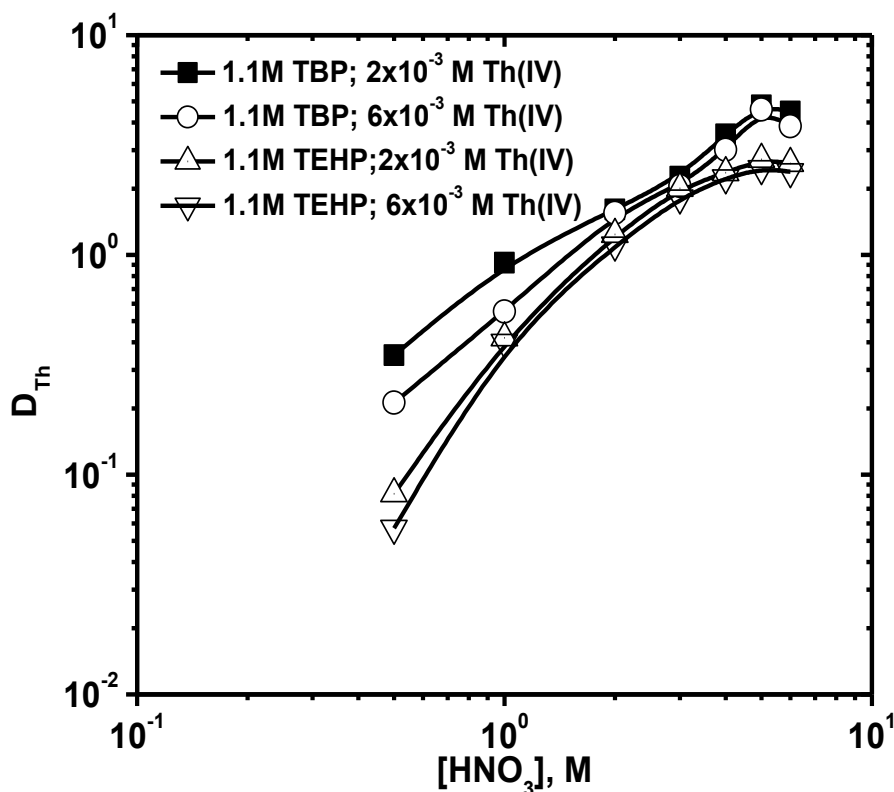


Figure 5.2. Variation of D_{Th} with HNO_3 concentration for 1.1M TEHP and TBP; Diluents: *n*-paraffin; T: 298 K.

5.3.3. Effect of extractant concentration

The effect of TEHP concentration on extraction of Th(IV) and U(VI) from nitric acid medium was investigated using different concentration of TEHP dissolved in *n*-paraffin at constant metal ions and nitric acid concentration and at room temperature. **Figure 5.3** shows the plot of log D of both the metal ions with log [TEHP] concentration at 4M HNO_3 and at 2×10^{-3} M metal ions

concentration. With increase in extractant concentration the distribution ratio of both the metal ions increases. From log-log plot it is observed that the slope for U(VI) is 1.5, where as for Th(IV) it is 2.3. Ideally there must be 2 molecule TEHP associated with U(VI) complex ($\text{UO}_2(\text{NO}_3)_2 \cdot 2\text{TEHP}$) and 3 molecule of TEHP associated with Th(IV) complex ($\text{Th}(\text{NO}_3)_4 \cdot 3\text{TEHP}$) and slope of $\log D$ vs $\log [\text{TEHP}]$ must be 2 and 3 for U(VI) and Th(IV) respectively in limiting condition [159]. The less and fractional values of slopes are because of non ideal behavior of the biphasic system due to high concentration of nitric acid, metal ions etc in aqueous phase and use of concentration term for evaluation of distribution ratio instead of activity of the species. Suresh *et al.*, observed similar results for study of extraction of U(VI) and Th(IV) from different concentration of nitric acid medium using various tri alkyl phosphate [160].

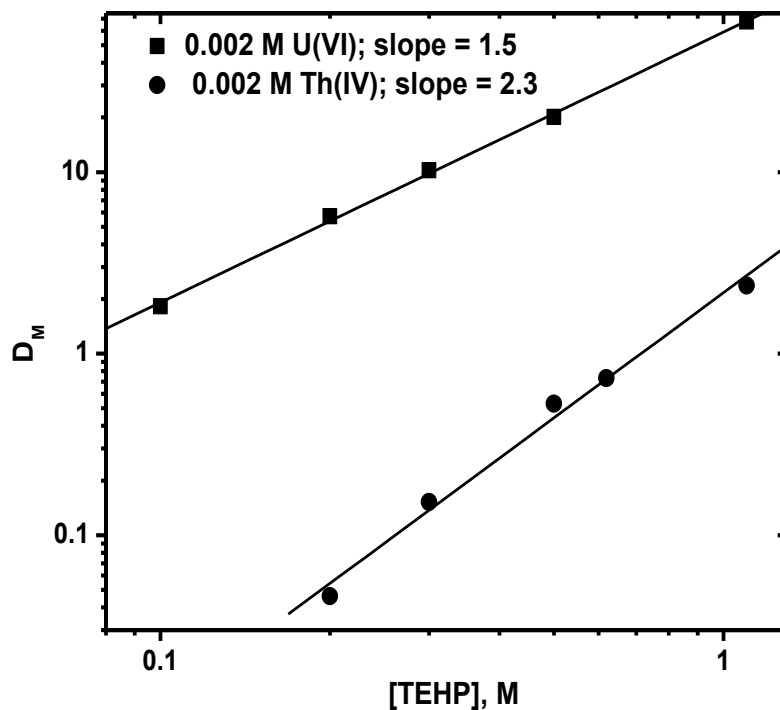


Figure 5.3. Variation of $\log D$ vs $\log [\text{TEHP}]$; $[\text{HNO}_3]$: 4 M; $[\text{U(VI)}]$: 2×10^{-3} M; $[\text{Th(IV)}]$: 2×10^{-3} M; Diluents: *n*-paraffin; T: 298 K

5.3.4. Separation of U(VI) from Th(IV)

The separation of U(VI) from binary mixtures of U(VI) and Th(IV) at different aqueous phase acidities was investigated to optimize the conditions for the development of a solvent extraction flow sheet. **Table 5.1** compares the separation factor (β) values for U(VI) over Th(IV) (2×10^{-3} M) mixtures at different aqueous phase acidities (from 2-6 M HNO₃) using 1.1 M TEHP or 1.1 M TBP dissolved in *n*-paraffin as solvents. It is observed that β values do not change much with increase in nitric acid concentration in the aqueous phase for both the extractants. However, at fixed aqueous phase acidity, the β values for TEHP are better than those of TBP. These studies suggest TEHP is better extractant than TBP for the separation of U(VI) from a binary mixture of U(VI) and Th(IV). Based on these studies, 2 M HNO₃ was chosen as the feed acidity for the separation of U(VI) from a binary mixture of U(VI) and Th(IV). It was of interest to vary TEHP concentrations to achieve better U(VI), Th(IV) separation at different feed acidities. **Table 5.2** compares the β values (D_U/D_{Th}) for U(VI), Th(IV) mixtures at different TEHP concentrations (0.2, 0.5, 1.1 M) in the acid range of 2-6 M HNO₃. The data suggest that lower in TEHP concentration offers better separation factor for U(VI) over Th(IV) at all nitric acid concentrations. This behavior can be explained in terms of the stoichiometries of the extracted species of U(VI) and Th(IV) as per equations 2 and 4. Based on these studies, 0.2 M TEHP dissolved in *n*-paraffin was found to be suitable choice for better separation factor and loading capacity of U(VI) at 2 M HNO₃ (**Table 5.3**).

Table 5.1. Separation factor (β) of U(VI), Th(IV) extracted from various concentration of nitric acid medium using 1.1M TEHP and TBP in *n*-paraffin; [U]_{aq,in} or [Th]_{aq,in}: 2×10^{-3} M; T: 298 K

[HNO ₃], M	1.1M TEHP			1.1M TBP		
	$D_{U(VI)}$	$D_{Th(IV)}$	β	$D_{U(VI)}$	$D_{Th(IV)}$	β
2	21.1	1.2	17.1	10.6	1.4	7.6
3	34.1	1.9	17.4	17.4	2.4	7.2
4	51.4	2.5	20.4	29.8	4.2	7.1
6	40.7	2.3	17.6	23.6	3.3	7.1

$\beta: D_{U(VI)}/D_{Th(IV)}$

Table 5.2. Result of evaluation of separation factor (β) for U(VI), Th(IV) mixture under different aqueous phase acidity and at various TEHP concentrations; [U]_{aq,in} or [Th]_{aq,in}: 2×10^{-3} M; Diluent: *n*-paraffin, T: 298 K

[HNO ₃], M	Separation factor (β)		
	1.1M TEHP	0.5 M TEHP	0.2 M TEHP
2	17.1	47.8	299.9
3	17.5	44.2	179.1
4	20.5	52.1	92.6
6	17.6	50.9	164.9

$\beta: D_{U(VI)}/D_{Th(IV)}$

Additional experiments were also performed to investigate the effect of different concentration ratio of U(VI) and Th(IV) on the β values for the separation of U(VI) from a binary mixtures at 2 M HNO₃ and using 0.2 M TEHP dissolved in *n*-paraffin as the solvent. **Table 5.4** shows that β values are better for lower concentration of metal ions and relatively poor separation is achieved at higher metal ion concentration.

Table 5.3. Maximum loading capacity of uranium at various concentrations of TEHP in *n*-paraffin; [HNO₃]: 2 M; T: 298 K

[TEHP], M	Maximum loading of U(VI), g/L
0.1	11.2
0.2	23.7
0.5	57.3
1.1	120.7

Table 5.4. Separation factors of U(VI), Th(IV) under various feed concentrations; Extractant: 0.2 M TEHP in *n*-paraffin; [HNO₃]: 2M; T: 298 K

[U(VI)], g/L	[Th(IV)], g/L	$D_{U(VI)}$	$D_{Th(IV)}$	Separation Factor (β)
0.1	1	13.3	0.13	106.3
0.2	5	10.1	0.04	273.3
0.5	10	4.6	0.03	197.2
1	20	3.5	0.05	65.7
10	50	2.3	0.04	56.6

$$\beta: D_{U(VI)}/D_{Th(IV)}$$

5.3.5. Separation of U(VI) from a mixture of U(VI) and Y(III)

The monazite leach liquor contains varying concentrations of lighter and heavier lanthanides along with yttrium. The chemical properties of Y(III) have a resemblance with the heavier lanthanides. It is reported that lighter lanthanides display lower extraction compared to the heavier ones. In fact, the extraction order for different metal ions using organophosphorous extractants follows the order: U(VI) > Th(IV) > heavy REE > light REE [161]. Therefore, extraction studies were performed using binary mixtures of U(VI) and Y(III) (2×10^{-3} M each) at different nitric acid concentrations using 1.1M TEHP and TBP dissolved in *n*-paraffin as solvents. **Table 5.5** shows that the extraction of Y(III) from nitric acid medium using TEHP and TBP as extractants is lower than that of U(VI). This behavior can be explained in terms of its small size and high hydration energy and poor complexation with the extractant molecules as compared to U(VI). With increase in nitric acid concentration from 2 to 6M, the β values of U(VI) over Y(III) increased gradually from ~94 (2 M HNO₃) to ~167 (6 M HNO₃) because of rapid increase in D_U values as compared to D_Y .

Table 5.5. Separation factors of U(VI), Y(III) from nitric acid medium using TEHP and TBP in *n*-paraffin; [U]_{aq,in} or [Y]_{aq,in}: 2×10^{-3} M; T: 298 K

[HNO ₃], M	1.1M TEHP			1.1M TBP		
	$D_{U(VI)}$	$D_{Y(III)}$	β	$D_{U(VI)}$	$D_{Y(III)}$	β
2	31.6	0.15	210.4	15.3	0.16	94.6
3	51.3	0.16	320.4	23.8	0.24	99.4
4	76.8	0.17	451.7	34.1	0.27	126.0
6	73.2	0.14	522.5	30.1	0.18	167.3

$$\beta: D_{U(VI)}/D_{Y(III)}$$

5.3.6. Separation of U(VI) from a mixture of U(VI), Th(IV), and Y(III)

The separation of U(VI) from a ternary mixture of U(VI), Th(IV) and Y(III) was also performed at 2 M HNO₃ as feed acidity, using 0.2 M TBP and 0.2 M TEHP dissolved in *n*-paraffin as solvents. Generally, the “thorium cake” after dissolution in nitric acid yields a solution containing 1g/L U(VI), 20 g/L Th(IV) and 20 g/L REEs [2]. Therefore, the U(VI), Th(IV) and Y(III) concentrations in feed solution were fixed as 1 g/L, 20 g/L and 20 g/L to simulate with the concentration of metal ions in actual monazite leach solutions. The separation factors (β) of U(VI)-Th(IV) and U(VI)-Y(III) were 24.3 and 944.4 for 0.2 M TBP, and 80 and 2666.6 for 0.2 M TEHP, respectively (Table 5.6). Based on this studies, the relative concentrations of [U(VI)] : [Th(IV)] : [Y(III)] were maintained as 1: 20 : 20 (g/L), for process flow sheet development using 0.2 M TEHP in *n*-paraffin as solvent.

Table 5.6. Separation of U(VI) from a mixture of U(VI), Th(IV) and Y(III) from nitric acid medium using TBP and TEHP; Diluent: *n*-paraffin; [U]_{aq,in}: 1g/L; [Th]_{aq,in}: 20g/L; [Y]_{aq,in}: 20g/L; [HNO₃]: 2M; T: 298 K

	$D_{U(VI)}$	$D_{Th(IV)}$	$D_{Y(III)}$	$(D_{U(VI)} / D_{Th(IV)})$	$D_{U(VI)} / D_{Y(III)}$
0.2 M TBP	1.7	0.07	1.8×10^{-3}	24.3	944.4
0.2 M TEHP	4.0	0.05	1.5×10^{-3}	80.0	2666.6

5.3.7. Separation of U(VI) from multi-component system

The separation of U(VI) were carried out from 4M HNO₃ concentration containing a number of impure elements using 1.1M TEHP and TBP and results are given in Table 5.7. The concentration level of impurities is 5 ppm each. It is observed that the separation factor of non transition and transition elements are higher than rear earth elements for both the extractant.

However, each element has higher separation factor with respect to U(VI) for 1.1M TEHP than same concentration of TBP. The reason behind higher separation factor is the higher distribution ratio of U(VI) in case of TEHP as compared to same concentration of TBP.

Table 5.7. Separation of U(VI) from multi component metal ion system using 1.1 M TEHP/ TBP in *n*-paraffin; U(VI) : 1×10^{-2} M; [HNO₃] : 4 M; T: 298 K.

Elements	D_M with TBP	Separation factor(β)	D_M with TEHP	Separation factor (β)
Al	0.013	1889.23	0.014	3992.86
Cd	0.075	327.47	0.07	798.57
Cr	0.068	360.29	0.077	725.97
Dy	0.211	116.39	0.183	305.46
Er	0.349	70.37	0.349	160.17
Eu	0.359	68.41	0.339	164.89
Gd	0.305	80.52	0.281	198.93
Mg	0.234	104.96	0.217	257.60
Mn	0.028	912.86	0.035	1597.14
Ni	0.203	120.98	0.175	319.43
Sm	0.079	310.88	0.029	1927.59

5.3.8. McCabe-Thiele diagram for extraction and stripping of U(VI)

The McCabe-Thiele plot for extraction of uranium from 2 M HNO₃ medium using 0.2 M TEHP dissolved in *n*-paraffin was constructed by varying the aqueous and organic phase ratio (A/O) within 1:5 to 5:1 at constant metal ion concentration. The data plotted in **Figure 5.4** indicate the

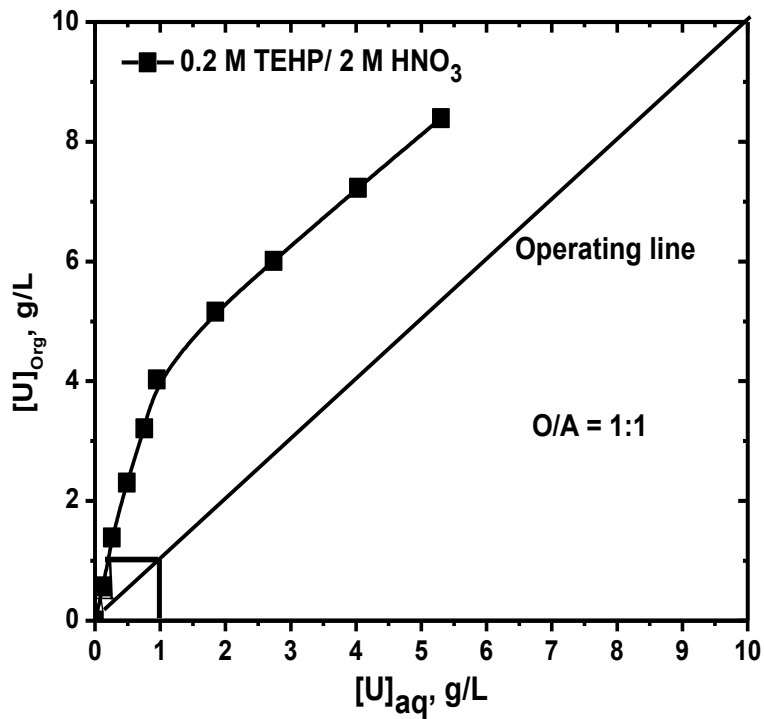


Figure 5.4. McCabe-Thiele diagram of extraction of U(VI) from 2 M HNO₃ medium using 0.2 M TEHP, Diluent: *n*-paraffin; T: 298 K

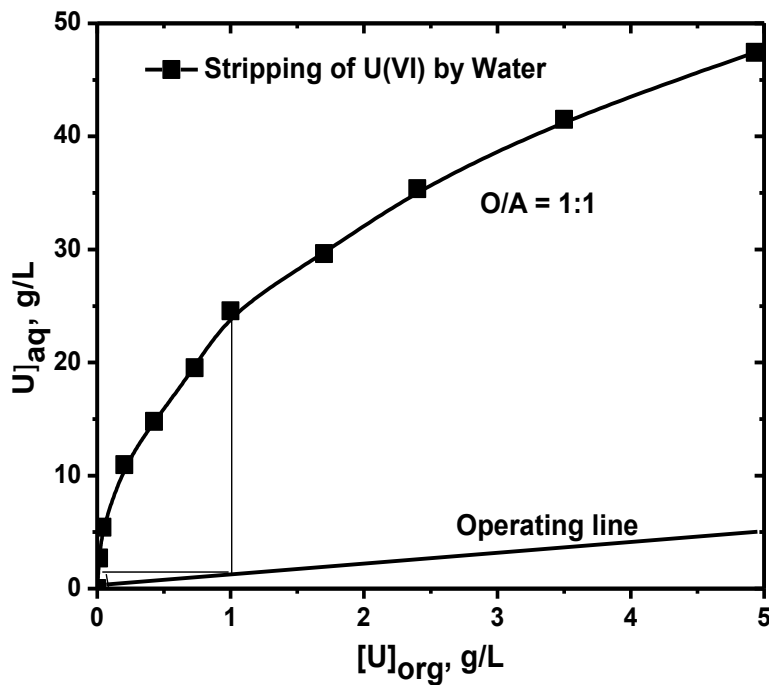


Figure 5.5. McCabe-Thiele diagram of stripping of U(VI) from 0.2 M TEHP; Strippant: water; Diluent: *n*-paraffin; T: 298 K

three extraction stages are required at organic-to-aqueous phase ratio (O:A) as 1 for complete extraction of uranium (>99.9 %) from a feed solution containing 1g/L U(VI) at 2 M HNO₃. It would be possible to enrich uranium in organic solution if extraction is performed at higher A: O and at higher feed acidity. Similarly, the McCabe-Thiele plot for stripping of uranium from loaded 0.2 M TEHP dissolved in *n*-paraffin using distilled water as strippant was constructed by varying the organic and aqueous (O:A) ratio within 1:5 to 5:1. **Figure 5.5** indicates that two-stage stripping are required at O: A 1:1 for complete stripping of uranium from loaded organic containing 1g/L uranium. Here also, it would be possible to enrich uranium in the strip solution if stripping studied were carried out at higher O: A ratio.

5.3.9. Conceptual process flow-sheet

Monazite sand is initially digested with hot alkali (NaOH) and the digested mass is washed with water to separate Th(IV), U(VI) and REEs hydroxides as precipitates. This mass is called “thorium concentrate”. The next step is the selective dissolution of most of REEs in HCl medium as chloride at pH ~3 leaving Th, U as hydroxide cake (Thorium cake). This cake is dissolved in HNO₃ which is the feed solution for the present work. The feed acidity is generally maintained between 2-3 M HNO₃. A typical feed solution contains 1 g/L U(VI), 20 g/L Th(IV) and 20 g/L REEs. Based on the experimental results, the optimize conditions for separation of U(VI) from a crude thorium cake are: [TEHP] : 0.2 M, Feed acidity: 2 M HNO₃ (**Figure 5.6**). Distilled water is used as the strippant as it works well for the purpose and does not add any other chemical to the product stream. Numbers of stages required for quantitative extraction (> 99.9 %) as well as stripping are 3.

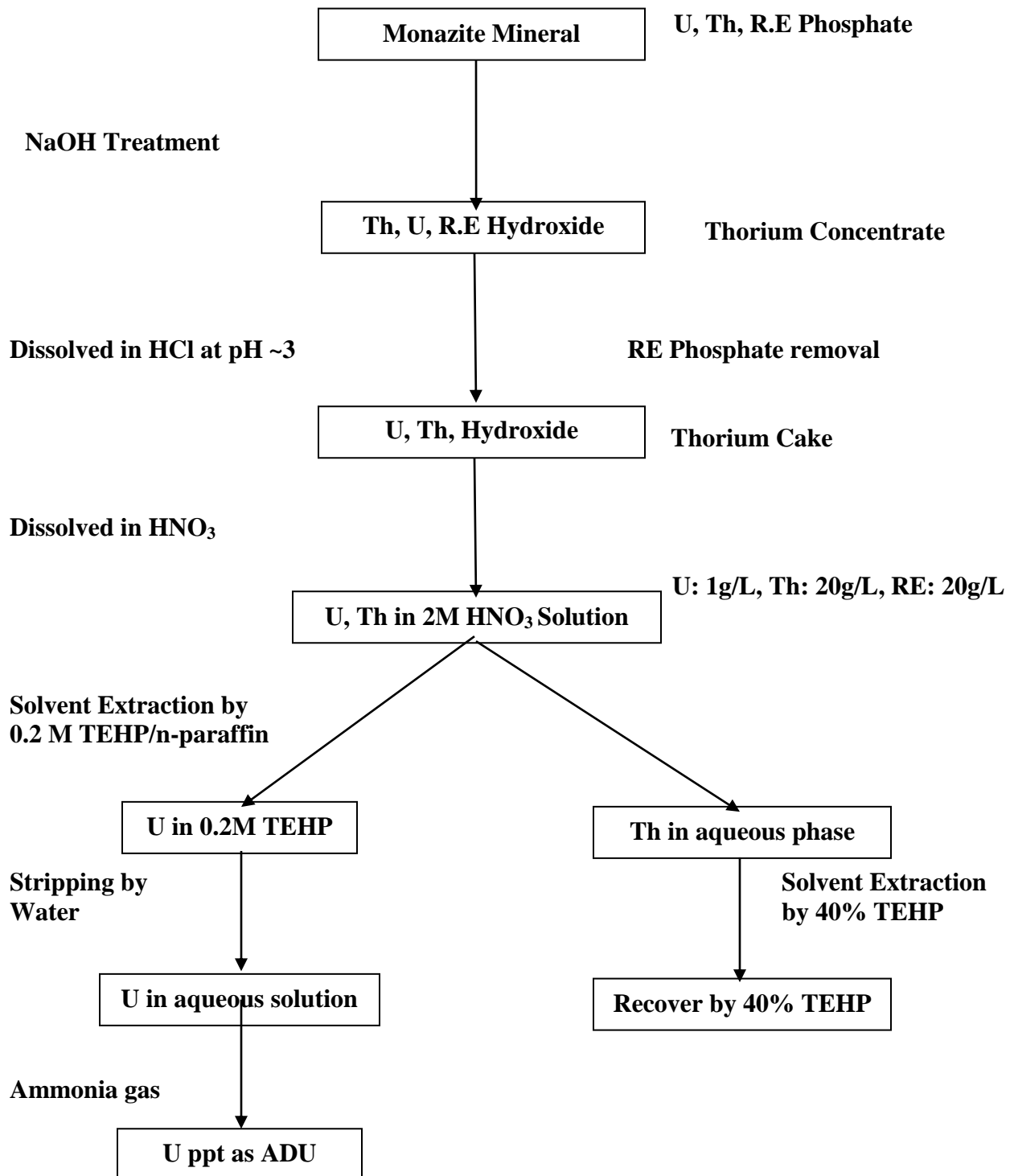


Figure 5.6. Process flow-sheet for separation of U(VI), Th(IV), REEs during processing of Monazite mineral, TEHP: 0.2 M, Diluent: *n*-paraffin; T: 298 K.

5.4. Conclusions

Extraction behavior of U(VI) and Th(IV) were investigated using TEHP dissolved in *n*-paraffin. The performance of TEHP was compared with TBP under identical experimental conditions. The distribution ratio values increase with aqueous phase nitric acid concentration and reach a maximum at 5 M HNO₃ beyond which a decrease is observed. The separation factor of U(VI) (β) with respect to elements like Th(IV) and Y(III), are higher in the case of TEHP as compared to those of TBP. McCabe-Thiele diagram for extraction and stripping of U(VI) shows that for 2M HNO₃ feed solution containing 1g/L U, 0.2 M TEHP and water as strippant, three stages for extraction and two stages for stripping are sufficient for complete separation of U(VI) from the monazite leach solution (nitric acid medium). The U(VI), Th(IV) separation method developed was successfully used for separation of U(VI) from thorium concentrate after dissolving in nitric acid solution. A conceptual process flow-sheet for separation of U(VI) from a mixture of uranium, thorium and other rare earth elements in nitric acid solution has been proposed.

CHAPTER VI

**URANIUM PERMEATION STUDIES FROM NITRIC ACID
MEDIUM ACROSS SUPPORTED LIQUID MEMBRANE
USING ORGANOPHOSPHOROUS EXTRACTANTS**

6.1. Introduction

Separation and recovery of uranium from various industrial wastes as well as from secondary sources is gaining importance in view of its increasing demand in nuclear industry [116, 118, 162-164]. Conventionally, solvent extraction, ion exchange, and precipitation methods have been used to recover such valuable elements from sources of different origins. There is always an emphasis on the development of new separation technologies which may require relatively low inventory of the reagents for recovery purpose. In this context, liquid-membrane based separation holds promise for the recovery of metal ions from lean effluent solutions and has received considerable attention in separation science and technology [165]. The prominent features of this technique are: low solvent inventory, low operation cost, clean separation, high selectivity and reasonably high efficiency. Extensive studies have been carried out in our laboratory as well as elsewhere to evaluate different types of extractants including some novel extractants such as dialkyl amides, diamides, and diglycolamides for separation of actinides like uranium, plutonium, and americium etc. from solutions of different origin [153, 152, 27, 18, 158, 166-168].

Supported liquid membrane (SLM) studies were carried out employing di-2-ethyl hexyl phosphoric acid (D2EHPA) with and without neutral oxodonors such as tri *n*-butyl phosphate (TBP), di-butyl butyl phosphonate (DBBP), tri *n*-Octyl phosphine oxide (TOPO), and Cyanex 923 (a mixture of four trialkyl phosphine oxides viz. R₃PO, R₂R'₁PO, RR'₂PO and R'₃PO where R: *n*-octyl and R': *n*-hexyl chain), evaluated for the recovery of U(VI) from phosphoric acid medium [65, 67, 169-171]. Similarly, conditions were optimized for uranium recovery from phosphoric acid medium using synergistic mixtures of 2-ethyl hexyl phosphonic acid 2-ethyl hexyl monoester (PC88A) with either TOPO or octyl (phenyl)-*N,N*-diisobutylcarbamoyl methyl

phosphine oxide (CMPO) as the carriers [72,73]. The optimized conditions were applied to recover uranium from analytical waste solutions generated in the laboratory during uranium analysis in phosphoric acid medium. Kedari *et al.* investigated the transport mechanism of U(VI) and Pu(IV) across a SLM and emulsion liquid membrane (ELM) from nitric acid medium using PC88A as the carrier under varying experimental conditions such as stirring speed, carrier concentration, nature of anions and acidity of source phase [71,172]. Uranium transport studies from nitric acid solutions across SLMs containing PC88A suggested that transport process was diffusion controlled. The analytical as well as process applications of this method were evaluated by the transport of uranium across the SLM from solutions containing diverse ionic impurities.

The raffinate generated during the purification of uranium yellow cake (diuranate) by TBP route generally contains significant amounts of uranium (0.3-1 g/L). It is treated with MgO or calcium hydroxide to precipitate uranium as magnesium or calcium diuranate and disposed as a solid waste [111, 112]. It is desirable to develop process flow sheet to recover uranium from uranyl nitrate raffinate (UNR). In this context, extraction studies of U(VI) from nitric acid medium were carried using PC88A as extractant either alone or in combination with neutral extractants such as TBP, TOPO, and DOSO. These studies were extended for the recovery of uranium from UNR waste. It was of interest to evaluate membrane-based separation technique in view of relatively low concentration of uranium from UNR waste solutions.

6.2. The present work

The transport of uranium from nitric acid medium has been investigated across a SLM impregnated with several organophosphorous extractants, neutral donors such as: TBP, tris n-butyl ethyl phosphate (TBEP), tris 2-ethylhexyl phosphate (TEHP), and TOPO or Cyanex 923 and acidic, such as: PC88A, bis[2,4,4 trimethyl pentyl] phosphinic acid (Cyanex 272), di nonyl

phenyl phosphoric acid (DNPPA) either alone or its mixtures with neutral donors. The effects of various experimental parameters such as feed acidity, carrier concentration, receiver phase composition, metal ion concentration, membrane thickness, membrane pore size and other metal ions on uranium transport have been investigated. The study has been extended for uranium recovery from UNR waste generated during uranium purification from yellow cake.

6.3. Results and Discussion

6.3.1. Uranium permeation studies from HNO₃ medium using neutral organophosphorous extractants

In this section, permeation and transport studies of U(VI) from HNO₃ medium has been investigated using various neutral organophosphorous extractants such as TBP, TBEP, and TEHP dissolved in *n*-paraffin. An attempt has been made in the investigation to compare uranium transport behavior across SLM using trialkyl phosphates having different alkyl substituents viz. TBP, TBEP, and TEHP as carriers.

6.3.1.1. Effect of alkyl substituents on U(VI) transport

To understand the effect of alkyl substituent's of neutral organophosphorous extractants, uranium transport studies were carried out employing 1.1 M solutions of TBEP, TBP and TEHP in *n*-paraffin as carriers, 2×10^{-3} M U(VI) at 1.12 M HNO₃ as feed solution, and distilled water as receiver phase (**Figure 6.1**). There was a distinct effect of alkyl substituents on U(VI) transport and it followed the order: TEHP \geq TBP > TBEP. The lower transport of U(VI) in case of TBEP was attributed to the presence of extra oxygen atom in the alkyl substituent, which decreased the basicity/donor capacity of the P=O group due to -I effect. On the other hand, marginal difference in the uranium transport was observed in the case of TBP and TEHP. Burger reported

the correlation between P = O bond stretching frequency (reflecting the basicity of the ligand) and the distribution data of various organophosphorous extractants [173].

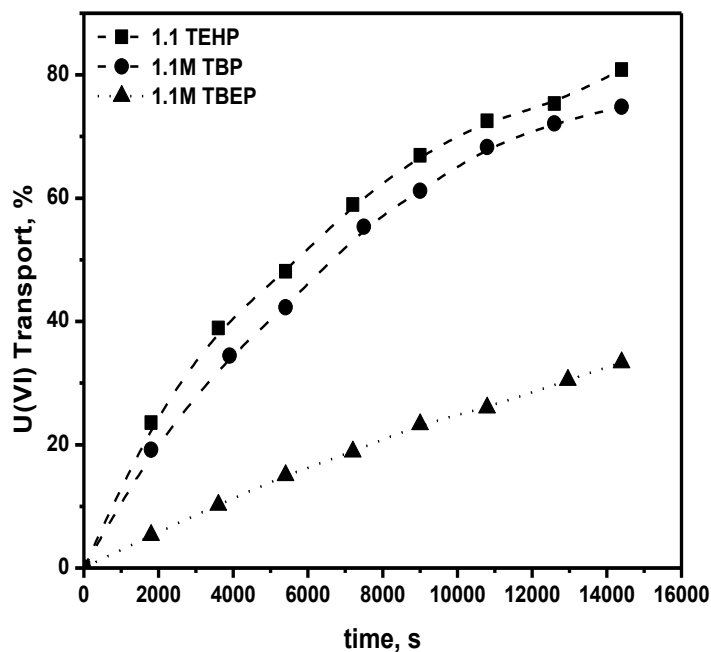


Figure 6.1. Uranium transport behavior of various organophosphorous carrier in the membrane phase; $[U(VI)]_{\text{feed}}: 2 \times 10^{-3} \text{ M}$ at 1.12 M HNO_3 ; Carrier concentration: 1.1 M in *n*-paraffin

More shift of IR stretching frequency of P = O bond in lower side indicate more basicity of the ligand and large distribution ratio for extraction of the metal ions. The phosphoryl IR absorption bands shifted towards lower wave numbers in the order: $(\text{RO})_3 \text{PO} > (\text{RO})_2 \text{R PO} > (\text{RO}) \text{R}_2 \text{PO} > \text{R}_3 \text{PO}$. The absorption bands at 1273 cm^{-1} for TBP and $1275 - 1270 \text{ cm}^{-1}$ for TEHP suggested that the basicities of the two ligands are almost similar. The U(VI) transport from HNO_3 medium through SLM using TBP as a carrier has been investigated by many authors [67,69,76,77], but there is no report on U(VI) transport from HNO_3 medium across SLM using TEHP as a carrier. Therefore TEHP was chosen for further experiments because of its high selectivity towards U(VI) over other metal ions [150].

6.3.1.2. Effect of feed acidity

The transport of U(VI) was investigated from feed solutions at various nitric acid concentrations ($\sim 2 \times 10^{-3}$ M U at 1.1 – 3.3 M HNO₃) employing 1.1 M TBP/TBEP/TEHP solutions as carrier.

Figure 6.2 shows an increase in uranium transport with increased feed acidity. Both TBP and TEHP display similar transport behavior of uranium at all acidities. Typically, $\sim 90\%$ uranium transport was observed in 4 h for TBP and TEHP at 3.3 M HNO₃ as feed acidity.

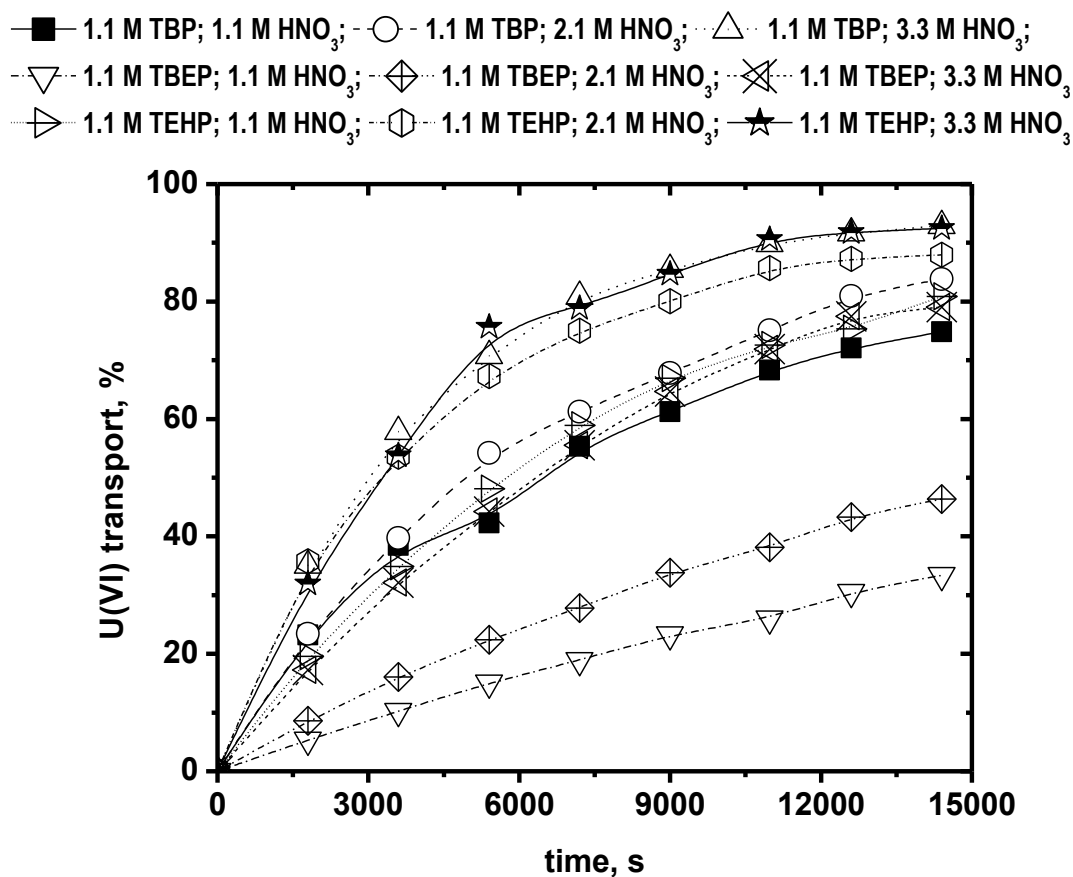


Figure 6.2. Comparison of uranium transport across PTFE supported membrane impregnated with different carriers and with different feed solutions; Carrier(s): 1.1 M TBP/TBEP/TEHP in *n*-paraffin; Feed solution(s): 2×10^{-3} M U(VI) at 1.1 - 3.3 M HNO₃; Strippant: Distilled Water

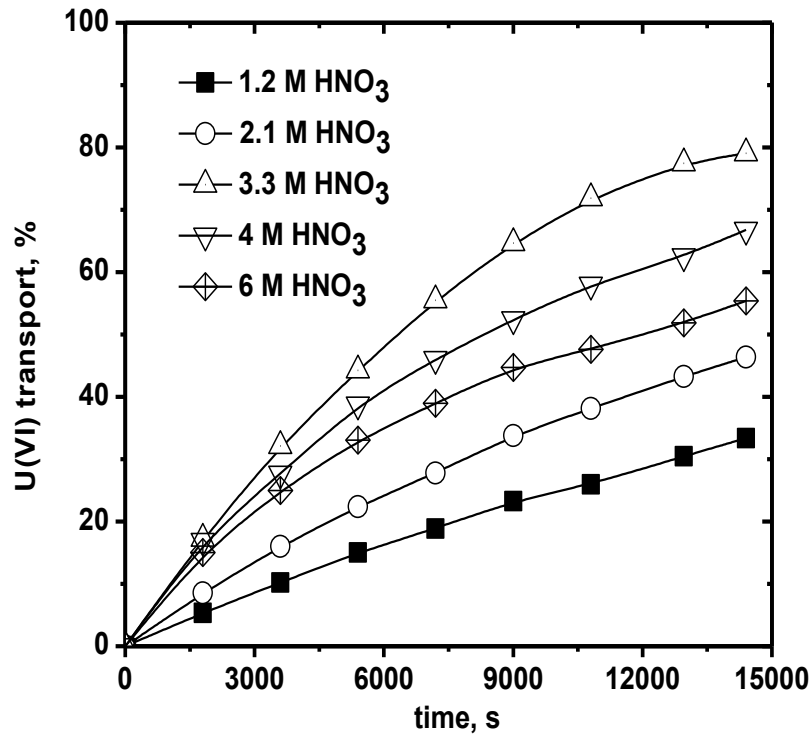
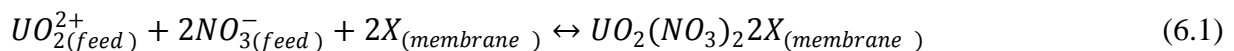


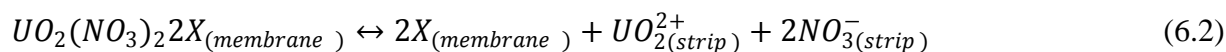
Figure 6.3. Effect of acidity on uranium transport using 1.1M TBEP in *n*-paraffin as a carrier; $[U(VI)]_{feed}: 2 \times 10^{-3} \text{ M}$; Strippant: Distilled Water

By contrast, only ~ 80 % uranium transport was observed in the case of 1.1 M TBEP under identical experimental conditions. Further increase in feed acidity decreases the transport (Figure 6.3). This behavior was attributed to increase in the strip phase acidity thereby leading to poor stripping from the membrane phase. Typically, the acid transport from 1-6 M HNO₃ feed solutions were found to be as high as 15% in 4 h. The transport of U(VI) by neutral organophosphorous extractant occurs via co-transport mechanism where NO₃⁻ ion act as a co-ion Figure 6.4 [73]. The chemical reaction for this coupled transport can be given as follows:

At feed-membrane interface:



At membrane-strip interface:



Where X = TBEP, TBP or TEHP

From equation (6.1), it is observed that the transport of U(VI) through membrane will increase with increase in nitrate ion concentration in the feed and hence with the nitric acid concentration. The decrease in transport of U(VI) after 3.3 M HNO₃ is due to the formation of HNO₃.X complexes which lower both the concentration of NO₃⁻ ions in feed as well as extractant X in the membrane phase.

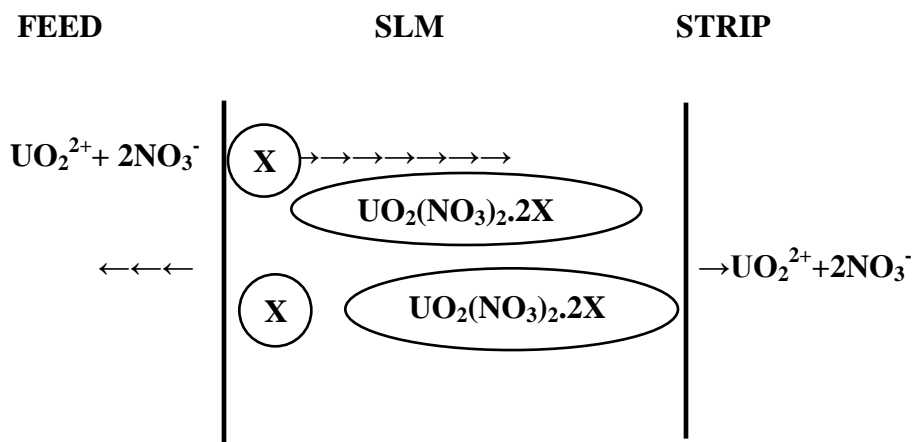


Figure 6.4. Transport steps of uranium in SLM in presence of neutral extractant

6.3.1.3. Effect of extractant concentration

Uranium transport was studied as a function of TEHP concentration employing 2×10^{-3} M U(VI) solution at 4 M HNO₃ as the feed and distilled water as the receiver phase. **Table 6.1** shows the variation of permeation coefficient (*P*) of U(VI) at various concentration of TEHP/ *n*-paraffin.

Table 6.1. Effect of carrier concentration on U(VI) transport from HNO₃ medium using TEHP/*n*-paraffin, U(VI): 2x10⁻³ M, Volume of feed & strip solutions: 25mL; Feed acidity: 4 M HNO₃; Strippant: Distilled water; Stirring speed: 200 rpm

Carrier concentration	Px10 ⁴ cm/sec	% T
0.1 M TEHP	3.95	69.07
0.2 M TEHP	7.86	87.56
0.3 M TEHP	9.58	92.74
0.5 M TEHP	11.11	95.64
1.1 M TEHP	11.43	96.64

Uranium transport increases initially with increased carrier concentration in the membrane phase up to 0.5 M beyond which no appreciable increase was observed. It appears that the increased viscosity of the carrier is responsible for slow increase in uranium permeation across the membrane.

6.3.1.4. Effect of uranium concentration

Figure 6.5 shows the variation of flux with uranium concentration (4.2x10⁻⁴ to 3.4x10⁻³ M) at 2 M HNO₃ as feed acidity, distilled water as receiver phase using 1.1 M TEHP/*n*-paraffin as carrier. As expected, there was a linear increase in the flux (though small) with increased metal ion concentration in the feed solution, which was attributed to the presence of limited ligand in the membrane phase. However, transport of U(VI) initially increase with metal ion concentration and become maximum (**Figure 6.6**) any further increase in metal ion concentration causes decrease in transport of the metal ion. Initially presence of few numbers of U(VI) ions cannot

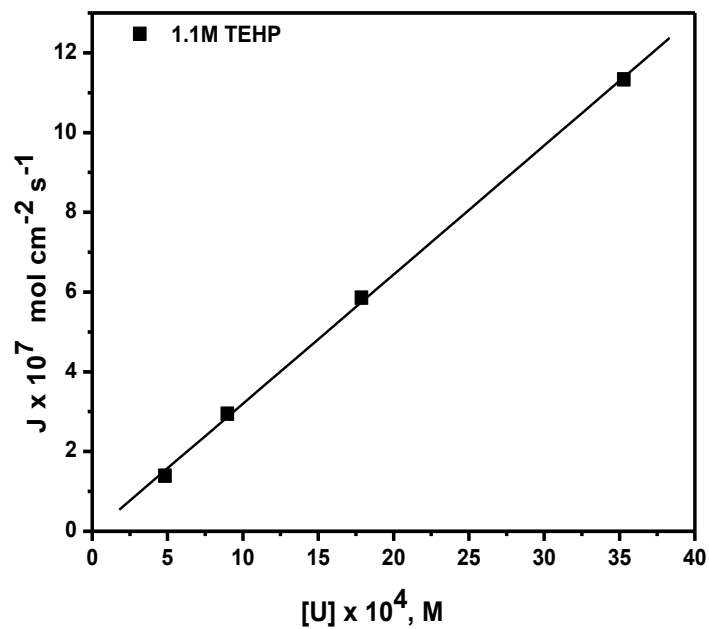


Figure 6.5. Variation of flux (J) with U(VI) concentration in the feed solution; Carrier: 1.1 M TEHP/*n*-paraffin; Feed acidity: 2 M; Receiver phase: Distilled Water

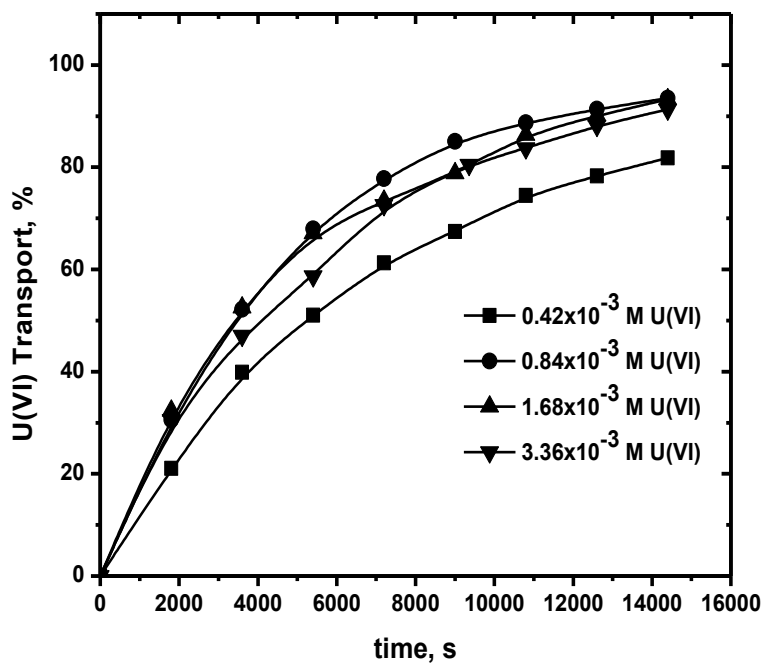


Figure 6.6. Effect of U(VI) concentration in the feed solution on its permeation; Feed acidity: 2 M HNO₃; Carrier: 1.1 M TEHP in *n*-paraffin; Receiver phase: Distilled Water

saturate the amount of ligand present in membrane phase and hence the ligand has more capacity to complex metal ions. However, after certain metal ion concentration ($8.4 \times 10^{-4} \text{ M}$) the carrier gets saturated by metal ions and any further increase in metal ion concentration in feed solution decrease the metal ion transport across the membrane.

6.3.1.5. Effect of pore

U(VI) transport across supported liquid membrane was investigated using 1.1 M TEHP/*n*-paraffin impregnated in membranes of two different pore sizes and porosities (0.20 μm , 55 % and 0.45 μm , 64 %). **Figure 6.7** shows that uranium transport increased with membrane pore size suggesting that larger pore size provides relatively easy passage for the metal cations. However, it has to be noted that too large a pore size would lead to poorer holding of the carrier molecules in the pores of the membrane and therefore may leach out of the membrane.

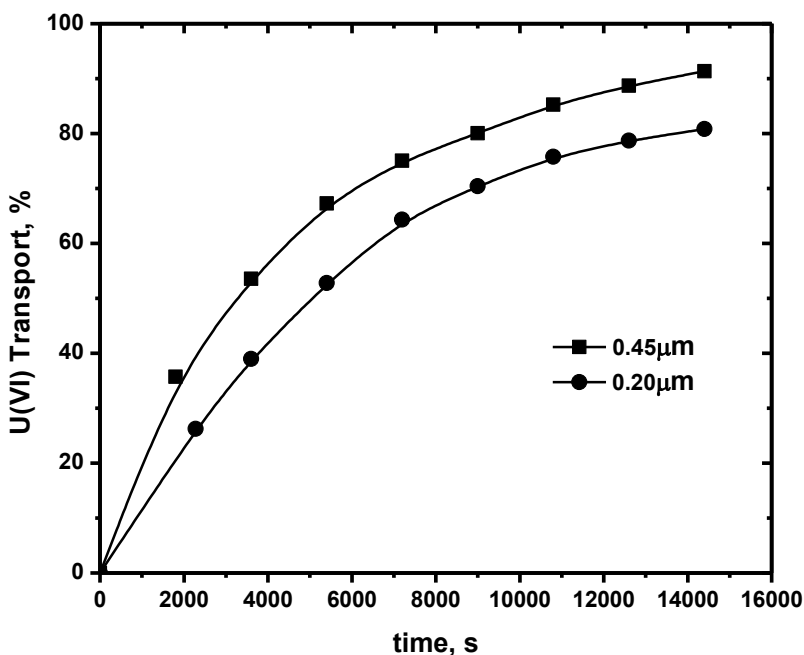


Figure 6.7. Effect of membrane pore size on U(VI) transport across SLM employing 1.1 M TEHP/*n*-paraffin; Feed: $2 \times 10^{-3} \text{ M}$ U(VI) at 2 M HNO_3 ; Receiver phase: Distilled Water

Similar observations were made during the transport of Am(III), and U(VI) using dimethyldibutyltetradecyl-1,3-malonamide (DMDBTDMA) and a tertiary amine as carrier [75,64]. The hindered diffusion of the metal-carrier complex across the membrane pores indicates predominant contribution from tortuosity (defined as effective diffusion path length) which may change with porosity.

6.3.1.6. Effect of membrane thickness

In diffusion controlled transport process permeability (P) of the metal ion is dependent on the effective diffusion path length in the membrane phase. It depends on the distribution coefficient (D_U) by the following equation:

$$P = D_U / \{D_U(d_{(a)}/D_{(a)} + (\tau d_{(o)}/D_{(o)})\} \quad (6.4)$$

where d_a , $d_{(o)}$ are the thickness of diffusion layer of aqueous phase and membrane phase and D_a , $D_{(o)}$ are the diffusion coefficient of aqueous phase and membrane phase respectively.

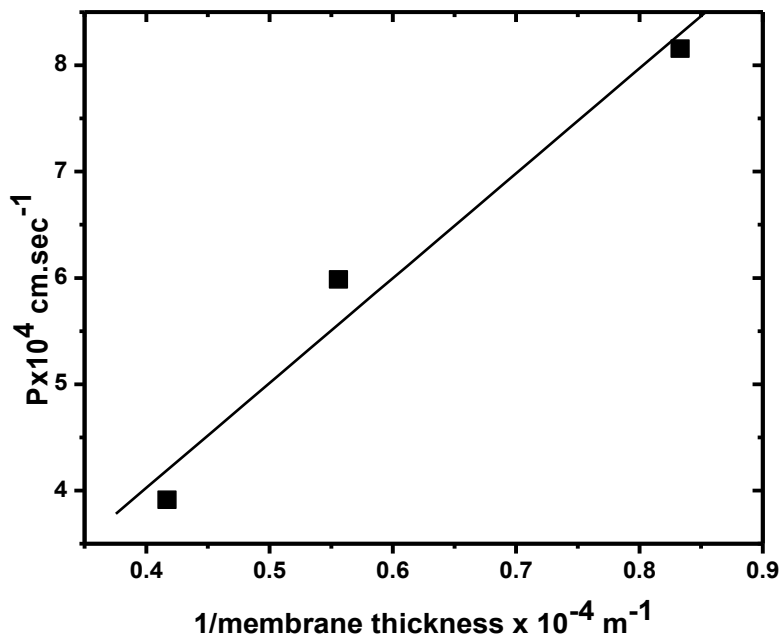


Figure 6.8. Effect of membrane thickness on U(VI) transport across SLM employing 1.1M TEHP/*n*-paraffin; Feed: 2×10^{-3} M U(VI) at 2 M HNO_3 ; Receiver phase: Distilled Water

Uranium transport experiments were carried out by compressing a number of membranes (pore size: 0.45 μm , and effective thickness: 60 μm) using 1.1 M TEHP/*n*-paraffin, 2×10^{-3} M U at 2 M HNO_3 and distilled water as carrier, feed, and the receiver phase, respectively. The membranes were immersed separately in to the carrier solution of desired concentration and were stacked together to increase the thickness. With increase in membrane thickness there was a gradual decrease in permeability of uranium across SLM (**Figure 6.8**) which is a characteristic property of diffusion control process.

6.3.2. Uranium permeation studies using acidic organophosphorous extractants and their synergistic mixtures

This section deals with the detailed permeation of U(VI) from nitric acid medium across SLM containing various acidic organophosphorous extractants (Cyanex 272, PC88A and DNPPA) along or with their mixture with neutral donors (TBP, TOPO, TEHP and Cyanex 923).

6.3.2.1. Evaluation of acidic extractants

The permeation of U(VI) was studied across SLM containing 0.1 M solution of various organophosphorous extractants viz. Cyanex272, PC88A, DNPPA dissolved in *n*-paraffin as carrier from 2×10^{-3} M U(VI) at 2 M HNO_3 as feed and 2 M H_2SO_4 as the receiver. **Figure 6.9** shows that uranium transport across the membrane varied with their pK_a values in the order: Cyanex 272 (8.7) > PC88A (7.1) > DNPPA (2.5) [174]. For effective U(VI) transport across SLM, the distribution ratio of U(VI) (D_U) values of the system at feed – membrane interface must be very high as compared to D_U values at membrane – strip interface. The high permeation of U(VI) in case of Cyanex 272 was due to higher pK_a value which facilitated faster release of UO_2^{2+} ions from $\text{UO}_2(\text{HA}_2)_2$ complex at the membrane - receiver interface. Similar observations

were reported in solvent extraction studies of U(VI) from nitric acid medium employing different organophosphorous acidic extractants such as Cyanex 272, PC88A, D2EHPA having different pK_a values [174]. The extractant with lower pK_a values form stronger complex with metal ion at feed-membrane interface and it becomes relatively difficult to release the metal ion at the membrane-strip interface. This results in overall decrease in U(VI) transport across SLM. Further studies were carried out using Cyanex 272 as extractant in the carrier phase.

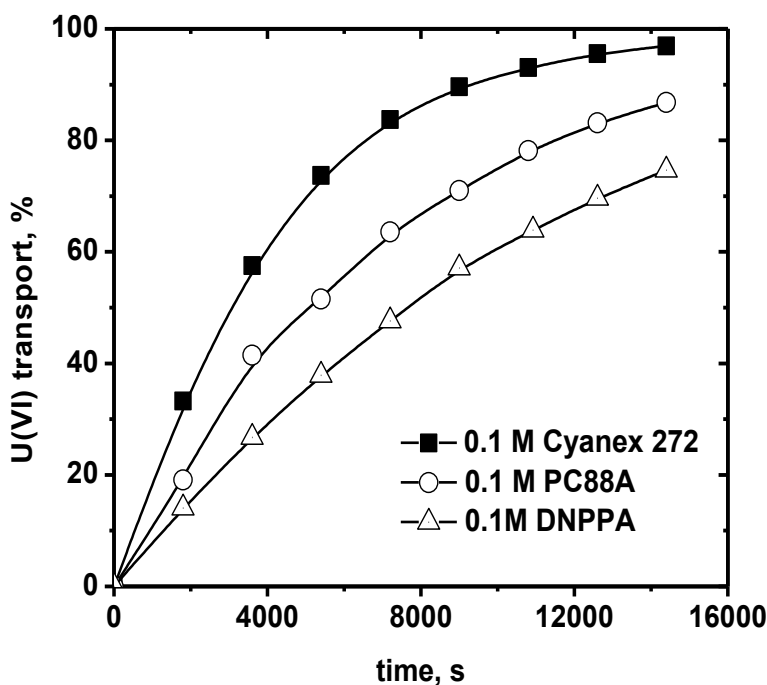


Figure 6.9. Uranium transport across SLM impregnated with various acidic extractants as carrier; $[U(VI)]_{\text{feed}}: 2 \times 10^{-3} \text{ M}$ at 2 M HNO_3 ; Carrier: 0.1 M in *n*-paraffin; Receiver phase: $2 \text{ M H}_2\text{SO}_4$

6.3.2.2 Evaluation of different strippants as receiver phase

Several solutions such as $0.5 \text{ M H}_2\text{SO}_4$, 0.5 M oxalic acid, 0.5 M citric acid and $1 \text{ M Na}_2\text{CO}_3$ were evaluated as receiver phases for efficient uranium transport from a feed solution containing

2×10^{-3} M U(VI) at 2 M HNO₃ across SLM impregnated with 0.1 M Cyanex 272/*n*-paraffin as the carrier (**Figure 6.10**). There was negligible transport of U(VI) across SLM when citric acid was used as receiver phase which was attributed to poor complexation of U(VI) under the conditions of this experiment. Interestingly, an increase in the volume of the receiver phase was noticed when Na₂CO₃ was used as strippant essentially due to formation of CO₂ and therefore was not used as strippant. On the other hand, efficient U(VI) transport was observed in 4 h employing 0.5 M H₂SO₄ (90%) and 0.5 M oxalic acid (83%) as the receiving phase. Usually oxalate ions form relatively stronger complexes with U(VI) as compared to sulphate anions [174,175] Even though, oxalic acid can also be used strippant in the present work, the choice of H₂SO₄ as the receiver phase was guided by the generation of sulphate waste after precipitation of U(VI) as ammonium diuranate (ADU), which can be disposed off as solid cake.

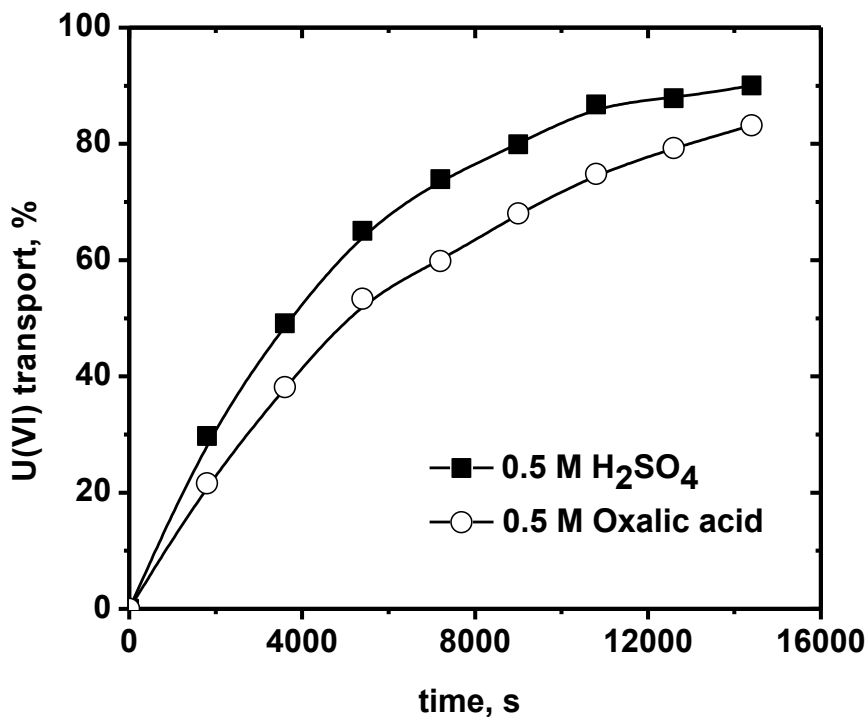


Figure 6.10. Effect of receiver phase on U(VI) transport; [U(VI)]_{feed}: 2×10^{-3} M at 2 M HNO₃; Carrier: 0.1 M Cyanex 272 in *n*-paraffin

6.3.2.3 Effect of neutral donors

U(VI) permeation across SLM was studied employing Cyanex 272 along with various neutral donors viz. TBP, TEHP, Cyanex 923 dissolved in *n*-paraffin as carrier, 2×10^{-3} M U(VI) in 2 M HNO₃ as feed, and 2 M H₂SO₄ as the receiver phase. There was a synergistic enhancement in uranium transport in the presence of these oxodonor ligands which followed the order of their basicity or acid uptake constant (K_H): Cyanex 923 (8.1) > TBP (0.16) > TEHP (0.16) [176-186] (Figure 6.11).

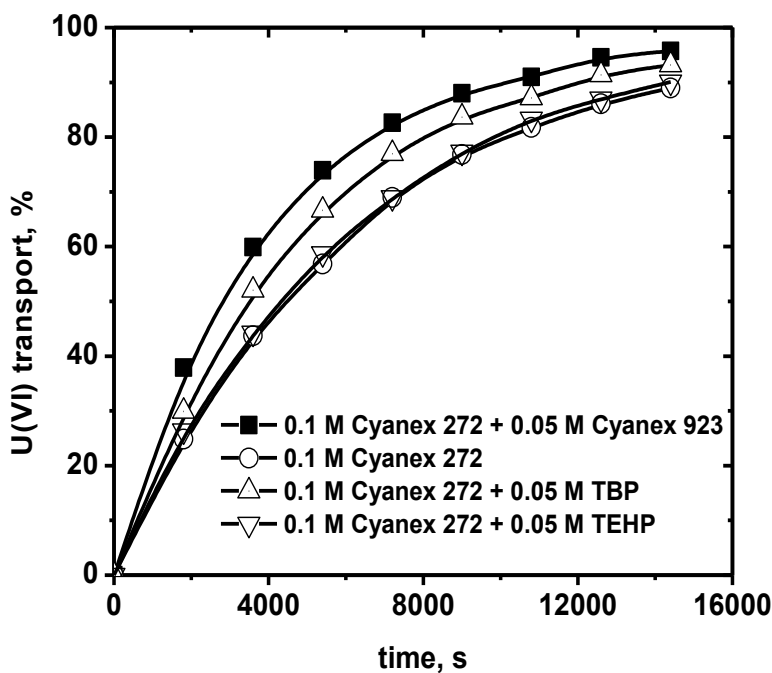
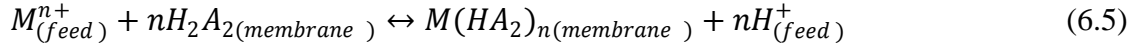


Figure 6.11. Effect of various neutral donors in the carrier solution in presence of 0.1 M Cyanex 272 on uranium transport; Feed: 2×10^{-3} M U(VI) at 2 M HNO₃; Diluent: *n*-paraffin; Receiver phase: 2 M H₂SO₄

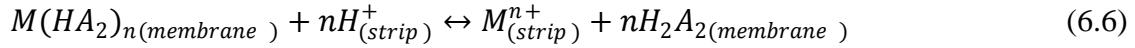
Even though both TBP and TEHP have same basicity, the relatively less transport in the case of the latter can be due to steric hindrance of the branched 2-ethylhexyl group during the complexation with UO₂²⁺-Cyanex272 species. Based on these studies, Cyanex 923 was chosen as

neutral donor for synergistic transport of uranium from nitric acid medium. The permeation of U(VI) from nitric acid medium across SLM using Cyanex 272 is cation exchange mechanism.

At feed-membrane interface:

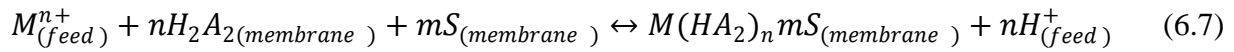


At membrane-strip interface:

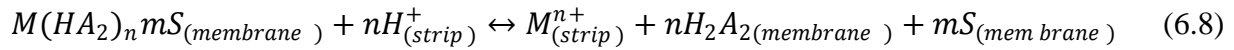


In the presence of neutral donor (S) in carrier solvent, there is an adduct formation in the membrane phase, which enhances the permeation of the U(VI) across SLM.

At feed-membrane interface:



At membrane-strip interface:



The values of n and m in the present work was determined by independent solvent extraction experiments varying Cyanex 272 and Cyanex 923 concentrations as 2 and 1, respectively.

6.3.2.4 Effect of H₂SO₄ concentration on uranium transport in the receiver phase

Uranium transport studies across a SLM impregnated with 0.1 M Cyanex 272 + 0.05 M Cyanex 923 as the carrier, were carried out from a feed solution containing 2x10⁻³ M U(VI) from 2 M HNO₃, and varying concentrations of H₂SO₄ as the receiver phase. There was an increase in U(VI) transport with increase in H₂SO₄ concentration in the receiver phase up to 2 M beyond which a decrease was observed (**Figure 6.12**). The transport mechanism of U(VI) across SLM in the presence of 0.1 M Cyanex 272 + 0.05 M Cyanex 923 as carrier solvent can be divided in the following three steps:

- (i) Transport of U(VI) from feed to feed-membrane interface and formation of synergistic complex of U(VI) with Cyanex 272 (H_2A_2) and Cyanex 923 (S),
- (ii) Diffusion of uranium complex through the membrane, and
- (iii) Dissociation of $UO_2(HA_2)_2 \cdot nS$ complex at membrane-strip interface and regeneration of carrier solvent which will diffuse back at the membrane-feed interface.

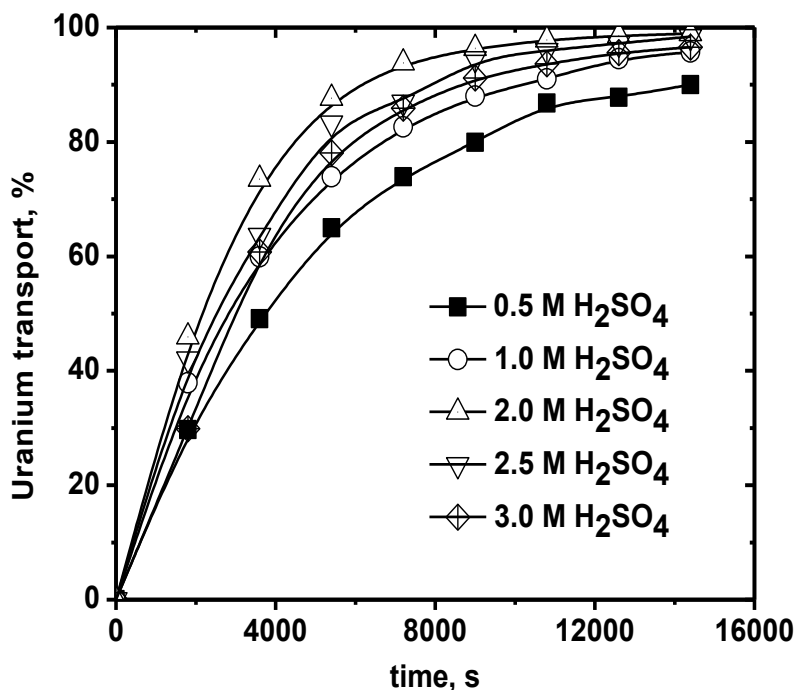


Figure 6.12. Uranium transport as a function of H_2SO_4 concentration in the receiver phase; $[U(VI)]_{\text{feed}}: 2 \times 10^{-3} \text{ M}$ at 2 M HNO_3 ; Carrier: $0.1 \text{ M Cyanex 272} + 0.05 \text{ M Cyanex 923}$ in *n*-paraffin

Receiver phase plays an important role in the dissociation of $UO_2(HA_2)_2 \cdot nS$ complexes at membrane-strip interface and in the regeneration of carrier solvent for further transport of metal ions. With increase in H_2SO_4 concentration in receiver phase, U(VI) transport across SLM increases due to increased H^+ concentration which accelerate the dissociation of $UO_2(HA_2)_2 \cdot nS$ complexes at membrane-strip interface. Beyond $2 \text{ M H}_2\text{SO}_4$, the decrease in the uranium

transport may be due to adduct formation of Cyanex 923 with acid molecules thereby decreasing the free ligand concentration which should be available for synergistic complex formation.

6.3.2.5. Effect of feed acidity

The effect of feed acidity on U(VI) transport across SLM containing 0.1 M Cyanex 272 + 0.05 M Cyanex 923 as carrier solvent was investigated using 2×10^{-3} M U(VI) and 2 M H_2SO_4 as receiver phase. **Figure 6.13** shows that a decrease in U(VI) transport with increased feed acidity indicating counter-current transport mechanism of the metal ions across SLM. In such cases, an acidic extractant, H_2A_2 , forms a complex $\text{M}(\text{HA}_2)_n$ with a metal cation (M^{n+}) at the feed-membrane interface.

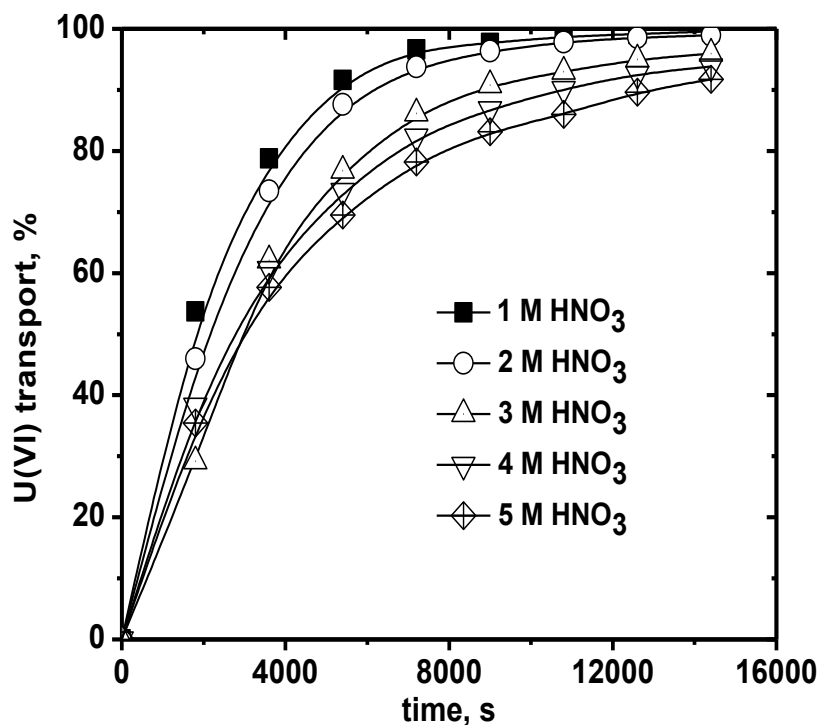


Figure 6.13. Uranium transport as a function of feed acidity; Carrier: 0.1 M Cyanex 272 + 0.05 M Cyanex 923 in *n*-paraffin; $[\text{U(VI)}]_{\text{feed}}: 2 \times 10^{-3}$ M; Receiver phase: 2 M H_2SO_4

The complex diffuses through membrane to membrane-strip interface and liberates the metal cation to the strip solution and simultaneously picks up H^+ ions from strip solution to form H_2A_2 . This species diffuses back to feed-membrane interface, picks up more metal ions and the process continues. It is evident from the discussion that lower acidity on the feed side favors the release of proton from the acidic extractant and hence facilitates the faster transport of uranium. The extractant molecules shuttles between feed and strip interfaces as shown in **Figure 6.14** during the transport of the metal ions. The presence of neutral donors further enhances the transport of U(VI) due to formation of more hydrophobic complexes which leads to the high distribution ratio values of the metal ions at the feed membrane interface. Even though 0.5 M HNO_3 in feed solution provides better transport of uranium in the presence of 2 M H_2SO_4 as the receiver phase, further experiments were carried out using 2 M HNO_3 as the feed solution because the aim of the present study is to recover uranium from UNR waste solution.

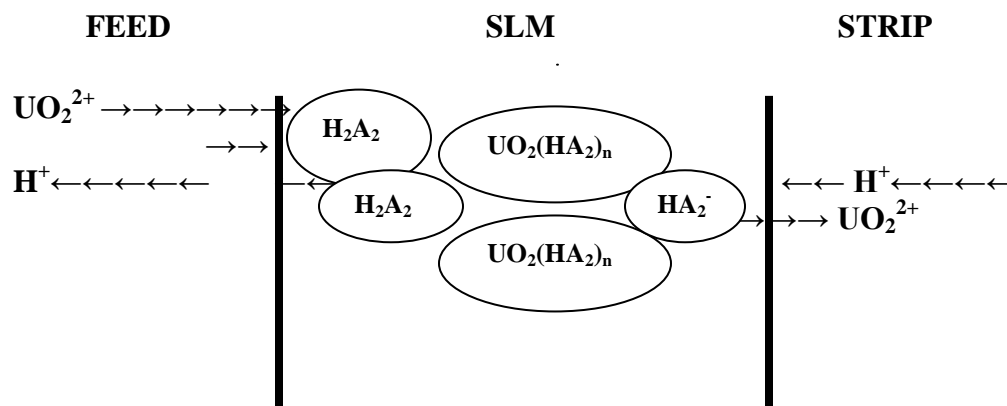


Figure 6.14. Counter-current U(VI) transport steps in SLM using acidic extractants (H_2A_2)

6.3.2.6. Effect of U(VI) concentration

Figure 6.15 shows the effect of uranium concentration (4.2×10^{-4} – 3.36×10^{-3} M) on its permeation through membrane containing 0.1 M Cyanex 272 + 0.05 M Cyanex 923 /*n*-paraffin as carrier

maintaining 2 M HNO₃ as the feed acidity and 2 M H₂SO₄ as the receiver phase. Marginal variation in uranium transport rate with increased uranium concentration from 4.2x10⁻⁴ M to 3.36x10⁻³ M suggested the availability of sufficiently high ligand concentration in the membrane. **Figure 6.16** shows that flux is directly proportional to metal concentration in the feed solution. Similar behavior has been observed in case of Co(II) and U(VI) transport through supported liquid membrane system employing triethanolamine/cyclohexanone and di(2-ethylhexyl)isobutyramide (D2EHIBA) as carriers [187,170].

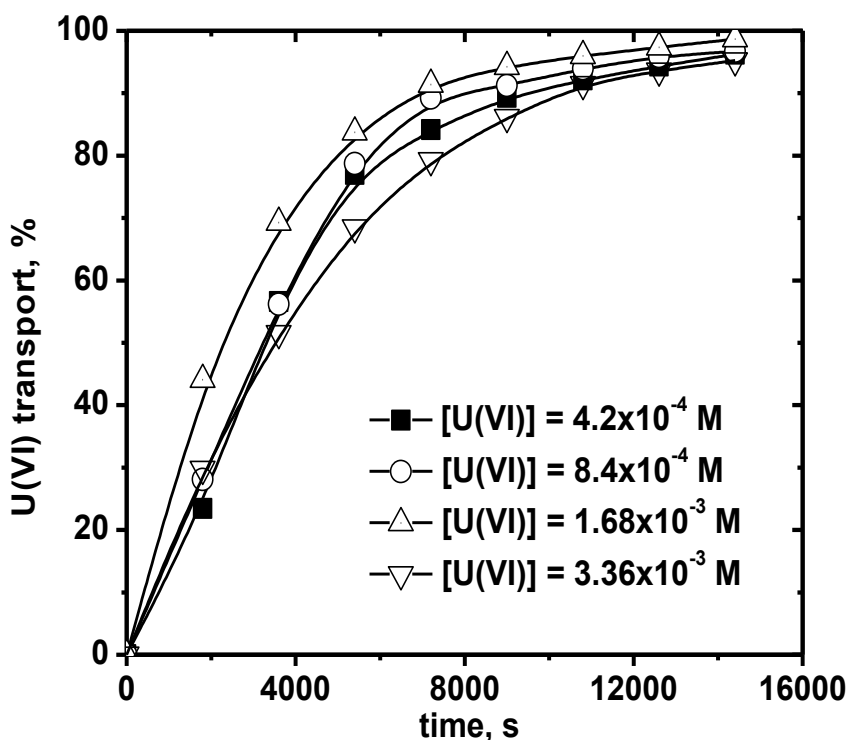


Figure 6.15. Effect of U(VI) concentration in the feed solution on its permeation; Carrier: 0.1 M Cyanex 272 + 0.05 M Cyanex 923 in *n*-paraffin; Feed acidity: 2 M HNO₃; Receiver phase: 2 M H₂SO₄

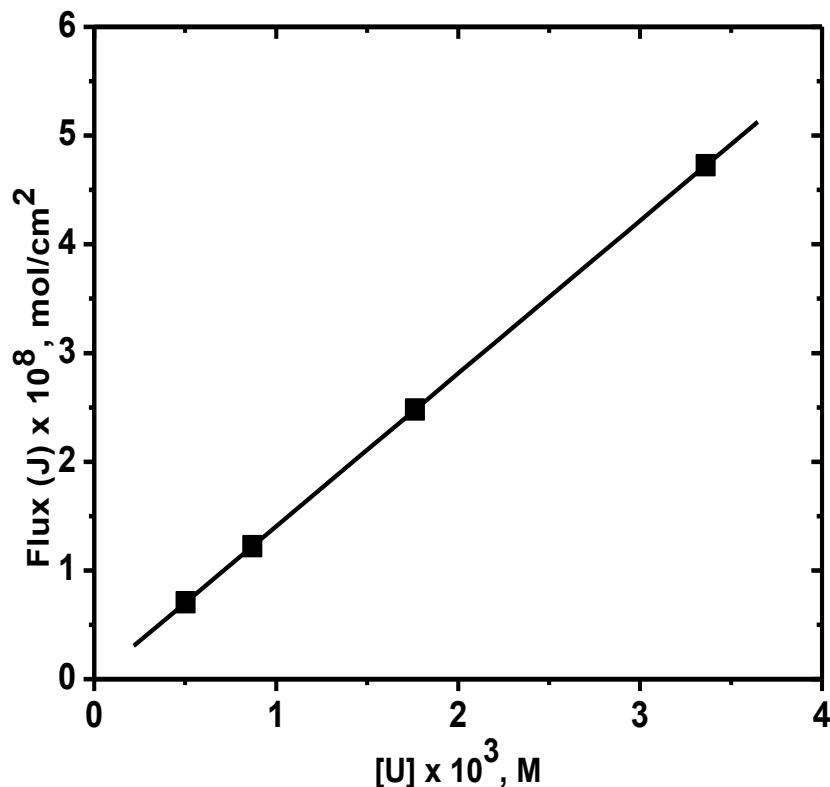


Figure 6.16. Variation of flux (J) with U concentration in the feed solution; Carrier: 0.1 M Cyanex 272 + 0.05 M Cyanex 923/ n -paraffin; Receiver phase: 2 M H_2SO_4

6.3.2.7. Effect of membrane thickness

In diffusion control transport process, permeability (P) of the metal ion depends on the effective diffusion path length in the membrane phase and on the distribution coefficient (D_U) by the following equation (6.4). The uranium transport experiments were carried out by stacking a number of membranes (up to 4 nos., pore size: 0.45 μm , effective thickness: 60 μm) and using a feed solution 2×10^{-3} M $U(VI)$ at 2 M HNO_3 . 0.1 M Cyanex 272 + 0.05 M Cyanex 923/ n -paraffin was used as carrier in the membrane phase and 2 M H_2SO_4 was the receiver phase. These membranes were immersed separately in to the carrier solution were stacked together to increase the thickness.

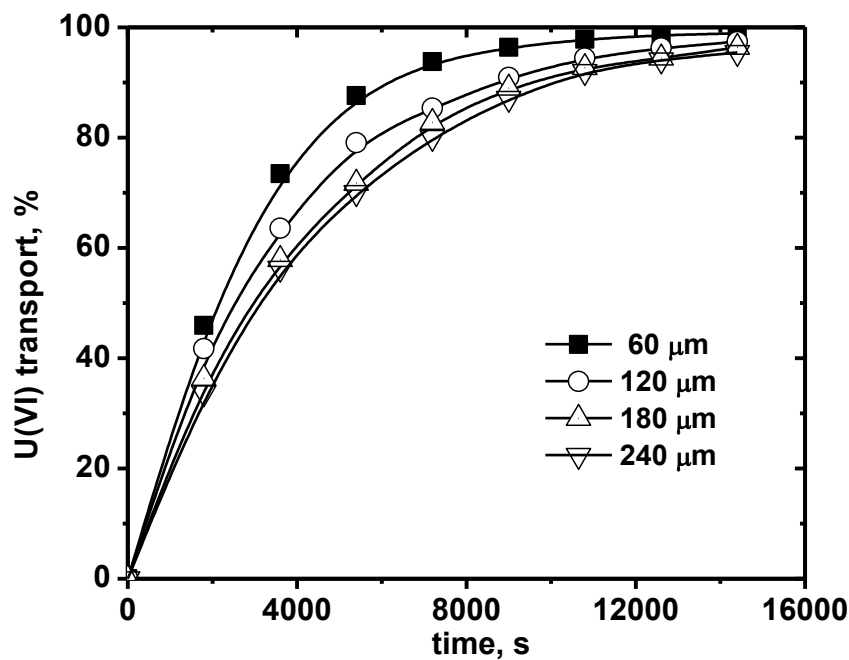


Figure 6.17. Variation of U(VI) transport with membrane thickness; Feed: 2×10^{-3} M U(VI) at 2 M HNO₃; Carrier: 0.1 M Cyanex 272 + 0.05 M Cyanex 923 in *n*-paraffin; Receiver phase: 2 M H₂SO₄

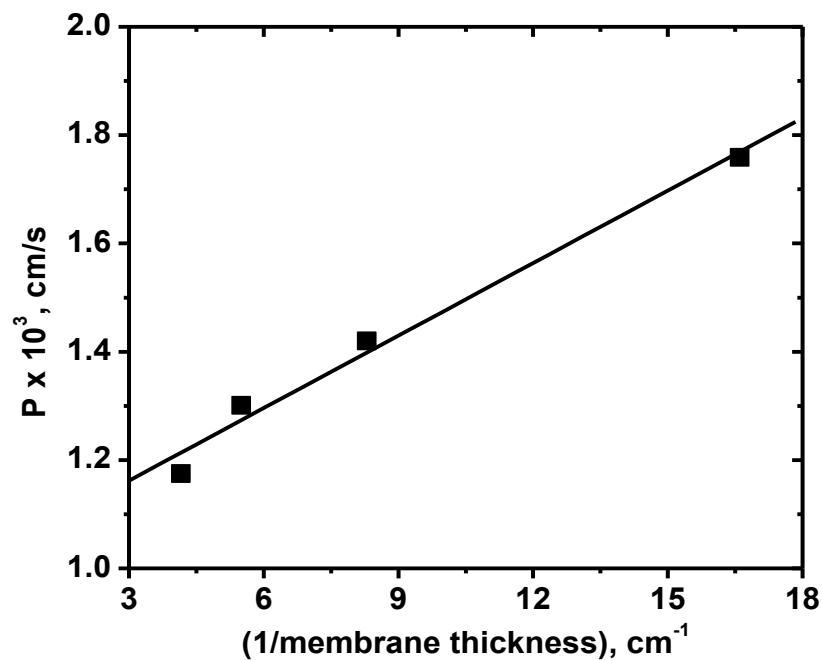


Figure 6.18. Variation of U(VI) permeability with membrane thickness; $[U(VI)]_{\text{feed}}: 2 \times 10^{-3}$ M; Receiver phase: 2 M H₂SO₄; Carrier: 0.1 M Cyanex 272 + 0.05 M Cyanex 923 in *n*-paraffin

With increase in membrane thickness, there was a gradual decrease in uranium transport from 99 % (no.1) to 95% (no.4) (**Figure 6.17**). **Figure 6.18** indicates that P values for uranium transport are inversely proportional to the membrane thickness which is a characteristic of a diffusion control transport process

6.3.2.8. Effect of membrane pore size

Transport of uranium across SLM is influenced by membrane pore size. The effects of membrane pore size on uranium transport were studied using 0.45 μm and 0.20 μm pore size employing 0.1 M Cyanex 272 + 0.05 M Cyanex 923/*n*-paraffin as carrier solvent in presence of 2 M H_2SO_4 as receiver phase. The composition of feed solution was maintained 2×10^{-3} M U(VI) at 2 M HNO_3 .

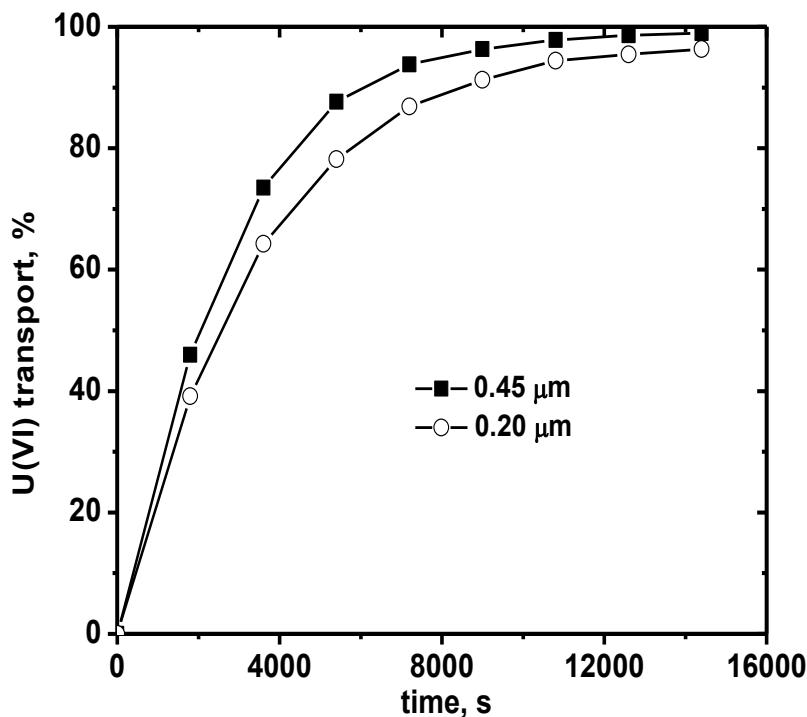


Figure 6.19. Effect of pore size on U(VI) permeation; Feed: 2×10^{-3} M U(VI) at 2 M HNO_3 ; Carrier: 0.1 M Cyanex 272 + 0.05 M Cyanex 923 in *n*-paraffin; Receiver phase: 2 M H_2SO_4

Figure 6.19 shows that with decrease in pore size of the membrane from 0.45 μm to 0.2 μm uranium transport across SLM decreased from 93.5 % to 88.0 %. The reason behind this observation was reduced porosity of the membrane which led to decrease in uranium flux at the feed membrane-interface. Similar results were reported in case of uranium transport across SLM containing PC88A as carrier solvent [22,24].

6.3.3. Transport studies using DNPPA and its mixture with neutral donors

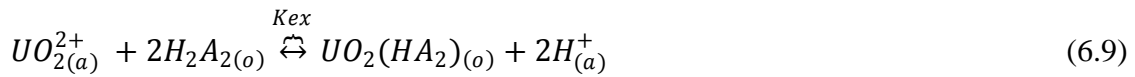
DNPPA a close analog of D2EHPA is widely used for recovery of uranium from wet phosphoric acid by solvent extraction [16-19]. Synergistic extraction of uranium from nitric acid and sulphuric acid medium was also reported using DNPPA and other neutral donors like TBP, TOPO etc.. Recently, Singh et.al. has investigated on selective extraction of yttrium from phosphoric acid medium using DNPPA and TOPO as synergistic mixture [188]. Although, few reports have been published on separation of uranium from phosphoric acid medium and other medium, but no attempt has been made on membrane separation of uranium from nitric acid medium using SLM and DNPPA as the carrier. In the present study it is our interest to investigate detail uranium permeation from HNO_3 medium across SLM using DNPPA as a carrier solvent under various parameters such as composition of receiver phase, concentration of receiver phase, optimization of carrier concentration, pore size, membrane thickness, presence of neutral donors etc.

6.3.3.1. Kinetic Modeling

The experimental data (**Table 6.2**) were fitted to a kinetic model to evaluate the diffusion coefficient of U-DNPPA complex across SLM. The proposed kinetic model was based on the following assumptions:

- (a) Interfacial mass transfers at feed-membrane and membrane–receiver interface are instantaneous and hence the the interfacial fluxes were neglected.
- (b) The interfacial chemical reactions at feed-membrane and membrane–receiver interface are faster than diffusion.
- (c) The rate of mass transfer across SLM was diffusion controlled.
- (d) Complex formation of uranium with DNPPA at the feed-membrane interface is a single step process.

The extraction of U(VI) from HNO₃ medium using DNPPA/*n*-paraffin was studied and extraction mechanism described elsewhere [37]. The extraction equilibria at 2 M HNO₃ concentration can be described by the following equations and extractants constants:



$$K_{ex} = \{[UO_2(HA_2)_2]_{(o)} \cdot [H^+]_{(a)}^2\} / \{[UO_2^{2+}]_{(a)} \cdot [H_2A_2]_{(o)}^2\} \quad (6.10)$$

Where ‘H₂A₂’ refers to dimeric form of DNPPA. K_{ex} is the conditional extraction constant and subscripts (a) and (o) represent the aqueous and organic phases, respectively. The value of K_{ex} was calculated as 8.954x 10⁴ using slope ratio technique [82]. The flux of metal ion transport through the membrane was given by the Fick’s first law of diffusion to the diffusion layer on the feed side to the membrane. According to the law, the permeability coefficient (P) can be written as [106, 107]:

$$P = J/[UO_2^{2+}] \quad (6.11)$$

$$P = D_U/(D_U\Delta_{(a)} + \Delta_{(o)}) \quad (6.12)$$

Where D_U is the distribution ratio of U(VI) with DNPPA at feed-membrane interface and $\Delta_{(a)}$ & $\Delta_{(o)}$ are the resistance in transport in bulk feed phase and membrane phase respectively.

Combining equations (6.10) and (6.12) the following equation can be derived:

$$P = K_{ex} [H_2A_2]_{(o)}^2 \cdot [H^+]_{(a)}^2 / \{ \Delta_{(o)} + \Delta_{(a)} (K_{ex} \cdot [H_2A_2]_{(o)}^2 \cdot [H^+]_{(a)}^2) \} \quad (6.13)$$

$$1/P = \Delta_{(a)} + \Delta_{(o)} / (K_{ex} [H_2A_2]_{(o)}^2 \cdot [H^+]_{(a)}^2) \quad (6.14)$$

Figure 6.20 showed the plot of $1/P$ as a function of $1/K$ where $K = (K_{ex} \cdot [H_2A_2]_{(o)}^2 \cdot [H^+]_{(a)}^2)$ for different extractant concentration at 2M HNO₃ concentrations is a straight line with a slope $\Delta_{(o)}$ and intercept $\Delta_{(a)}$. The value of $\Delta_{(o)}$ and $\Delta_{(a)}$ were determined from proposed kinetic model as 69046.4 ± 6757 and $975.64 \pm 374.34 \text{ s} \cdot \text{cm}^{-1}$, respectively. The transport resistance due to diffusion by the membrane ($\Delta_{(o)}$) was expressed as follows: $\Delta_{(o)} = \tau d_{(o)} / D_{(o)}$, where τ is the tortuosity of the membrane, $d_{(o)}$ thickness of organic layer and $D_{(o)}$ is the diffusion coefficient of the metal complex across the membrane. Considering the known value of τ as 2.7 [170] and $d_{(o)}$ as $60 \times 10^{-4} \text{ cm}$, the $D_{(o)}$ value was evaluated from proposed model as $2.35 \times 10^{-7} \text{ cm}^2 \cdot \text{s}^{-1}$. The mass transfer coefficient was calculated as $\Delta_{(a)}^{-1} = 1.02 \times 10^{-3} \text{ cm} \cdot \text{s}^{-1}$. A comparison of the diffusion coefficient, $D_{(o)}$ of different metal ions-extractant system is listed in **Table 6.3**. Observation indicate that the diffusion coefficient, $D_{(o)}$ calculated in the present work is comparable with the reported values.

Table 6.2: Variation of carrier (DNPPA) / *n*-paraffin concentration; U(VI): $2 \times 10^{-3} \text{ M}$; Feed acidity 2 M HNO₃; Receiver phase: 6 M H₂SO₄; Duration: 4h

[DNPPA], M	$P \times 10^4 \text{ cm/sec}$	% T
0.01	0.79	20.01
0.02	1.13	27.38
0.03	2.55	51.02
0.05	3.23	60.29
0.1	9.45	93.45
0.2	12.25	96.76

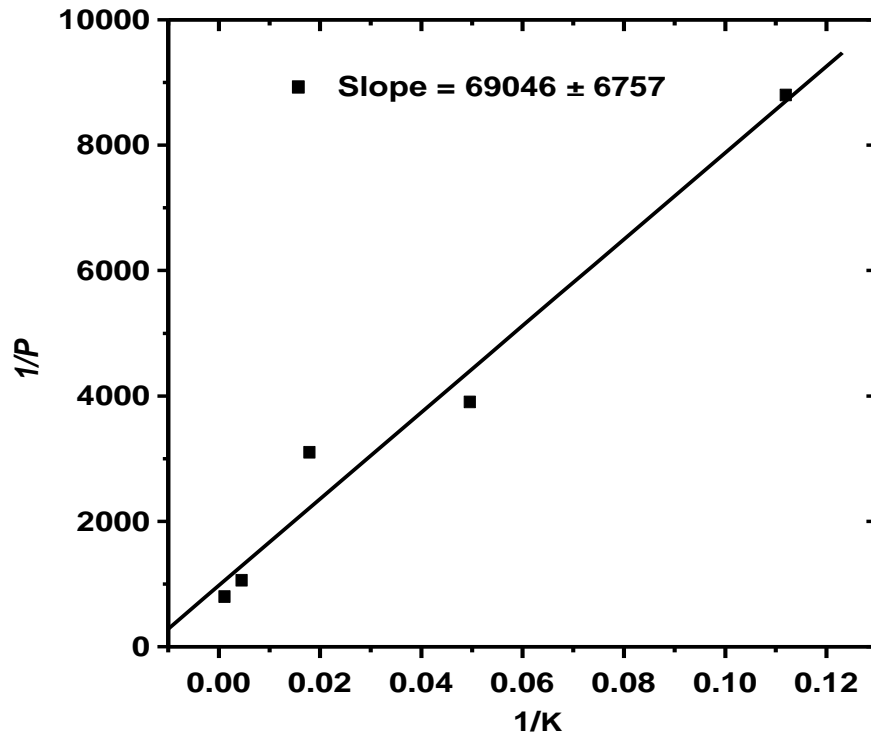


Figure 6.20. Plot of $1/P$ vs $1/K$ at different DNPPA concentration; Feed acid: 2 M HNO_3 ; U(VI) : 2×10^{-3} M Receiver phase: 6 H_2SO_4 , $[\text{U(VI)}]_{\text{feed}}$: 2×10^{-3} M

The diffusion coefficient of the uranium complex in the bulk organic phase ($D_{(o), b}$) can be calculated from the diffusivity in the membrane, $D_{(o)}$ using following equation [107]:

$$D_{(o)} = \varepsilon \cdot D_{(o),b} / \tau^2 \quad (6.15)$$

Where ε is the porosity of the membrane (0.72). The value of $D_{(o), b}$ was found to be $2.38 \times 10^{-6} \text{ cm}^2 \cdot \text{s}^{-1}$. The above result showed that the value of diffusion coefficient in membrane is less than the bulk diffusion coefficient. The less value of diffusion coefficient in membrane is caused by the diffusional resistance offered by the microporous thin PTFE membrane placed between feed and receiver phase.

Table 6.3. Comparison of diffusion coefficient $D_{(o)}$ of different metal ion extractant systems

Sr. No.	Metal ion-extractant system	diffusion coefficient $D_{(o)}$	Ref.
1	Co(II)-Cyanex 272	$3.25 \times 10^{-12} \text{ m}^2 \cdot \text{s}^{-1}$	[184]
2	Eu(III)-DTMPPA	$2.07 \times 10^{-10} \text{ m}^2 \cdot \text{s}^{-1}$	[189]
3	Cu(II)-MOC-55 TD	$1.2 \times 10^{-8} \text{ cm}^2 \cdot \text{s}^{-1}$	[190]
4	Cd(II)-Cyanex 923	$6.5 \times 10^{-6} \text{ cm}^2 \cdot \text{s}^{-1}$	[191]
6	U(VI)-DNPPA	$2.35 \times 10^{-7} \text{ cm}^2 \cdot \text{s}^{-1}$	[Present work]

6.3.3.2. Effect of membrane thickness

As described in the previous Section 2.5, the transport of uranium across SLM is a diffusion control phenomena. For such transport process, the permeability (P) of the metal ion is depends on the membrane thickness (effective diffusion path length). The permeability coefficient (P) depends on the membrane thickness $d_{(o)}$ and distribution coefficient (D_U) of the metal ion by the following equation (6.4). The U(VI) transport experiments were carried out by compressing a number of membranes (up to 4 no., pore size: $0.45 \mu\text{m}$, effective thickness: $60 \mu\text{m}$) and using $2 \times 10^{-3} \text{ M}$ U(VI) in the feed solution containing 2 M HNO_3 . $0.1 \text{ M DNPPA/ } n\text{-paraffin}$ were used as carrier solvent in the membrane phase in presence of $6 \text{ M H}_2\text{SO}_4$ as the receiver phase. The membranes were immersed separately in to the carrier solution of desired concentration and were stacked together to increase the thickness. With increase in membrane thickness, there is a gradual decrease in U(VI) transport from 93.5 % (no.1) to 40.8 % (nos.4) (**Figure 6.21**) due to increase in diffusional resistance with effective path length. Assuming the diffusion of U(VI)- $(\text{HA}_2)_2$ across membrane is rate determining step, the first term in the denominator of equation (6.4) can be ignored and P can be represented as:

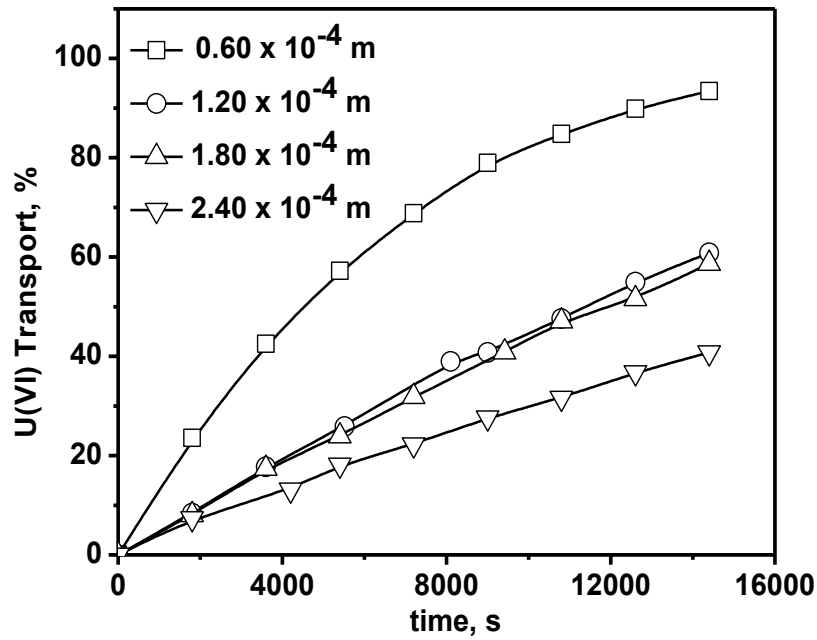


Figure 6.21. Variation of U(VI) transport with membrane thickness; Feed: 2×10^{-3} M U(VI) at 2 M HNO_3 ; Carrier: 0.1 M DNPPA in *n*-paraffin; Receiver phase: 6 M H_2SO_4

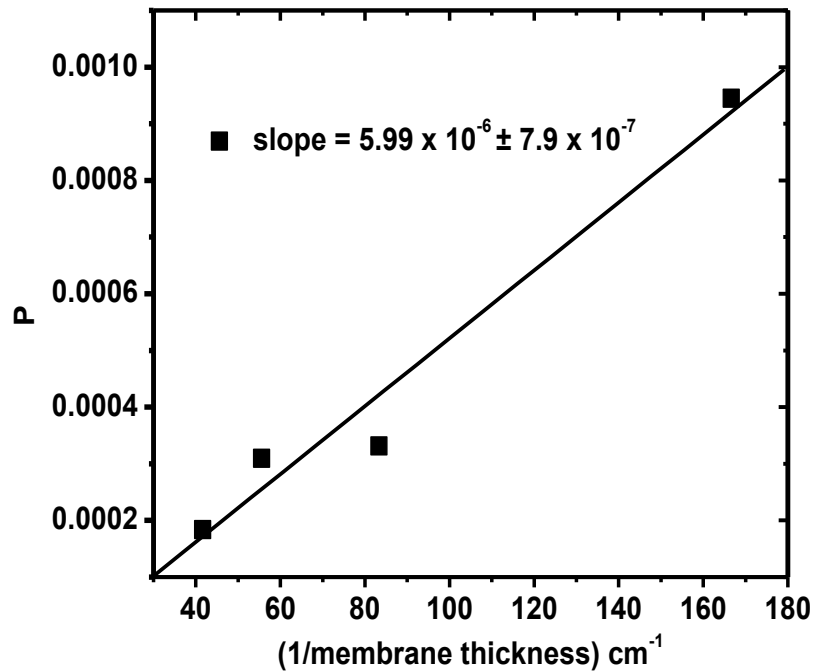


Figure 6.22. Variation of U(VI) permeability with membrane thickness; $[\text{U(VI)}]_{\text{feed}}: 2 \times 10^{-3}$ M; Receiver phase: 6 M H_2SO_4 ; Carrier: 0.1 M DNPPA in *n*-paraffin

Figure 6.22 shows the plot of P vs $1/d_{(o)}$ yield a straight line with a slope of $5.99 \times 10^{-6} \pm 7.9 \times 10^{-7}$. Assuming the known value of D_U (1.05×10^{-2}) and τ (2.7), $D_{(o)}$ was calculated as $1.58 \times 10^{-7} \text{ cm}^2 \cdot \text{s}^{-1}$. The $D_{(o)}$ calculated from kinetic modeling and membrane thickness variation methods are in good agreement. Similar results of $D_{(o)}$ were reported for uranium permeation from nitric acid medium across SLM using a synergistic mixture of 0.1M DNPPA + 0.05 M Cyanex 923/*n*-paraffin as carrier. Permeability (P) value for U(VI) transport inversely proportional to the membrane thickness which is a characteristic of a diffusion control transport process.

6.3.3.3. Synergistic transport of uranium

U(VI) transport experiments were carried out using the synergistic mixtures of 0.1 M DNPPA and 0.05 M neutral oxodonor (like Cyanex 923, TOPO, TEHP and TBP) in *n*-paraffin as the carrier. 2×10^{-3} M U(VI) at 2 M HNO₃ was used as feed and 2 M H₂SO₄ was the receiver phase unless stated otherwise (**Figure 6.23**). It should be noted that 2 M H₂SO₄ was chosen as receiver phase to clearly demonstrate the synergistic enhancement in U(VI) transport in the presence of neutral oxodonor in the carrier solutions. As expected, there was a significant enhancement in U(VI) transport across the membrane in the presence of neutral oxodonor in membrane phase as compared to that in the absence of oxodonor. Typically, % T values in 4 hours were ~74 (no oxodonor), 79 with TBP as oxodonor and ~90 with TOPO/Cyanex 923 as oxodonor. The order of synergism was in accordance of the basicities of these neutral donors as TOPO ~ ($K_H = 8.2$) Cyanex923 ($K_H = 8.1$) > TBP ($K_H = 0.16$) ~ TEHP ($K_H = 0.16$), where K_H = acid uptake constant. Similar observations were reported during solvent extraction studies of U(VI) using mixtures of DNPPA and TOPO from nitric acid medium [192]. However, it was interesting to observe that even though the TBP and TEHP have same acid uptake constant, there was no enhancement in U(VI) transport when DNPPA + TEHP mixture was used as synergistic carrier (**Table 6.4**). This

can be attributed to the steric hindrance due to the branched alkyl group (2-ethylhexyl) in TEHP during complexation. Based on these studies, Cyanex 923 was chosen as neutral donor for synergistic transport of uranium from nitric acid medium. The permeation of U(VI) from nitric acid medium across SLM using DNPPA is cation exchange mechanism (equation 6.4 to 6.7).

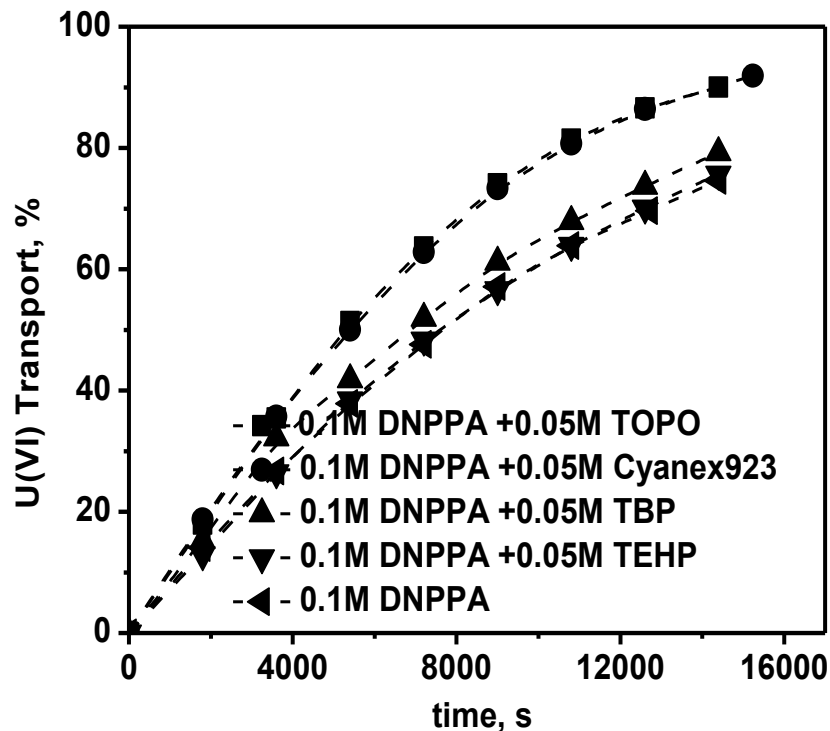


Figure 6.23. Effect of different neutral donors on U(VI) transport across SLM containing 0.1M DNPPA/*n*-paraffin in the membrane phase; Feed: 2×10^{-3} M U(VI) in 2 M HNO₃; Receiver phase: 2 M H₂SO₄

Table 6.4. Synergistic transport of uranium using DNPPA and various neutral donors in presence of 2 M H₂SO₄ as a receiver phase; [U(VI)]: 2x10⁻³ M; Feed acidity 2 M HNO₃; Duration: 4 hour

Composition	P×10 ⁴ cm/sec	% T
0.1 M DNPPA	4.8	74.6
0.1 M DNPPA+0.05 M TEHP	4.9	75.7
0.1 M DNPPA+ 0.05 M TBP	5.5	79.2
0.1 M DNPPA+ 0.05 M TOPO	8.4	90.0
0.1 M DNPPA+ Cyanex923	8.4	90.0

5.2.3.4. Effect of variation of mole ratio of extractants

The effect of neutral donor (Cyanex 923) concentration was investigated from a feed solution containing 2x10⁻³ M U(VI) in 2 M HNO₃ medium. The concentration of DNPPA and H₂SO₄ were fixed at 0.1M in membrane phase and 2M in the receiver phase respectively. **Figure 6.24** shows that with increase in Cyanex 923 concentration from 0.01 to 0.25 M; U(VI) transport (%) across SLM increased from ~81 to 99 % in 4 hour. However, further increase in the concentration of Cyanex 923 suppressed the transport of U(VI) across the SLM. The initial increase in uranium transport across SLM due to increase in Cyanex 923 in the membrane phase was attributed to synergistic effect of the mixed carrier solvent. Beyond 0.25 M Cyanex 923 concentration, the decrease in uranium transport across SLM may be due to increase in viscosity of the membrane phase which reduces the mass transfer across SLM (**Table 6.5**).

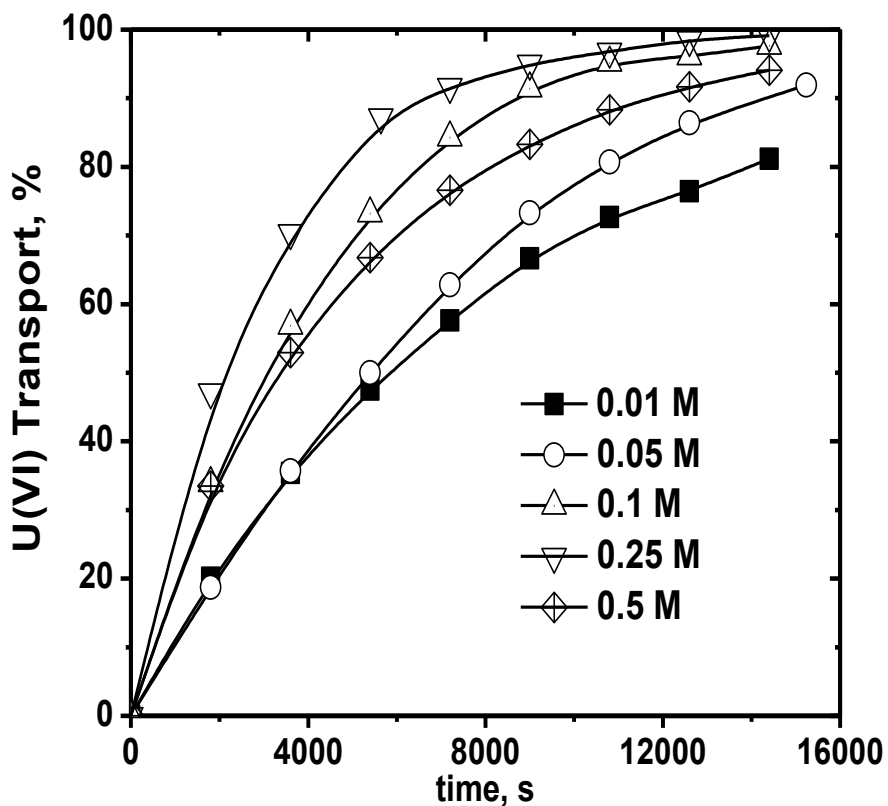


Figure 6.24. Effect of varying concentrations of Cyanex 923 on U(VI) transport across SLM; [DNPPA]: 0.1 M DNPPA; Diluent: *n*-paraffin; Feed: 2×10^{-3} M U(VI) in 2 M HNO₃; Receiver phase: 2 M H₂SO₄

Table 6.5. Viscosity and density measurements of different concentration of synergistic mixture containing 0.1M DNPPA and varying concentration of Cyanex 923 dissolved in *n*-paraffin

Cyanex 923, M	Density, g/cc	Viscosity, mPa.s
0.01	0.7635	1.7224
0.05	0.7676	1.7812
0.1	0.7689	2.0369
0.25	0.7758	2.3189
0.5	0.7875	2.9326

It is to be noted that, after 0.05M neutral donor concentration, there is a very small increase in U(VI) transport (from 97 to 99 %) across SLM, although the neutral donor concentration increase is very high (from 0.1 to 0.25 M). Hence, further U(VI) transport experiments were carried employing 0.1M DNPPA+ 0.05 M Cyanex 923 dissolved in *n*-paraffin as the carrier.

5.2.3.5. Comparison of U(VI) permeation with other synergistic solvent mixture

Transport of uranium was carried out from 2M HNO₃ as a feed solution using different synergistic mixture such as 0.1M DNPPA + 0.05M Cyanex 923, 0.1M D2EHPA + 0.05M Cyanex 923, 0.1M PC88A + 0.05 M Cyanex 923 and 0.1M Cyanex 272 + 0.05M Cyanex 923 dissolved in *n*-paraffin to compare the U(VI) permeability of different solvent mixture under identical experimental conditions. 2M H₂SO₄ was used as receiver phase at room temperature. The permeability order of U(VI) across SLM was given as follows: 0.1M Cyanex 272 +0.05M Cyanex 923> 0.1M PC88A + 0.05 M Cyanex 923 > 0.1M D2EHPA + 0.05 M Cyanex 923 > 0.1M DNPPA + 0.05M Cyanex 923(**Table 6.6**). The results are well agreement with the pK_a values of acidic organophosphorous extractants. Solvent extraction studies of U(VI) from nitric acid medium using different organophosphorous extractant having varying pK_a values shows that the extractant with higher pK_a values have higher extraction [**26,28**].

Table 6.6. Comparison of uranium transport with different synergistic solvent system

Solvent mixture	P (cm/sec)	% T
0.1M DNPPA + 0.05M Cyanex 923	8.8×10^{-4}	90.0
0.1M D2EHPA + 0.05M Cyanex 923	10.7×10^{-4}	94.8
0.1M PC88A + 0.05M Cyanex 923	12.7×10^{-4}	96.4
0.1M Cyanex 272 + 0.05M Cyanex 923	17.9×10^{-4}	98.9

6.2.4. Recovery of U(VI) from UNR solution

The SLM based separation process developed was applied for selective recovery of uranium from UNR waste solution generated during purification of uranium from crude raw material through U(VI)- HNO₃- TBP route in the front end of fuel cycle. PTFE membrane having pore size of 0.45 μm was used as solid support at 200 r.p.m stirring speed. It was observed that, 0.1 M Cyanex 272 + 0.05 M Cyanex 923/*n*-paraffin was the best choice for selective recovery of uranium from UNR solution under present experimental conditions (**Table 6.7**).

Table 6.7. Transport behavior of different metal ions present in a typical UNR solution at 1.1 M HNO₃ employing various combinations of carrier and receiver phases; Diluent: *n*-paraffin; Duration: 4 hours; Stirring speed: 200 r.p.m.

Elements	% U(VI) transport		
	0.1M Cyanex 272 + 0.05 M Cyanex 923/ 2M H ₂ SO ₄ *	0.1M DNPPA + 0.05 M Cyanex 923/ 2M H ₂ SO ₄ *	0.1 M DNPPA/ 6 M H ₂ SO ₄ *
U(VI)	98	93	94.2
Al(III)	<1	<1	< 1
Co(III)	<1	<1	1.7
Cr(III)	1	1	< 1
Er(III)	<1	< 1	< 1
Fe(III)	2	1	3.8
Gd(III)	<1	<1	< 1
Mg(II)	2	3	< 1
Mn(II)	<1	<1	< 1.
Ni(II)	1	3	< 1
Y(III)	2	1	< 1

*Receiver phase

6.3. Conclusions

The U(VI) permeation studies from HNO₃ medium was investigated using neutral (such as TEHP, TBP, TBEP) and acidic (such as PC88A, Cyanex 272, D2EHPA, DNPPA) organophosphorous extractants either alone or in combination using various receiver phases. It was observed that for all the neutral extractants uranium transport increases with aqueous phase acidity, become maximum and then decrease. The comparative transport studies of uranium using these extractants shows the order of transport is TEHP \geq TBP > TBEP. That shows there is a distinct effect of substitution of nature of alkyl group in uranium transport from nitric acid medium across supported liquid membrane.

On the other hand, uranium transport across SLM using acidic organophosphorous extractants decreased with increased in feed acid concentration. The presence of neutral donors such as TBP, TEHP, TOPO, Cyanex 923 along with PC88A, Cyanex 272 and DNPPA as carrier shows synergistic effect in uranium transport across SLM. The order of synergistic effects vary according to the acid uptake constant of the neutral donors (TOPO~ Cyanex 923 > TBP > TEHP). It was found that the 0.1 M Cyanex 272 + 0.05 M Cyanex 923/ and *n*-paraffin 2 M H₂SO₄ as receiver phase was the best combination for selective recovery of uranium from UNR solution.

CHAPTER VII

STUDY ON AGGREGATION BEHAVIOR OF DINONYL PHENYL PHOSPHORIC ACID (DNPPA)

7.1. Introduction

The ligands or organic extractants used in the solvent extraction to complex the metal ions in the organic phase are generally surface active amphiphiles containing polar metal binding functional groups. The non-polar moieties such as alkyl or aryl group, are required to make the resultant metal-ligand complex organophilic. The biphasic solvent extraction system containing common surfactants such as dialkyl naphthalenesulphonates, dialkyl phosphate or tetra alkyl diglycolamide, etc. are mostly explained with the help of thermodynamics, coordination chemistry and self-association of the solvents [193-200]. Di nonyl phenyl phosphoric acid (DNPPA), is one of the most promising extractants for the recovery of uranium from wet phosphoric acid (WPA) as well as other aqueous acidic solutions [200-203]. However, the studies of metal-DNPPA complexes in the organic phase show unusual interesting features that are difficult to explain with the framework of traditional coordination chemistry interpretation. Extraction behavior of metal ions such as U(VI) from nitric acid medium using DNPPA shows unusual behaviour at all acidities in comparison to the other commercially available acidic organophosphorous extractants such as di (2 ethyl hexyl) phosphoric acid (D2EHPA), 2-ethyl hexyl phosphonic acid 2-ethyl hexyl monoester (PC88A), and bis (2,4,4-trimethylpentyl) phosphonic acid (Cyanex 272) [28,115-118]. The anomalous extraction behaviour of DNPPA is attributed to aggregate formation in non-polar diluents and requires to be confirmed by Dynamics Light Scattering (DLS) and UV-Visible spectrometry.

7.2. The present work

DLS and spectrophotometric, studies were carried out to investigate the aggregation behavior of DNPPA under varying experimental conditions such as aqueous phase acidity, nature of diluents, and ligand concentration.

7.3. Results and Discussion

7.3.1. Effect of feed acidity and diluents on aggregation of DNPPA

DNPPA dissolved in different diluents such as *n*-dodecane and 1-Octanol forms reverse micelle due to its amphiphilic nature. The reverse micelles are formed due to Van der Waals force of attraction among the polar group present in DNPPA molecule dissolved in non polar diluents. The effect of feed acidity on the aggregation behaviour of DNPPA was studied at various concentration of nitric acid medium using 0.05M DNPPA dissolved in *n*-dodecane and 1-Octanol. **Figure 7.1** shows the variation of DNPPA aggregate particle size with the variation of HNO₃ concentration in the aqueous phase. The DNPPA aggregate particle size decrease with increased in HNO₃ concentration indicating an interaction of reverse micelle due to uptake of HNO₃ by DNPPA which was independently confirmed by UV-visible spectrophotometry.

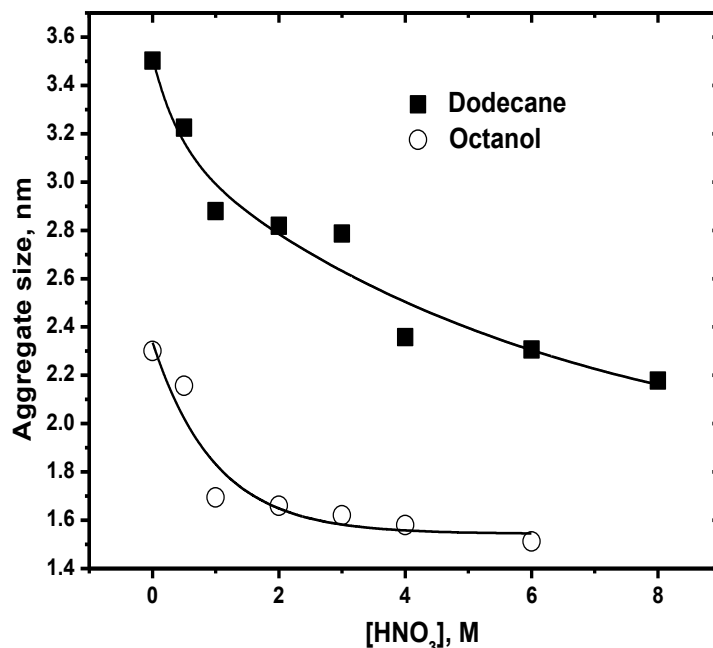


Figure 7.1. Effect of diluents on the aggregation behavior of 0.05 M DNPPA pre-equilibrated with different nitric acid solutions; [DNPPA] : 0.05M; Temperature: 25 °C

Figure 7.2 shows the UV-visible spectra of DNPPA dissolved in dodecane equilibrated with different concentration of HNO_3 . DNPPA/*n*-dodecane has a characteristic absorption peak at 293 nm in UV-visible region without equilibration with HNO_3 . With increase in HNO_3 concentration, the peak intensity at 293 nm decreased with appearance of a new peak arise at 354 nm which indicates the formation of new reverse micelle of smaller size. However, reverse micelle size measure of neutral extractant systems such as diglycomides, malonamides, TBP using various techniques (DLS, SANS, SAXS etc.) indicate the increase in reverse micelle size with increase in HNO_3 concentration in the organic phase [201-206].

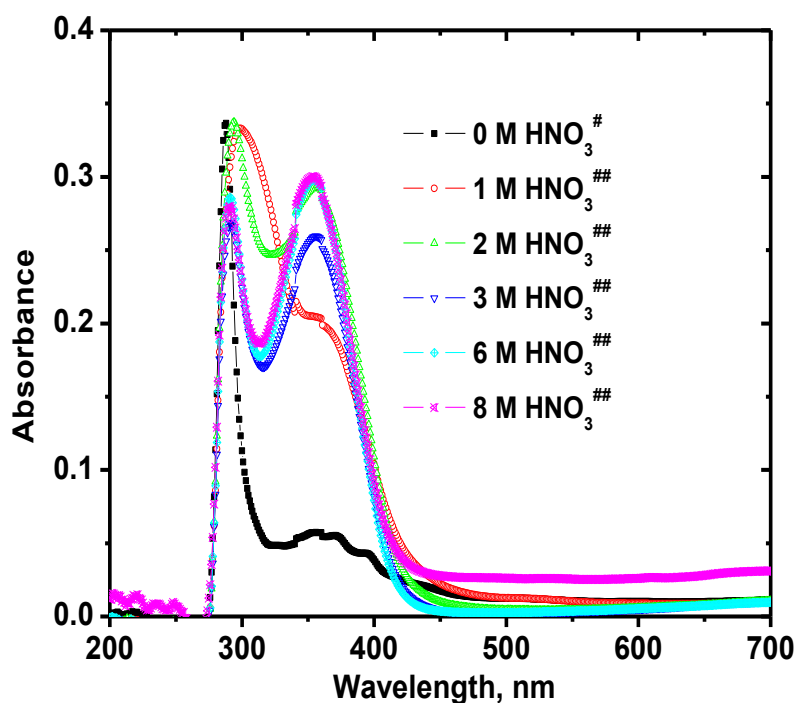


Figure 7.2. Absorbance spectra of DNPPA solutions dissolved in *n*-dodecane and pre-equilibrated with different nitric acid solutions [#] 5×10^{-3} M DNPPA; ^{##} 5×10^{-4} M DNPPA

The acidic organophosphorous extractants such as D2EHPA and DNPPA, adsorb at organic diluents/ water interface due to the acidity (electrophilicity) of the O-H group present in the extractant. The presence of H^+ ion in the form of HNO_3 in organic phase decreases the surface

tension of the DNPPA -micelles system. The decrease in reverse micelle size with increase in HNO_3 concentration in organic medium may be due to complexation of DNPPA with HNO_3 which decrease the interfacial surface tension of the acidic extractant in different organic diluents and hence decrease in the Van der Waals force of attraction among the polar group present in DNPPA reverse micelle. The effect of diluents such as 1-octanol shows that with increase in dielectric constant of diluents the size of DNPPA nano aggregate decrease due to interaction of polar diluents with DNPPA. Pathak et al. has also observed similar diluents effect on reverse micelle size of TODGA dissolved in different organic diluents in the presence of HNO_3 [202]. A direct correlation between DNPPA aggregate particle size and extraction of metal ion U(VI) from HNO_3 medium was observed. **Figure 7.3** shows the extraction behavior of U(VI) from different concentration of HNO_3 at constant DNPPA concentration in *n*-dodecane.

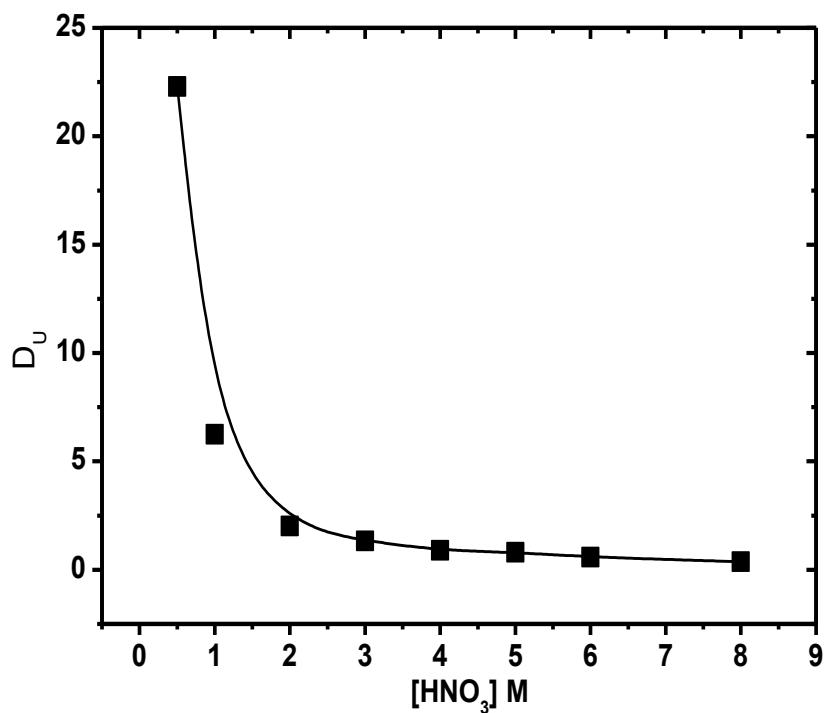


Figure 7.3. Variation of D_U with aqueous phase acidity; $[\text{U(VI)}]: 1 \times 10^{-3} \text{ M}$; Extractant: $1 \times 10^{-2} \text{ M DNPPA}$; Diluent: *n*-dodecane; temperature: 25°C

It was observed that with increase in HNO₃ concentration in aqueous phase, D_U decreased which can be correlated with the variation of DNPPA aggregate particle size variation with HNO₃ concentration.

7.3.2. Effect of DNPPA concentration on aggregation

The effect of DNPPA concentration in *n*-dodecane medium on nano aggregation size has been studied at constant HNO₃ concentration (1 and 3 M) and results are given in **Figure 7.4**. It was observed that with increased in ligand (DNPPA) concentration the size of aggregates increased indicating that the aggregation process was facilitated with ligand concentrations. Hence, the reason behind increase in reverse micelle size supposed to be due to increase in number of DNPPA molecules in the reverse micelle. Y. Meridiano et al. has also observed an increase in reverse micelle size with increase in ligand concentration in N,N'-dimethyl-N,N'-dioctylhexylethoxymalonamide (DMDOHEMA)/*n*-dodecane-water reverse micelle system [204]. Further, the result was supported by distribution ratio values of U(VI) in HNO₃ medium with DNPPA [203]. The UV-Visible spectroscopic study on ligand (DNPPA) variation also showed a distinct difference in the absorption spectra (**Figure 7.5**). At lower DNPPA concentration, the absorption spectra had a double hump containing peaks positions at 291 nm and 358 nm with equal intensities, and with increased in DNPPA concentrations 291 nm peak intensity decreased and a single broad peak with higher intensity appeared at 354 nm.

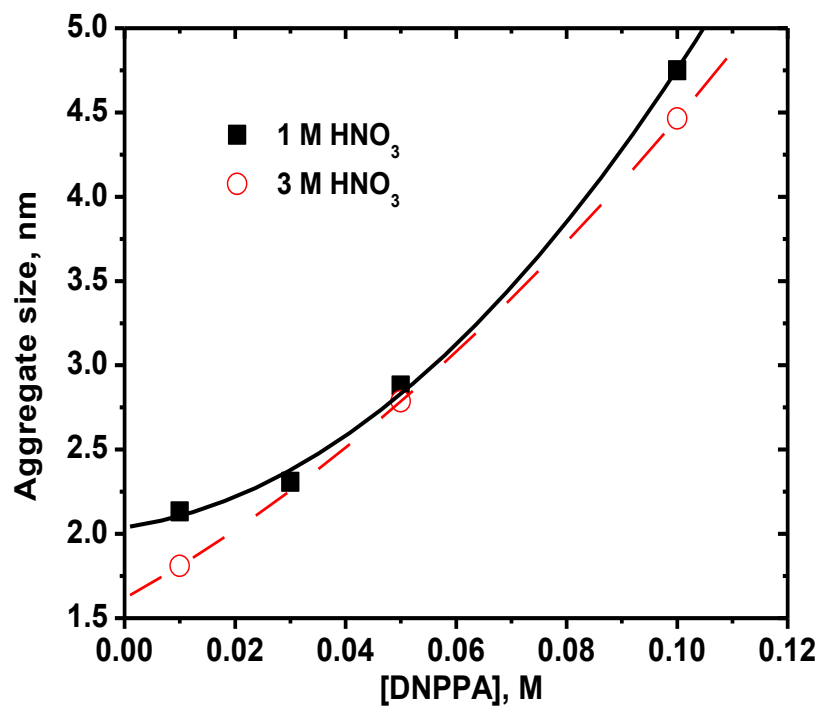


Figure 7.4. Effect of DNPPA concentration on its aggregation behavior pre-equilibrated with 1 & 3 M HNO₃; Diluent: *n*-dodecane; Temperature: 25 °C

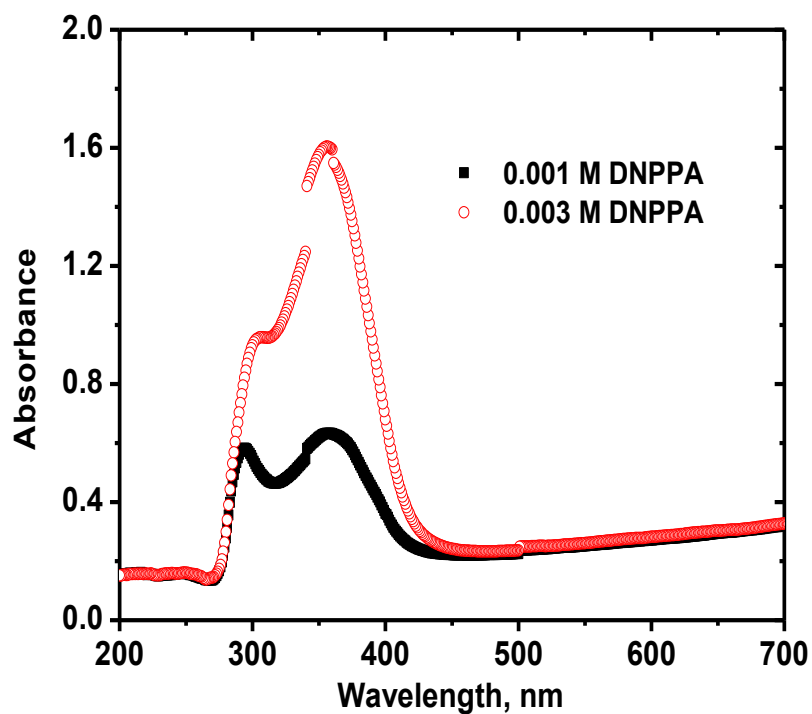


Figure 7.5. Absorbance spectra of DNPPA solutions dissolved in *n*-dodecane and pre-equilibrated with 3 M HNO₃

7.3.3 Effect of metal ions on aggregation

The presence of different metal ions (An/Ln) on the aggregation behaviour of DNPPA in *n*-dodecane was studied at constant extractant concentration (0.05M) under varying nitric acid concentrations (**Figure 7.6**) shows that the presence of metal ions such as U(VI), Eu(III) increased the particle size of DNPPA aggregate which can be explained on the basis of increased tendency of reverse micelle formation through ion-dipole interaction. It appears that metal ions with relatively higher charge enhance the energy of attraction between the extractant molecules in reverse micelles [201].

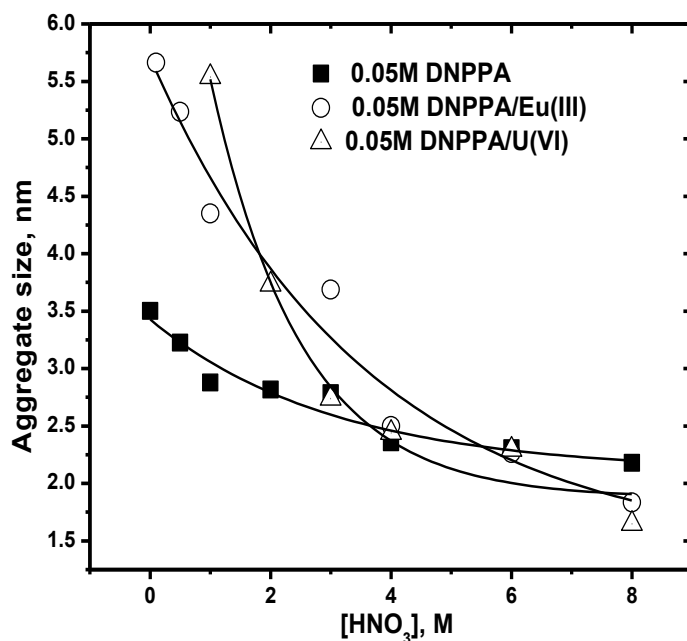


Figure 7.6. Effect of Eu(III)/U(VI) on the aggregation behavior of 0.05 M DNPPA pre-equilibrated with different nitric acid solutions; Diluent: *n*-dodecane; temperature: 25 °C

7.3.4. Influence of neutral donors on aggregation behavior

The presence of neutral donors such as Cyanex 923, TBP on aggregate formation of DNPPA/*n*-dodecane was investigated at different nitric acid concentrations using DLS technique. The

presence of Cyanex 923 in DNPPA increase the reverse micelle particle size where as TBP showed the reverse trend (**Figure 7.7**). Cyanex 923 will complex with HNO_3 present in the DNPPA/*n*-dodecane reverse micelle as has high acid uptake constant ($K_H : 8.2$). Further, the presence of Cyanex 923 in DNPPA reverse micelle will decrease the free HNO_3 concentration in the organic phase which will leads to the increase in the increase in interfacial surface tension and hence formation of bigger reverse micelle in the organic phase [19]. Antonio et al. observed that presence of DMDOHEMA malonamide in D2EHPA forms mixed reverse micelle in *n*-dodecane with larger size suing electrospray ionization mass spectrometry in combination with SAXS and SANS techniques [205].

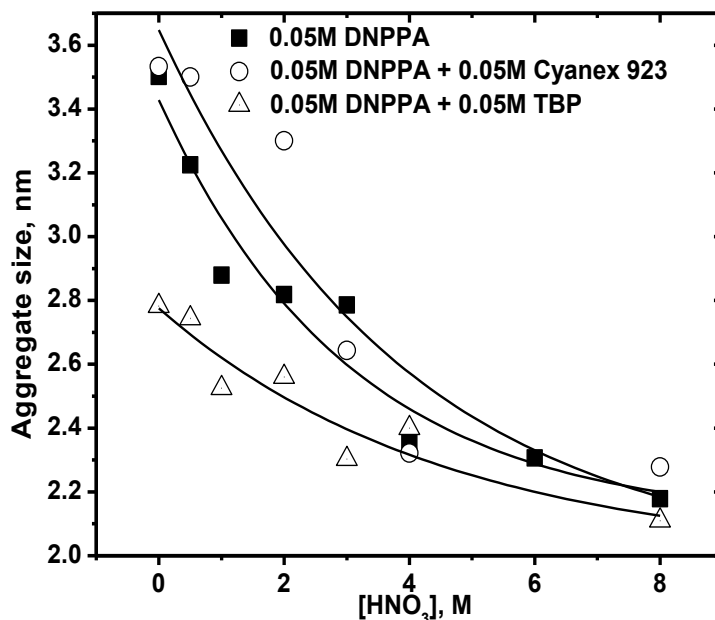


Figure 7.7. Effect of neutral donors on the aggregation behavior of 0.05 M DNPPA in *n*-dodecane pre-equilibrated with different nitric acid solutions; temperature: 25 °C

The reverse result in case of TBP may be due to very low acid uptake constant ($K_H: 0.2$) which interact very little with nitric acid present in organic medium. Further the spectroscopic data shows there are difference in absorption characteristic between DNPPA + Cyanex 923/

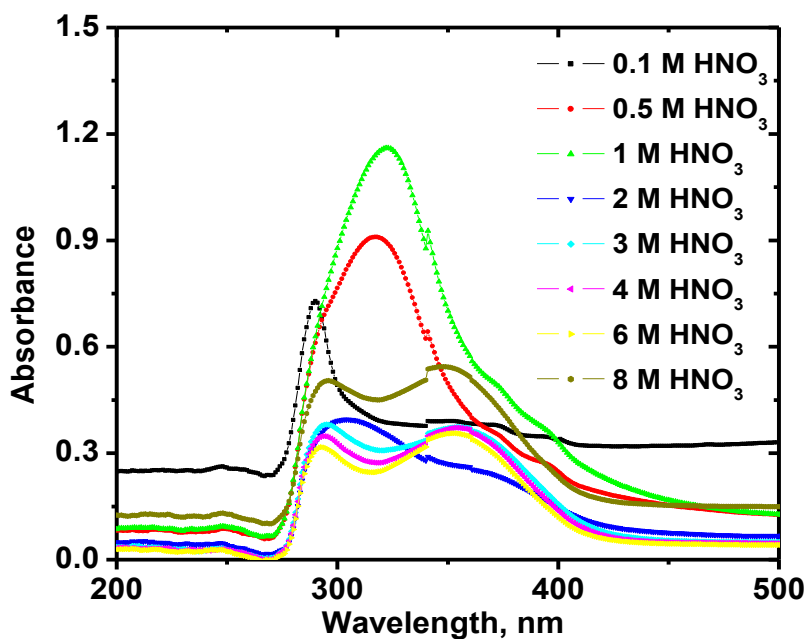


Figure 7.8: Absorbance spectra of 5×10^{-4} M DNPPA + 5×10^{-4} M Cyanex 923 solutions in *n*-dodecane pre-equilibrated with different nitric acid solutions

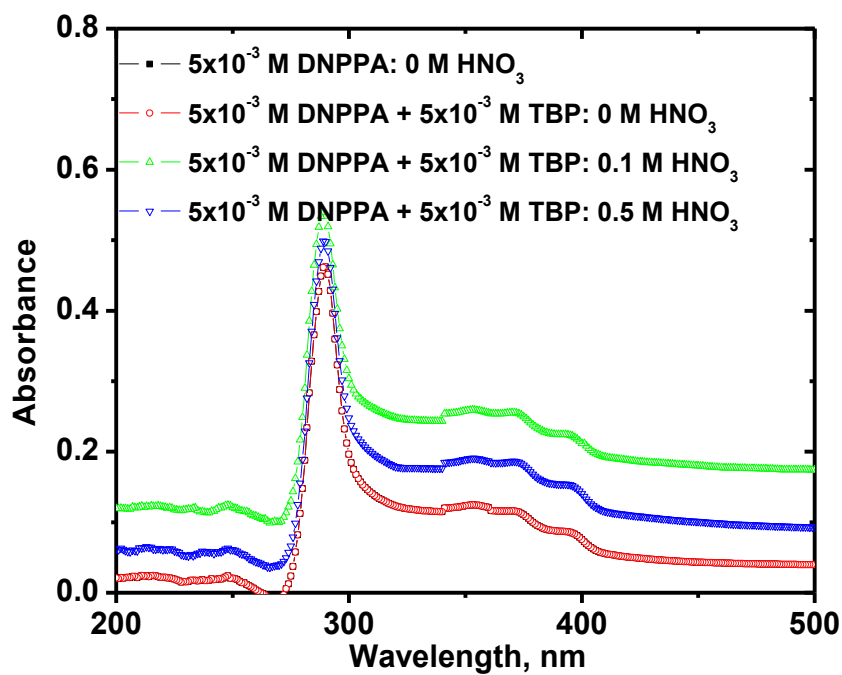


Figure 7.9 (a). Absorbance spectra of 5×10^{-4} M DNPPA + 5×10^{-4} M TBP solutions in *n*-dodecane pre-equilibrated with 0.1 - 0.5 M HNO_3

n- dodecane and DNPPA + TBP/*n*-dodecane (**Figures 7.8, 7.9a & 7.9b**). Presence of Cyanex 923 broaden the absorption spectra at low acidity (up to 3 M) with peak shift from 288 nm to 322 nm where as for TBP up to 0.5M HNO₃ there is no change in absorption maxima, but from 2M acid concentration double hump peak arise at 294 nm and 350 nm with equal intensities.

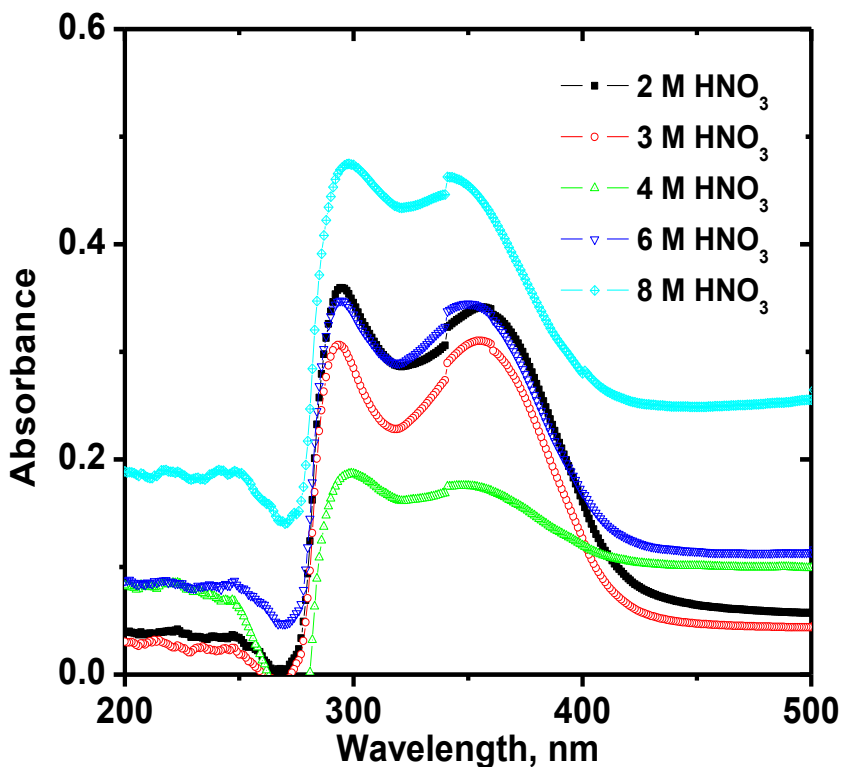


Figure 7.9 (b). Absorbance spectra of 5×10^{-4} M DNPPA + 5×10^{-4} M TBP solutions in *n*-dodecane pre-equilibrated with 2- 8 M HNO₃

7.4. Conclusions

The aggregation tendency of DNPPA decreases with increase in HNO₃ concentration equilibration and increase with DNPPA concentration. The aggregation behavior was also influenced by the nature of diluents and it was observed the aggregate size decrease in polar

diluents (Octanol). Presence of metal ions such as Eu(III)/U(VI) facilitated the aggregation behaviour of DNPPA at all HNO₃ concentration. Similarly presence of neutral donor such as Cyanex 923 increases the aggregation tendency of DNPPA where as in case of TBP it was reversed.

CHAPTER VIII

DEVELOPMENT OF EXTRACTIVE SPECTROPHOTOMETRIC METHOD FOR THE ANALYSIS OF URANIUM

8.1. Introduction

Uranium is an important element in the actinides series due to its wide applications in nuclear industry as a nuclear fuel. The primary source of uranium is naturally occurring uranium ore present in the earth crust. The recovery of uranium from ore is carried out via two step process viz. (a) acid, alkali or bio leaching, and (b) separation from the ore leach solution [207-213]. Monitoring of uranium concentration in ore leach solution is an important aspect for its effective and efficient recovery. A large number of analytical techniques have been used for the determination of uranium in a wide variety of samples such as environmental, sea water, process streams, effluent/waste streams, ores and ore leach solutions. The increasing availability of powerful instrumentals techniques such as Neutron Activation Analysis (NAA), Energy Dispersive X-Ray Fluorescence (EDXRF), Inductively Coupled Plasma Emission Spectrometry (ICPAES), Inductively Coupled Plasma Emission Mass Spectrometry (ICPMS) has enabled the analysis of complex mixtures with high accuracy and precision [214-219]. However, these advanced techniques require sophisticated high value instruments (including nuclear reactors). On the other hand, the low cost techniques (such as spectrophotometry) cannot be used successfully without prior chemical separations due to spectral interference of rare earths and transition elements [220,221]. Nevertheless, the association of spectrophotometric techniques employing chelating agents and chemometric methods, such as Partial Least Squares (PLS), multivariate calibration procedures, offers outstanding advantages for the analysis of complex matrices [222,223]. In this context, 2-(5-bromo-2-pyridylozo)-5-diethyl aminophenol (Br-PADAP) as chelating agent has been extensively used for the spectrophotometric analysis of U(VI) in various matrices [99,100]. Das *et al.* demonstrated the determination of trace amounts of U(VI) in nitric acid medium by selective extraction of U(VI) from a mixture of U(VI), Pu(IV),

Fe(III), Th(IV) in to organic phase comprising of TOPO/cyclohexane and simultaneous color development using Br-PADAP [101].

8.2. *The present work*

A method has been developed for the measurement of trace amounts of U(VI) present in ore leach solutions containing a large number of other metal ions *viz.* rare earths, transition elements (Fe, Mn, Ni, Cr etc.) in sulphate medium (**Table 8.1**). In view of non selective nature of Br-PADAP, U(VI) has been selectively extracted from ore leach solution in to organic medium containing a synergistic mixture of PC88A + TOPO in cyclohexane and simultaneously color development in organic medium using Br-PADAP in presence of a buffer solution at pH 7.8. NaF and ascorbic acid were used as additive in the aqueous phase for masking of extraction of other elements. The complexation of Br-PADAP with U(VI) is pH dependent and is optimum at ~8. Several common laboratory buffers such as phosphate, borate and *N*-cyclohexyl-3-aminopropanesulfonic acid (CAPS) are capable of maintaining the pH within the acceptable range. Because of limited water solubility of Br-PADAP, stock solution of Br-PADAP was prepared in absolute ethanol prior to addition to the reaction mixture. After addition of Br-PADAP, color development is very rapid in the presence of sufficient amount of U(VI). This results in a bathochromic shift of the absorbance maxima from 444 nm to 576 nm (**Figure 8.1**). The wavelength shift can be detected with a visible-light spectrophotometer. PC88A in combination with TOPO shows quantitative extraction of uranium from 1M HNO₃. Conditions have been optimized for extraction and spectrophotometric estimation of uranium in ore leach solution containing 2.5 – 250 µg mL⁻¹ uranium.

Table 8.1. Metal tested for the ability to bind Br-PADAP

Do not bind	Bind but can be masked	Bind, not masked
Li	Co	U
Cs	Cd	
Ta	Ni	
Na	Pb	
Mg	Zn	
Ce	Fe	
Cr	Cu	
W	Th	
K		
Ca		
Mo		
Rb		
Ba		
Ag		
Gd		
Al		

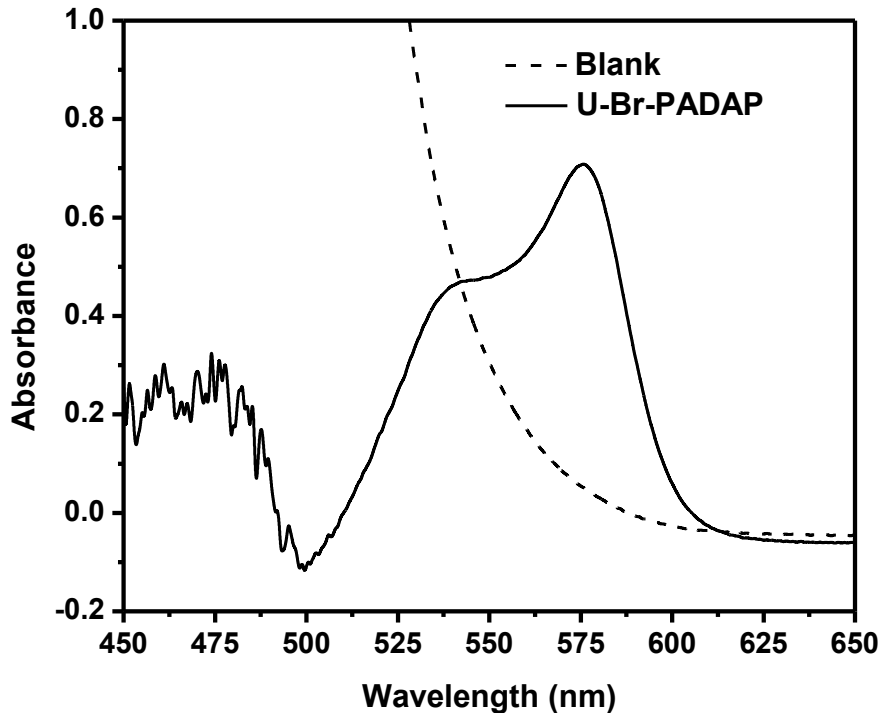


Figure 8.1. Absorption spectra of U-Br-PADAP complexes in PC88A+TOPO/Cyclohexane medium

8.3. Experimental procedure

The sample aliquot was taken in 20 mL 1M HNO₃ in an extraction vial. To this following reagents were added carefully 2 mL of 5 % ascorbic acid, 5 mL of 2 % NaF and the equilibrated with 5 mL organic phase for 2-3 minutes. After equilibration, the aqueous phase was discarded. To 1mL of complexing solution in a 25 mL standard flask, 2 mL of extracted organic phase was taken and then other reagents added in the following orders; 4 mL Br-PADAP solution, 1 mL buffer, 16 mL ethanol. The solution was diluted to 25 mL by distilled water. The solutions were kept for 10 minutes and then optical density was measured at 576 nm against a reagent blank. The calibration curve was drawn by taking average value of five measurements of each standard solution.

8.4. Results and Discussion

8.4.1. Effect of time on color stability

Figure 8.1 shows the absorption of U(VI)- Br-PADAP complex in 0.1M PC88A + 0.05M TOPO/cyclohexane synergistic mixture (used as extractant) and which reveals that absorption maximum appears at 576 nm. The molar extension coefficient (ϵ) at $\lambda_{\max} = 576$ nm is $36750 \pm 240 \text{ Lmol}^{-1}\text{cm}^{-1}$ in the presence of 64 % ethanol in the colored sample solution. The color stability of U(VI)-Br-PADAP complex was monitored as a function of time, which was extended up to several hours. It was observed that the color of U(VI)-Br-PADAP complex is stable up to > 24 hours (**Table 8.2**). **Figure 8.2** shows the calibration plot for the determination of U(VI) in sulphuric acid medium. It is observed that the calibration curve is linear up to $250 \mu\text{g U(VI) mL}^{-1}$ of sample solution and obeyed the following equation:

$$Y = m \cdot X + C \quad (8.1)$$

Where 'm' is the slope ($0.00386 \pm 3.47 \times 10^{-5}$) of the calibration curve, 'C' is the constant (-0.00549 ± 0.00448), Y and X are the variables respectively. The colored complex obeys Beer's law in the range of $0\text{-}250 \mu\text{g} \cdot \text{mL}^{-1}$ sample solution. A number of metal ions can interfere in the color development of U(VI)-Br-PADAP complex leading to error in absorbance measurement (**Table 8.1**). Therefore, the solvent extraction step is introduced for selective separation of uranium in to 0.1M PC88A + 0.05M TOPO/cyclohexane from the aqueous medium prior to color development in the organic phase by Br-PADAP reagent in the presence of complexing agent and buffer of pH 7.8. The reaction between Br-PADAP and U(VI) is pH sensitive and the main function of buffer solution is to maintain constant pH (7-8) to allow stable color development using the organic extracts containing uranium. It helps in the quantitative determination of U(VI) present in sample solutions. It is important to mention that ascorbic acid

is added to prevent the extraction of Fe(III) present in aqueous samples by reducing to Fe(II) state. Similarly, the acidity of the aqueous phase was maintained 1M by adding HNO₃ to prevent extraction of transition metal as well as rare earth elements from aqueous phase to organic phase during selective extraction of uranium using synergistic mixture. NaF present in the aqueous phase acts as masking agent for elements like Al(III), Fe(III), and Th(IV) etc. by forming most stable complexes in the aqueous phase. Thus, the complexing agents CyDTA and NaF suppress the extraction of impurities extracted in to the organic phase along with uranium. Application of Job's method revealed, the Stoichiometry of uranium and Br-PADAP complex is 1: 1 with the following chemical formula [U-Br-PADAP]⁺ [101]. At pH 7-8 both F⁻ and OH⁻ ion could be co anion forming complex with [U-Br-PADAP]⁺ ion. However, F⁻ ion is the most probable co anion as the possibility of OH⁻ as a co anion is ruled out as hydroxyl complex of U-Br-PADAP complex is highly unstable [99].

Table 8.2. Color Stability of U(VI)-Br-PADAP complex, λ_{max} : 576 nm

U- STD, $\mu\text{g mL}^{-1}$	Absorbance		
	10 minutes	4 hours	24 hours
10	0.025	0.026	0.025
20	0.076	0.076	0.075
30	0.098	0.098	0.099
50	0.174	0.175	0.174
100	0.366	0.368	0.367
200	0.759	0.759	0.761
250	0.958	0.953	0.971

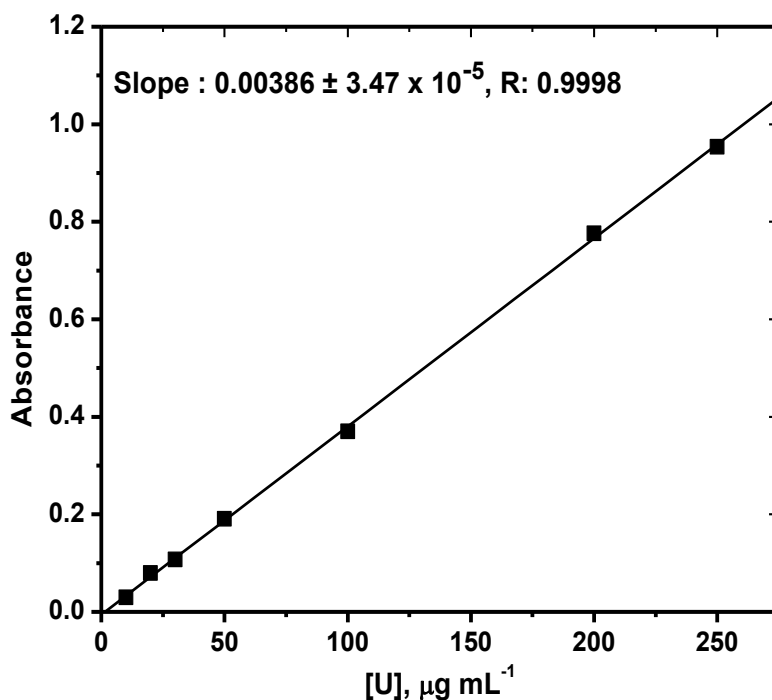


Figure 8.2. Calibration plot of determination of U(VI) in sulphate medium using Br-PADAP in 0.1M PC88A + 0.05M TOPO/Cyclohexane organic medium

The chemical reaction between Br-PADAP and uranium in presence of F⁻ anions can be written as:



8.4.2. Optimization of ethanol concentration

Ethanol plays an important role in this method. The solubility of Br-PADAP as well as U(VI)-Br-PADAP complex in aqueous phase is very poor, and may offer to phase separation and the addition of ethanol increases the solubility of U(VI)-Br-PADAP complex in the sample solutions. Thus, ethanol is act as a phase modifier. There was a decrease in aqueous solubility of U(VI)-Br-PADAP complex leading to phase separation for ethanol (v/v) content < 56 %. However, there was a decrease in the absorbance values (~23 %) of U(VI)-Br-PADAP complex in the sample solutions with increased ethanol proportions from 56 % to 64 %; and

correspondingly the molar extension coefficient (ϵ) decreased from $47886 \pm 450 \text{ L.mol}^{-1}\text{cm}^{-1}$ to $36750 \pm 240 \text{ L.mol}^{-1}\text{cm}^{-1}$ at $\lambda_{\text{max}} = 576 \text{ nm}$ (**Figure 8.3**).

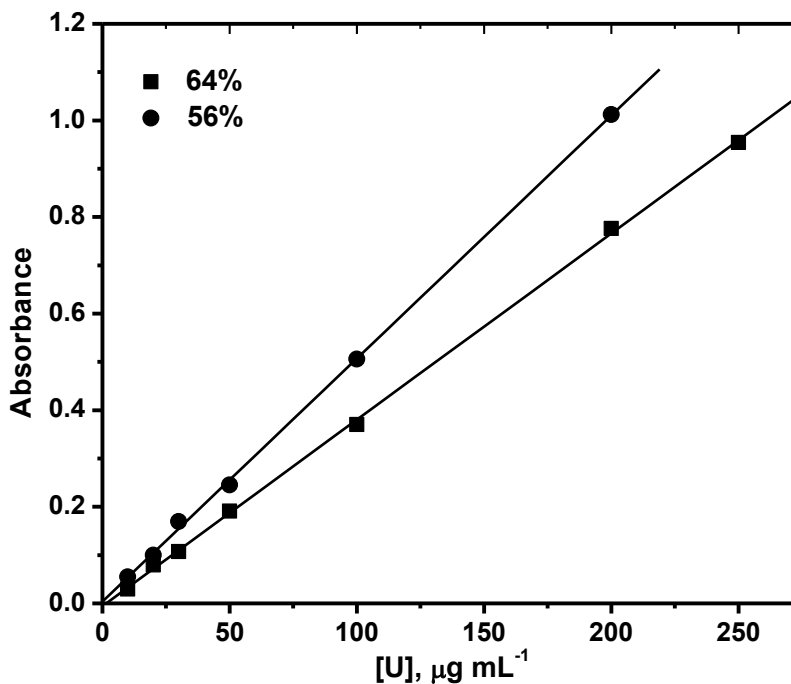


Figure 8.3. Effect of ethanol content in absorbance of U(VI)-Br-PADAP complexes in 0.1M PC88A+ 0.05M TOPO/cyclohexane medium

Based on this observation, the ethanol concentration was maintained as 64 % for further studies. This helped in avoiding the phase separation by increasing solubility of U(VI)-Br-PADAP complexes.

8.4.3. Accuracy of the analytical method

The accuracy of the developed analytical method was tested by standard addition method. Uranium standards of various concentrations were added to actual ore leach solution containing $19.4 \mu\text{g.mL}^{-1}$ U(VI) and a large number of other elements as impurities. The recoveries of the added standards were within $101.5 \pm 3.5 \%$ (**Table 8.3**).

Table 8.3. Recovery study of the analytical technique on the basis of added/found concentration of uranium standards

$[U]_{\text{added}}, \mu\text{g mL}^{-1}$	$[U]_{\text{found}}, \mu\text{g mL}^{-1}$	% Recovery	\pm % Difference
29.4	29.9	101.7	+ 1.70
39.4	38.8	98.5	- 1.52
49.4	51.0	103.2	+ 3.20
69.4	71.0	102.3	+ 2.30
119.4	119.7	100.2	+ 0.25
219.4	221	100.7	+ 0.73

8.4.4. Effect of other ions

Table 8.4 shows the tolerable limits of different impurities ions in the presence of $200 \mu\text{g mL}^{-1}$ of U(VI) in ore leach solution. The extraction and interference of transition metal ions and rare earths are less due to presence of F^- as well as ascorbic acid. The main role of F^- is to mask metal ions like Al(III), Zr(IV), Fe(III), La(III), where as the role of ascorbic acid is to reduce the oxidation state of Fe(III) to Fe(II) to prevent its extraction in to the organic phase. It is observed that the presence of Th(IV) decrease the tolerance limit. The probable reason for low tolerance limit of Th(IV) was the presence of insufficient amount of F^- in the aqueous phase as well as in the organic phase. On the other hand, ascorbic acid cannot mask it due to its stable +4 oxidation states. Hence, Th(IV) ions get extracted in the organic phase along with U(VI) which reduce the signal of U(VI) to $> 10\%$. However, Th(IV) content in uranium ore leach solution is generally in the range of $<10 \mu\text{g mL}^{-1}$ [224]. Our studies suggest that the presence of thorium in this concentration range in leach solutions will not have any positive bias on the measured uranium concentration.

Table 8.4. Effect of various ions on the determination of U(VI) concentration in ore leach solution; [U(VI)]: 200 $\mu\text{g mL}^{-1}$

Ions	Amount (μg)	Error (%)
Al(III)	1214	<1
Ce(III)	44	<2
Cr(III)	20	<2
Fe(III)	3330	<5
Mg(II)	1017	<2
Mn(III)	3440	<2
Y(III)	15	<2
Zr(IV)	500	<1
Mo(V)	500	<2
Th(IV)	200	<10

number of measurement for single sample is 3 (n= 3)

8.4.5. Precision of the developed method

The precision of the methods was evaluated by analyzing standard uranium solution 10 times under identical conditions and it was found to < 2 % at 50 $\mu\text{g mL}^{-1}$ U (**Table 8.5**). The repeated analysis of standard solution and ore leach solution by the above methods shows that the overall accuracy and precision is better than 2 %.

Table 8.5. Evaluation of relative standard deviation of the methods

S.N.	[U] _{stand.} , $\mu\text{g mL}^{-1}$	[U] _{ore leach.} , $\mu\text{g mL}^{-1}$
1	51.29	51.55
2	48.19	51.55
3	50.26	52.85
4	48.96	51.81
5	48.96	50.78
6	48.94	52.07
7	48.94	50.52
8	51.04	53.37
9	51.55	51.04
10	51.81	50.78
Average	49.82	51.63
rsd	1.6 %	0.58 %

rsd: relative standard deviation

8.4.6. *t* and *F* test

For better comparison of proposed method with the existing method such as ICPAES, *t* and *F*-test were carried out employing a ore leach solution containing $51.630 \mu\text{g}\cdot\text{mL}^{-1}$ uranium solution in sulphuric acid medium for total number of analysis $n= 10$. The value of absolute *t* was calculated using following equation [23]:

$$|t| = \frac{(\bar{X}_1 - \bar{X}_2)}{\text{sv}\sqrt{(1/n_1 + 1/n_2)}} \quad (8.3)$$

Where \bar{X}_1 and \bar{X}_2 are the average value of uranium evaluated from ICPAES and Br-PADAP methods, s is the pooled variance; n_1 and n_2 are the number of data point taken for the two methods respectively. The value of pooled variance 's' was calculated by the following equation:

$$s^2 = \{(n_1 - 1)s_1^2 + (n_2 - 1)s_2^2\}/(n_1 + n_2 - 2) \quad (8.4)$$

Where s_1^2 and s_2^2 are the variance of ICPAES and Br-PADAP method, respectively. **Table 8.6** shows the results of determination of uranium ore leach solution using ICPAES and Br-PADAP methods. The absolute value of t was found to be 0.53 where as the tabulated critical value of t at 95% confidence limit for degrees of freedom $v = 9$ is 2.262 [225]. This exceeds the calculated value of 0.53; therefore there is no difference between the means of results obtained. Similarly, the F-test of the two methods was carried out to compare the precision of the above two methods. The F value of the above two methods was calculated by dividing larger variance to the smaller variance and its value was found as 1.965. The tabulated critical value of F at 95 % confidence limit is 3.184 which means the method proposed for extractive spectrophotometric determination of uranium using Br-PADAP is precious, convents and acceptable.

Table 8.6. t and F- Test comparison of means from two (ICPAES and Br-PADAP) methods using a single ore leach solution

Sample no.	Experimental results		Squares of deviations	
	ICPAES	Br-PADAP	ICPAES	Br-PADAP
1	50.925	51.550	0.260	0.013
2	52.171	51.550	0.542	0.013
3	51.394	52.850	0.002	2.002
4	52.392	51.810	0.916	0.141
5	52.347	50.780	0.832	0.429
6	50.625	52.070	0.656	0.403
7	51.229	50.520	0.042	0.837
8	51.635	53.370	0.040	3.744
9	50.581	51.040	0.729	0.156
10	51.05	50.780	0.148	0.429
Sum	514.349	516.320	4.167	8.168
	51.435	51.630	0.462	0.908
	Mean		Variance	

8.4.7. Evaluation of detection limit

The detection limit of the above method was investigated by measuring absorbance of the blank solution several times (n= 10) without adding any sample aliquot. The detection limit of the

analytical technique is assumed to be three times of standard deviation of blank solution (3σ).

The detection limit of this method was determined to be $\geq 2.5 \mu\text{g mL}^{-1}$ (**Table 8.7**).

Table 8.7. Evaluation of detection limit of the method for measurement of uranium in ore-leach solution

S.N.	Absorbance (λ_{max} : 576 nm)	[U], $\mu\text{g mL}^{-1}$
1	0.006	1.6
2	0.005	1.3
3	-0.002	-0.5
4	0.01	2.6
5	0.002	0.5
6	-0.002	-0.5
7	0.003	0.8
8	0.001	0.3
9	0.002	0.5
10	0.004	1.04
Average	0.003	0.75

detection limit = $2.5 \mu\text{g /mL}$

8.4.8. Application of the developed method to real samples

The proposed method was applied successfully for the determination of uranium in ore leach solutions containing a large number of other impurities (**Table 8.8**). It was observed that the

results are very close to the reported value using ICPAES technique and the method can be helpful for the monitoring of uranium during ore leaching in front end of fuel cycle. The main advantages of the above method over the other are its simplicity, accuracy and higher analytical range (2.5 -250 $\mu\text{g mL}^{-1}$). However, the only disadvantage of the proposed method is the very little tolerance limit of Th.

Table 8.8. Comparison of extraction spectrometric and ICPAES analysis of some typical ore leach solutions

Ore leach samples	[U], $\mu\text{g mL}^{-1}$		
	Br-PADAP	ICPAES	\pm % Difference
1	2.76	2.56	+ 0.20
2	3.88	4.20	- 0.32
3	7.70	7.60	+ 0.10
4	19.46	19.40	+ 0.06
5	51.63	50.40	+ 1.23
6	194.20	193.90	+0.30

Number of measurement for single sample is 3 (n= 3)

8.5. Comparison with the other existing methods

The present method has been compared with the existing methods such as oxine and ferron methods of determination of U(VI) from HNO_3 medium using solvent extraction technique in combination with spectrophotometry and results are tabulated in **Table 8.9**. In oxine methods the U is extracted in oxine/chloroform medium (pH~8.8) in presence of EDTA where as in ferron methods the U-ferron complex was extracted in tertiary amine /chloroform (pH~4.5).

Table 8.9: Comparison of Br-PADAP method with the other existing methods

Method	Wavelength	Molar absorptivity, ϵ	Range ($\mu\text{g/mL}$)	Sensitivity ($\mu\text{g/mL}$)	Accuracy and precision
Br-PADAP	576 nm	47886	2.5 -250	0.00386	< 2 %
Ferron	380 nm	7920	100- 700	0.028	< 2%
Oxine	400 nm	-	30-300	-	< 2 %

8.6. Conclusions

The proposed method provides a simple, very sensitive and low cost spectrophotometric procedure for determination of uranium in ore leach solutions. The solvent extraction step employing 0.1M PC88A + 0.05M TOPO/cyclohexane was used to recover uranium selectively in organic phase. Br-PADAP, CyDTA as well as buffer were used for development of intense color for spectrophotometric measurement of uranium. Addition of NaF, ascorbic acid before the extraction step reduces the interference from transition as well as lanthanide/actinide elements. The optimum concentration of ethanol was determined as 64% to increase the solubility of Br-PADAP in the aqueous phase. The tolerance limit of Th(IV) is relatively low as compared to other elements due to strong complex formation of Th(IV) with synergistic mixture during solvent extraction step. The method could be applied for the determination of uranium in ore leach solution in the range of 2.5 -250 $\mu\text{g mL}^{-1}$ with the precision of < 2 %. A comparison of developed method and standard ICPAES method indicate that the former method is simple, low cost and faster than the later.

RECOMMENDATION FOR FURTHER RESEARCH

In the examples of SLM (chapter 6) applications presented above, the possibility to separate high quantities of metal ions using small volumes of organic phases shows that this method is still a very attractive choice when an efficient and selective method is necessary. Also, as a result of the development and commercialization of hydrophobic hollow-fiber membrane contactors, SLM might be applied successfully for industrial purposes. This is due to the high membrane surface per unit of volume with satisfactory liquid membrane stability and that HF-SLM technology is easily scalable. Therefore, there is much research to increase the applicability of SLM in the metal separation and recovery, wastewater treatment and analytical chemistry. Many of the new, interesting applications of SLM describe the use of the SLM concept. Thus, in the uranium purification plant, SLMs can be utilized in the recovery of U from effluent solution. One such possibility is already described in chapter 6, the recovery of uranium from uranyl nitrate raffinate solution (UNR) of which is a very challenging task. The process described in this thesis could be scale-up for commercial application in nuclear waste treatment using HF-SLM technology. Further, the chemical as well as radiation stability of different support can be evaluated in detail in particular emphasis of nuclear waste treatment. The agglomeration of DNPPA studied in chapter 7 is an interesting topic from the view point of surface chemistry. Further experiment may be carried out to determine the shape of the agglomerate and the number of molecule take part in agglomeration using advanced technique such as small angle X-ray scattering and neutron scattering. The analytical method developed for determination of uranium in ore leach solution using spectrophotometric technique in chapter 8 is an interesting analytical technique as the technique is cost effective and easy. The technique may be validated for other solution such as phosphoric acid medium (except ore leach) containing trace amount of uranium.

References

1. Bhattacharjee, B., An overview of R&D in fuel cycle activities of AHWR, 14th Indian Nuclear Society Annual Conference (INSAC), IT-1 (2003) 1-27.
2. Mukherjee, T.K., Singh H., 14th Indian Nuclear Society Annual Conference (INSAC), IT-7 (2003) 1-9.
3. Integrated Energy Policy: Report of the Expert Committee. Planning Commission Document, Government of India, 2006, p.1-147.
4. Mellor, J.W., Comprehensive Treatise on Inorganic and Theoretical Chemistry, Vol.XII, Longmans, Green and Co., London.
5. Holden, N.E., Isotopic Composition of the elements and Their Variation in Nature – A Preliminary Report, BNL-NCS-50605, Pure Appl. Chem., 52 (1979) 2349-2384.
6. Gmelin Hand Book of Inorganic Chemistry, System No. 55, Uran and Isotope mit einem Anhang uber Transurane, (1936) Main volume, Verlag Chemie, Berlin.
7. Holden, A.N., Physical Metallurgy of Uranium, (1958) Addison-Wesley, London.
8. Finch, R.J. and Murakami, T., Rev. Miner., 38 (1999) 91-180.
9. Plant, J., Simpson, P.R., Smith, B., and Windley, B.F., Rev. Miner., 38 (1999) 255-319.
10. Burns, P.C., and Finch, R.J., Am. Miner., 84 (1999) 1456-1460.
11. Fuchs, L.H., and Gebert, E., Am. Miner., 43 (1958) 243- 248.
12. Gmelin Hand Book of Inorganic Chemistry, Suppl. Ser., Uranium, (1981) Vol. C14, Springer-Verlag, Berlin, Heidelberg, and New York.
13. Gupta, C.K., Singh, H., Uranium Resource Processing: secondary Resources, (2003) Springer, Germany.

14. Production of yellow cake and uranium fluorides, IAEA, Vienna, June 5-8 (1979)
SIT/PUB/553.
15. Singh, H., Gupta, C.K., Min. Pro. Ext. Met. Rev., 21 (2000) 307-349.
16. Singh, H., Mishra, S.L., Vijayalakshmi, R., Giriyalkar, A.B., Gupta, C.K., US Pat. No. 6,645,453B2, Nov. 11, 2003.
17. Singh, H., Vijayalakshmi, R., Mishra, S.L., Gupta, C.K., Hydrometallurgy 59 (1) (2001) 69– 76.
18. Singh H., Mishra S.L., Vijayalakshmi R., Hydrometallurgy 73 (2004) 63–70.
19. Mishra, S.L., Giriyalkar, A.B., Vijayalakshmi, R., Iyer, N.S., Kotekar, M.K., Anitha, M., Singh, H. In the proceedings of International Symposium on Solvent Extraction, September 26-27 (2002) Bhubaneswar, India, pp. 393-398.
20. Korfan. S., J. Radioanal. Nucl. Chem., 238 (3) (1998) 145- 148.
21. Singh, S.K., Misra, S.K., Sudersanan, M., Dakshinamoorthy, A., Sep. Sci. Technol., 44 (2009) 169-189.
22. Singh, S.K., Misra, S.K., Tripathi, S.C., Singh, D.K., Desalination 250 (2010) 19-25.
23. Sawant, S.R., Sonawane, J.V., Venugopalan, A.K., Dey, P.K., Kumar, A., Mathur, J.N., Ind. J. Chem. Technol., 10 (2003) 531-538.
24. Singh, S.K., Misra, S.K., Sudersanan, M., Dakshinamoorthy, A., Munshi, S.K., Dey, P.K., Hydrometallurgy, 87 (2007) 190-196.
25. Joshi, J.M. Pathak P.N., Pandey A.K., Manchanda V.K., Hydrometallurgy, 96 (2009) 117-122.
26. Douglas, S.F., J.Orgmet. Chem, 690 (2005) 2426-2438.
27. Huang, C.T., Huang, T.C., Solv. Extr. Ion Exch., 5 (1987) 611-631

- 28.** Madane, N. S., Nikam, G. H., Mahanwar, K. R., Mohite, B. S., J. Radioanal Nucl Chem 288 (2011) 285–290
- 29.** OUT, E.O., Solvent Extr.Ion Exch., 15 (1993) 1-10.
- 30.** Harrington, C. D., Ruehle, A. E.,(Ed.) Uranium Production Technology, (1959) D.Van Nostrand Company .Inc., New Jersey.
- 31.** Gmelin Hand Book of Inorganic Chemistry, 8th edn, Thorium, System No.44, 1989, Vol. A4, Springer-Verlag, Berlin.
- 32.** Gmelin Hand Book of Inorganic Chemistry, 8th edn, Thorium, System No.44, 1997, Vol. B1, Springer-Verlag, Berlin.
- 33.** Calkins, G.D., Filbert, R.B., Bearnse, A.E., and Clegg, J.W., US Atomic Energy Commission Report, BMI-2431 (1950)
- 34.** Gmelin Hand Book of Inorganic Chemistry, 8th edn, Thorium, System No.44, 1990, Vol. A1a, Springer-Verlag, Berlin.
- 35.** Gmelin Hand Book of Inorganic Chemistry, 8th edn, Thorium, System No.44, 1991, Vol. A1b, Springer-Verlag, Berlin.
- 36.** Taylor, M., and Ewing, R.C., Acta Crystallogr., B34 (1978) 1074-1075.
- 37.** Jamrack, W.D., “Rare Metal Extraction by Chemical Engineering Technique”, International Series, Monograph in Chemical Engineering, Vol.II, p.162 and 187, Pergamon press, New York (1963).
- 38.** Navratil, J.D., and Schutz, W.W., (Eds): Science and Technology of TBP, CRC Press, Boca Raton (1984).
- 39.** Gmelin Hand Book of Inorganic Chemistry, 8th edn, Thorium, System No.44, 1985, Vol. C2, Springer-Verlag, Berlin.

40. Dean, O.C. and Chandler, J.M., Nucl.Sci. Eng., 2 (1957) 57-72.
41. Leber, A., Z.Anorg. Allg.Chem., 166 (1927) 16-26.
42. Smith, J.F., Carlson, O.N., Peterson, D.T., and Scott, T.E., Thorium: Preparation and Properties, 1975, Iowa State University Press, Ames, Iowa.
43. Thorium fuel cycle: potential benefits and challenges. International Atomic Energy Agency (IAEA) Technical Document 1450, May 2005.
44. Seaborg, G.T., Katz, J.J., "The Actinide elements" (1954) Mcgro Hill Book Co. Inc. p 131.
45. Keller C., "The chemistry of Trans uranium elements" Verlag Chemie GmbH., p. 333-335 (1971).
46. Morss, L.R., Edelstein, N.M., Fuger, J., Katz, J.J., The chemistry of actinides and transactinide elements, 3 (1) (2006).
47. Seaborg, G.T., Chem. Eng. News., 23 (1945) 2190-2193.
48. Seaborg, G.T., "Man made Transuranium Elements"., Printice Hall Inc. Eaglwood Cliffs, N.J., 1963.
49. Maltra, O.L., Molecular Physics, 42 (1) (1981) 65-72.
50. Richardson, F.S., Saxe, D.J., Davis, A.S., Faulkner, R.T., Molecular Physics, 42 (6) (1981) 1401-1429.
51. Berthelot, M., and Jungfleisch, J., Ann. Chim. Phys, 26 (1872) 396.
52. Merit, R.C., The Extractive Metallurgy of Uranium, Colorado School of Mines Research Institute, Colorado (1971).
53. Arnold,W.D., Hurst, F.J., and Ryon, A.D., Chim. Eng., 84 (1977) 56.

- 54.** Markus, Y., and Kertes, A.S., Ion Exchange and Solvent Extraction of Metal Complexes, Wiley Interscience, New York, (1969).
- 55.** Gupta, C.K., and Mukherjee, T.K., Hydrometallurgy in Extraction Process, Vol.II, (1990), CRC Press.
- 56.** Ritcey, G.M., and Ashbrook, A.W., Solvent Extraction: Principle and Application to Process Metallurgy, Part I & Part II (Elsevier, Oxford, New York, 1984).
- 57.** Habashi, F., Text Book of Hydrometallurgy, Second Edition (1999), Metallurgie Extractive Quebec, Canada.
- 58.** Rydberg, J., Cox, M., Musikas, C., Choppin, G.R., Solvent Extraction Principle and Practice (2004).
- 59.** Base, Jr. C.F., J. Inorg. Nucl. Chem., 24 (1962) 707-720.
- 60.** Peppard, D.F., and Mason, G.W., Nucl. Sci. and Eng., 16 (1963) 8-382.
- 61.** Ho, W.S.W. and Sirkar, K.K., Membrane Handbook, Van Nostrand Reinhold, New York, 1992.
- 62.** Mohapatra, P.K. and Manchanda, V.K., Ind. J. Chem., 42A (2003) 2921-2925.
- 63.** IUPAC Technical Report Series No. 431, Application of Membrane Technologies for Liquid Waste Processing. IAEA, Vienna, 2004.
- 64.** Babcock, W.C., Baker, R.W., Kelly, D.J., Lachapella, E.D., J. Memb. Sci., 7 (1980) 71-78.
- 65.** Sifniades, S., Largman, T., Tunick, A.A., Koff F.W., Hydrometallurgy, 7 (1981) 201-212.
- 66.** Akiba, K., Kanno, T., Sep. Sci. Tech., 18 (1983) 831-841.
- 67.** Chaudry, M.A., Islam M.N., J. Radioanal. Nucl. Chem., 109 (1987) 11-12.

68. Moskvin, L.N., Krasnaperov, V., Grigorev G.L., Tsaitsyana G.L., Radiokhimiya, 6 (1976) 851.
69. Shukla, J.P., Misra, S.K., J. Memb. Sci., 64 (1991) 93-102.
70. Panja, S., Mohapatra, P.K., Tripathi, S.C., Manchanda, V.K., J. Memb. Sci., 337 (1991) 274-281.
71. Kedari, C.S., Pandit, S.S., Ramanujam, A., J. Memb. Sci., 156 (1999) 187-196.
72. Ansari, S.A., Mohapatra, P.K., Raut, D.R., Adya, V.C., Thulasidas, S.K., Manchanda, V.K., Sep. Purif. Technol., 63 (2008) 239-242.
73. Matsuoka, H., Aizawa, M. and Suzuki, S., J. Memb. Sci., 7 (1980) 11-19.
74. Huang, T.C. and Huang, C.T., J. Memb. Sci., 29 (1986) 295-308.
75. Sriram, S., Mohapatra, P.K., Pandey, A.K., Manchanda, V.K., Badheka, L.P., J. Memb. Sci., 177 (2000) 163-175.
76. Shukla, J.P., Singh, R.K. and Kumar, A., Radiochim. Acta, 54 (1991) 73-77.
77. Shukla, J.P., Kumar, A. and Singh, R.K., Sep. Sci. Technol., 27 (1992) 447-465.
78. Shukla, J.P., Misra, S.K., Ind. J. Chem., 31 (1992) 323-338.
79. Vladimir, S. Kislik, Liquid Membranes: Principle & Applications in Chemical Separation & Wastewater Treatment, Elsevier, Oxford OX28DP, UK, 2010.
80. Singh, R.K., Dhadke, P.M., J. Radioanal. Nucl. Chem., 254 (2002) 607-612.
81. Behera, P., Mishra, M.S., Mohanty, M.I., Chakravorty, V., J. Radioanal. Nucl. Chem., 178 (1994) 179-192.
82. Singh, D.K., Singh, H., Mathur, J.N., Radiochim. Acta, 89 (2001) 573-578.
83. Rout, K.C., Mishra, P.K., Chakravorty, V. and Dash, K.C., Radiochim. Acta, 62 (1993) 203-206.

- 84.** Mansingh, P.S., Chakravorty, V., and Dash, K.C., *Radiochim. Acta*, 73 (1996) 139–143.
- 85.** Godbole, A.G., Mapara, P.M., Swarup, R., *J. Radioanal. Nucl. Chem.*, 200 (1995) 1-8.
- 86.** Chetty, K.V., Gamare, J.S., Godbole, A.G., Vaidya, V.N., *J. Radioanal. Nucl. Chem.*, 269 (2006) 15-20.
- 87.** Suresh, A., Srinivasan, T.G., Vasudeva Rao, P.R., Rajagopalan, C.V., Koganti, S.B., *Sep. Sci. and Tech.*, 39(10) (2005) 2477-2496.
- 88.** Suresh, A., Srinivasan, T.G., Vasudeva Rao, P.R., *Solv.Ext.Ion Exch.*, 12(4) (1994) 727-744.
- 89.** El-Taher, A., *Appl. Rad. and Isoto.* 68 (2010) 1189-1192.
- 90.** El-Taher, A., Nossair, A., Azzam, A.H., Kratz, K.L., Abdel-Halim, A.S., *J. Environ. Prot. Eng.* 29 (2004) 19-30.
- 91.** Afzal, M., Javed Hanif, M. S., Imtiaz, H., Riaz, A., *J. Radioanal. Nucl. Chem.*, 152 (1991) 251-259.
- 92.** Shrivastav, P., Menon, S. K., Agrawal, Y. K., *J. Radioanal. Nucl. Chem.*, 250 (2001) 459–464.
- 93.** Freitas, M. C., Hipólito, C. S., *J. Radioanal. Nucl. Chem.*, 271 (2007) 179–183.
- 94.** Osamu, F., Shigeo, U., Eiji, U., Kazunori, S., Takashi, M., *Anal. Chim. Acta*, 420 (2000) 65–71.
- 95.** Philip, A. Greene, Christine, L., Copper, D. E. B., Ramsey, J. D., Greg, E. C., *Talanta* 66 (2005) 961–966.
- 96.** Aziz, M., Beheir, S. G., Shakir, K., *J. Radioanal. Nucl. Chem.*, 172 (1993) 319-327.
- 97.** Stanislaw Ku, Norbert OBARSKI and Zygmunt Marczenko, *Analytical Sciences* April 8 (1992) 213.

- 98.** Ali, N., *J. Braz. Chem. Soc.*, 17 (2006) 1020-1026.
- 99.** Johnson, D.A., Florence, T.M., *Anal. Chim. Acta*, 53 (1971) 73-79.
- 100.** Singh, S.K., Misra, S. K., Pandit, S. S., Parikh, K. J. and Tripathi, S. C., *J. Radioanal. Nucl. Chem.*, 280 (2009) 33-39.
- 101.** Das, S. K., Kedari, C. S. and Tripathi, S. C., *J. Radioanal. Nucl. Chem.*, 280 (2010) 675-681.
- 102.** Kosolapoff, G.M., *Organophosphorous compounds* (1950), Wiley, New York, p.211.
- 103.** Singh, D.K., Anita, M., Yadav, K.K., Kotekar, M.K., Vijayalakshmi, R., Singh, H., *Des. Water Treat.* 38 (2012) 236-244.
- 104.** Sharma, J.N., Sakhalkar, P.M., Iyer, K.S., Marwah, U.R., *J. Radioanal. Nucl. Chem.* 240 (3) (1999) 959-961.
- 105.** Davies, W., Gray, W., *Talanta* 11 (1964) 1203–1211.
- 106.** Danesi, P.R., *Sep. Sci. Technol.*, 19 (1984) 857–894.
- 107.** Danesi, P.R., Chiarizia, R., Rickert, P., Horwitz, E.P., *Solv. Ext. Ion Exch.*, 3 (1985) 111–147.
- 108.** Cao, A., *Anal. Lett.*, 36 (15) (2003) , 3185–3225.
- 109.** Ganguly, R., Sharma, J.N., Choudhury, N., *J. Collo. Inter. Sci.*, 355 (2011) 458–463.
- 110.** Jeffery, G.H., Bassett, J., Mendham, J. and Denney, R. C. (Eds.), “*Vogel’s Textbook of Quantitative Analysis*”, 5th ed., ELBS Longman Publishers, UK (1996), p. 329.
- 111.** Balasubramanian, G.R., Chitnis, R.T., Ramanujam, A., Venkatesan, M., BARC Report, Report-940, Bhabha Atomic Research Centre, Mumbai, India, 1977.
- 112.** Gupta, R, Pandey, V.M., Pranesh, S.R., Chakravarty, A.B., *Hydrometallurgy* 71 (2004) 429-434.

- 113.** Schulz, W.W., Navratil, J.D., Bess, T., Science and technology of tributyl phosphate, selected technical and industrial uses, vol 1. (1987) CRC Press, Boca Raton.
- 114.** Schulz, W.W., Burger, L.L., Navratil, J.D., Bender, K.P., Science and technology of tributyl phosphate, applications of tributyl phosphate in nuclear fuel reprocessing, vol 3. (1990) CRC Press, Boca Raton.
- 115.** Mathur, J.N., Choppin, G.R., Solvent Extr. Ion. Exch., 16 (1998) 739-749.
- 116.** Hurst, F.J., Crouse, D.J., Brown, K.B., Ind. Eng. Chem. Process. Des. Dev., 11 (1972) 122-128.
- 117.** Dreisinger, D.V., Cooper, W.C., Hydrometallurgy 12 (1984) 1-20.
- 118.** Mishra, S., Chakravorty, V., Hydrometallurgy 44 (1997) 371-376.
- 119.** Mathur, J.N., Solvent Extr Ion Exch 1 (1983) 349-412.
- 120.** Sahu, S.K., Chakravorty, V., Reddy, M.L.P., Ramamohan, T.R., Talanta 51 (2000) 523-342.
- 121.** Singh, D.K., Singh, H., Mathur, J.N., Radiochim. Acta., 89 (2001) 573-578.
- 122.** Mishra, S.L., Singh, H., Gupta, C.K., Hydrometallurgy 56 (2000) 33-40.
- 123.** Godbole, A.G., Mapara, P.M., Swarup, R., J. Radioanal. Nucl. Chem., 200 (1) (1995) 1-8.
- 124.** Sarkar, S.G., Bandekar, S.V., Dhadke, P.M., J. Radioanal. Nucl. Chem., 243 (2000) 803-807.
- 125.** Mayankutty, P.C., Ravi, S., Nadkarni, M.N., J. Radioanal. Nucl. Chem., 68 (1982) 145-150.
- 126.** Stas, J., Al-Merey, R., Karjou, J., J. Radioanal. Nucl. Chem., 250 (2001) 525-529.
- 127.** Hoffmann, P., Pilz, N., Lieser, K.H., J Radioanal. Nucl. Chem., 132 (1989) 121-129.

- 128.** American Society for Testing and Materials, ASTM, vol 12.1 359 (2005) 1254–1299
- 129.** Dogmane, S.D., Singh, R.K., Bajpai, D.D., Mathur J.N., J. Radioanal. Nucl. Chem. 253(3) (2002) 477-482.
- 130.** Shukla, J.P., Pai, S.A., Subramanian, M.S., J. Radioanal. Nucl. Chem.; 56 (1980) 53-63.
- 131.** Biswas, S; Singh, D.K; Hareendran, K.N; Sharma, J.N; Roy, S.B; J. Radioanal. Nucl. Chem.; 284 (2010) 201-205.
- 132.** Kolarik, Z., Petrich, G., A., Berichte der Bunsengesellschaft für physikalische Chemie, 83 (1979)1110-1113.
- 133.** Jožef, J. Čomor; Miroslav M. Kopečni; Djordje M. Petkovič, Solv. Ext. Ion.Exch, 15 (1997) 991-1006.
- 134.** Singh, D.K., Singh, H., Gupta, C.K., J. Radioanal. Nucl. Chem. 245, (2000) 575-580.
- 135.** Sato, T.: J. Inorg. Nucl. Chem. 24, (1972) 699-706.
- 136.** Mukherjee, T.K.; Singh, H. (2006) Recovery of uranium and thorium from secondary resources, in Nuclear Fuel Cycle Technologies – Closing Fuel Cycles, B. Raj, P.R. Vasudeva Rao (Eds.), Board of Research in Nuclear Sciences, Mumbai, India, pp. 70.
- 137.** Deqian, L.; Yong, Z.; Shulan, M. J. Alloys Comp. 374 (2004) 431-433.
- 138.** Habashi, F., Hand Book of Extractive Metallurgy, Wiley-VCH, (1997) pp. 1649.
- 139.** Miyawaki, R.; Nakai, I., Crystal chemical aspects of rare earth minerals. In: A.P. Jones, F. Wall and C.T. Williams, Editors, Rare Earth Minerals: Chemistry, Origin and Ore Deposits, The Mineralogical Society Series vol. 7, Chapman and Hall, London (1996) pp. 21.

- 140.** Silva, A.S.; Almendra, E.R.E.; Ogasawara, T.; Andrade, M.C., Lixiviação sulfúrica da monazita em autoclave: análise termodinâmica. Anais do III Encontro de Metalurgia, Mineração e Materiais, vol. 1. UFMG, Belo Horizonte/MG, Brasil, (1995) pp. 223–234.
- 141.** Vijayalakshmi, R., Mishra, S.L., Singh, H., Gupta, C.K., Hydrometallurgy. 61(2) (2001) 75-80.
- 142.** Gupta, C.K., Krishnamurthy, N., Extractive metallurgy of rare earths. Inter. Mater. Reviews. 5(37) (1992) 204-207.
- 143.** Muthuchamy, S., Nair, V.R., Maharana, L.M., Application of solvent extraction technique for the separation of rare earths, thorium and uranium , Proceedings of International Symposium on Solvent Extraction, September, 26-27, Bhubaneswar, India, (2002) pp.511-523.
- 144.** Soe, N.N., Shwe, L.T., Lwin, K.T., World. Acad. Sci. Engg. Technol. 22 (2008) 142-145.
- 145.** Mckay, H.A.C., Miles, J.H., Swanson, J.L., The Purex Process. In Science and Technology of Tributyl Phosphate. Schulz, W.W.; Burger, L.L.; Navratil, J.D.; Bender, K.P. (Eds.), CRC Press, Boca Raton, Florida, USA, volume 3, (1990) pp.1.
- 146.** Bond, W.D., The Thorex Process. In Science and Technology of Tributyl Phosphate. Schulz, W.W.; Burger, L.L.; Navratil, J.D.; Bender, K.P. (Eds.), CRC Press, Boca Raton, Florida, USA, volume 3, (1990) pp. 225.
- 147.** Healy, T.V., Mckay, H.A.C., Trans. Faraday Soc. 52 (1956) 633-642.
- 148.** Shoun, R.R., Thompson, M.C., Schulz, W.W., Navratil, J.D., Talbot, A.E., (Eds.) Chemical properties and reactions., Science and Technology of Tributyl Phosphate, CRC Press, Boca Raton, Florida, USA, 1(1984) pp.137.

- 149.** Barney, G.S., Cooper, T.D., The chemistry of tributyl phosphate at elevated temperature in the plutonium finishing plant process vessels Report WHC-EP-0737, Washington, USA (1994).
- 150.** Pathak, P.N., Veeraraghavan, R., Prabhu, D.R., Mahajan, G.R., Manchanda, V.K., Sep. Sci. and Tech., 34(13) (1999) 2601-2614.
- 151.** Mowafy, E.A., Aly, H.F., Solv. Extr. Ion Exch. 19(4) (2001) 629-641.
- 152.** Suresh, A., Srinivasan, T.G., Vasudeva Rao P.R., Rajagopalan, C.V., Koganti, S.B., Sep. Sci. and Tech. 39(10) (2005) 2477-2496.
- 153.** Suresh, A., Srinivasan, T.G., Vasudeva Rao, P.R., Solv. Ext. Ion Exch. 12(4) (1994) 727-744.
- 154.** Koladkar, D.V., Dhadke, P.M., J. Radioanal. Nucl. Chem., 253 (2002) 297-302.
- 155.** Sharma, J.N., Ruhela, R., Harindran, K.N., Mishra, S.L., Tangri, S.K., Suri, A.K., J. Radioanal. Nucl. Chem., 278 (2008) 173-177.
- 156.** Siddall III, T.H., Ind. Eng. Chem. 51(1) (1959) 41-44.
- 157.** Pathak, P.N., Veeraraghavan, R., Manchanda, V.K., J. Radioanal. Nucl. Chem. 240 (1999) 15-18.
- 158.** Suresh, A., Srinivasan, T.G., Vasudeva Rao, P.R., Solv. Ext. Ion Exch., 27 (2009) 258-294.
- 159.** Kulkarni, P.G., Gupta, K.K., Gurba, P.B., Janardan, P., Changrani, R.D., Dey, P.K., Manchanda, V.K., Radiochim. Acta., 94 (2006) 325-329.
- 160.** Thompson, M. C., Distribution of selected lanthanides and actinides between 30% TBP in *n*-paraffin and various metal nitrate solutions. Separations Chemistry Division, E. I. du Pont de Nemours & Co. 62-L I-06, Savannah River Laboratory, DP-1336(1973).

- 161.** Kraikaew, J., Srinuttrakul, W., Chayavadhanakur, C., *J. Met. Mater. Min.* *15*(2) (2005) 89-95.
- 162.** Goldenberg, J. F., Abbruzzese, C., *Int. Journal of Mineral Processing*, *10*(4) (1983) 241-254.
- 163.** Sood, D.D., Patil, S.K., *J. Radioanal. Nucl. Chem. Articles*, *203*(2) (1996) 547-573.
- 164.** Korbisch, J., Actinides. In: *Handbook of Ion Exchange Resin: Their Application to Inorganic Chemistry*, **vol. 2**, 1989, CRC Press, pp. 6–53.
- 165.** Kluge, E., Lieser, K.H., *Radiochim. Acta*, **27** (1980) 161–171.
- 166.** Mincher, B.J., Modolo, G., Mezyk, S.P., *Solv. Extr. Ion Exch.*, 27(1) (2009) 1-25.
- 167.** IUPAC Technical Report Series No. 431, *Application of membrane technologies for liquid waste processing*. IAEA, Vienna, 2004.
- 168.** Babcock, W.C., Baker, R.W., Lachapelle, E.D., Smith, K.L., *J. Memb. Sci.*, *7* (1980) 71-87.
- 169.** Mohapatra, P.K., Manchanda, V.K., *Handbook of Membrane Separations: Chemical, Pharmaceuticals, Food and Biological Applications*, Anil Kumar Pabby, S.S.H. Rizvi, Ana Maria Sastre (Eds.), Chapter-31, *Liquid membrane-based separations of actinides*. pp. 883-910, CRC Press, Taylor & Francis Group, 2009.
- 170.** Shailesh, S., Pathak, P.N., Mohapatra, P.K., Manchanda, V.K., *Desalination*. *232* (1-3) (2008) 281-290.
- 171.** Panja, S., Mohapatra, P.K., Tripathi, S.C., Manchanda, V.K., *J. Memb. Sci.*, *337* (2009) 274-281.
- 172.** Kedari, C.S., Pandit, S.S., Misra, S.K., Ramanujam, A., *Hydrometallurgy*, *62* (2001) 47-56.

- 173.** Burger, L.L., *J. Phys. Chem.*, 62 (1958) 590-593.
- 174.** Sella, C., Becis, A., Cote, G., Bauer, D., *Solv. Extr. Ion Exch.*, 13 (4) (1995) 715 – 729.
- 175.** Di Bernardo, P., Zanonato, P.L., Tian, G., Tolazzi, M., Rao, L., *Dalton Trans.*, (2009) 4450-4457.
- 176.** Naik, P.W., Dhami, P.S., Misra, S.K., Jambunathan, U., Mathur, J.N., *J. Radioanal. Nucl. Chem.* 257 (2003) 327–332
- 177.** Ansari, S.A., Mohapatra, P.K., Manchanda, V.K., *Ind. Eng. Chem. Res.* 48 (2009) 8605-8612.
- 178.** Huang, T.-C., Huang, C.-T., *J. Memb. Sci.*, 29 (1986) 295-308.
- 179.** Shukla, J.P., Kumar, A., Singh, R.K., *J. Nucl. Sci. Technol.*, 31 (1994) 1066-1072.
- 180.** Darvishi, D., Haghshenas, D.F., Keshavarz Alamdari, E., Sadrnezhad, S.K., Halali, M., *Hydrometallurgy*, 77 (3-4) (2005) 227-238.
- 181.** El-Hefny, N.E., El-Nadi, Y.A., Daoud, J.A., *Sep. Purif. Technol.*, 75 (3) (2010) 310-315.
- 182.** Parhi, P.K., Sarangi, K., *Sep. Purif. Technol.*, 59 (2) (2008) 169-17.
- 183.** Lindell, E., Jääskeläinen, E., Paatero, E., Nyman, B., *Hydrometallurgy*, 56 (3) (2000) 337-357.
- 184.** Swain, B., Jeong, J., Lee, Jae-chun, Lee, Gae-Ho, *J. Memb. Sci.*, 297 (1-2) (2007) 253-261.
- 185.** Ramakul, P., Supajaron, T., Prapasawat, T., Pancharoen, U., Lothongkum, A.W., *J. Ind. and Eng. Chem.*, 15 (2) (2009) 224-226.
- 186.** Chiarizia, S R., Horwitz, E.P., Rickert, P.G., Hodgson, K.M., *Sep. Purif. Technol.*, 25(13-15) (1990) 1571-1586.
- 187.** Bukhari, N., Chaudry, M.A., Mazhar, M., *J. Membr. Sci.* 234 (2004) 157-165.

- 188.** Singh, D.K., Vijayalakshmi, R., Singh, H., *Des. Water Treat.* 38 (2012) 138-145.
- 189.** Juang, R.S., Lee, S.H., *J. Memb. Sci.*, 110 (1996) 13-23.
- 190.** Alguacil, F.J., Alonso, M., Sastre, A.M., *J. Memb. Sci.*, 184 (2001) 117-122.
- 191.** Alonso, M., Delgado, A.L., Sastre, A.M., F.J., *Chem. Eng. J.*, 118 (2006) 213-219.
- 192.** Mishra, S.L., Vijayalakshmi, R., Singh, H., *Ind. J. Chem. Technol.*, 12 (2005) 708.
- 193.** Neumana, R. D., Zhoua, N. F., Wuab, J., Jonesac, M. A., Gaonkarad, A. G., Parka, S. J., Agrawal, M. L., *Sep. Sci. Tech.*, 25(13-15), (1990) 1655-1674.
- 194.** Chiarizia, R., Nash, K. L., Jensen, M. P., Thiyagarajan, P., and Littrell, K.C., *Langmuir* 19 (2003) 9592-9599.
- 195.** Rosen, M. J., *Solubilization by Solutions of Surfactants: Micellar Catalysis. Surfactants and Interfacial Phenomena*, 2nd ed.; Wiley: New York, 1989; pp 171-206.
- 196.** Hinze, W. L., Pramauro, E.A., *Crit. Rev. Anal. Chem.*, 24 (1993) 133-177.
- 197.** Hoffmann, H., Kielman, H.S., Pavlovic, D., Platz, G., Ulbricht, W., *J. Colloid Interface Sci.*, 80 (1981) 237-239.
- 198.** Yua, Z.J., Ibrahima, T. H., Neuman, R. D., *Solvent Extr. Ion Exch.*, 16(6) (1998) 1437-1463.
- 199.** Chiariziaa, R., Briandb, A., Jensena, M. P., Thiyagarajan, P., *Solvent Extr. Ion Exch.*, 26 (2008) 333-359.
- 200.** Wanga, D., Lia, Y., Wua, J., Xua, G., *Solvent Extr. Ion Exch.*, 14 (4) (1996) 585-601.
- 201.** Jensen, M. P., Yaita, T., and Chiarizia, R., *Langmuir* 23 (2007) 4765-4774.
- 202.** Pathak, P.N., Ansari, S.A., Sumit Kumar, Tomar, B.S., Manchanda, V.K., *J. Colloid Interface Sci.*, 342 (2010) 114-118.

- 203.** Vijayalakshmi, R., Mishra, S.L., and Singh, H., *Int. J. Nucl. Ener. Sci. Technol.*, 1 (2-3) (2005) 178-183.
- 204.** Meridiano, Y., Berthon, L., Crozes, X., Sorel, C., Dannus, P., Antonio, M.R., Chiarizia, R., Zemb, T., *Solvent Extr. Ion Exch.*, 27 (2009) 607–637.
- 205.** Nave, S., Mandin, C., Martinet, L., Berthon, L., Testard, F., Madic, C., Zemb, T., *Phys. Chem. Phys.*, 6 (2004) 799-808.
- 206.** Antonio, M.R., Chiarizia, R., Gannaz, B., Berthon, L., Zorz, N., Hill, C., Cote, G., *Sep. Sci. Tech.*, 43 (2008) 2572- 2605.
- 207.** Uranium and uranium compounds, *Encyclopedia of Chemical Technology*, 3rd ed., vol. 23, p. 514.
- 208.** Brierley, J.A., Brierley, C.L., *Hydrometallurgy* 59 (2001) 233–239.
- 209.** McCready, R.G., Gould, W.D., Biobleaching of uranium, in: H.L. Ehrlich, C.L. Brierley (Eds.), *Microbial Mineral Recovery*, McGraw-Hill, New York, 1990, p. 107.
- 210.** Lizama, H.M., Fairweather, M.J., Dai, Z., Allegretto, T.D., *Hydrometallurgy* 69 (2003) 109–116.
- 211.** Swamy, K.M., Rao, K.S., Narayana, K.L., Murthy, J.S., Ray, H.S., *Min. Pro. Ext. Metal. Rev.*, 14 (1995) 179-192.
- 212.** Swamy, K.M., Sukla, L.B., Narayana, K.L., Kar, R.N., Panchanadikar, V.V., *Ultrason Sonochem.*, 2 (1995) S5–S9.
- 213.** Tekin, T., Tekin, D., Bayramoglu, M., *Ultrason. Sonochem.*, 8 (4) (2001) 373–377.
- 214.** El-Taher, A. *Appl. Rad. and Isoto.* 68 (2010) 1189-1192.
- 215.** El-Taher, A., Nossair, A., Azzam, A.H., Kratz, K-L., Abdel-Halim, A.S., *J. Environ. Prot. Eng.*, 29 (2004) 19-30.

- 216.** Afzal, M., Javed, Hanif, Saleem, M., Imtiaz Hanif, Ahmed, Riaz, J. *Radioanal. Nucl. Chem.*, 152 (1991) 251-259.
- 217.** Shrivastav, P., Menon, S. K., Agrawal, Y. K., *J. Radioanal. Nucl. Chem.*, 250 (2001) 459-464.
- 218.** Freitas, M. C., Hipólito, C. S., *J. Radioanal. Nucl. Chem.*, 271 (2007) 179-183.
- 219.** Osamu Fujino, Shigeo Umetani, Eiji Uenoa, Kazunori Shigeta, Takashi Matsuda, *Anal. Chim. Acta*, 420 (2000) 65-71.
- 220.** Philip, A., Greene, Christine L., Copper, David, E., Berv, Jeremy D. Ramsey, Greg, E., Collins, *Talanta* 66 (2005) 961-966.
- 221.** Aziz, M., Beheir, Sh. G., Shakir, K., *J. Radioanal. Nucl. Chem.*, 172 (1993) 319-327.
- 222.** Stanislaw Ku, Norbert OBARSKI and Zygmunt Marczenko, *Analytical Sciences* April 8 (1992) 213.
- 223.** Ali Niazi, *J. Braz. Chem. Soc.*, 17 (2006) 1020-1026.
- 224.** Suresh, A., Patre, D.K., Srinivasan, T.G., Vasudeva Rao, P.R., *Spectrochim. Acta A*, 58 (2002) 341-347.
- 225.** Roy Ko, Weiler, M. R., *Anal. Chem.*, 34 (1962) 85-87.

Statement under section 0.771

The work reported in this thesis was planned, carried out and interpreted by me. I was helped by Dr. P.N. Pathak through valuable discussions. Part of the work reported in this thesis has been published as listed below.

List of Publications

Journals

1. Synergistic extraction of uranium with Mixtures of PC88A and neutral donors, **S.Biswas**, P.N.Pathak, D.K.Singh, S.B.Roy, V.K.Manchanda, **J. Radioanal. Nucl.Chem.** 284 (2010) 13-19.
2. Mathematical modeling of solvent extraction of uranium from sulphate media employing 2-ethylhexyl phosphonic acid-mono-2-ethylhexyl ester (PC88A) and its mixture with tri octyl phosphine oxide (TOPO) as extractants, **S. Biswas**, P.N. Pathak, D.K. Singh, S.B. Roy, V.K. Manchanda, **J. Radioanal. Nucl.Chem.** 289 (2011) 557-564.
3. Evaluation of dinonyl phenyl phosphoric acid (DNPPA) and its synergistic mixtures with neutral oxodonors for extraction and recovery of uranium from nitric acid medium, **S. Biswas**, P.N. Pathak, D.K. Singh, S.B. Roy, V.K. Manchanda, **Int.J.Miner.Process.**, 104-105 (2011) 17-23.
4. Evaluation of 2-Ethylhexyl Phosphonic Acid Mono 2-Ethylhexyl Ester (PC88A) and its Synergistic Mixtures for Uranium Transport Studies from Nitric Acid Medium, **Sujoy Biswas**, P.N. Pathak, S.B. Roy and V.K. Manchanda , **Sep. Sci. Technol.** 46 (2011) 592-600.
5. Uranium permeation from nitric acid medium across supported liquid membrane impregnated with acidic organophosphorous extractants and their synergistic mixtures with neutral oxodonors, **Sujoy Biswas**, P.N. Pathak, Sangita Pal, S.B. Roy, P.K.Tewari and V.K. Manchanda, **Sep. Sci. Technol.** 46 (2011) 2110-2118.
6. Effect of Alkyl Substituents of Organophosphorous Extractants on Uranium Permeation for Recovery from Uranyl Nitrate Raffinate, **Sujoy Biswas**, P.N. Pathak, S.B. Roy and V.K. Manchanda, **Des. Water. Treat.**, 38 (2012) 151–158.
7. Carrier facilitated transport of uranium across supported liquid membrane using dinonyl phenyl phosphoric acid and its mixture with neutral donors, **S.Biswas**, P.N.Pathak, S.B.Roy, **Desalination** 290 (2012) 74–82.
8. Development of an extractive spectrophotometric method for estimation of uranium in ore leach solutions using 2-ethylhexyl phosphonic acid-mono-2-ethylhexyl ester (PC88A) and tri-*n*-octyl phosphine oxide (TOPO) mixture as extractant and 2-(5-bromo-2-pyridylozo)-5-diethyl aminophenol (Br-PADAP) as chromophore, **S.Biswas**, P.N.Pathak, S.B.Roy, **Spectrochimica Acta Part A** 91 (2012) 222– 227.

9. Kinetic Modeling of Uranium Permeation Across a Supported Liquid Membrane Employing Dinonyl phenyl phosphoric acid (DNPPA) as the Carrier, **Sujoy Biswas**, P.N. Pathak, S.B. Roy, **Int. J. Ind. Eng. Chem.** 19 (2013) 547–553.
10. An insight into the speciation and extraction behavior of Eu(III) with dinonyl phenyl phosphoric acid and di(2-ethylhexyl) phosphoric acid: Solvent extraction and fluorescence Studies, **Sujoy Biswas**, P.N. Pathak, S.V. Godbole, S.B. Roy, **Sep. Sci. Technol**, **48: 2418–2424, 2013**.
11. Separation of U(VI) and Th(IV) from thorium concentrate of monazite sand using tri(2-ethylhexyl) phosphate (TEHP)/ *n*-paraffin as the solvent, **Sujoy Biswas**, P.N. Pathak, D.K.Singh, S.B. Roy, **Sep. Sci. Technol. Sep. Sci. Technol**, **48: 2013–2019, 2013**.
12. Aggregation Behavior of Dinonyl Phenyl Phosphoric Acid (DNPPA): Dynamic Light Scattering and Spectrophotometric Investigations, **Sujoy Biswas**, P.N. Pathak, P.K. Mohapatra, S.B. Roy, *Int.J.Miner.Process.*, 125 (2013) 101–105.

Conferences

13. Synergistic Extraction of U(VI) from Nitric Acid Medium Using PC88A and Neutral Donors, **Sujoy Biswas**, K.N.Hareendran, V.H.Rupawate, D.K.Singh and S.B.Roy, Proceedings of Nuclear and Radiochemistry Symposium, January 7-10, 2009, SVKM Mithibai College, Mumbai, Paper No B-14.
14. Recovery of Uranium from Uranul Nitrate Raffinate obtained during Purification of Uranium, **Sujoy Biswas**, K.N.Hareendran, P.N.Pathak, S.B.Roy and V.K.Manchanda, Proceedings of Nuclear and Radiochemistry Symposium, January 7-10, 2009, SVKM Mithibai College, Mumbai, Paper No B-48.
15. Effect of alkyl substituents of Organophosphorous Extractants on uranium permeation for Recovery from Uranyl Nitrate Raffinate, **Sujoy Biswas**, P.N. Pathak, K.N.Hareendran, D.K.Singh, J.N. Sharma, S.B. Roy and V.K. Manchanda, DAE- BRNS Biennial Symposium on Emerging Trends in Separation Science and Technology SESTEC -2010, March 1- 4, 2010, Indira Gandhi Centre for Atomic Research, IGCAR, Kalpakkam -603 102, India, Paper No. H-9.
16. Evaluation of PC88A and its Synergistic Mixtures for Uranium Transport Studies from Nitric Acid medium, **Sujoy Biswas**, P.N. Pathak, S.B. Roy and V.K. Manchanda, DAE- BRNS Biennial Symposium on Emerging Trends in Separation Science and Technology SESTEC - 2010, March 1- 4, 2010, Indira Gandhi Centre for Atomic Research, IGCAR, Kalpakkam - 603 102, India, Paper No. H-15.

17. Separation of U(VI) and Th(IV) from monazite using tri(2-ethylhexyl) phosphate (TEHP)/ *n*-paraffin, **S. Biswas**, P.N. Pathak, D.K. Singh, S.B. Roy, V.K. Manchanda, DAE- BRNS Biennial Symposium on Nuclear and Radiochemistry (NUCAR) -2011, February 22-26, 2011, GITAM Institute of Science, Visakhapatnam, India, Paper No. B-104.
18. Evaluation of different Organophosphorous Extractants for Uranium Permeation from Nitric acid Medium Across a Supported Liquid Membrane, **S. Biswas**, P.N. Pathak, S.B. Roy, V.K. Manchanda, DAE- BRNS Biennial Symposium on Nuclear and Radiochemistry (NUCAR) - 2011, February 22-26, 2011, GITAM Institute of Science, Visakhapatnam, India, Paper No. B-108.
19. Carrier facilitated transport of uranium from nitric acid medium using di-nonyl phenyl phosphoric acid (DNPPA) as a carrier solvent, **S. Biswas**, P.N. Pathak, S.B. Roy, V.K. Manchanda, DAE- BRNS Biennial Symposium on Nuclear and Radiochemistry (NUCAR) - 2011, February 22-26, 2011, GITAM Institute of Science, Visakhapatnam, India, Paper No. B-109.
20. Determination of uranium in ore leach solution using 2-(5-Bromo-2-pyridylazo)-5- diethyl aminophenol (Br-PADAP) as chromogenic reagent, **S. Biswas**, P.N. Pathak, S.B. Roy, V.K. Manchanda, DAE- BRNS Biennial Symposium on Nuclear and Radiochemistry (NUCAR) - 2011, February 22-26, 2011, GITAM Institute of Science, Visakhapatnam, India, Paper No. C-24.
21. Empirical Modeling of Solvent Extraction of Uranium from Sulphuric Acid Medium Using PC88A and TOPO as Extractant, **S. Biswas**, P.N. Pathak, D.K. Singh, S.B. Roy, V.K. Manchanda, DAE- BRNS Biennial Symposium on Nuclear and Radiochemistry (NUCAR) - 2011, February 22-26, 2011, GITAM Institute of Science, Visakhapatnam, India, Paper No. B-86.
22. Carrier facilitated transport of uranium using different organophosphorous extractants and its recovery from uranyl nitrate solution, **S. Biswas**, P.N. Pathak and S.B. Roy, 24th Research Scholar's Meet-2012, 17th -18th February 2012, SIS College, Mumbai-400022, India, Abstract-23.
23. Aggregation Behavior of Dinonyl Phenyl Phosphoric Acid (DNPPA): Dynamic Light Scattering (DLS) and Spectrophotometric Studies, **S. Biswas**, P.N. Pathak, S.A. Ansari, P.K. Mohapatra, S.B. Roy, DAE- BRNS Biennial Symposium on Emerging Trends in Separation Science and Technology SESTEC -2012, Feb 27 -March 1, 2012, SVKM Mithibai College, Mumbai, India, Paper No. SNFC-10.
24. Uranium Permeation across Supported Liquid Membrane Using Dinonyl Phenyl Phosphoric Acid (DNPPA) and Its Mixture with Neutral Donors as Carriers, **Sujoy Biswas**, P.N. Pathak, S.B. Roy, DAE- BRNS Biennial Symposium on Emerging Trends in Separation Science and Technology SESTEC -2012, Feb 27 -March 1, 2012, SVKM Mithibai College, Mumbai, India, Paper No. MST-14.

